UNIVERSITY OF SOUTHAMPTON

FACULTY OF MEDICINE

Clinical and Experimental Sciences

Innovative Techniques for Retinal Pigment Epithelium Transplantation

by

Philip Alexander BSc MBBS MBA FRCOphth

Thesis for the degree of Doctor of Medicine

November 2016

UNIVERSITY OF SOUTHAMPTON

ABSTRACT

FACULTY OF MEDICINE

Clinical Neurosciences

Thesis for the degree of Doctor of Medicine

INNOVATIVE TECHNIQUES FOR RETINAL PIGMENT EPITHELIUM TRANSPLANTATION

Philip Alexander

Age-related macular degeneration (AMD) occurs due to changes in Bruch's Membrane (BrM), leading to Retinal Pigment Epithelium (RPE) dysfunction. RPE transplantation has potential as a regenerative strategy but previous attempts have been unsuccessful because BrM replacement has not been taken into consideration. Previous work at the University of Southampton has led to the development of a 60:40 P(MMA-co-PEGM-succinimidyl carbonate) electrospun fibrous co-polymer scaffold, as a potential artificial BrM. The aim of this project was to characterise and evaluate the co-polymer scaffold, and to develop methods to use it for RPE transplantation. The characteristics of an ideal BrM substitute, as espoused by Binder *et al.* (2007), were used as benchmarks.

RPE transplanted on an artificial BrM is likely to be positioned on the surface of the existing BrM and therefore needs to be more permeable than BrM. Diffusional flux studies showed that, allowing for differences in thickness, the polymer was 48x more permeable than human post-mortem BrM samples. Measurements of transepithelial electrical resistance across monolayers of ARPE-19 cells and primary rabbit RPE cells, cultured either on the co-polymer surface or directly on to tissue culture plates, supported the existence of tight electrical contacts between neighbouring RPE cells. VEGF concentrations were 50% higher in apical vs. basal compartments of culture wells, confirming RPE polarisation.

In vitro evaluation of a novel surgical instrument, POLARIS (**Pol**ymer **A**nd **R**PE **I**njector – **S**outhampton), designed to deliver cell-seeded polymer into the subretinal space, could detect no statistical difference in apoptotic cell death between POLARIS (21%) and the unejected controls (21%). ARPE-19 cells showed no increased cytotoxicity from application of a range of ophthalmic viscoelastic devices during cell culture, with baseline cytotoxicity maintained at less than 20%. This supports the potential use of viscoelastic devices within the subretinal space, to prevent bleb collapse during transplantation.

Three-port pars plana vitrectomy was performed in 25 rabbits, and creation of a localised retinal detachment allowed the successful delivery of polymer scaffolds into the subretinal space of 11 rabbit eyes. Pre-operative intravitreal saline was found to increase the likelihood of successful surgical induction of posterior vitreous detachment at the time of surgery.

The findings of this study show that the 60:40 P(MMA-co-PEGM-succinimidyl carbonate) electrospun copolymer scaffold mimics the desirable properties of an artificial BrM and allows formation of an electrically resistant, polarised RPE monolayer. The polymer has been successfully transplanted into rabbit eyes. These results support use of this copolymer to facilitate RPE transplantation, as a future potential treatment for AMD.

Table of Contents

ABSTRACT ..... **i**

Table of Contents ..... **iii**

List of tables ..... **ix**

List of figures ..... **xi**

List of accompanying materials ..... **xv**

DECLARATION OF AUTHORSHIP ..... **xvii**

Acknowledgements ..... **xix**

Definitions and Abbreviations ..... **xxiii**

Chapter 1: INTRODUCTION **25**

1.1 Eyes are important and expensive **25**

1.2 Structure of the Human Eye **27**

1.3 Photoreceptor cells are responsible for vision **29**

1.4 Retinal Pigment Epithelium in Health and Disease **31**

1.5 Bruch's Membrane **35**

1.5.1 Diffusion Regulation 36

1.5.2 RPE Cell Adhesion, Migration and Differentiation 36

1.5.3 Physical Barrier 37

1.6 Age Related Macular Degeneration **37**

1.7 Innovative therapeutic solutions for Retinal Degeneration **42**

1.8 RPE Transplantation **43**

1.8.1 Macular translocation 44

1.8.2 Autologous RPE-Choroid Patch Graft 46

1.8.3 Submacular injection of RPE cell suspension 48

1.8.4 Sources of Cells 48

1.8.4.1 Autologous Iris Pigment Epithelial cells 49

1.8.4.2 Ex-vivo cell sheet expansion prior to transplantation 50

1.8.4.3 Pluripotent Stem Cells 50

1.8.5 Surgical Considerations 53

1.8.6 Delivery of cells 54

1.8.7 Age-Related Changes in Bruch's Membrane 55

1.8.8 Effect of BrM Age on RPE Transplantation 56

1.9 BrM Substitutes 59

1.9.1 Natural membranes 59

1.9.2 Tissue engineered BrM substitutes 60

1.9.3 Previous work in the Lotery Laboratory on Tissue Engineered Polymer Scaffolds for RPE Transplantation 62

1.10 Aims, Hypothesis and Objectives 65

Chapter 2: DIFFUSION ACROSS BRUCH'S MEMBRANE 67

2.1 Introduction 67

2.1.1 Hydraulic Conductivity of BrM 67

2.1.2 Diffusion of macromolecules across BrM 68

2.2 Aims and Objectives 69

2.3 Methods 70

2.3.1 Preparation of human Bruch's Membrane 70

2.3.2 Preparation of polymer fibre 72

2.3.3 Preparation of the Ussing chamber 72

2.4 Results 75

2.4.1 Diffusion across human BrM Samples 76

2.4.2 Diffusion across Polymer, with and without ARPE-19 cells 77

2.5 Discussion 79

2.6 Conclusions 82

Chapter 3: RPE POLARISATION 83

3.1 Introduction 83

3.1.1 Polarity of the RPE 83

3.1.1.1 Cell Structure 84

3.1.1.2 Distribution of Organelles 84

3.1.1.3 Membrane protein distribution 85

3.1.1.4 Secreted growth factors 87

3.1.1.4.1 Pigment Epithelium-Derived Factor (PEDF) 87

3.1.1.4.2 Vascular Endothelial Growth Factor (VEGF) 88

3.1.1.5 Mechanism of RPE Polarisation 90

3.1.2 The RPE as a barrier 91

3.1.2.1 Techniques for studying barrier and polarisation 92

3.1.3 Cellular models of RPE polarisation and barrier function 95

3.1.3.1 Cell culture techniques 95

3.1.3.2 In vitro RPE models 96

3.1.4 Measurement of VEGF and PEDF using Sandwich ELISA 97

3.2 Aims and Objectives 99

3.3 Methods 100

3.3.1 Preparation of Transwells 100

3.3.2 Preparation of polymer 100

3.3.3 Preparation of ARPE-19 cells 101

3.3.4 Preparation of Primary Rabbit RPE cells 101

3.3.5 Immunocytochemistry of human and rabbit RPE cells 103

3.3.6 VEGF Sandwich ELISA 103

3.3.7 PEDF Sandwich ELISA 105

3.3.8 Transepithelial Electrical Resistance (TEER) 106

3.4 Results 110

3.4.1 Immunocytochemistry of Human and Rabbit RPE Cells 110

3.4.2 PEDF assay 112

3.4.3 VEGF Assay 119

3.4.4 Transepithelial Electrical Resistance (TEER) 126

3.5 Discussion 128

3.6 Conclusions 132

Chapter 4: SURGICAL INSTRUMENTATION 133

4.1 Surgical Instrumentation 133

4.1.1 Ophthalmic Viscoelastic Device (OVD) 135

4.1.2 Removing residual RPE 136

4.1.3 Delivery of RPE cells 137

4.1.3.1 Delivery of an RPE cell suspension 137

4.1.3.2 Delivery of a patch graft 138

4.2 Aims and Objectives 140

4.3 Methods 141

4.3.1 RPE cell culture 141

4.3.2 Effect of Viscoelastic on RPE cells in culture 141

4.3.2.1 Ophthalmic Viscoelastic Devices (OVD) 141

4.3.2.2 Cytotoxicity assay 142

4.3.3 Design and Assessment of RPE/Polymer Injector 143

4.3.3.1 Injector Design 143

4.3.3.2 Preparation of Polymer 145

4.3.4 TUNEL assay 146

4.4 Results 148

4.4.1 Viscoelastic experiment 148

4.4.2 Evaluation of POLARIS Injector 149
4.4.2.1 POLARIS Mark I 149
4.4.2.2 POLARIS Mark II 151
4.4.2.3 Polymer and Cell survival after POLARIS II ejection 152
4.4.3 Comparison between POLARIS II & Bonn-Shooter instrument 155
4.5 Discussion 159
4.6 Conclusions 160

Chapter 5: SURGICAL TECHNIQUES 161
5.1 Introduction 161
5.1.1 Pars Plana Vitrectomy 162
5.1.2 Animal Models for Ocular Surgery 169
5.1.3 Comparative Ocular Anatomy 170
5.1.4 Surgical Anatomy of the Rabbit Eye 175
5.1.4.1 Orbital, adnexal and ocular surface anatomy 175
5.1.4.2 Pars plana anatomy of the rabbit eye 177
5.1.4.3 Retinal anatomy of the rabbit eye 177
5.2 Aims and Objectives 180
5.3 Methods 181
5.3.1 In vivo transplantation experiments in rabbits 181
5.3.1.1 Animal handling 181
5.3.1.2 Anaesthetic 181
5.3.1.3 Surgical Technique 182
5.3.1.4 Polymer preparation 182
5.3.2 Histological Examination 183
5.3.2.1 Paraformaldehyde fixation and frozen sections 183
5.3.2.2 Haematoxylin and eosin (H&E) 183

5.3.2.3 Davidson's fixative solution and paraffin sectioning 184

5.3.2.4 Optimising Histological Sectioning using Porcine Eyes 184

5.3.2.5 Optimising Histological Sectioning using Lapine eyes 185

5.3.2.6 Perfusion Fixation of Lapine Eyes 186

5.3.3 Optical Coherence Tomography of Rabbit Eyes 190

5.4 Results 190

5.4.1 Surgical Technique 190

5.4.1.1 Pre-operative saline injection 190

5.4.1.2 Animal Positioning and Surgical Access 192

5.4.1.3 Incisions 195

5.4.1.4 Lensectomy 197

5.4.1.5 Vitrectomy 197

5.4.1.6 Bleb formation 198

5.4.2 Optimisation of Histology 205

5.4.2.1 Fixation with 4% paraformaldehyde vs. Davidson's fixative 205

5.4.2.2 Duration of Fixative and Size of Keratotomy 208

5.4.2.3 Histology of Rabbit Eyes 210

5.4.2.4 Histological processing of polymer 214

5.4.2.5 Histological result of polymer in the subretinal space 216

5.4.3 OCT of Rabbit Eyes 218

5.5 Discussion 219

5.6 Conclusions 223

Chapter 6: CONCLUSIONS & FUTURE WORK 225

Appendix 231

List of References 243

List of tables

Table 1.1: Functions of the Retinal Pigment Epithelium.....31
Table 1.2: Classification of AMD. 39
Table 1.3: Age related changes in Bruch's Membrane. 55
Table 1.4: Potential scaffolds for RPE transplantation 61
Table 2.1: Demographic data and thickness measurements for human BrM-choroid samples. 70
Table 3.1: A comparison of the conventional epithelial localisation of various membrane proteins with the localisation in RPE. 86
Table 3.2: Isoforms of Vascular Endothelial Growth Factor (VEGF) and their biological effects. 89
Table 4.1. Table comparing frequency of polymer damage after ejection of polymer from surgical instruments (POLARIS Mark II, or Bonn-Shooter) vs. control. 156
Table 5.1: Indications for pars plana vitrectomy surgery. 165
Table 5.2: Ocular anatomy of animals used for experimental surgery. 171
Table 5.3: Table showing the different types of fixative tested and points at which keratotomy was created in porcine eyes, to try to improve histological processing and preserve tissue architecture. 185
Table 5.4: Table showing the different sizes of keratotomy that were tested in lapine eyes, to optimise histological sectioning. 185
Table 5.5. Details of all rabbit vitrectomy procedures performed. 204

List of figures

Figure 1.1: Structure of the human eye. 27
Figure 1.2: Normal fundus photograph of the left eye. 28
Figure 1.3: OCT scan of a healthy macula 29
Figure 1.4: Healthy RPE 34
Figure 1.5: RPE degeneration in AMD 38
Figure 1.6: Clinical photographs of Dry AMD. 40
Figure 1.7: Clinical photographs of Neovascular ("Wet") AMD. 41
Figure 1.8: Macular translocation. 45
Figure 1.9: Autologous RPE-Choroid Patch Graft 46
Figure 1.10: Clinical photographs of autologous RPE-Choroid Patch graft 47
Figure 1.11: Schema showing manufacture of the P(MMA:PEGM-DSC) polymer 63
Figure 2.1: Photograph of human BrM in a 60mm petri dish 71
Figure 2.2: Structure of a modified Ussing chamber. 73
Figure 2.3: Photographs showing apparatus for diffusion studies 74
Figure 2.4: Diffusional Flux of FITC-Dextran (MW 40,000) across samples of human BrM over 24 hours. 76
Figure 2.5: Plot of diffusion flux per unit area of human BrM at 24 hours against age at time of death. 77
Figure 2.6: The diffusional flux of FITC-Dextran across human BrM compared with polymer, both with and without ARPE cells. 78
Figure 3.1: RPE Cell structure and Organelle Distribution 84
Figure 3.2: Subconfluent vs. confluent RPE cells. 92
Figure 3.3: Transwells ® [Corning, USA]) allow cell culture in media designed to resemble the apical and basal environments of *in vivo* epithelium. 93
Figure 3.4: Components of Transepithelial Electrical Resistance. 94
Figure 3.5: Principle of Sandwich ELISA. 98
Figure 3.6: Rabbit eye dissection to harvest primary rabbit RPE cells for culture 102
Figure 3.7: Method for measuring transepithelial electrical resistance using the EVOM2 (electrovoltohmmeter) and the STX2 electrode. 107
Figure 3.8: ARPE-19 cells stained with DAPI (blue) and Phalloidin (green) 110
Figure 3.9: Primary rabbit RPE cells stained with DAPI (nuclei = blue) and Phalloidin (actin filaments = green). 111
Figure 3.10: Standard curve for PEDF Sandwich ELISA assay. 112

Figure 3.11: Mean PEDF concentrations measured in the Transwells for ARPE-19 cells and Primary rabbit RPE cells, either with or without polymer. .. 113
Figure 3.12: Mean PEDF concentrations measured in the apical and basal chambers of the Transwells for ARPE-19 cells and primary rabbit RPE cells, either with or without polymer, one week after seeding. 115
Figure 3.13: Mean PEDF concentrations measured in the apical and basal chambers of the Transwells for ARPE-19 cells and primary rabbit RPE cells, either with or without polymer, four weeks after seeding. 116
Figure 3.14: Mean PEDF concentrations measured in the apical and basal chambers of the Transwells for ARPE-19 cells and primary rabbit RPE cells, either with or without polymer, eight weeks after seeding. 117
Figure 3.15: Bar chart comparing PEDF concentrations (average of all time points) in the apical and basal chambers of the Transwells. 118
Figure 3.16: Standard 'curve' for VEGF Sandwich ELISA assay. 119
Figure 3.17: Mean VEGF concentrations measured in the Transwells for ARPE-19 cells and primary rabbit RPE cells, either with or without polymer.... 120
Figure 3.18: Mean VEGF concentrations measured in the apical and basal chambers of the Transwells for ARPE-19 cells and primary rabbit RPE cells, either with or without polymer, one week after seeding. 121
Figure 3.19: Mean VEGF concentrations measured in the apical and basal chambers of the Transwells for ARPE-19 cells and primary rabbit RPE cells, either with or without polymer, four weeks after seeding. 122
Figure 3.20: Mean VEGF concentrations measured in the apical and basal chambers of the Transwells for ARPE-19 cells and primary rabbit RPE cells, either with or without polymer, eight weeks after seeding. *(error bars=SEM)* 123
Figure 3.21: Mean VEGF concentrations measured in the apical and basal chambers of the Transwells for ARPE-19 cells and primary rabbit RPE cells, either with or without polymer, across all time points. 124
Figure 3.22: Degree of polarisation of VEGF and PEDF secretion by rabbit RPE and ARPE-19 cells, with and without polymer, at all time points..... 125
Figure 3.23: Transepithelial Electrical Resistance Measurements of ARPE-19 and primary rabbit RPE cells, with and without polymer. 126
Figure 3.24: Time course for TEER development. 127
Figure 4.1: Instrumentation required during stages of subretinal surgery 134
Figure 4.2: Cytotoxicity of cohesive and dispersive ophthalmic viscoelastic devices to RPE cells..... 148

Figure 4.3: Photographs of the **POL**ymer **A**nd **R**PE **I**njector from **S**outhampton (POLARIS), Mark I. 149
Figure 4.4: Photographs showing failed ejection of a polymer (without cells) from POLARIS Mark I. 150
Figure 4.5: Photograph panel showing successful ejection of polymer (without cells) from POLARIS Mark II. 151
Figure 4.6: Image demonstrating that structural integrity of the 2mm diameter polymer disc was maintained even after ejection from POLARIS Mark II. 152
Figure 4.7: TUNEL assay of polymer ejected from POLARIS Mark II. 153
Figure 4.8: A bullet-shaped polymer segment, measuring 2mm x 1mm 155
Figure 4.9: Polymer damage following ejection from surgical instruments 156
Figure 4.10: Photographs showing cells remaining on polymer immediately after ejection from the Bonn-Shooter and POLARIS instruments. 157
Figure 4.11: Apoptotic cell death following ejection from the Southampton Injector (POLARIS) and the Geuder Injector (Bonn-Shooter), compared to unejected controls. 158
Figure 5.1: Number of pars plana vitrectomies performed in England, 2006-2014. 163
Figure 5.2: Initial steps of pars plana vitrectomy. 167
Figure 5.3: Cross-sectional illustrations showing the method for surgical inducing posterior vitreous detachment (PVD) in a human eye. 168
Figure 5.4: Schematic eyes for human and mouse 172
Figure 5.5: Schematic eyes of the human, mouse and rabbit. 174
Figure 5.6: The nictitating membrane of the rabbit eye 176
Figure 5.7: Photograph of the rabbit retina 178
Figure 5.8: Schematic showing perfusion fixation 187
Figure 5.9: Photographs of Perfusion Fixation 189
Figure 5.10: Photographs showing preparation before vitrectomy surgery 192
Figure 5.11: Photograph showing the Lang speculum 193
Figure 5.12: Photographs showing technique for globe proptosis 194
Figure 5.13: Photograph showing scleral ischaemia in a proptosed rabbit eye. 195
Figure 5.14: Photograph panel showing method for insertion of self-retaining 23-gauge cannulae in a human eye 196
Figure 5.15: Photographs illustrating stages in vitrectomy and subretinal implantation of polymer. 199
Figure 5.16: Light micrograph (10x) showing ESC-derived RPE monolayer on a 4mm disc of polymer, day 25 *in vitro*. 200
Figure 5.17: Histological results after fixation with 4% paraformaldehyde. 206

Figure 5.18: Histological results after fixation with Davidson's fixative 207
Figure 5.19: Histological results after fixation for either 24h or 48h with Davidson's fixative 209
Figure 5.20: Histology of normal rabbit eyes (Davidson's fixative, 6mm post-processing aperture, H&E stain) 210
Figure 5.21: Examples of histological artefact in normal rabbit eyes. 211
Figure 5.22: Examples of the retinal distortion that can occur following vitrectomy and submacular polymer implantation 212
Figure 5.23: Examples of histological results from rabbit eyes that had undergone vitrectomy surgery and subretinal implantation. 213
Figure 5.24: Photographs of polymer that has been exposed to Davidson's fixative and then undergone histological processing. 214
Figure 5.25: Verhoeff's staining of polymer and retina 215
Figure 5.26: Single example of polymer detection in the subretinal space 216
Figure 5.27: Results of perfusion-fixation with 4% PFA. 217
Figure 5.28: Examples of Rabbit OCT scan using the Zeiss Stratus OCT 218

List of accompanying materials

Reprint of the following publication is shown in the Appendix:

Alexander P, Thomson HA, Luff AJ, Lotery AJ. Retinal pigment epithelium transplantation: concepts, challenges, and future prospects. Eye (Lond) 2015 Aug;29(8):992-1002. doi: 10.1038/eye.2015.89. Epub 2015 Jun 5.

DECLARATION OF AUTHORSHIP

I, PHILIP ALEXANDER, declare that this thesis entitled “INNOVATIVE TECHNIQUES FOR RETINAL PIGMENT EPITHELIUM TRANSPLANTATION” and the work presented in it is my own and has been generated by me as the result of my own original research.

I confirm that:

1. This work was done wholly or mainly while in candidature for a research degree at this University;
2. Where any part of this thesis has previously been submitted for a degree or any other qualification at this University or any other institution, this has been clearly stated;
3. Where I have consulted the published work of others, this is always clearly attributed;
4. Where I have quoted from the work of others, the source is always given. With the exception of such quotations, this thesis is entirely my own work;
5. I have acknowledged all main sources of help;
6. Where the thesis is based on work done by myself jointly with others, I have made clear exactly what was done by others and what I have contributed myself;
7. Parts of this work have been published as:

   Alexander P, Thomson HA, Luff AJ, Lotery AJ. Retinal pigment epithelium transplantation: concepts, challenges, and future prospects. Eye (Lond) 2015 Aug;29(8):992-1002. doi: 10.1038/eye.2015.89. Epub 2015 Jun 5.

Signed: .....

Date: 10th August 2016

Acknowledgements

I am using this opportunity to express my gratitude to everyone who supported me throughout the course of this project. I make no apology at all that these acknowledgements run to over three pages in length.

I would like to express the deepest appreciation to my main supervisor Professor Andrew Lotery, clinician and researcher extraordinaire. He continually and persuasively conveys a spirit of adventure with regard to research, and demonstrates the importance of bridging the gap between research and patient care by allowing one to directly influence the course of the other. Without his supervision and extensive network of connections and collaborators, this work would not have been possible.

I would like to thank my two co-supervisors Dr Martin Grossel and Dr Heather Thomson, both of whom continue to supervise my project despite officially leaving academia. Martin has always been approachable and supportive and I am grateful that he continues to provide me with new perspectives for my project. Dr Heather Thomson left academia to become a clinician but continues to provide me with a great deal of encouragement and support by email, or by late night texts. I express my gratitude to Angela Cree, who ensured that every aspect of this project, be it academic, organisational or financial, ran as smoothly as possible. Both Heather and Angela are meticulous and I particularly appreciate their punctilious proof-reading of my thesis.

My particular thanks go to Mr Andrew Luff, who has been my clinical and surgical mentor for the last 4 years. His vast vitreoretinal knowledge and experience have been invaluable in tackling the surgical aspects of this project. His presence in the animal operating theatre was truly invaluable and I feel privileged to have worked with him and to consider him my friend.

My sincere thanks go to Jenny Scott and Helen “The Rabbit Whisperer” Griffiths. Both have been present for every animal vitrectomy we have performed. During these procedures, their care and diligence for both surgeon and patient were outstanding and they are first-rate scrub nurses, surgical assistants and anaesthetists. In addition, I am grateful to Jenny for teaching me so many laboratory techniques, and for providing a seemingly never-ending supply of ginger biscuits for when the going got tough.

I am grateful to Gareth Ward, a fellow doctoral student and our resident polymer chemist, who provided a constant supply of the polymer that has been so essential for both *in vitro* and *in vivo* studies.

For the animal work, thanks go to Yvonne Morrison, Theatre Manager at the Southampton Eye Unit, for sourcing all of the surgical equipment and for supporting my animal experiments despite her own personal reservations about vivisection. I am grateful to Amanda at the Spire Southampton Hospital for donating a fragmatome, and to the Nuffield Health Wessex Hospital for donating the vitrectomy machine. I am indebted to Cillairné O'Reilly for providing me with a constant supply of high-pressure medical air to drive the vitreous cutter. Thanks also go to Stuart Albright from Stat One Services, who recognised our particular needs and financial constraints and gave us substantial discount on the inverter and BIOM which have truly revolutionised our surgery. Thanks to Jenny Baltrop, Matron for Anaesthetics and Theatre Services at University Hospital Southampton, for providing us with a second-hand fully functioning motorised operating table for use with the rabbits, at a cost far less than the original purchase price of £50,000.

Many thanks to all in the Biomedical Imaging Unit (BIU), but particularly to Dr Dave Johnston for his advice on optimum methods for capturing intraoperative photographs and video. I am also grateful to Helena Lee, Academic Clinical Lecturer in Ophthalmology, for her expertise in trying to improve the quality of OCT scans in rabbit eyes.

My veterinary colleagues Dr Cameron Black, Dr Penny Courtney, and particularly Dr Neil Smyth, have provided much advice on how to anaesthetise and operate on patients that are smaller and furrier than those that I have previously encountered. I am particularly thankful to Neil for performing the neck dissections of rabbits undergoing perfusion fixation. I am grateful to my ophthalmology colleagues Dr Hari Jayaram and Professor David Charteris, both of the Institute of Ophthalmology, for allowing me to observe their technique for rabbit vitrectomy. I am also grateful to Dr Boris Stanzel and Dr Fabian Thieltges of the University of Bonn for sharing their experience with rabbit subretinal surgery. Thanks go to all the staff in the Biomedical Research Facility, including Richard Reid, Lesley Lawes, Caroline Mercer, Lorraine, Mike and the many technicians whose names I still don't know.

For histology of the rabbit eyes I am grateful to Sammy Reynolds for her initial advice, and to Helen Rigden, Jenny Norman and Jon Ward for their patience and expertise in developing an optimal method for fixing and sectioning.

For their expertise in graphics and digital illustration, I would like to thank Miguel Velasquez and Alan Morris, for their assistance with the pictures of RPE in this thesis.

I am truly indebted to Andy Luff of Sapphire Eye Care and Christian Fallon, previously of QFX trader, who generously sponsored my studentship. Without their financial support I would have been unable to undertake this project. I was privileged to be awarded the Fellowship Project Award by the Global Ophthalmology Awards Programme (GOAP) from Bayer. Rabbits and their upkeep are expensive but the GOAP grant provided sufficient funding for all of the consumables related to this project. Many of the team from Bayer, including Sebastian Schwerdt and Maria Bell, have been very encouraging and kindly allowed me to present my work at the GOAP ceremony in 2014. I am also grateful to the Brian Mercer Charitable Trust, who provided funding for the initial part of this research, and to the De Lazlo Foundation for providing a travel grant that allowed me to attend the ARVO conference in 2014.

I express my utmost gratitude to my clinical mentors. Mr Parwez Hossain supported my part-time appointment as a Clinical Research Fellow in the Eye Unit in Southampton, which enabled me to maintain my clinical and surgical skills during the period of my research. I was privileged not only to be able to work with Mr Chris Canning between May 2013 and May 2014, but then to take on the role of Locum Consultant Vitreoretinal Surgeon from June 2014. Since April 2015, I have been working as a Senior Fellow in Vitreoretinal Surgery at Moorfields Eye Hospital, working with Professor Lyndon da Cruz. On 11th August 2015, I was privileged to be the second surgeon on the world's first RPE/BrM transplantation into a patient with AMD. The second patient underwent transplantation in October 2015.

I am grateful to my friends, particularly to Mr Nainglatt Tint and Mr Phil Banerjee, for their wisdom on how to maintain balance between research, clinical work, and home life.

My parents, both doctors, have instilled in me the love for learning, and allowed me to witness first-hand the benefits and rewards of dedication and discipline. My successes throughout life are in fact their successes. My failures are my own.

My daughters Rebecca and Sophia, and my son Joseph who was born during this period of research, have contributed more than they will ever know. Their smiles, laughter and fun-loving nature make them the joy of my life, and they have seen me through both good times and bad, and not just over the course of this project.

But my most sincere gratitude goes to my wife Chinnu, for her encouragement, patience, tolerance, and love. Without her support, this work would have been impossible. I dedicate this thesis to her.

Definitions and Abbreviations

AGE	**A**dvanced **G**lycation **E**nd product
AIDS	**A**cquired **I**mmuno**d**eficiency **S**yndrome
AM	**A**mniotic **M**embrane
AMD	**A**ge-related **M**acular **D**egeneration
ARPE-19	A Human **A**dult **R**etinal **P**igment **E**pithelium cell line
BrM	**Br**uch's **M**embrane
CNV	**C**horoidal **N**eo**v**ascularisation
DAPI	4′,6-**di**a**i**midino-2-**p**heny**l**indole
DNA	**D**eoxyribo**n**ucleic **a**cid
ELISA	**E**nzyme-**l**inked **i**mmuno**s**orbent **a**ssay
ESC	**E**mbryonic **S**tem **C**ell
FBS	**F**oetal **b**ovine **s**erum
Healon	Cohesive OVD – 1.0% sodium hyaluronate (MW 4 million Da)
Healon-GV	Cohesive OVD – 1.4% sodium hyaluronate (MW 5 million Da)
HIV	**H**uman **I**mmunodeficiency **V**irus
HPMC	**H**ydroxy**p**ropyl**m**ethyl**c**ellulose
IPE	**I**ris **P**igment **E**pithelium
iPSC	**I**nduced **P**luripotent **S**tem **C**ell
LDH	**L**actate **D**e**h**ydrogenase

mRNA	**M**essenger **R**ibo**n**ucleic **A**cid
OCT	**O**ptical **C**oherence **T**omogram
OVD	**O**phthalmic **V**iscoelastic **D**evice
PBS	**P**hosphate **B**uffered **S**aline
PEDF	**P**igment **E**pithelium **D**erived **F**actor
PEGM	**P**oly (**e**thylene **g**lycol) **m**ethacrylate
PFA	**P**araformaldehyde
PIL	**P**ersonal animal **L**icence awarded by the Home Office
PMMA	**P**oly(**m**ethyl **m**eth**a**crylate)
POLARIS	**Pol**ymer **A**nd **R**PE **I**njector - **S**outhampton
Polymer	Unless otherwise specified, the term 'polymer' in this thesis refers to 60:40 P(MMA-co-PEGM-succinimidyl carbonate)
PPV	**P**ars **P**lana **V**itrectomy
PVD	**P**osterior **V**itreous **D**etachment
RPE	**R**etinal **P**igment **E**pithelium
rt	**Room temperature**
TEER	**T**rans**e**pithelial **E**lectrical **R**esistance
VEGF	**V**ascular **E**ndothelial **G**rowth **F**actor

Chapter 1: INTRODUCTION

1.1 Eyes are important and expensive

Eyes are important. Eyes are responsible for vision which, rightly or wrongly, is widely regarded as the most important of the five senses.[1] Loss of vision is associated with acute and significant psychopathology, even when compared with loss of other senses such as hearing.[2] In a 2014 survey of Americans, blindness ranked among the top four "worst things that could happen to you" for all respondents, alongside cancer, Alzheimer's disease and HIV/AIDS.[1]

Sound is a two-way process, and therefore a communication tool, in a way that vision is not – humans cannot emit light in the way that they emit sound. However, much non-verbal communication comes from how we listen and express ourselves through our eyes. Pupil size, blink rate, gaze direction and movement of the eyelids and eyebrows all send clear non-verbal messages. Our eyes can reflect our mood, and to a certain degree, our health and wellbeing.

The value of the eye is evident from the observation that it has evolved independently more than once. Both cephalopods and humans have independently developed camera-type eyes consisting of an iris, lens, vitreous cavity, photoreceptor cell and pigment cell. [Of interest, humans have an inverted retina, which is sometimes thought to be inferior in design to the cephalopod eye].[3] Although eyes are valuable, they are also metabolically expensive. Photoreceptors are the most metabolically active tissue in the body.[4] The observation that cave animals have poor vision has long been attributed to the scarcity of food in subterranean habitats, and the high energetic cost of neural tissue. Moran *et al.* have recently quantified the metabolic cost of vision in Mexican cavefish, and estimated vision to be responsible for 15% of the resting metabolism of a young fish.[5] Eyeless cavefish require 30% less brain mass than cavefish that possess eyes.[5]

The influence of eyes on the development of the head was first described by the Greek physician Galen, who lived in the 2nd century, and then again by Vesalius in 1543, in his book "De Humani Corporis Fabrica" [meaning The Fabric of the Human Body].[6] It had been noted that animals that did not possess a head, such as crabs, beetles and lobsters, had eyes on long processes. Since humans did not possess the hard

"testaceous" skin of these animals, eyes on long processes would not be without danger. However eyes need to have an elevated position, and it was not possible for eyes to be attached to bare necks. Therefore,

> *Nature was willing neither to prevent the use of eyes nor to diminish their safety, she built a lofty part [cavitas orbitale] that also nicely protected the eyes from danger.*

Therefore the head was formed for the sake of the eyes. Since the brain should not be too far from the eyes, the brain was also located in the head. The organs of smell, hearing and taste were located in the head because they needed to be close to the brain.[6]

Eyes are important indeed.

1.2 Structure of the Human Eye

The eye is an organ of photoreception. Specialised nerve cells in the retina, known as photoreceptors, convert light energy from the outside world to an electrical signal, which in turn can be relayed via the optic nerve to the brain, where information is processed and then consciously appreciated as vision. The retina is, therefore, the most important structure in the eye, and all other eye structures serve to enhance and support the basic physiological process of photoreception, either by focus and transmission of light (e.g. cornea, lens, iris) or by nourishment of ocular tissue (e.g. choroid, aqueous, lacrimal apparatus). The structure of the eye is shown in Figure 1.1.

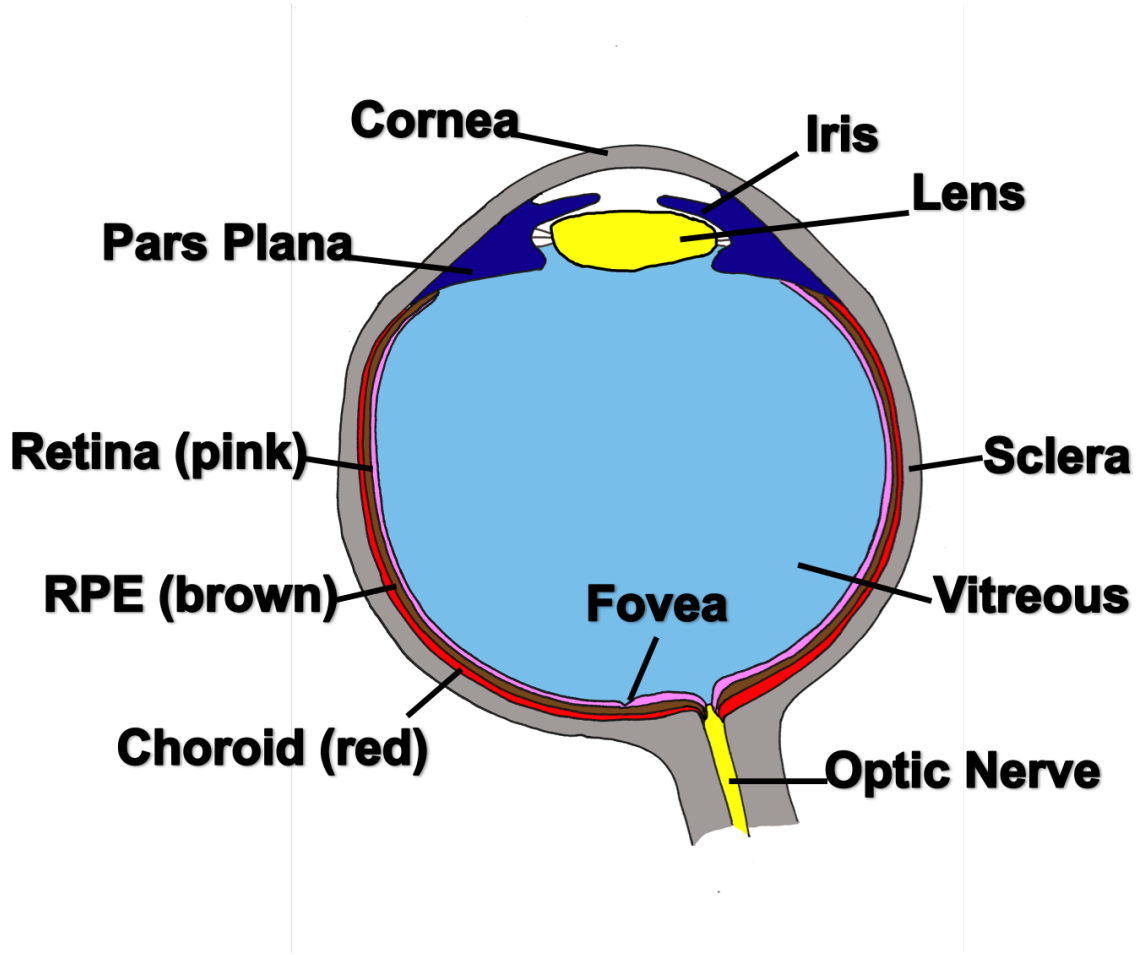

Figure 1.1: Structure of the human eye.

The retina lines the inside of the posterior eye wall. It has two primary layers, the neurosensory retina and the retinal pigment epithelium (RPE), both of which are embryologically derived from neuroectoderm. Invagination of the optic vesicle leads to

formation of the double-layered optic cup, of which the inner layer becomes the neurosensory retina, whilst the outer layer becomes RPE. In the adult eye, the neurosensory retina remains in apposition with the RPE but is only firmly attached at its anterior edge (the ora serrata) and at the margins of the optic nerve head. Figure 1.2 shows a photograph of a normal ocular fundus. Figure 1.3 shows a cross-sectional image of the centre of the retina, known as the macula, obtained using Optical Coherence Tomography scanning.

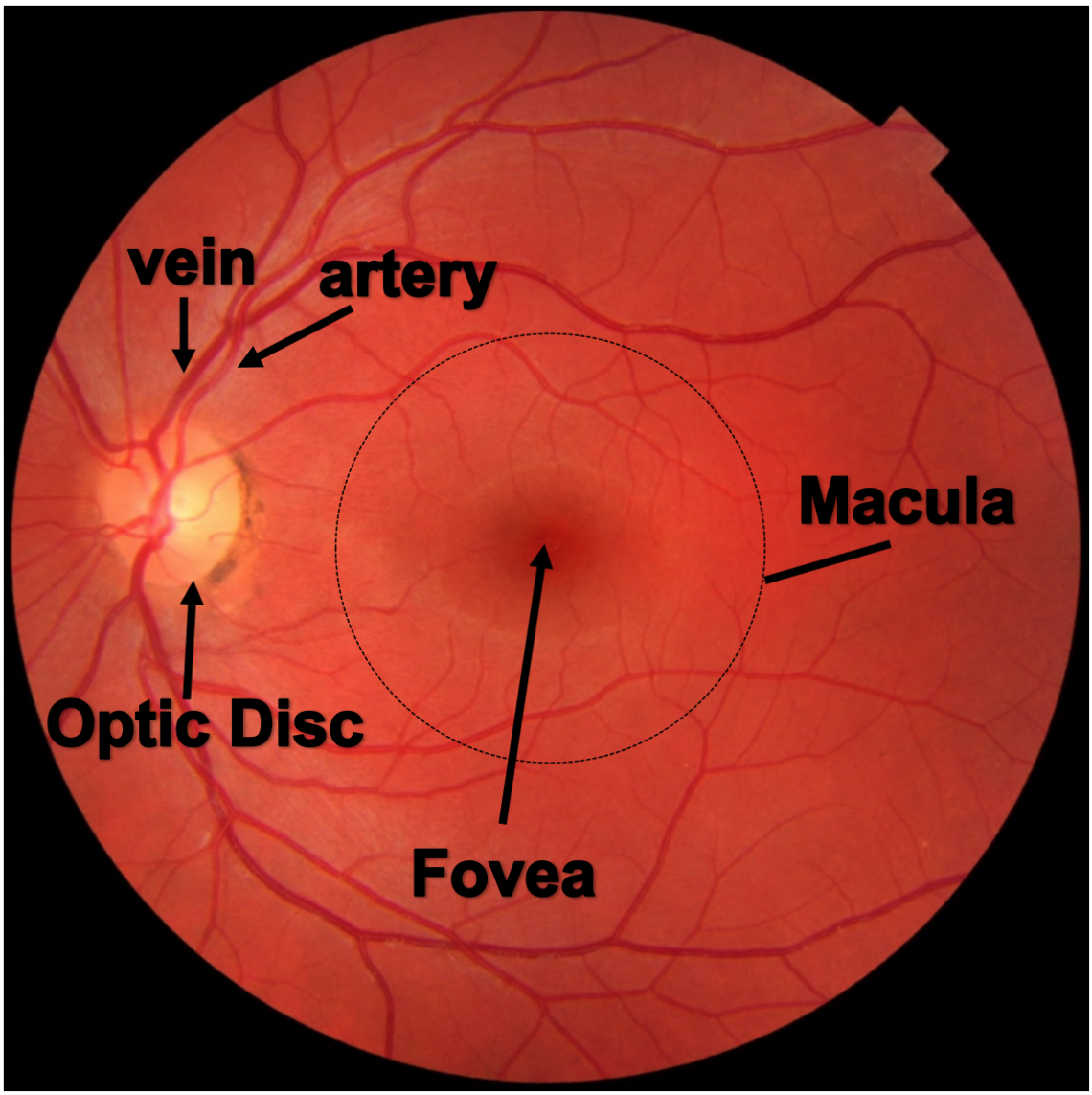

Figure 1.2: Normal fundus photograph of the left eye.

The ocular fundus is the interior surface of the posterior segment of the eye, and includes the optic disc, retina, BrM and choroid. The outer retina is supplied by the choroidal circulation. The retinal circulation, which is

supplied by the central retinal artery, a branch of the ophthalmic artery, supplies only the inner retina. Retinal veins are darker and slightly wider than retinal arteries. The macula can be defined histologically as the area of the retina that has two or more layers of ganglion cells. The centre of the macula is the fovea. Confusingly, in clinical practice the term 'macula' often refers to the anatomical fovea. Image courtesy of Moorfields Eye Hospital.

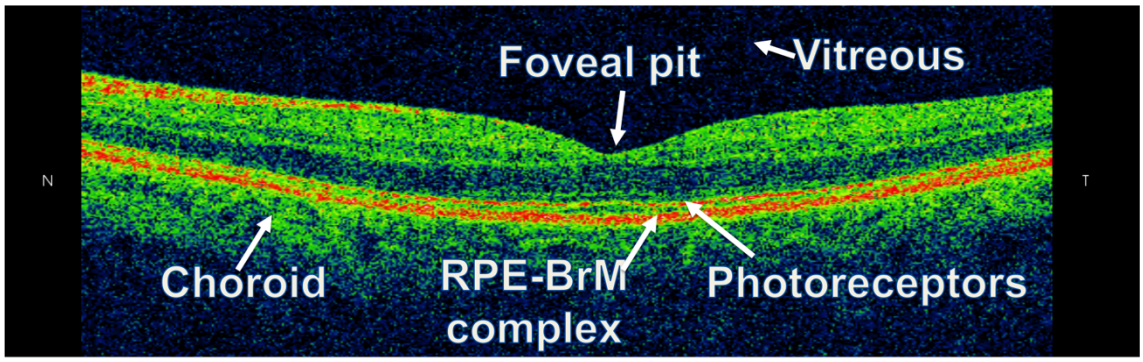

Figure 1.3: OCT scan of a healthy macula

OCT scanning is a non-invasive test that allows rapid cross-sectional imaging of the macula. This has revolutionised the diagnosis, treatment and monitoring of patients with AMD and other macular disorders. Taken with Topcon OCT 1000. Image courtesy of Moorfields Eye Hospital.

The metabolic activity of the retina correlates with its blood supply. Photoreceptors are the most metabolically active cells in the human body[7] and together with the RPE receive their blood supply from the choroid. The inner two-thirds of the retina is much less metabolically demanding and is supplied by the retinal circulation.

1.3 Photoreceptor cells are responsible for vision

The photoreceptors are situated in the outermost layer of the neurosensory retina, and are classified as rods or cones. In a typical human eye there are 115 million rods, which are responsible for sensing contrast, brightness and motion, and 6.5 million cones, which allow fine resolution, spatial resolution, and colour vision. The macula is the central part of the retina and its extent is defined by a ganglion cell layer that is at least 2 cells thick. The fovea, a depression at the centre of the macula, is responsible

for fine vision, and has a photoreceptor population that consists exclusively of cones. However, the parafoveal region is rod-dominated. Considering the eye as a whole, rods outnumber cones 20:1, but within the young adult macula, rods outnumber cones 9:1, and the macula can therefore be considered cone-enriched but not cone-dominated.[8]

Each photoreceptor cell has a long and narrow configuration. The cell body lies within the outer nuclear layer of the retina, and axons pass into the outer plexiform layer, where they form synaptic terminals (either cod pedicles or rod spherules) with other cell types such as bipolar or horizontal cells. The inner and outer segments of the cell, which are joined by a connecting stalk consisting of a modified cilium, lie on the outer side of the cell body. The outer limiting membrane separates the photoreceptor nucleus from the inner and outer segments of the cell.

The outer segment contains discs of visual pigment, a G protein coupled receptor that consists of a protein, known as opsin, which is covalently bound to a Vitamin A, derived chromophore, 11-cis-retinal.[9] Absorption of photons leads to isomerisation of the chromophore from 11-cis-retinal to all-trans retinal, which in turn induces the pigment to change into its physiologically active metarhodopsin-II state. In the resting state, the dark currents produced by open non-selective cGMP-gated cation channels are accompanied by high levels of neurotransmitter release at the photoreceptor's synaptic junction with the bipolar cells. The activated visual pigment molecule triggers a transduction cascade, ultimately resulting in closure of the cation channel in the photoreceptor outer segment, leading to hyperpolarisation of the photoreceptor. Therefore, in light there is a decrease in neurotransmitter release, altering the transmission of electrical potentials in bipolar cells.

Photoreceptors are unable to reisomerise all-*trans*-retinal, formed after photon absorption, back into 11-*cis*-retinal.[7] Therefore, to maintain its own excitability, the photoreceptor is reliant on another cell type that forms a simple (i.e. single cell thickness) epithelium and lies in apposition with the outer segments in the interphotoreceptor matrix: The Retinal Pigment Epithelium (RPE).

1.4 Retinal Pigment Epithelium in Health and Disease

The RPE consists of a monolayer of cells that are cuboidal in cross section, and hexagonal when viewed from above. The cells are joined together by tight junctions (zonulae occludens) that block the free passage of ions and water; the RPE is therefore the second site of the blood retinal barrier (the first site being the capillary endothelium of the retinal vessels). Figure 1.4 illustrates the anatomy of the healthy RPE monolayer in cross-section, and demonstrates its relationship with the choroid and with the photoreceptors of the outer neurosensory retina.

The most important function of the RPE is the regeneration of bleached rhodopsin, which occurs in the RPE cell cytosol. During phototransduction, photons of light cause the conversion of 11-*cis*-retinal to all-*trans*-retinal, which is then released from the photoreceptor into the interphotoreceptor matrix. The all-*trans*-retinal then enters the RPE independent of outer segment tip phagocytosis, and is converted back to 11-*cis* retinal by retinol isomerase, an enzyme that is unique to the RPE.

Functions of the RPE
Visual cycle
Spatial buffering of ions in the subretinal space
Phagocytosis
Secretion
Transepithelial transport
Absorption of light and protection against photooxidation
Blood retinal barrier

Table 1.1: Functions of the Retinal Pigment Epithelium

The RPE cell has long and short microvilli on its apical surface. Long microvilli (5-7μm) maximise the surface area for epithelial transport, whilst short microvilli form photoreceptor sheaths that allow phagocytosis of the photoreceptor outer segments. Proteins on the apical cell surface are those that would be typically expressed basolaterally in other epithelia, including N-CAM (a cell adhesion molecule) and EMMPRIN (extracellular matrix metalloproteinase inducer) and these are likely to be involved in photoreceptor adhesion and phagocytosis respectively.

The outer retina lies within an oxygen-rich environment. Perfusion of the choroid is 1400ml/min/100g of tissue, which is higher than the kidney; oxygen saturation of choroidal venous blood is 90%, suggesting very little O2 extraction during flow through choriocapillaris. Photo-oxidation (i.e. oxidation occurring due to the presence of light) can lead to oxidative damage of the outer retina, especially because of the reactive oxygen species generated from the phagocytosis by the RPE of the photoreceptor outer segments. However, the RPE provides three lines of defence against oxidative damage. Firstly, the RPE has melanin-containing melanosomes that, in conjunction with the photoreceptor pigments lutein and zeaxanthin, absorb light. Secondly, the RPE contains a number of antioxidants, both enzymatic (e.g. superoxide dismutase, and catalase) and a number of non-enzymatic antioxidants including lutein, zeaxanthin, melanin, ascorbate, alpha-tocopherol and beta-carotene. Thirdly, the RPE is able to repair DNA, lipids and proteins that have been damaged by oxidative stress.

The polarity of the RPE cell is essential for it to be an ion-transporting epithelium. The intercellular tight junctions establish a strong barrier between the subretinal space and the choroid, such that paracellular resistance is 10 times higher than transcellular resistance. The high metabolic activity of the photoreceptors leads to the generation of a large amount of water and the eye's intrinsic pressure (the intraocular pressure) causes a net flow of water through the retina from the vitreous. By transporting ions and water from its apical side to its basolateral surface, the RPE cell ensures the removal of water from the subretinal space but also establishes an adhesive force between the retina and the RPE. The constant requirement for removal of water from the retina is fulfilled by the RPE's ability to transport water and ions from its apical side to its basolateral surface.

Whilst electrolyte and water transport occurs from the subretinal space to the choroid, the RPE also transports glucose and other nutrients in the opposite direction, from the choroid to the photoreceptors, and therefore has large numbers of glucose transports GLUT1 and GLUT3 in both the apical and basolateral surfaces. Vitamin A (all-trans-retinol) uptake from the choroid occurs through the basolateral RPE surface, before being isomerised and then delivered to photoreceptors. Docosahexanoic acid, a fatty acid that cannot be synthesised by neuronal tissue but is essential for new photoreceptor outer segments, is preferentially taken up by the RPE from the blood stream for delivery to photoreceptors.

The RPE produces a number of growth factors that are essential for the structural integrity of the neurosensory retina, and for supporting the choroid. Pigment Epithelium Derived Factor (PEDF) is secreted from the apical surface and not only has a neuroprotective effect, by preventing glutamate- or hypoxia-induced apoptosis, but is also antiangiogenic and thereby prevents endothelial cell proliferation. Vascular Endothelial Growth Factor (VEGF) is secreted from the basal RPE surface where it prevents choroidal endothelial cell apoptosis. The RPE also secrete factors that suppress CD4 and CD8 T cell activity, thereby contributing to immune privilege in the eye.

The functions of the RPE have been considered with respect to a single cell. However, when considering the RPE as a layer, it is clear that its ability to perform its many functions is reliant on two factors. Firstly, the RPE layer must be a confluent monolayer, with intercellular tight junctions. Secondly, the cells must be polarised. Both of these factors are therefore reliant on the RPE basement membrane, which itself is a single layer of a pentalaminar structure that underlies the RPE: Bruch's Membrane.

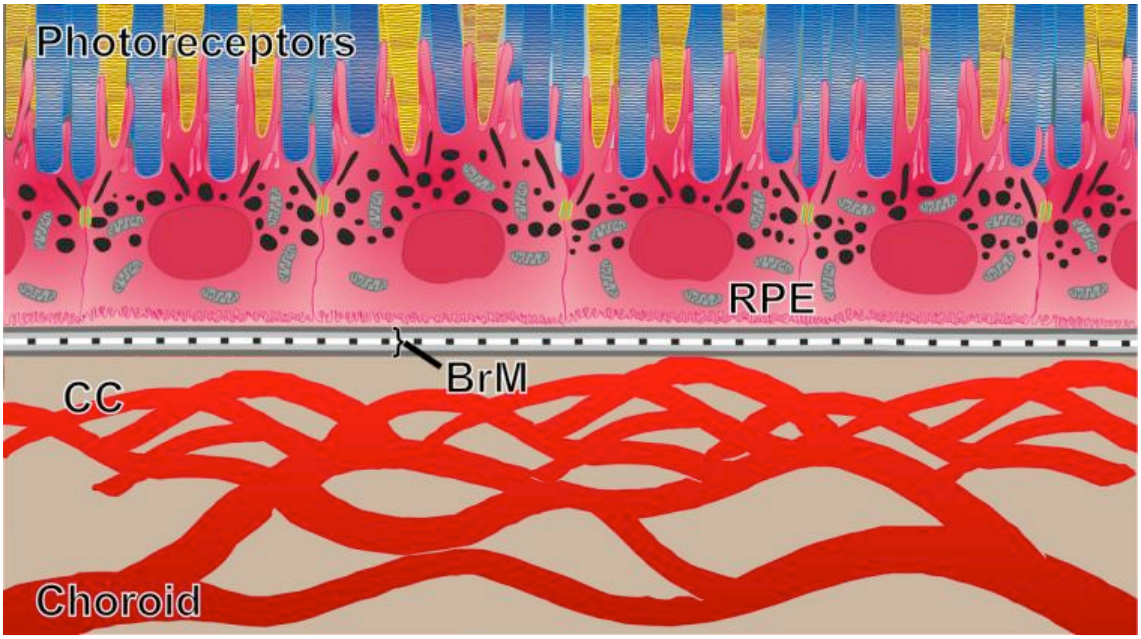

Figure 1.4: Healthy RPE

Healthy RPE exists as a polarised monolayer with tight junctions (green). Melanin is located in the apical cytoplasm and acts to absorb scattered light, thereby improving the optical quality of the eye. Microvilli on the apical RPE membrane interdigitate with the photoreceptors (rods shown in blue; cones shown in yellow). Microvilli allow phagocytosis of the shed photoreceptor outer segments and recycling of the visual pigments. The tight junctions ensure that the RPE can maintain its function as the outer blood retinal barrier. Bruch's membrane (BrM) is a pentilaminar structure; the innermost layer of BrM is formed by the basement membrane of the RPE. The outer layer of BrM is formed by the basement membrane of the choriocapillaris (CC). Breaches of BrM lead to growth of choroidal vessels into the sub-RPE and subretinal space, known as choroidal neovascularisation.

1.5 Bruch's Membrane

Bruch's Membrane (BrM) is acellular. Its histological structure was first described in 1961 by Hogan, who identified 5 distinct layers[10]: RPE basement membrane, inner collagenous layer, elastin layer, outer collagenous layer, and the basement membrane of the choriocapillaris.

The basement membrane of the RPE is approximately 0.14μm thick[11] and is similar to the choriocapillaris basement membrane. Both basement membranes contain collagen type IV, fibronectin, laminin, heparin sulphate and chondroitin/dermatan sulphate. Additionally, the choriocapillaris basement membrane contains collagen type VI, which is the product of pericytes and acts to anchor fenestrated capillaries to the choroid.

The inner collagenous layer is 1.4μm thick and consists of a grid of collagen types I, III and V, embedded in glycosaminoglycans, and components of the coagulation and complement systems. Type I collagen provides tensile strength to the tissue, Type III is normally present in tissues with elastic properties, and Type V collagen acts to anchor basement membranes. The outer collagenous layer is similar but is slightly less thick. Between the two collagenous layers lies the 0.8μm thick elastin layer, consisting of multiple layers of elastin fibres that are frequently crossed by the collagen fibres of the inner and outer collagenous layers.

BrM has three main functions:

- to regulate diffusion between RPE and choroid
- to provide physical support for RPE adhesion, migration and (perhaps) differentiation
- to create a barrier between retina and choroid and therefore prevent cellular migration from one tissue to the other.

1.5.1 Diffusion Regulation

Since the BrM is acellular, diffusion across BrM is passive and dependent upon the molecular composition, which in turn depends on both age and location within the retina. Starita *et al.* have shown that water conductivity depends on pore size.[12] Diffusion of molecules depends not only on hydrostatic pressure on each side of BrM, but also on the concentration of specific molecules. A number of molecules (as outlined above) pass from the choroid to the RPE and are essential for normal functioning of the outer neurosensory retina. Waste products that pass from RPE to choroid include carbon dioxide, water, ions, oxidised lipids and oxidised cholesterol.

Using Ussing chambers, Moore *et al*.[13] and Starita *et al*.[14] have demonstrated an age-related decrease in water conductivity, which tends to occur early in life long before any BrM debris can be visualised.

1.5.2 RPE Cell Adhesion, Migration and Differentiation

BrM from young donors is far better at allowing attachment of RPE cells than BrM from older donors. Integrins are a group of RPE basal membrane proteins that kind bind to a number of BrM components such as laminin isoforms and type IV collagen[15], in “anchoring plaques”, and RPE cells made to over-express integrins in culture show more adhesion to BrM than normal RPE cells.[16]

In humans, the RPE continues to develop until six months after birth, but is then considered post-mitotic,[17] although it is recognised that mechanical or light induced damage can induce RPE cell proliferation for large defects; small defects tend to heal by RPE migration. In vitro wound healing is impaired by integrin inhibition. Studies in cats, pigs and monkeys have shown that RPE can resurface intact BrM, usually as a monolayer, but resurfacing is incomplete on damaged aged human submacular BrM, demonstrating the importance of healthy BrM to RPE wound healing.[18]

1.5.3 Physical Barrier

The outer blood-retinal barrier is formed by RPE intercellular tight junctions, and is supported by BrM, which acts as a semi-permeable molecular sieve. Despite this physical barrier, however, inflammatory cell migration through pores in BrM, and between RPE cells, can occur without apparent physical disruption of the RPE cell layer.[19]

1.6 Age Related Macular Degeneration

Despite its myriad unique metabolic processes, primary RPE dysfunction is an uncommon cause of eye disease.[20] Single gene disorders affecting the RPE include those arising from mutations in lecithin retinol acyltransferase (LRAT) [21, 22], RPE 65 [23, 24], MerTK [25] or bestrophin[26]. Primary photoreceptor dysfunction, leading to secondary RPE atrophy, is more common. However, more important in terms of visual morbidity is the role of the RPE in the modulation of complex disease processes such as inflammation and neovascularisation.

Age-related macular degeneration (AMD) is the leading cause of visual impairment in the Western world for people over the age of 50.[27] The prevalence increases with age, and AMD affects up to one third of those aged over 75.[28] AMD is characterised by progressive deterioration of the RPE-BrM-choriocapillaris complex, leading to subsequent damage of photoreceptor cells. The primary locus of damage remains contentious but is thought to be the RPE cell rather than BrM.[29] A schematic diagram showing the pathological changes of the RPE and BrM in AMD is shown in Figure 1.5.

Clinical features of AMD are shown in Figures 1.6 and 1.7 and include:

- Drusen, which are discrete white/yellow spots that are external to the retina and RPE.
- Areas of outer retinal hyperpigmentation associated with drusen.
- Areas of RPE hypopigmentation, often more sharply demarcated than drusen without any visibility of choroidal vessels associated with drusen.

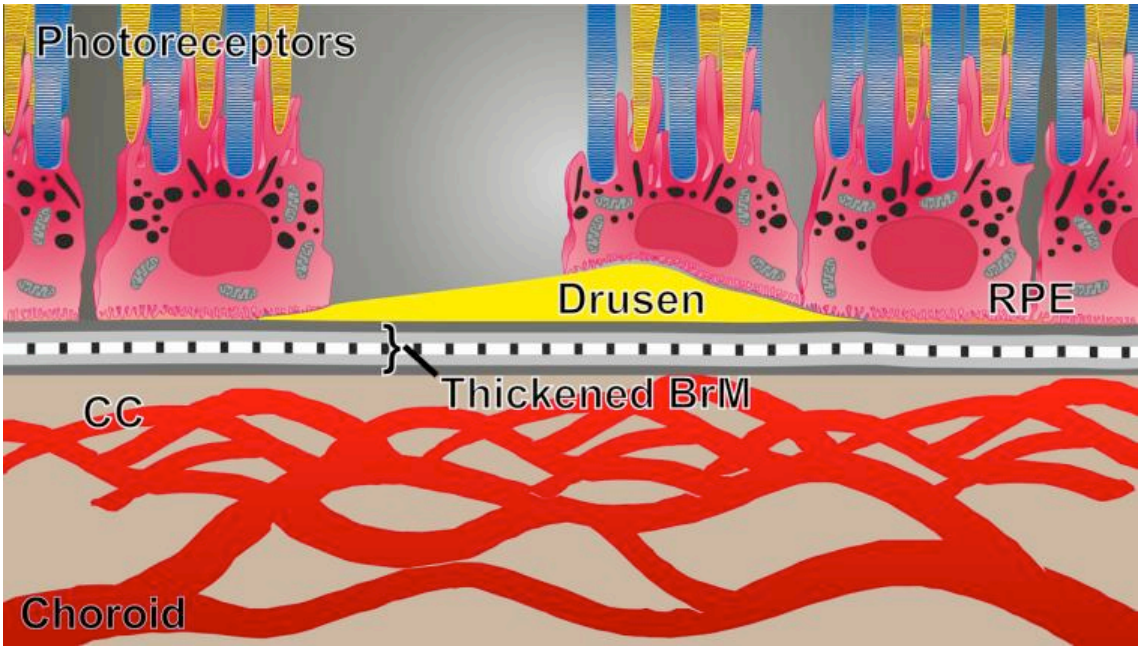

Figure 1.5: RPE degeneration in AMD

BrM is thickened, impairing diffusion between the choriocapillaris and the neurosensory retina. Drusen are clinically visible deposits that occur beneath the RPE. RPE cell death occurs, and there is loss of tight junctions between the remaining RPE cells, resulting in a discontinuous cell layer. These changes all lead to secondary photoreceptor cell loss, resulting in visual impairment.

Late AMD is usually associated with visual loss. It can be divided into “dry” and “wet” forms:

- Dry AMD, also known as geographic atrophy, is characterised by sharply defined areas of depigmentation/absent RPE in which choroidal vessels are more visible than the surrounding areas.

- Wet AMD, also known as neovascular AMD, is characterised by the growth of abnormal vessels originating from the choroid. This process is known as choroidal neovascularisation. Growth of abnormal blood vessels originating within the retina, known as Retinal Angiomatous Proliferation, has also been identified in a subset of patients with neovascular AMD.

Several groups have proposed classification systems of AMD, and it is likely that classification systems will be continually refined as imaging technology improves.[30] Until recently, the most universal classification, proposed by Bird *et al.* in 1995,[31] distinguished between early and late stages of Age-Related Maculopathy (ARM). Recently, a consensus committee has abandoned use of the term "ARM" and has produced a new clinical classification for AMD.

Classification	**Definition (lesions assessed within 2 disc diameters of fovea in either eye)**
No apparent ageing changes	No drusen *and* No AMD pigmentary abnormalities
Normal ageing changes	Only drupelets (small drusen ≤63μm) *and* No AMD pigmentary abnormalities
Early AMD	Medium drusen >63μm and ≤125μm *and* No AMD pigmentary abnormalities
Intermediate AMD	Large drusen >125μm *and/or* Any AMD pigmentary abnormalities
Late AMD	Neovascular AMD and/or Any geographic atrophy

Table 1.2: Classification of AMD.

Based on Ferris *et al.* (2013). Ophthalmology 120:844–851.[32]

Recent advances in anti-Vascular Endothelial Growth Factor (anti-VEGF) therapy for AMD have revolutionised the management of patients with neovascular AMD (nvAMD).[33, 34] However, initial enthusiasm for this therapy has been dampened by the observation that up to one fifth of patients treated will develop geographic atrophy,[35] resulting in visual impairment due to photoreceptor cell loss. Therefore, therapy to combat the development of dry AMD as well as nvAMD is needed. At present there is no effective treatment for dry AMD, which is the more prevalent form of the disease.[36] As the primary pathogenic process in AMD appears to occur within the RPE, a logical approach would be to repair the RPE via either transplantation or translocation of RPE cells.

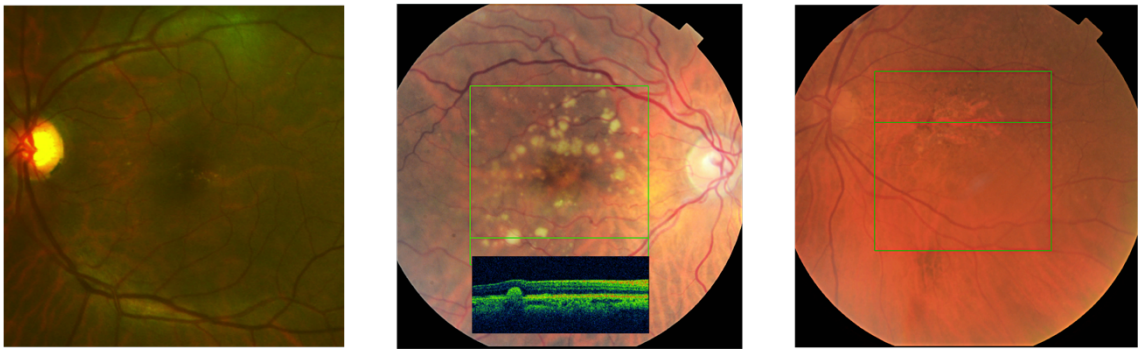

Figure 1.6: Clinical photographs of Dry AMD.

Left photograph: Early AMD. Optos widefield photograph showing fine drusen.

Middle photograph: Intermediate AMD. Soft drusen at the macula are seen as yellow spots in the central retina. These drusen are larger than 125µm (the diameter of the retinal vein as it emerges from the optic disc). These drusen are therefore classified as 'large'. Inset image showing an OCT scan through a druse, which are typically located beneath RPE and BrM.

Right photograph: Late AMD - geographic atrophy affecting the fovea.

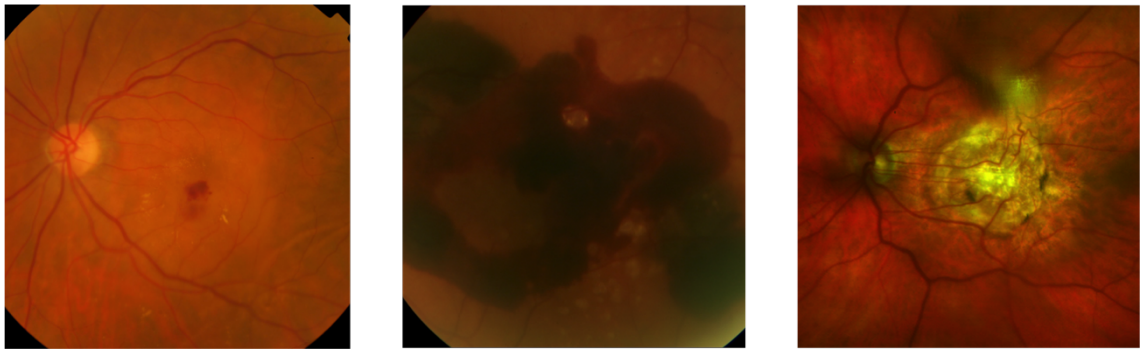

Figure 1.7: Clinical photographs of Neovascular ("Wet") AMD.

Left photograph: Active neovascular AMD. Abnormal blood vessels from the choriocapillaris, known as choroidal neovascularisation, have caused bleeding, exudation, and retina swelling. This patient is amenable to treatment with intravitreal anti-VEGF therapy.

Middle photograph: Severe widespread subretinal and subepithelial haemorrhage. This patient would be a candidate for surgery, to allow displacement of the haemorrhage away from the fovea.

Right photograph: Disciform scar due to untreated neovascular AMD. The central retina is dead and the white/yellow area visible is sclera and choroidal vessels. The disease will not respond to intravitreal anti-VEGF therapy.

1.7 Innovative therapeutic solutions for Retinal Degeneration

The have been a number of innovative therapeutic approaches for patients with retinal degeneration.

- Gene therapy involves incorporation of new DNA into retinal cells via a carrier vector, to either replace a diseased or non-functioning gene, or to silence the expression of a mutated gene. It is of most benefit in monogenic disorders such as Leber's Congenital Amaurosis[37] and Choroideremia[38] but is less beneficial for AMD, which has a polygenic origin and a pathogenesis arising from a complex interplay between genetic and environmental factors.

- Optogenetics is an off-shoot of gene therapy and utilises a vector to deliver a novel gene to the inner retina. Since photoreceptor degeneration usually precedes inner retinal degeneration, expression of the novel gene coding for a light-activated channel can render the inner retinal cells photosensitive, bypassing the need for photoreceptor input.[39]

- Electronic implants can be subretinal, epiretinal, suprachoroidal or cortical visual prostheses. The Argus-II Retinal Prosthesis System is the first and currently the only prosthetic vision device to obtain regulatory approval in both Europe and the USA.[40] It has a robust safety profile and has been shown to improve visual function,[41] but the resolution and visual field provided by the prosthesis remains limited. The device is currently being evaluated in patients with AMD.[42]

- Retinal rejuvenation, using a nanosecond laser treatment, is able to reduce drusen load and improve BrM structure, while maintaining integrity of the neurosensory retina. These changes persist for at least 2 years after treatment and this may have potential in reducing progression in patients with dry AMD.[43]

- Cellular replacement, in the form of RPE and/or photoreceptor transplantation.

1.8 RPE Transplantation

Human RPE cells were first isolated and characterised over 30 years ago.[44-46] RPE cell structure and function are well understood, the cells are readily sustainable in culture under laboratory conditions, and unlike other cell types within the retina, RPE cells do not require synaptic connections to perform their role. These factors, together with the relative ease of imaging with ophthalmoscope and Optical Coherence Tomography (OCT) scanning, make RPE cells an attractive target for cell transplantation compared to other cell types in the retina or central nervous system. Compared to other forms of cell replacement therapy, the number of cells required for a given lesion site is relatively small.[47] RPE replacement would prevent secondary photoreceptor degeneration, thereby preserving visual function.

Seminal experiments by Li & Turner used the Royal College of Surgeons (RCS) rat, an animal model of retinal dystrophy, to demonstrate proof of principle of RPE transplantation.[48] The inherited retinal degeneration within the RCS rat was first discovered in 1938 but it was only in 1962 that Dowling and Sidman discovered an accumulation of outer segments on electron microscopy, suggesting abnormal phagocytosis by the RPE.[49] In 2000, D'Cruz *et al*. discovered that the RCS strain had a defect in the *merTK* gene and is therefore unable to produce RPE cells that phagocytose shed rod outer segments; this results in photoreceptor death and degeneration of the neurosensory retina within two months.[25] However, Li & Turner demonstrated that subretinal injection of healthy RPE cells allows preservation of the outer nuclear, outer plexiform, and photoreceptor layers.[48] Since then, successful RPE transplantation has also been demonstrated in RPE65 knockout mice that are unable to isomerise all-*trans*-retinal to 11-*cis*-retinal.[50]

Surgical strategies to allow RPE transplantation in humans arose primarily due to the absence of effective treatments for nvAMD prior to the development of anti-VEGF intravitreal injections. Submacular surgery aimed to remove the subfoveal choroidal neovascular membrane (CNV) and any associated haemorrhage, and the first randomised controlled trial to evaluate this technique, the Submacular Surgery Trial, was initiated in 1998. However the visual outcomes were poor and this disappointing result was attributed to mechanical removal of the RPE at the time of CNV excision.[51]

Since then, three approaches to RPE transplantation have been attempted:

(1) Macular translocation
(2) Autologous RPE-Choroid Patch graft
(3) Subretinal injection of a suspension of autologous RPE cells

1.8.1 Macular translocation

Macular translocation is a procedure in which the neurosensory retina is surgically detached, rotated and reattached so that the macula, and in particular the fovea, is repositioned from an area of diseased RPE to an area of healthy RPE.[20] Therefore, although the RPE itself is not moved, macular translocation surgery can be regarded as a functional RPE transplantation. Figure 1.9 shows illustrative diagrams and clinical photographs demonstrating macular translocation.

This procedure can confer long-term visual stability, and in a significant proportion of patients leads to an improvement in both visual acuity[52] and quality of life.[53] Of interest, in a series of seven patients undergoing macular translocation for non-exudative AMD, new geographic atrophy was reported in the new subfoveal RPE of one patient.[54] All patients undergoing macular translocation require further surgery to reposition extra-ocular muscles to prevent intractable torsional diplopia and the large retinotomies can have significant complications including retinal detachment, proliferative vitreoretinopathy (PVR), macular pucker, and macular hole.[52] Due to the high rate of complications, macular translocation surgery has been abandoned by clinicians.

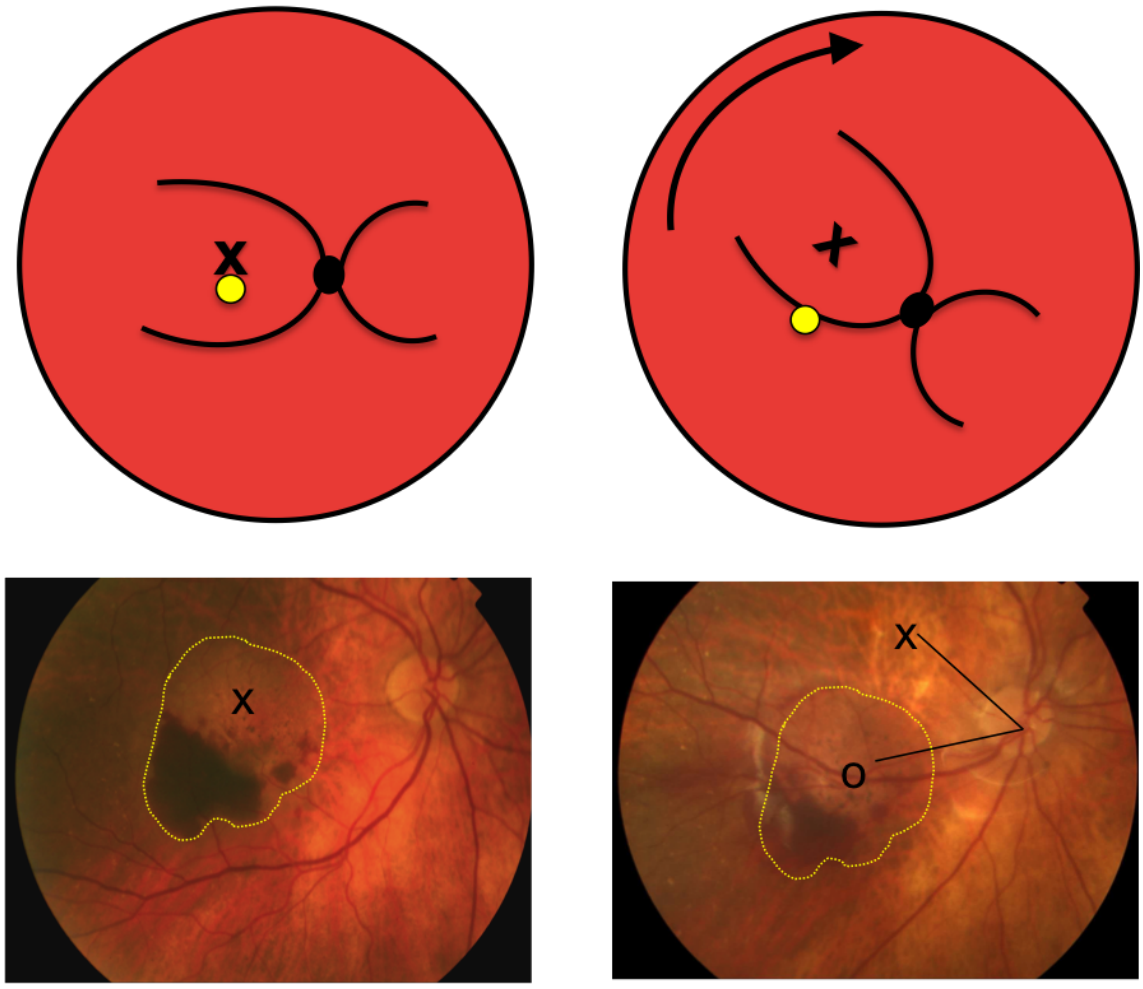

Figure 1.8: Macular translocation.

Preoperatively, the patient had wet AMD in the right eye. Submacular haemorrhage is visible, and right fovea is affected by serous macular detachment (see diagram top left and photograph bottom left). The outline of the choroidal neovascular membrane (CNV) is marked by the dotted yellow line. Macular translocation was performed to allow the neurosensory retina to be rotated around the optic disc so that the fovea rests on a more healthy area of RPE. The bottom right picture shows atrophic retina in the area overlying the CNV (marked O). The fovea (marked X) remains supported by healthy RPE. This patient's visual acuity was 6/60 preoperatively and five years postoperatively the visual acuity was maintained at 6/9. (Courtesy of Professor Lyndon da Cruz, Moorfields Eye Hospital, London)

1.8.2 Autologous RPE-Choroid Patch Graft

Numerous investigators have attempted autologous RPE sheet transplantation, with the aim of using healthy peripheral RPE, on a bed of BrM and partial thickness choroid, and moving the multi-layered patch graft to the submacular space, as illustrated in the diagram in Figure 1.9. Figure 1.10 shows fundus photographs of a patient in whom this procedure has been performed.

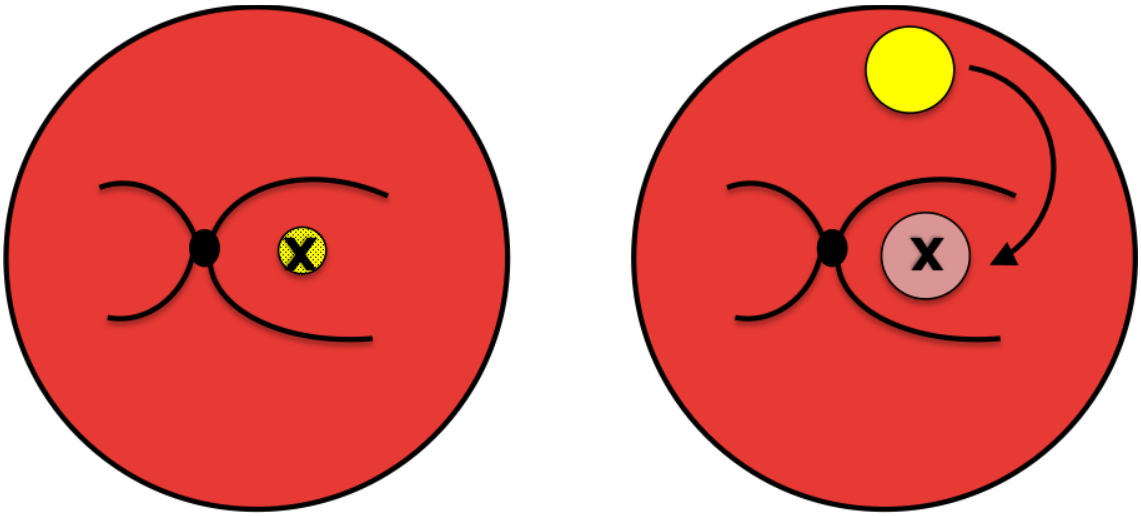

Figure 1.9: Autologous RPE-Choroid Patch Graft

In this technique, an RPE-choroid graft is removed from the peripheral retina and placed in the subretinal space at the fovea. This technique transplants RPE, BrM and partial thickness choroid.

Peyman *et al.* were the first to describe this technique, and report two patients who underwent vitrectomy and CNV excision, combined with RPE transplantation. Visual acuity improved in the patient that received an autologous pedicle RPE graft, while the patient that received RPE and BrM transplant from an enucleated donor eye did not improve.[55] Stanga *et al.* operated on six patients, and performed vitrectomy and CNV excision with translocation of RPE/BrM from the paramacular area to the subfoveal space. Using a small retinotomy, they fashioned a free RPE/choroid graft in five patients and a pedicled RPE/choroid graft in one patient, followed by air fluid exchange and face down posturing. Four of the six patients could detect a fixation target projected onto the fovea overlying the translocated RPE, although none of the patients

showed any improvement in visual acuity. Three out of six patients experienced significant complications, including subretinal bleeding, PVR-related total retinal detachment, and insertion of an upside-down RPE graft.[56] Later studies used grafts from the mid peripheral retina, rather than from the edge of the macular RPE defect.

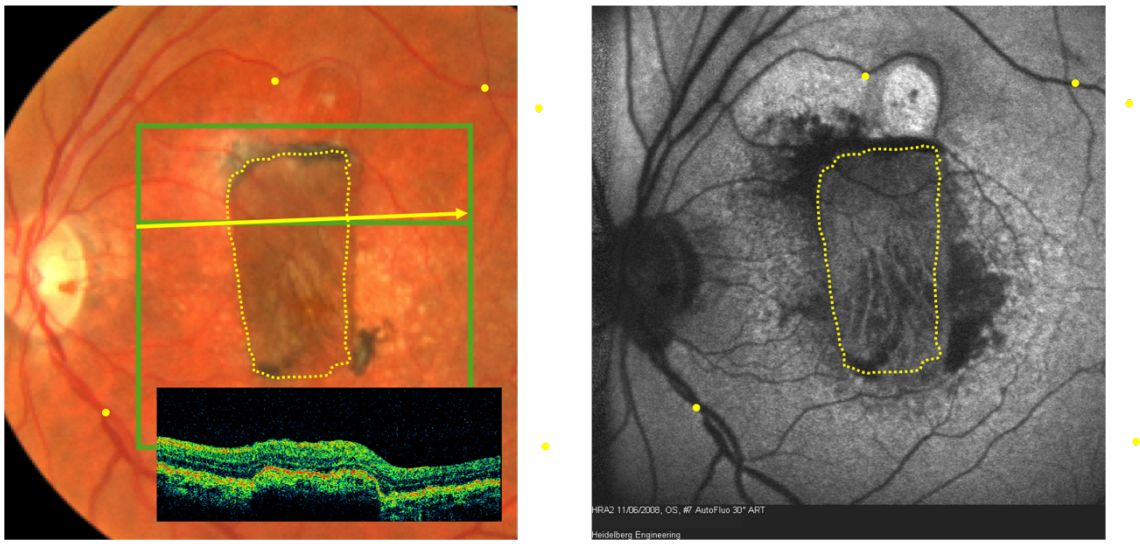

Figure 1.10: Clinical photographs of autologous RPE-Choroid Patch graft

Left panel shows area of patch graft beneath the fovea. Inset figure shows presence of the graft on OCT scan. Right figure shows vascularisation and integration of the graft into the macula. (Courtesy of Professor Lyndon da Cruz, Moorfields Eye Hospital, London)

Van Meurs *et al.* also used an internal approach in six patients undergoing subfoveal CNV excision with transplantation of a full thickness patch of RPE and choroid from under the peripheral retina, to the subfoveal space, to cover the excision site.[57] Four of the six patients showed improvement in visual acuity but this technique still carries with it a significant risk of intraocular haemorrhage, retinal detachment, and PVR. Van Meurs' group recently published the long-term outcomes of 133 patients who underwent CNV excision followed by autologous RPE-Choroid grafting. The postoperative PVR rate in this cohort was 10%. The visual acuity outcomes overall were modest but four years after surgery, 5% of patients had Best Corrected Visual Acuity [BCVA] better than 20/40. [58]

1.8.3 Submacular injection of RPE cell suspension

In a series of 14 eyes, Binder *et al.* performed pars plana vitrectomy, and created a retinotomy nasal to the optic disc to allow formation of a subretinal bleb. Using a blunt instrument, RPE cells from this area were mobilised, aspirated into a micropipette, and then transplanted over an RPE defect in the macula,[59] but the dissociated RPE cells were unable to attach to the damaged BrM under the fovea. However, RPE cells from the extramacular site in the peripheral retina were able to restore RPE continuity, because of their ability to divide and adhere to undamaged BrM. **This observation suggests that it is the damaged host BrM that is the limiting factor for adherence of isolated cells, and not the age of the RPE donor cells.** Furthermore, *in vitro* studies have shown that embryonic RPE cells can adhere to normal, but not aged, BrM from post mortem specimens.[17] These age-related changes in BrM also represent one of the critical differences between human subjects and laboratory animals in which many of the successes of RPE transplantation experiments have been reported, because the latter are generally young and have a healthy BrM.[48, 60, 61] The inference from these findings is that successful RPE transplantation for AMD must take replacement of BrM into consideration.[62]

1.8.4 Sources of Cells

Although the aim of cell transplantation is to restore RPE function and prevent photoreceptor loss, the transplanted cells may not necessarily need to be RPE cells. Subretinal injection of iris pigment epithelial (IPE) cells,[63] Schwann cells,[64] human central nervous system stem cells,[65] and umbilical cord cells[66] all facilitate photoreceptor rescue in the RCS rat. Transplanted cells may be primary cells that have been harvested immediately before transplantation, or can instead be cultured *in vitro* prior to transplantation. Alternatively, a transformed RPE cell line such as ARPE-19 or h1RPE-7 can be used, although these tend to be utilised only for experimental purposes because of the risk of teratoma formation *in vivo*.

From the point of view of the transplanting surgeon, the original source of the cell is not as important as the technical aspects of harvesting and delivery. From the surgical point of view, cell sources can be divided into three types:

(1) autologous RPE cells (already discussed in section 1.8.2 and section 0)
(2) autologous Iris Pigment Epithelial (IPE) cells
(3) *in vitro* cultured allogenic cells

1.8.4.1 Autologous Iris Pigment Epithelial cells

IPE cells are a source for autologous cell transplantation because they are similar to RPE cells but are much easier to harvest.[67] Surgical iridectomy is a relatively straightforward procedure and iridectomy specimens have been successfully used to produce dissociated IPE cells that can be propagated in culture.[68]

RPE and IPE cells are derived from the same embryonic cell line, and both cell types have apical/basal polarisation, microvilli and tight junctions that serve as a barrier to regulate the passage of ions and small molecules and to restrict diffusion of membrane lipids and proteins. Importantly, RPE and IPE tight junctions are morphologically similar. IPE cells can survive for up to 20 weeks in the subretinal space of rabbits[69, 70] and *in vivo* phagocytosis of photoreceptor outer segments of RCS rats has also been demonstrated.[71]

Gene expression in IPE cells differs from that of RPE cells. Gene expression for intra and extracellular retinal binding proteins, which are essential for metabolism of the visual pigments, is lower in IPE cells than RPE cells.[72] *In vitro*, IPE cells are able to phagocytose photoreceptor outer segments but are less able to degrade them compared to RPE cells.[73] The level of expression of mRNA of VEGF is also lower in IPE cells than in RPE cells,[74] but it has been suggested that this may in fact make IPE cells more suitable than RPE cells for subretinal transplantation especially in cases of exudative AMD where presence of VEGF can stimulate recurrence of CNV.[67] It is not known to what degree IPE cells acquire RPE properties when transplanted into the subretinal space in patients with AMD. However, Abe *et al.* report 56 AMD patients who underwent pars plana, vitrectomy, CNV excision, IPE transplantation into the subretinal space, and gas tamponade. Despite an initial deterioration in visual acuity, there was a long-term logMAR visual acuity improvement, with at least 2 years follow-

up in all patients (1.26 vs. 1.48, p=0.02). Four of the 56 developed surgical complications including rhegmatogenous retinal detachment (three patients) and vasculitis (one patient).[67]

1.8.4.2 Ex-vivo cell sheet expansion prior to transplantation

For non-autologous transplants, donor RPE cells can be removed from an enucleated eye cup either by using trypsin digestion for the collection of a cell suspension, or alternatively, dispase can be used to separate the basement membrane from the RPE monolayer, thereby allowing harvest of an intact RPE cell sheet.[20] Authors that have utilised foetal human RPE cells have cultured the cells *in vitro* prior to surgical injection. Gouras *et al.* excised a 0.6mm RPE monolayer patch from foetal human RPE cells cultured *in vitro*, and by aspiration into a glass pipette were able to deliver the patch into the subretinal space. [75] Primary cell cultures have a limited lifespan because after a number of population doublings (known as the Hayflick limit), cells undergo senescence and stop dividing. This is beneficial because while the cells retain viability there is very little risk of non-regulated growth.[76]

Transformed RPE cells can be defined as cell lines that have either spontaneously or deliberately acquired genetic modifications that lead to a state of unregulated growth. They are useful in cell culture because they show long-term stability *in vitro*. RPE cell transformations can occur spontaneously, such as with the ARPE19 and the D407 cell lines, [77] [78] but may also be genetically engineered e.g. H1RPE7.[79] RPE cells can also be genetically modified to alter some other aspect of their behaviour, so that they either express a marker (e.g. Green Fluorescent Protein (GFP)-labelled RPE) or modify gene expression. However, after repeated passage it has been established that these adult human cell lines can dedifferentiate and lose their morphology and RPE gene expression, and express neuronal cell markers instead.[80, 81]

1.8.4.3 Pluripotent Stem Cells

The potential of stem cell therapy has captured the imagination of scientists, clinicians and tabloid newspaper editors worldwide. Stem cell therapy has in fact been used for decades, in the form of bone marrow transplantation. Haematopoietic stem cells (HSC) in the bone marrow have the capacity to grow, divide and replace all types of blood cell for patients receiving chemotherapy or radiation therapy for leukaemia.

Research into stem cells began after the devastation of Hiroshima and Nagasaki caused by atomic bombs in World War II, and initial research efforts were focussed on understanding radiation and treating radiation exposure. Bone marrow transplants are the only widely used form of stem cell therapy, but are limited to the regeneration of haematopoietic cells.

The use of pluripotent stem cell technology holds promise as a novel source of cells for transplantation in AMD and other degenerative diseases. Like haematopoietic stem cells, pluripotent stem cells are able to self-renew indefinitely, while maintaining a stable undifferentiated state, but since they are pluripotent they can differentiate into any cell type in the body (except into placental cells).[82]

The retina is an ideal candidate for experimental stem cell therapy. It is an easily accessible tissue, and the transparent cornea facilitates clinical assessment after transplantation, and also allows objective monitoring with low-intervention imaging modalities such as standard photography and OCT scanning. The area of transplantation required is small compared to other organs. The fellow eye, which because of the blood retinal barrier is relatively protected from the effects of transplantation, can be used as a control. Furthermore, the eye is not essential to sustain life. For research purposes, this allows full characterisation for the life of the graft, even if the recipient organ continues to fail.[83] For these reasons, it is unsurprising that ophthalmic disease has been the target for pioneering clinical trials using pluripotent stem cells. Although the first ever pluripotent stem cell trial was for spinal cord injury, the second and third trials of pluripotent stem cells were for Stargardt Macular Dystrophy and dry AMD, and utilised RPE cells derived from human embryonic stem cells.[84, 85]

Human embryonic stem cells (hESC) can be isolated from the inner cell mass of the human blastocyst at approximately five days post fertilisation. These cells can then be maintained indefinitely under defined conditions *in vitro*, as pluripotent cells, and, when required, can be differentiated into RPE cells.[86]

Using hESC-derived RPE, Lu *et al.* have demonstrated photoreceptor rescue and sustained cell function in the RCS rat. The first use of hESC-derived RPE cells in human patients was described by Schwartz *et al.*, in one patient with Stargardt macular dystrophy and another with dry AMD.[84] Initial results show no significant improvement

in visual function, but do suggest a good safety profile. The use of hESC for RPE transplantation not only entails ethical obstacles, but also carries a risk of immune rejection, especially since surgical trauma is likely to compromise the blood retinal barrier and the immune privilege status of the subretinal space.

The difficulties associated with hESC can be overcome with the use of induced pluripotent stem cells (iPSCs). This technology was first described in 2006 by Yamanaka, who was awarded the 2012 Nobel Prize for his work.[87] This technique uses viral vectors to insert four key genes into the DNA of any mature somatic cell, which then causes reprogramming of the cell into a stem cell capable of producing any cell lineage of the three germ layers.

The intrinsic attraction of iPSC technology is not only the avoidance of the ethical issues of using embryonic cells, but also that iPSC-derived cell transplantation would obviate the need for continual immunosuppression. In a model scenario, tissue would be obtained from a somatic cell of the patient with AMD, the cells would be reprogrammed to a pluripotent state, and then differentiated into RPE cells and expanded *in vitro*, prior to transplantation. Autologous transplantation of iPS-derived RPE cells, without any artificial scaffold, into a nonhuman primate showed no immune rejection or tumour formation. However, the immunogenicity of iPSC has not been well studied and while they certainly have an advantage over ESC, there is some evidence that iPSC derivatives can induce T-cell dependent immune responses even in genetically identical organisms.[88]

Rather than simply being used as a regenerative source, the use of iPSCs in combination with gene therapy may enrich their therapeutic potential. Autologous iPSCs could be screened for common genetic mutations that could then be corrected *in vitro* by gene therapy. Cells would then be differentiated into RPE cells before surgical transplantation. Assuming that sufficient photoreceptors remained functionally intact, this could allow a disease-free phenotype to be maintained, but this tandem technique relies on complete elimination of any diseased host cells prior to transplantation.[89]

A significant concern associated with the use of iPSC technology is the risk of tumourigenicity. The four key genes used by Yamanaka all code for transcription factors: c-Myc, Sox2, Oct4, and Klf4. Of these, c-Myc is known to be an oncogene and the remaining factors have been implicated in tumourigenicity. Yu *et al.* have demonstrated that a different combination of transcription factors – Oct4, Sox2, Lin28

and Nanog – can also induce pluripotency in human somatic cells, but Nanog is also known to be expressed in some tumours, and can promote breast cancer tumourigenesis and metastasis.[90] The iPSC technology uses viral DNA that could incorporate itself into the genome of the somatic cell and potentially cause harm. However an approach that uses non-integrating adenoviruses, could avert the cancer risks of iPSCs, and no tumours have been observed in mice derived from integration-free iPSCs up to 20 weeks of age.[91] However exclusion of these oncogenic factors has a significant and detrimental effect on reprogramming efficiency and it is unknown whether reprogramming itself may lead to tumourigenesis.[92, 93]

In 2014, Obokata reported that strong external stimuli, such as a transient low-pH stressor, can generate pluripotent stem cells without the need for transcription factor integration into the genome. This cellular reprogramming, known as stimulus-triggered acquisition of pluripotency (STAP), generated much excitement and controversy but could not be reproduced despite fervent attempts by several other groups.[94, 95] The original paper has since been retracted,[96] the lead author discredited, and STAP cells are widely regarded as one of the most well-known scientific frauds in history. The observation by the original authors that STAP cell technology only seems to work on freshly harvested cells from the early postnatal period suggests that this technology, even if it were reproducible, is unlikely to be of major benefit, and would certainly preclude its use for patients with AMD.

1.8.5 Surgical Considerations

Autologous grafts overcome the risk of rejection and obviate the need for long-term systemic immunosuppression. Techniques for autologous grafts have been described in animals, but are based on human surgical procedures, and can be classified into external or internal approaches.

The external approach was first described in 1975 by Peyman *et al*., who performed a sclera-choroido-retinal biopsy in a patient with suspected malignant melanoma.[97] Choroidal haemorrhage was avoided by extensive diathermy but moderate vitreous loss occurred through the wound. This technique was subsequently adapted for RPE harvesting in pigs[98] and rabbits.[99] In 2002, Binder *et al.* described an internal

approach, and harvested RPE cells by first inducing a localised peripheral retinal detachment and then aspirating RPE cells with a microcannula, before injecting them into the subfoveal space. Van Meurs *et al.* also used an internal approach in 6 patients undergoing subfoveal CNV excision and dissected a 1.5mm x 2.0mm full thickness patch of RPE and choroid from peripheral retina that was then manipulated into the subfoveal space to cover the excision site. Four of the six patients showed improvement in visual acuity, and the van Meurs technique has since become the most widely used technique in humans.

The advantage of autologous RPE transplantation is that the procedure can be done at a single sitting. However, harvest of RPE cells from a different locus in the same eye is technically challenging, and this has led to non-RPE cells being considered for transplantation. IPE cells can be easily obtained from a peripheral iridotomy, but as outlined above in section 1.8.4.1, use of IPE cells is less than ideal.

1.8.6 Delivery of cells

The first description of RPE transplantation was by Gouras *et al.*, who transplanted cultured 3H thymidine labelled human RPE cells on to denuded Bruch's Membrane in owl monkeys. The investigators used an open-sky technique for this procedure (i.e. the cornea was removed, and the globe was therefore open for the duration of the procedure) and therefore experienced difficulties reattaching the neurosensory retina.[100] Following modification of the technique to a closed-eye method, consisting of pars plana vitrectomy, retinotomy and delivery of cells through a pipette,[101] early spontaneous retinal reattachment was achieved. In both of these studies, donor RPE cells successfully attached to Bruch's membrane and some phagocytosis of photoreceptor outer segments could be demonstrated. Following this, a number of investigators have continued to use an internal approach, whilst others favoured an external approach involving dissection of posterior sclera and trans-sclero-choroidal subretinal injection of RPE cells. The external approach is preferable in animal studies, especially in rodents, where the globe is small, the lens is extremely large, and there is no true vitreous cavity to operate within. However this technique not only requires rupture of Bruch's membrane but also causes choroidal trauma, leading to the risk of severe intraocular or suprachoroidal haemorrhage, or may possibly lead to inflammation and immune responses that would not occur with the transvitreal

approach. Nevertheless, the external approach has been successfully demonstrated in rats, rabbits and mice.

Various surgical instruments have been used to either harvest or deliver RPE cells. Blunt tipped needles and glass cannulae have been used for delivering RPE cell suspensions or small patches of RPE sheet, which can also be delivered in a slow, controlled injection by manually controlled oil-hydraulic microinjection pump, or by electronic motorised injectors.[102]

1.8.7 Age-Related Changes in Bruch's Membrane

Despite various elegant techniques to optimise RPE cell harvest and surgical delivery, it is now clear that the RPE graft survival is dependent on a healthy Bruch's Membrane, or alternatively a Bruch's membrane substitute. Tezel & Del Priore has shown that RPE cells are anchorage dependent, and without attachment to a suitable substrate the cells will undergo *anoikis*,[103] defined as apoptosis triggered in response to lack of extracellular matrix binding.

When considering RPE transplantation in human eyes with AMD, it is unlikely that the host Bruch's membrane is sufficient as a substrate for transplanted cells. Bruch's membrane undergoes a number of changes with normal ageing, as well as with AMD. Creating a distinction between ageing changes and pathological changes is difficult, but Booij *et al.* assert that molecular changes should only be viewed as pathological once they begin to affect BrM function.

Age related changes in BrM
Lipid accumulation
Collagen cross-linking
Increase in BrM thickness
AGE accumulation
Increase in proteoglycan size
Higher heparan sulphate fraction
Elastin layer calcification

Table 1.3: Age related changes in Bruch's Membrane.

Adapted from Booij *et al.* (2010).[104]

Progressive accumulation of lipids (phospholipids, triglycerides, fatty acids and free cholesterol) in BrM occurs with age, and particularly affects the macula. This lipid accumulation then impairs BrM's capacity to facilitate fluid and molecular exchange between the choroid and RPE.[105] Permeability of BrM is also affected by the increased collagen cross linking that occurs with age, which increases the strength and density of the collagen network, and thereby increases the BrM thickness, but reduces its elasticity and filtration capabilities.[106]

Proteoglycans are heavily glycosylated glycoproteins, whose exact function is determined by the type of core protein and its glycosaminoglycan side chains. Proteoglycan turnover is usually tightly controlled but with age there is a shift towards larger proteoglycan molecules.[104] In disease states such as retinitis pigmentosa, diabetic retinopathy and AMD, BrM proteoglycans exhibit a much higher proportion of heparan sulphate than in BrM from healthy controls. BrM associated heparan sulphate is known to modulate complement activity and interacts with complement factor H. Complement activity is thought to be important in AMD pathogenesis.

Advanced glycation end products (AGEs) are chemically modified glycosylated or oxidised fats and proteins. Exogenous AGEs are generated by smoking and cooking, whilst endogenous AGEs occur due to the combined metabolism of fats, proteins and sugars. High concentrations of AGEs activate the AGE receptor (RAGE) which is present on multiple cell types throughout the body and has been implicated in atherosclerosis, diabetic nephropathy and neurodegenerative disease. Specific AGEs, and AGE receptors, are present in BrM.

Calcium deposition in BrM correlates with age, and with AMD. BrM calcification makes the membrane more brittle, and therefore susceptible to breaks, which would allow the development of choroidal neovascularisation. This is corroborated by the pathology observed in the condition pseudoxanthoma elasticum (PXE), an autosomal recessive condition characterised by soft tissue calcification including BrM calcification, leading to BrM breaks visible on ophthalmoscopy as 'angioid streaks'.

1.8.8 Effect of BrM Age on RPE Transplantation

Donor RPE cells can attach to an undamaged BrM within two hours of delivery.[100] However, the age and layer of BrM available for cell attachment have a profound effect

on the fate of seeded RPE cells in vitro. Tezel *et al.* have conducted a number of studies in this area and has shown that RPE attachment, survival and repopulation is most likely if the RPE basal lamina of BrM is intact.[103] Tezel *et al.* also noted that inhibition of RPE cell repopulation occurs due to age related changes in the inner collagenous layer, but this could be partially reversed by coating of the ICL with ECM proteins such as fibronectin, laminin and vitronectin.[103]

It is unlikely that in an eye with AMD, host BrM can act as a substrate for transplanted RPE cells. Gullapalli *et al.* found that untreated aged submacular BrM did not support long term survival of foetal human RPE in vitro.[17] Furthermore, in the original studies by Binder, suspended RPE cells injected into the submacular space failed to adhere to submacular BrM, but interestingly the graft donor site (nasal to the disc) was able to restore RPE continuity in this area, presumably because of an undamaged BrM in the nasal retina. More recently, Schwartz *et al.* observed that following subretinal injection of ESC-derived RPE cells, pigmentation was most prominent at the edge of the atrophic areas being treated.[85] This may have occurred because of the fluidics of the bleb – particulate matter within a confined space is more likely to become trapped at the edges of the bleb rather than remain in the centre. A further observation was the high prevalence of preretinal cells, indicating a degree of inadvertent cell injection into the vitreous cavity, or alternatively reflux from the subretinal bleb into the vitreous cavity.[85] These unwanted effects are the result of using a cell suspension, and could be avoided if the cells were transplanted on a cell carrier that served as an artificial BrM. There would also be a greater control over the number of cells injected, with a more even distribution, and a cell carrier may also facilitate surgical handling, preventing egress of RPE cells into the vitreous cavity.

These findings have led to the consensus that reconstruction of BrM is as important as replacement of RPE cells. Much work has focussed on the development of an artificial or surrogate scaffold to act as a BrM substitute. A potential schema for the use of pluripotent stem cell derived RPE cells, on an artificial BrM substitute, is shown in Figure 1.11.

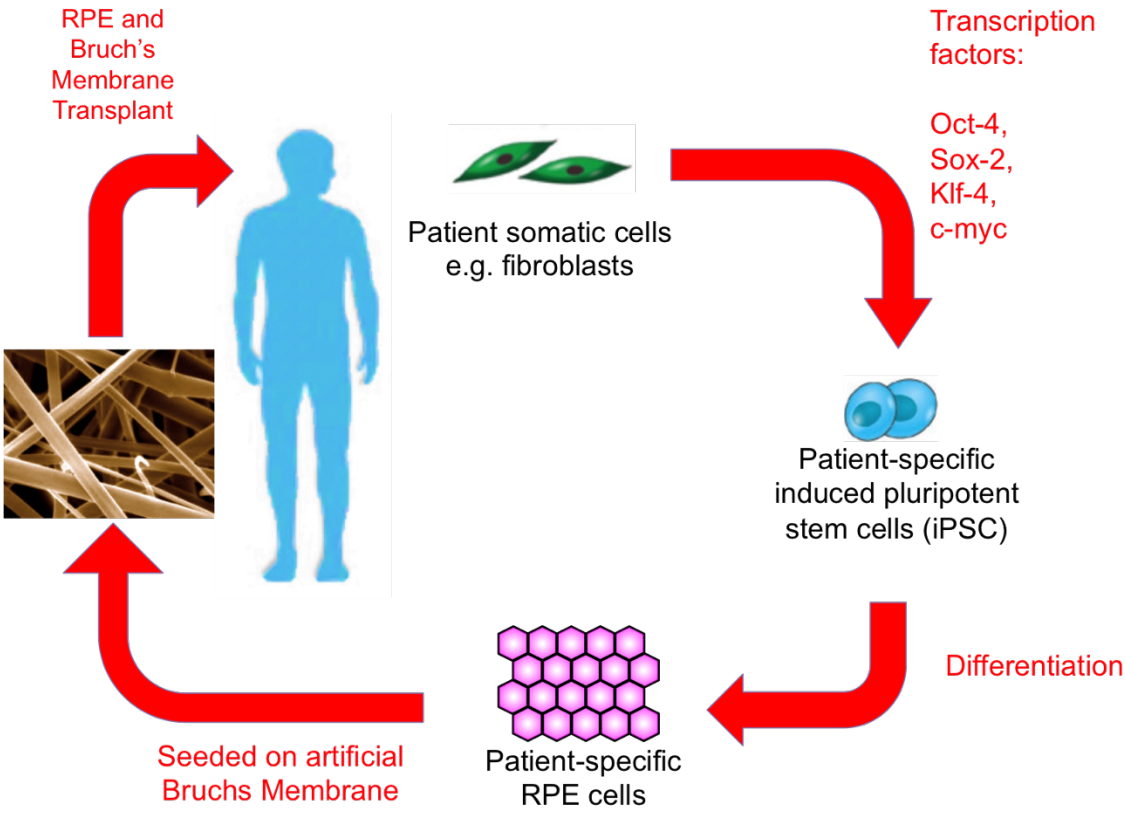

Figure 1.11: A potential schema for the use of iPS technology in treating retinal degenerations.

Fibroblasts are isolated from the patient's skin sample. Fibroblasts are converted into iPSC, which in turn are differentiated into RPE cells. These are specific for the individual patient and will therefore not induce an immunological reaction. The iPS-RPE cells are then seeded on to an artificial BrM, until confluent, and the RPE-BrM graft can then be transplanted into the patient's eye. Of note, the right hand part of the cycle (iPSC production, differentiation, seeding) is conducted by scientists in the lab, but the left hand side (patient selection, skin biopsy, RPE-BrM transplantation) is conducted by clinicians, many of whom will not have a laboratory science based background. For RPE transplantation to become clinically useful, the left hand side of the schema needs to be made as simple and straightforward as possible.

1.9 BrM Substitutes

Binder *et al.* have suggested the following characteristics of an ideal BrM substitute[18]:

- support acquisition and/or maintain the RPE phenotype
- allow for fluid transport, i.e. with porosity comparable to juvenile BrM
- enable easy surgical manipulation
- be well tolerated in the subretinal space
- biodegrade or integrate over time

Table 1.4 shows the variety of natural and synthetic membranes that have been tested experimentally for the purpose of RPE transplantation.

1.9.1 Natural membranes

Several natural membranes, including both ocular and non-ocular membranes, have been tried. The use of amniotic membrane (AM) is already well established in ophthalmology, for the purposes of ocular surface reconstruction following severe chemical injury to the cornea. In vitro studies have shown that AM supported RPE cell differentiation greater than plastic cell culture plates alone.[107] Furthermore, AM is well tolerated in the subretinal space, and causes minimal inflammation[108] but it is thought that AM does not allow sufficient diffusion between RPE and choroid, and would therefore lead to overlying neurosensory retinal atrophy, despite ideal RPE differentiation.[18]

Thumann *et al.* cultured porcine and bovine RPE and IPE on autologous Descemet's membrane, with good results, demonstrating formation of a confluent monolayer.[109] Porcine lens capsule was used by Turowski *et al.*, who noted that cultured ARPE-19 cells showed more uniform morphology, better phagocytosis, enhanced tight junction formation, and superior polarisation compared to cells cultured on porous polyester filters.[110]

There is also the possibility that natural membranes can be enhanced to either encourage or limit cell growth and proliferation. Lee *et al.* studied the effect of microcontact printing on human lens capsule.[111] Human lens capsule consists of collagen type IV, laminin and fibronectin, and is the thickest basement membrane in the human body, measuring 15μm in thickness. Microcontact printing (also known as soft lithography) is a modern material fabrication technique that allows surface engineering with chemically active patterns or topological features with sizes ranging from 30nm to 100μm.[111] The investigators used inhibitory growth molecules and noted successful cell growth inhibition on printed lens capsule, compared to untreated lens capsule.

1.9.2 Tissue engineered BrM substitutes

Tissue engineering can be defined as the combined use of cells, engineering and materials methods, and suitable biochemical and physio-chemical factors, to improve or replace biological functions.[112] The field has arisen, in part, to address the shortage of tissues and organs available for transplantation. It is being evaluated for a range of clinical applications, including skin, cartilage and bladder.[113-115]

The acellularity of BrM lends itself to tissue engineering solutions. A synthetic substitute for BrM has the advantage that technical parameters such as porosity, thickness, biodegradation or rigidity can be varied more readily. It also avoids any risk of immunological rejection.

Simple porous polyester or polycarbonate membranes support differentiation of foetal RPE cells, but differentiation does not persist beyond 1-3 weeks if aged human RPE cells are used.[116]

Tomita *et al.* were the first to use a polymer scaffold for stem cell delivery to the subretinal space, and utilised Poly-(L-lactic acid) (PLLA) and poly (D,L-Lactic-co-glycolic acid) (PLGA) because these polymers are biocompatible, easy to process and have been used successfully in other parts of the body.[117] The degradation rates of these polymers can be manipulated by changing properties such as molecular weight and the lactic:glycolic unit ratio.

Poly (methyl methacrylate) (PMMA) has been used to manufacture ultrathin (6μm) scaffolds for retinal progenitor cells (RPCs), which were shown to grow and differentiate well on these scaffolds both in vitro and in wild type mice.[118] Other scaffolds that have been used include poly(glycerol sebacate) (PGS) to produce a porous elastic scaffold,[119] and poly (ε-caprolactone) (PCL) to produce ultrathin nanowire scaffolds.[120]

Natural scaffold materials	
Collagen	Thumann *et al.* (2009)[63]
Gelatin	Ho *et al.* (1997)[121]
Natural membranes	
Descemet's Membrane	Thumann *et al.* (1997)[109]
Lens capsule	Lee *et al.* (2007)[111]
Biodegradable synthetic polymers	
Poly(a-hydroxy) esters	Lu *et al.* (2001)[122]
Polyurethanes	Williams *et al.* (2005)[123]
Bombyx mori silk fibroin	Shadforth *et al.* (2012)[124]
Poly(ε-caprolactone)	Christiansen *et al.* (2012)[120]
Antheraea pernyi silk fibroin (RWSF), PCL, gelatin	Xiang *et al.* (2014)[125]
Biostable synthetic polymers	
Polymethylmethacrylate (PMMA)	Tao *et al.* (2007)[118]
Poly(p-xylylene) [Parylene]	Lu *et al.* (2012)[126]
Polytetrafluoroethylene	Krishna *et al.* (2011)[127]
Polyethylene terephthalate	Stanzel *et al.* (2012)[128] Carr *et al.* (2013)[86]
Polyimide	Subrizi *et al.* (2012)[129]

Table 1.4: Potential scaffolds for RPE transplantation

1.9.3 Previous work in the Lotery Laboratory on Tissue Engineered Polymer Scaffolds for RPE Transplantation

Anton Formhals patented the technique of electrospinning in 1934.[130] This technique allows the fabrication of a non-woven matrix from randomly organised microfibres and nanofibres. It is utilised in industry and widely used in tissue engineering research, for the manufacture of biocompatible scaffolds for skin, bone and cartilage.

The technique of electrospinning involves liquid polymer, a syringe pump drive, a high voltage power supply and a collector plate. Application of a high voltage to the liquid polymer, which is being fed through the syringe pump driver causes electrostatic repulsion of the molecules within the polymer. The electrostatic repulsion causes the liquid polymer droplet to elongate. At a critical point, known as the Taylor cone, the electrostatic force overcomes the surface tension of the liquid polymer, and the droplet erupts. As long as the polymer is sufficiently cohesive, the emerging jet of charged liquid polymer will form a continuous stream as it travels towards the opposite electrode. As it passes through the air it is dries, and forms a mat of randomly orientated fibres on the metal collector plate. The concentration of the polymer, flow through the syringe driver, and the voltage and distance between the plates all determine the characteristics of the electrospun polymer scaffold.

The Lotery lab at the University of Southampton, in conjunction with the Department of Chemistry, has previously developed an electrospun polymer scaffold from poly(methyl methacrylate) (PMMA) and poly(ethylene glycol) methacrylate (PEGM). Figure 1.12 shows a schematic for the production of the Lotery lab polymer scaffold. PMMA has a long been used as a material for the manufacture of intraocular lens implants following cataract surgery and is safe and inert. PMMA is brittle, hydrophobic and does not allow cell adhesion, and is therefore unsuitable as an RPE scaffold. The inclusion of poly(ethylene glycol) not only increases hydrophilicity but also provides a spacer arm between the cell adhesion ligand and the polymer backbone. Peptides to promote cell adhesion can be added to the PEGM side chains, which need to be “functionalised” to allow the peptides to bind (see Figure 1.12).

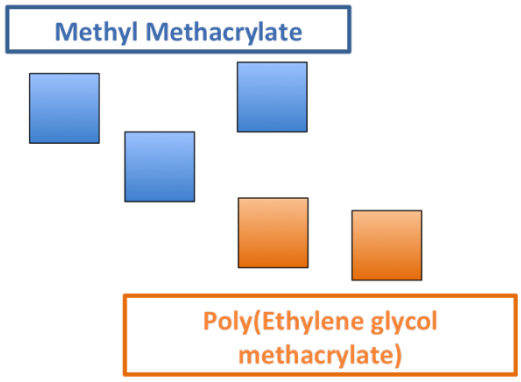

Methylmethacrylate and Poly ethylene glycol methacrylate are blended in a 60:40 ratio.

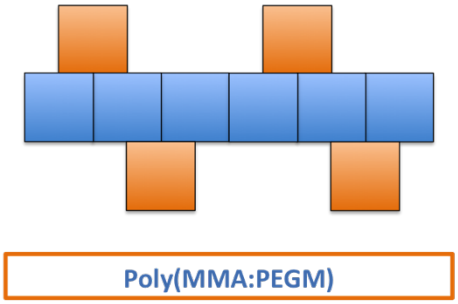

The resulting "unfunctionalised" polymer, if electrospun ,is fragile and poor at promoting cell adherence and cell survival.

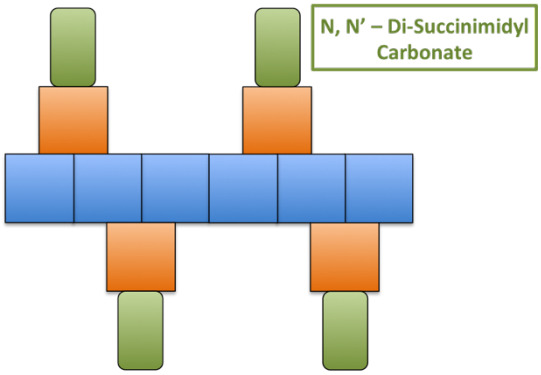

During manufacture of the polymer, incorporation of Di-Succinimidyl Carbonate (DSC) causes the polymer to be functionalised…

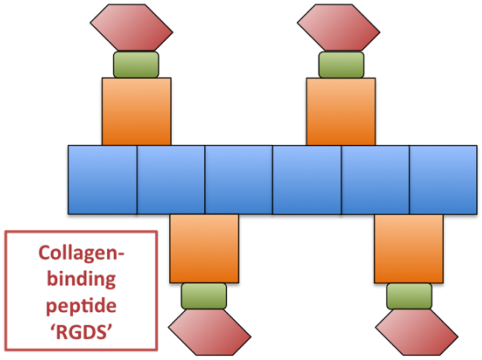

…thereby allowing the addition of peptide ligands to promote cell adhesion

Figure 1.12: Schema showing manufacture of the P(MMA:PEGM-DSC) polymer

Previous work has shown that when the MMA:PEGM ratio is 60:40, excellent RPE cell adhesion and cell survival can be demonstrated.[131] Therefore P(MMA-co-PEGM) is potentially a suitable scaffold for RPE transplantation. Further studies have shown that while cell survival is markedly improved on functionalised polymer compared to unfunctionalised polymer, addition of peptide ligands such as RGDS or YIGSR (the peptides that allows fibronectin and laminins respectively to interact with integrins on the cell surface) added minimal improvement to cell adhesion or cell survival, compared to functionalised polymer without any peptide.

Scanning electron microscopy demonstrates that the P(MMA-co-PEGM) co-polymer developed in Southampton has a fibrous structure similar to that of to native porcine BrM.

While the electron micrographical appearances are similar and RPE cell survival can be maintained, it is unclear whether the polymer fulfils the other characteristics suggested by Binder *et al.*[18]

1.10 Aims, Hypothesis and Objectives

The aim of this project was to further characterise and evaluate the P(MMA-co-PEGM) co-polymer as a potential artificial BrM and to develop methods to use this co-polymer for RPE transplantation. The characteristics of an ideal BrM substitute, as espoused by Binder *et al.*, were used as benchmarks (see Section 1.9).

The hypothesis for this thesis is that the 60:40 P(MMA-co-PEGM-succinimidyl carbonate) allows sufficient diffusional flux to act as an artificial BrM, and can support RPE cells as a polarised monolayer with tight junctions. Furthermore, I hypothesise that the polymer can be safely and effective implanted into the subretinal space.

The primary objectives were to:

1. Measure diffusional flux across the co-polymer, with and without RPE cells.
2. Determine if RPE cells growing on the polymer are polarised.
3. Evaluate the effect of the polymer on the transepithelial resistance of the RPE monolayer.
4. Determine the effect of viscoelastic on RPE cells.
5. Develop and evaluate a novel surgical instrument to inject polymer into the subretinal space.
6. Assess the safety and efficacy of vitrectomy and subretinal polymer implantation in rabbit eyes.
7. Assess histological and imaging techniques in eyes that have undergone subretinal polymer implantation.

- -

Chapter 2: DIFFUSION ACROSS BRUCH'S MEMBRANE

"Knowledge is not simply another commodity. On the contrary - knowledge is never used up. It increases by diffusion and grows by dispersion."

- Daniel J. Boorstin

2.1 Introduction

2.1.1 Hydraulic Conductivity of BrM

Like the cornea, the retina must remain in a physiologically dehydrated state for optimal visual function to be maintained. The corneal stroma and the interphotoreceptor matrix in the outer retina both have high concentrations of glycosaminoglycans (GAGs)[132, 133], which are large, highly charged molecules that maintain orderly and geometric spacing between cells. Within the cornea, this achieves destructive interference of light scatter from individual fibrils, thereby maintaining corneal transparency. In the retina, regular spacing between photoreceptors is vital for visual sampling. GAGs normally imbibe fluid, which would cause swelling, resulting in alteration of tissue geometry, and reduced visual function. In the retina, any fluid in the subretinal space is pumped by active transport back into the circulation. However this fluid must pass through BrM before it reaches the choroid and putative BrM replacements must allow transport of fluid.

Hydraulic conductivity of BrM, which represents the ease of fluid transport across a unit area of membrane, declines exponentially with age, and in old age is 200x lower than in a child's eye, and this decline in conductivity is more marked in the central retina compared to the peripheral retina.[13] In AMD, hydraulic conductivity is thought to be reduced even further, based on peripheral BrM samples of AMD patients and age-matched controls.[134]

2.1.2 Diffusion of macromolecules across BrM

The photoreceptors are the most metabolically active cells in the body[4] and in dark adapted conditions, photoreceptors are in a state of physiological hypoxia.[135] Photoreceptor survival is reliant on rapid and efficient supply of nutrients to maintain the metabolic rate and to renew the photoreceptor outer segments. The endothelium of the choriocapillaris is fenestrated and the outermost layer of BrM is therefore exposed to myriad circulating molecules within the bloodstream, ranging from simple sugars and amino acids to carrier bound species such as vitamin A, fatty acids, heavy metals, and lipoproteins.

Convection can be defined as the concerted, collective movement of groups or aggregates of molecules within fluids (e.g., liquids, gases). Convection can occur through either advection or diffusion. Advection is the transport of molecules through bulk fluid motion. Diffusion is the net movement of a substance from a high concentration to a low concentration. It would appear quite obvious that diffusion is the more important component of macromolecular transport across BrM, because the nutrients reaching the outer retina are moving in the opposite direction to the bulk fluid flow, and molecular movement cannot therefore be attributed to advection. The importance of advection relative to diffusion can be quantified using the Péclet number, Pe, where:

$$Pe = \text{advective transport rate / diffusive transport rate}$$

$$Pe = VL / D_0$$

where V is velocity of flow,
L is transport path length
D_0 is free diffusion coefficient of the species being transported

Curcio *et al.* have calculated Pe for human BrM, using a typical RPE pumping rate of 11 μL/h/cm^2 for V, a typical BrM thickness of 3μm for L, and using the diffusion coefficients of various molecules in saline (ranging from 2 x 10^{-7} cm^2/s for LDL to 2 x 10^{-5} cm^2/s for oxygen).[136] Therefore, the Péclet number for human BrM ranges from 5 x 10^{-5} to 5 x 10^{-3} i.e. it is negligible relative to diffusion in physiological conditions.

Diffusion follows Fick's law, which states that the amount of diffusion per unit area and per unit of time is proportional to the concentration difference across the medium, and

inversely proportional to the diffusion length. For the purposes of BrM studies, the diffusion length is the thickness of the membrane.

Fick's Law: $J = D\Delta C/L$

where J is diffusive flux per unit area
D is diffusion coefficient of the species in the medium
ΔC is concentration difference across the medium
L is diffusion length

Hussain *et al.* have previously demonstrated the use of fluorescein-isothiocyanate (FITC)-labelled dextran to assess the diffusion capacity of BrM for macromolecular transport.[134] Dextran is a complex, branched, polysaccharide that forms randomly coiled polymers, and are therefore distinct from globular proteins. However, FITC-labelled dextran is available in a highly pure, stable form and is easily detectable, and can therefore be used for experimental purposes to estimate diffusion. Hussain *et al.* measured the diffusional flux of FITC-Dextran through human macular BrM over a 12-hour period.[134] They identified a highly significant, negative linear correlation with age, and estimated a 16-fold reduction in diffusion flux in BrM over a person's lifetime, between the ages of 9 and 92.[134]

2.2 Aims and Objectives

The primary aim of this chapter was to assess diffusional flux in the polymer, both with and without human RPE cells, and compare it with post-mortem samples of human BrM. Since human BrM diffusional flux reduces with age, an ideal BrM substitute should provide at least as much diffusional flux as a juvenile human BrM.

The main objectives of this experiment:

- Obtain samples of human BrM from patients without AMD, and utilise FITC-labelled Dextran in a modified Ussing Chamber to assess diffusional flux over 24 hours.

- Determine if there was any relationship between human BrM diffusional flux and age.

- Assess diffusional flux of the polymer, both with and without human RPE cells on its surface, and compare it to human BrM samples.

2.3 Methods

2.3.1 Preparation of human Bruch's Membrane

Eleven human donor eyes were obtained from the Bristol Eye Bank by Dr Heather Thomson. Seven donors were female, four were male, and ages ranged from 46 to 80 years at time of death.

Date	Sample	Age	Gender	Cause of Death	Thickness of BrM-choroid complex (central to peripheral)			
19/05/10	A	56	Female	GI Bleed	9.158	13.64	14.06	16.34
19/05/10	B	68	Male	Cancer	10.28	12.96	15.28	16.64
06/07/10	C	67	Female	Unknown				
06/07/10	D	60	Male	Unknown	10.13	13.19	14.17	15.12
06/07/10	E	71	Female	Unknown	10.44	13.70	15.39	14.98
06/07/10	F	72	Female	Unknown	10.37	11.70	13.65	17.21
28/10/10	G	58	Female	CVA				
28/10/10	H	46	Female	Pneumonia	12.72	16.72	16.56	17.36
28/10/10	I	63	Female	Unknown	8.934	12.57	14.39	15.24
28/10/10	J	78	Male	Unknown	10.81	14.02	16.05	17.19
28/10/10	K	80	Male	Unknown				

Table 2.1: Demographic data and thickness measurements for human BrM-choroid samples.

After enucleation, eyes were maintained in saline-moistened containers at 4°C and then transferred on ice to the eye bank. The corneas were removed by the eye bank for corneal graft surgery, resulting in a delay (of several days) in receiving eyes in the laboratory.

For all samples, the following method was used by Dr Heather Thomson to isolate human BrM. A circumferential incision in the pars plana was used to dissect and remove the iris and the crystalline lens. The fundus was examined by Dr Charles Pierce (clinical research fellow, University of Southampton) for features of AMD and the posterior eye-cup was then cut in half. The neurosensory retina, and with it the vitreous, was peeled from the underlying RPE/BrM/Choroid complex. The BrM/Choroid complex was easily removed from the sclera by blunt dissection, but required cutting from around the optic nerve head. Once the BrM/Choroid sheet was free-floating, it was washed in PBS. A Pasteur pipette was used to wash off any residual RPE cells. Each specimen was then divided into four sections, placed on filter paper, and stored at -80°C until use.

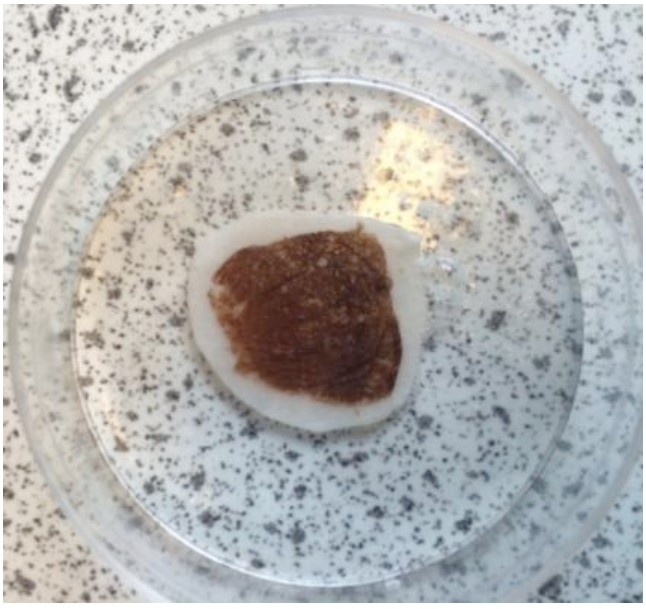

Figure 2.1: Photograph of human BrM in a 60mm petri dish

2.3.2 Preparation of polymer fibre

Using a pre-cut template, thirteen discs of 9mm diameter were cut from an electrospun P(MMA-co-PEGM-succinimidyl carbonate) copolymer scaffold sheet that had been manufactured by Gareth Ward, PhD student at the University of Southampton. Discs were UV-irradiated overnight, washed three times with phosphate buffered saline (PBS) and then placed in PBS in a 12-well tissue culture plate (Corning USA), ensuring complete wetting of the polymer disc. Six discs were then seeded with ARPE-19 cells (American Tissue Culture Collection [ATCC] Manassas, VA, USA) and maintained at 37°C for 5 days. Cell seeding density was 25,000 cells in 2µl, because previous experiments had established that this was sufficient to ensure confluent RPE cells at 5 days.[137] Cell culture medium (comprising 98% DMEM-high glucose-pyruvate [Sigma-Aldrich], 1% antibiotic antimycotic solution (10,000 units per ml Penicillin G, 10mg per ml streptomycin sulphate, 25mg per ml amphotericin B [Sigma-Aldrich], and 1% foetal bovine serum (FBS) [ATCC]) was changed every 48 hours. The remaining seven discs did not have any cells but were kept in a transwell, immersed in tissue culture medium for five days.

2.3.3 Preparation of the Ussing chamber

A modified Ussing chamber, kindly provided by Dr A. Hussain and Prof J .Marshall, was used to measure the diffusion characteristics of the BrM-choroid complex or polymer fibre using the method described by Hussain *et al*.[134] The two half chambers were separated by a tissue cassette, consisting of two plates with a central aperture of 4mm in diameter. Images of the apparatus are shown in Figure 2.2 and Figure 2.3.

The sample (either human BrM or polymer fibre sheet) was placed between the two plates within the cassette. There was a tendency for the BrM samples to scroll, and optimum placement within the cassette was best achieved by first placing one half of the cassette into a petri dish of PBS, with the interface upwards. PBS was added until the central aperture of the cassette was just covered. The sample was then placed over the central aperture and the PBS was then removed whilst ensuring that the sample remained flat, unfolded, and positioned to span the central aperture. The other half of the cassette was then carefully lowered onto the exposed surface of the tissue, and secured with screws. The entire Perspex blockware was clamped together by 3 large bolts. A magnetic stir bar was placed in each half chamber, which were then

filled with 2.5mls of fluorescein isothiocyanate–dextran (MW 40,000, Sigma-Aldrich, UK) and PBS respectively. The chambers were filled simultaneously to ensure an equal pressure on both sides of the sample at all times, to reduce the risk of sample rupture.

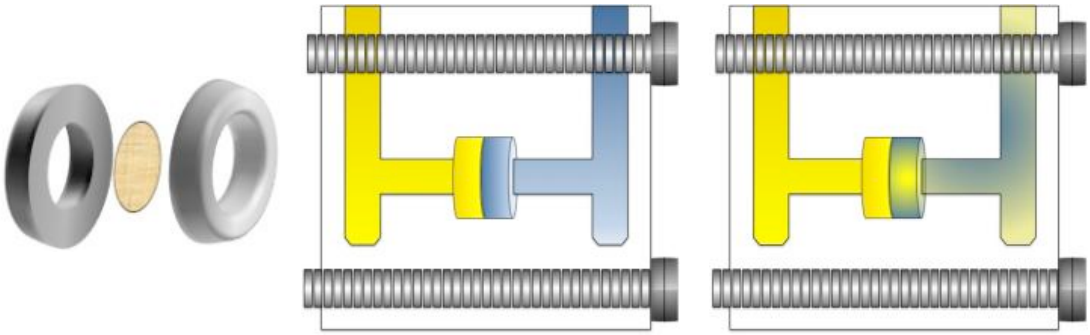

Figure 2.2: Structure of a modified Ussing chamber.

The polymer or BrM sample is secured between two halves of a cassette (LEFT) which is then placed between the two hemi-chambers of the apparatus (CENTRE). Fluorescein-isothiocyanate–dextran (FITC-Dextran, shown in yellow) is placed in one half chamber, and PBS (shown in blue) is placed in the other. Gradual diffusion of the FITC-dextran occurs with time (RIGHT), and the concentration can be interpolated by comparing it with a standard curve constructed from serial dilutions of FITC-Dextran.

Two of the cell-seeded polymer segments were tested with the ARPE-19 cells 'facing' the Dextran hemichamber, while the remaining four cell-seeded segments were tested with the polymer 'facing' the Dextran hemichamber, and the cells therefore facing the PBS.

Samples of fluid (200µl) were taken simultaneously from each hemi-chamber at prespecified time points. For Human BrM, samples were taken at baseline, 15 minutes, 30 minutes, 1 hour, 3 hours, 6 hours, 9 hours, and 24 hours. For the polymer scaffold, samples were taken at 5, 10, 20, 40, 80 and 120 minutes. A standard curve

was constructed with serial dilutions of fluorescein-labelled dextran. Absorbance was measured using a spectrophotometer (FLUOstar Optima, BMG Labtech) at 420 nm.

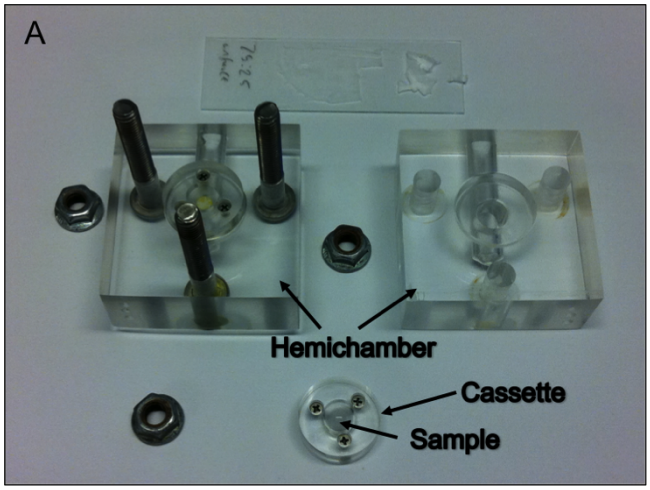

The polymer or BrM sample is secured between two halves of a cassette, which is then placed between the two hemi-chambers of the apparatus.

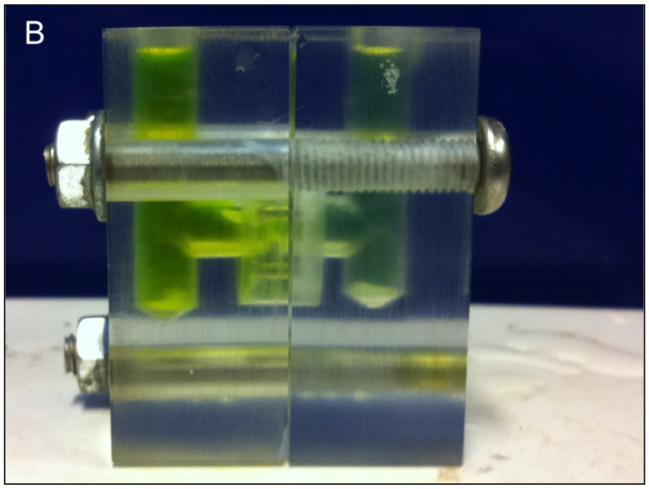

Fluorescein-isothiocyanate - dextran (FITC-Dextran) is placed in one half chamber, and PBS is placed in the other. Gradual diffusion of the FITC-dextran occurs with time, and the concentration can be interpolated by comparing it with a standard curve constructed from serial dilutions of FITC-Dextran.

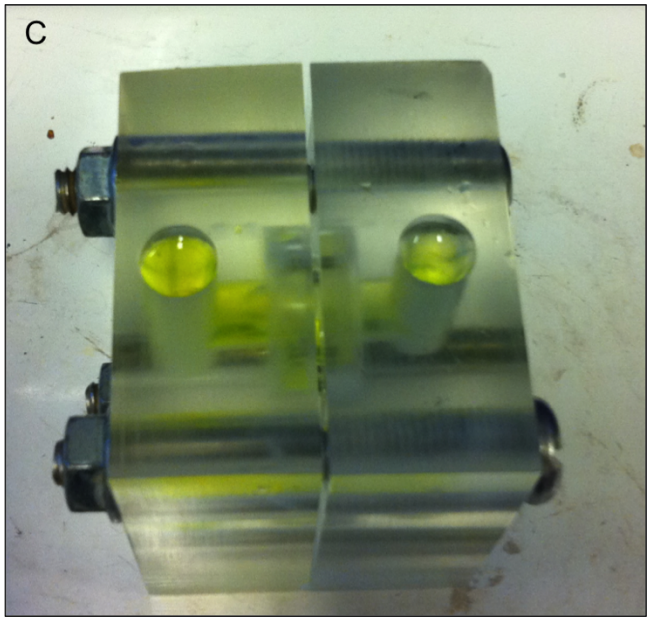

Care is taken to ensure that the height of the fluid level in each hemichamber is equal at the start of the experiment, and that samples are taken from each hemichamber simultaneously, to prevent hydraulic pressure from interfering with the assay.

Figure 2.3: Photographs showing apparatus for diffusion studies

Immediate leakage of fluorescein-labelled dextran into the PBS was interpreted as rupture of the sample either due to the pressure of the fluid column or due to a pre-existing hole. In the event of this, samples were discarded and the experiment was re-started with a new sample.

After use, each sample was placed on a slide, dried in an oven at 37 degrees for one hour, and then stored at -20°C. Thickness measurements of each sample were provided by Gareth Ward, who achieved this using the Ze-Scope (Ze-metrics, Tuscon, Arizona, USA), a sub-nanometer precision 3D optical profiler.

2.3.4 Statistical Analysis

The standard curve was used to interpolate the diffusional flux of FITC-Dextran across each sample (GraphPad Prism 6.0 for Mac OS). One way ANOVA was used to compare the diffusional flux of FITC-Dextran between human BrM samples, polymer with cells, and polymer without cells (IBM SPSS Statistics for Macintosh v22, Armonk, New York, USA). Levene's test was used to confirm heterogeneity of variance. A p-value of <0.05 was considered statistically significant. The Bonferroni method was used to make adjustments to take multiple comparisons into account. The adjusted alpha level was therefore 0.016667 (i.e. 0.05/3).

2.4 Results

The rate of diffusion across human BrM was observed to be much slower than for the polymer. This could be detected simply by observing how yellow the fluid in the PBS hemichamber was. Because of this, diffusional flux measurements across human BrM were measured over 24 hours. However, diffusional flux measurements across polymer were taken only over a period of 2 hours.

There were numerous difficulties with ensuring good diffusion measurements of the polymer. Immediate leakage of fluorescein-labelled dextran into the PBS was interpreted as rupture of the sample. For each successful polymer experiment, there were approximately 2-3 that were abandoned, because of an apparent immediate polymer rupture in the polymer causing FITC-Dextran to visibly seep into the PBS hemichamber. However, even after removal and microscopic examination of these

apparently damaged polymers, no cause for this immediate leak could be found in many of these polymer discs. It is unclear whether there was a microhole in these polymer samples that I did not detect microscopically, or whether the polymer is simply far more permeable than we had anticipated. It was observed that polymer rupture could be avoided by cutting a larger piece, and it is surmised that the tensile stress created at the central diffusion zone during cutting is minimised if the piece is larger, because the point of cutting is further away. Of note, there were no difficulties with immediate rupture of the human BrM samples.

2.4.1 Diffusion across human BrM Samples

The results of the human BrM diffusion experiments are shown in Figure 2.4. There was considerable variation between samples. Mean diffusion flux at 24 hours was 20.48 / 4mm / 24 hours (standard deviation 7.38 / 4mm / 24 hours)

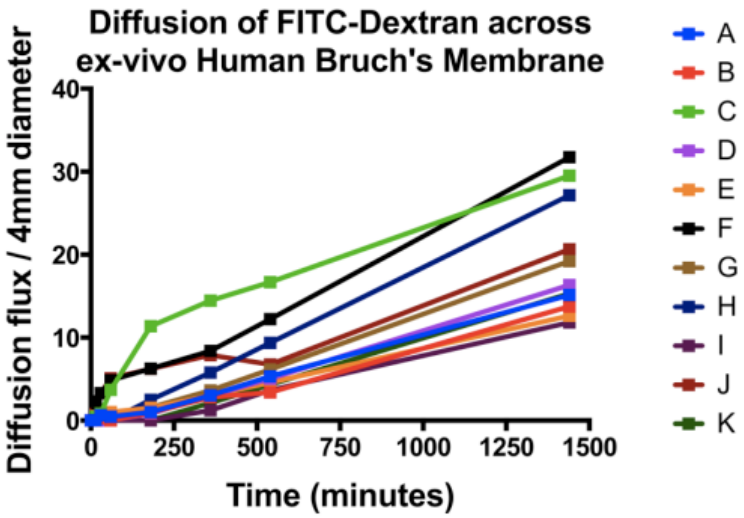

Figure 2.4: Diffusional Flux of FITC-Dextran (MW 40,000) across samples of human BrM over 24 hours.

Sample readings showed considerable variation between patients. There was an almost three fold difference in diffusional flux between sample I (11.81 / 4mm / 24 hours) and sample F (31.74 / 4mm / 24 hours).

Hussain *et al.* were able to demonstrate that age was highly correlated with a linear decrease in FITC-Dextran diffusion.[134] However we were unable to show a definitive

correlation. Linear regression was performed. As can be seen from the scatterplot in Figure 2.5, age was not a significant predictor of diffusion flux (R^2=0.011, F[1, 9] = 0.07, p=0.0762).

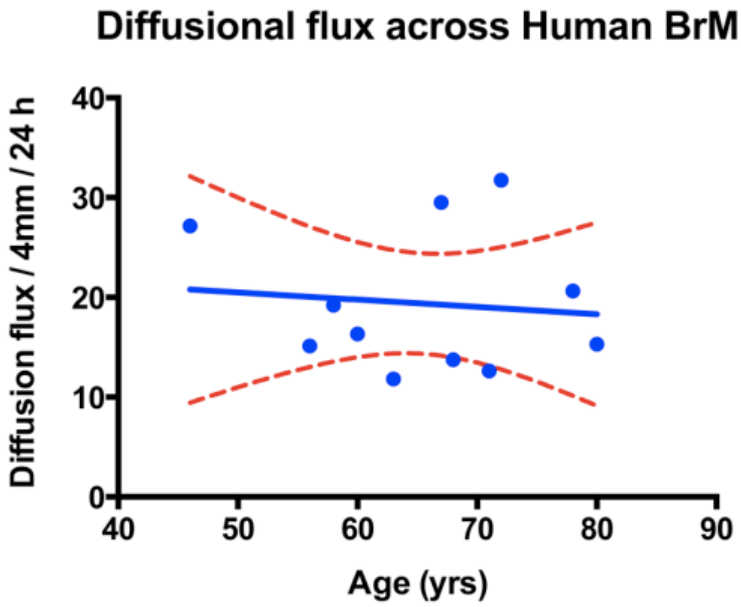

Figure 2.5: Plot of diffusion flux per unit area of human BrM at 24 hours against age at time of death.

Blue line = line of best fit; Red dashed lines indicate 95% confidence interval. Each blue dot represents a patient sample. Patient ages ranged from 46 to 80 years (mean 65.4 years, SD 10.1). There was no statistically significant correlation between age and diffusional flux of 40,000MW FITC-Dextran at 24 hours (p=0.76).

2.4.2 Diffusion across Polymer, with and without ARPE-19 cells

The diffusional flux across the polymer and human BrM is shown in Figure 2.6. Levene's test confirmed homogeneity of variance (p=0.350). A one-way ANOVA was conducted to determine if the diffusion flux was different between polymer without cells (n=7), polymer with cells (n=6), and human BrM (n=11). For polymer samples, the 120 minute timepoint was used for analysis. There was no 120 minute timepoint for the human BrM samples, therefore the 180 minute timepoint was used. Data is presented as mean ± standard deviation. Diffusion was statistically significantly different between

different groups, $F(2, 21) = 24.141$, $p < .0001$, $\omega^2 = 0.64$. Diffusion increased from human BrM (5.02 ± 3.88), to polymer with cells (22.07 ± 11.99) to polymer without cells (33.01 ± 10.50), in that order. Tukey post-hoc analysis, with adjustment of the alpha level to allow for multiple comparisons revealed that the diffusion increase from human BrM to polymer with cells (17.05, 95% CI (8.86 to 25.23)) was statistically significant ($p = 0.002$), but the increase between polymer with cells to polymer without cells did not reach statistical significance (p=0.08).

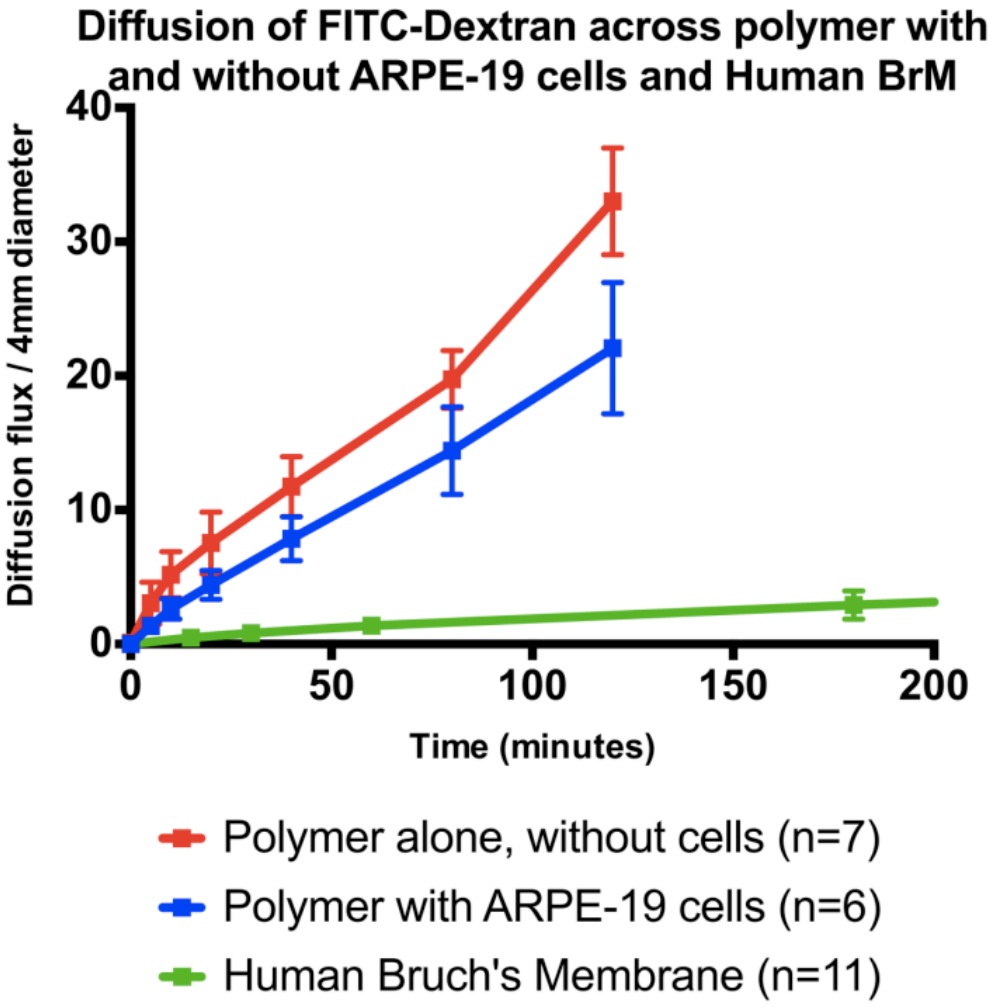

Figure 2.6: The diffusional flux of FITC-Dextran across human BrM compared with polymer, both with and without ARPE cells.

The polymer is around 15-fold more permeable (33 vs. 2.1nmol /4mm/120 minutes) than human BrM, but with an intact RPE monolayer the polymer is slightly less permeable (22 nmol/4mm/120 minutes), allowing diffusional

flux to be around 10 fold that of human BrM. Thickness of the specimen needs to be considered here, because diffusional flux is inversely proportional to thickness. Mean thickness of the human BrM samples was 13.8 microns (SD 0.9 microns), compared to mean thickness of 42 microns for the polymer. Diffusion across the polymer can be calculated as 48 times (33/2.1 x 42/13.8) higher than diffusion across human BrM.

2.5 Discussion

Hussain *et al.* used 21.2kDa fluorescein-isothiocyanate labelled Dextran to conduct extensive studies of the diffusion capacity of human BrM for macromolecular transport. They used 14 macular BrM samples (age range 9-92) and 19 peripheral BrM (age range 4-90), and identified three main findings. Firstly, there was a statistically significant decrease in diffusional flux with increasing age. Second, the decrease was far more marked for central BrM compared to peripheral BrM. Diffusional flux in BrM taken from 90-year-old donors was reduced to 6.5% and 44% for macular and peripheral regions respectively, compared to the first decade of life. Finally, BrM from 5 patients with AMD showed much lower diffusional flux than controls, and were outside the 99% confidence limit of the control population. Notably, only peripheral BrM could be used for these studies because the gross tissue architecture of the macular regions were too disturbed to allow adequate dissection of BrM, but it can be inferred that diffusional flux across macular BrM would lower still.

My experiments could not demonstrate a statistically significant correlation between increasing age and reduction in diffusional flux. All of the BrM samples for our experiments were taken from healthy eyes; there were no AMD eyes. The age range of our donors (46-80 years) was considerably narrower than studies by Hussain *et al.* and this may be one reason why we were not able to demonstrate a negative linear correlation between age and diffusional flux. Furthermore, we were using MW 40,000 Dextran and Hussain has previously shown that the age-related decrease in flux is more pronounced if lower molecular weight (e.g. 10,000 or 20,000) Dextrans were used. We had deliberately used MW 40,000 because the aim of our experiments was to determine differences in diffusional flux between polymer and human samples, rather than to demonstrate differences between the human donor samples.

Our results show that after allowing for differences in thickness, the polymer is approximately 48 times more permeable than BrM. One limitation of this experiment was that the time points between the polymer samples and the human BrM samples were different. This difference arose because during the very early stages of this project (before I joined the group), a variety of different polymers were being tested and variations in diffusion flux were evident even after 120 minutes. However, differing time points make it much more difficult to fairly compare the polymer samples with the human BrM samples. In retrospect it would have been helpful to prolong the polymer diffusion experiments from 120 minutes to 180 minutes. During the statistical analysis I have deliberately chosen the 180 minute data for the human BrM to compare with the 120 minute data for the polymer samples. This would tend to *underestimate* the difference between the human BrM and the polymer groups, yet the difference was still statistically significant.

The observation that numerous polymer samples had to be abandoned, because of apparent immediate leak suggesting polymer rupture, warrants some discussion. It was unclear what the cause of this was immediate leak was. In some cases there was an obvious hole in the sample but in many, no hole could be found even on microscopic examination. It is possible that there was a microhole that I did not detect microscopically. The additional observation that polymer rupture could be avoided by cutting a larger piece indicates another variable that may potentially contribute to the result that I had not considered when conducting these experiments.

Lu *et al.* have proposed a mesh-supported submicron parylene-C membrane (MSPM) as a potential artificial BrM for the treatment of AMD.[126] The investigators measured the diffusion coefficients of FITC-dextran molecules of a variety of molecular weights (ranging from 4000 to 250,000) for MSPMs with ultrathin parylene-C. They tested two thicknesses of parylene-C, 0.30μm and 0.15μm, and concluded that the diffusion coefficients of these membrane thicknesses were similar to that of healthy human BrM. Conceptually, RPE transplantation involves replacement of BrM but in reality, the term 'replacement' is misleading, because the host BrM is not being removed. Removal of host RPE is possible[138] but any surgical attempt at host BrM removal is likely to lead to massive choroidal haemorrhage. Transplanted RPE on a BrM substitute is likely to be placed on top of the existing BrM surface, and it is therefore insufficient for the BrM substitute to be as permeable as human BrM in the first decade of life – it needs to be *more* permeable than that, because it should not be the limiting factor in diffusion of solutes to and from the choroid. It therefore seems that even submicron parylene-C

membranes would not allow sufficient diffusion of macromolecules. Although the 60:40 P(MMA:PEGM) copolymer succeeds in allowing greater permeability than is normally seen in human BrM, it is unclear exactly *how* much more permeable a putative artificial BrM needs to be.

It is almost 30 years since Alan Bird and John Marshall first observed serous pigment epithelial detachments in elderly people, and hypothesised that this occurs due to a lipophilic barrier in BrM, leading to obstruction of the normal efflux of fluid directed from the RPE to the choroid.[139] Subsequent experiments have confirmed that the hydraulic resistivity does indeed correlate with esterified cholesterol in human BrM.[140] Liu *et al* observed pigment epithelial detachments in vitro, using foetal RPE cells cultured either on polyethylene terephthalate (PET) or on poly(L-lactide-co-ε-caprolactone), (PLCL).[141] Liu *et al* demonstrated that smooth scaffolds were associated with higher rates of RPE detachment than fibrillary, electrospun scaffolds, for both PET and PLCL.[141] These results taken in conjunction therefore suggest that the ideal scaffold to act as an artificial BrM would have to be both fibrillary and highly permeable, to prevent RPE detachment. With respect to these qualities, the polymer evaluated in the above experiments shows considerable promise.

Our experiments have studied diffusional flux across polymer and human BrM, which can be used as a surrogate measure of the transport of solutes. We have not made any attempt to take measurements of hydraulic conductivity i.e. the transport of fluid and this should be considered when planning future work.

2.6 Conclusions

- RPE transplanted on an artificial BrM is likely to be positioned on the surface of the existing BrM and therefore needs to be more permeable than BrM, to allow adequate transport of gases, nutrients, cytokines and waste products.

- After allowing for differences in thickness, the 60:40 P(MMA-co-PEGM-succinimidyl carbonate) is around 48 times more permeable than BrM.

- It is unclear how much more permeable the artificial BrM needs to be. It is also unknown whether an artificial BrM can be too permeable.

- AMD is associated with serous pigment epithelial detachments, which occur due to reduced hydraulic conductivity of BrM. We have not measured hydraulic conductivity of BrM or of the polymer but this is work that should be conducted in future.

Chapter 3: RPE POLARISATION

> "POLARITY, or action and reaction, we meet in every part of nature; in darkness and light, in heat and cold; in the ebb and flow of waters; in male and female; in the inspiration and expiration of plants and animals; in the systole and diastole of the heart; in the undulations of fluids and of sound; in the centrifugal and centripetal gravity; in electricity, galvanism, and chemical affinity. Superinduce magnetism at one end of a needle, the opposite magnetism takes place at the other end. If the south attracts, the north repels."
>
> - Ralph Waldo Emerson, *Compensation*, 1841

3.1 Introduction

The term "epithelium" is used to describe the cellular covering of the internal and external surfaces of the body. The main function of any epithelium is to form a dynamic barrier that regulates movement of fluid and molecules between body compartments. To achieve this, all epithelial surfaces show polarity, with the apical surfaces commonly facing an acellular lumen. The retinal pigment epithelium also demonstrates cell polarity and has distinct apical and basolateral zones. Cellular polarity is vital for normal RPE function. Unlike all other human epithelia, the apical surface of the RPE does not face an acellular lumen, but instead faces a tissue, the neurosensory retina.[142]

3.1.1 Polarity of the RPE

The polarity of the RPE is illustrated in Figure 3.1 and can be demonstrated in terms of cell structure, distribution of organelles, distribution of membrane proteins, and secretion of growth factors.[7]

3.1.1.1 Cell Structure

The basal surface of the RPE contrasts markedly with the apical surface. The RPE has long apical microvilli that extend into the subretinal space and surround the photoreceptor outer segments. Although the RPE and the neurosensory retina are apposed but not adhered, the apical microvilli establish a complex of close structural interaction with the retinal photoreceptors[7].

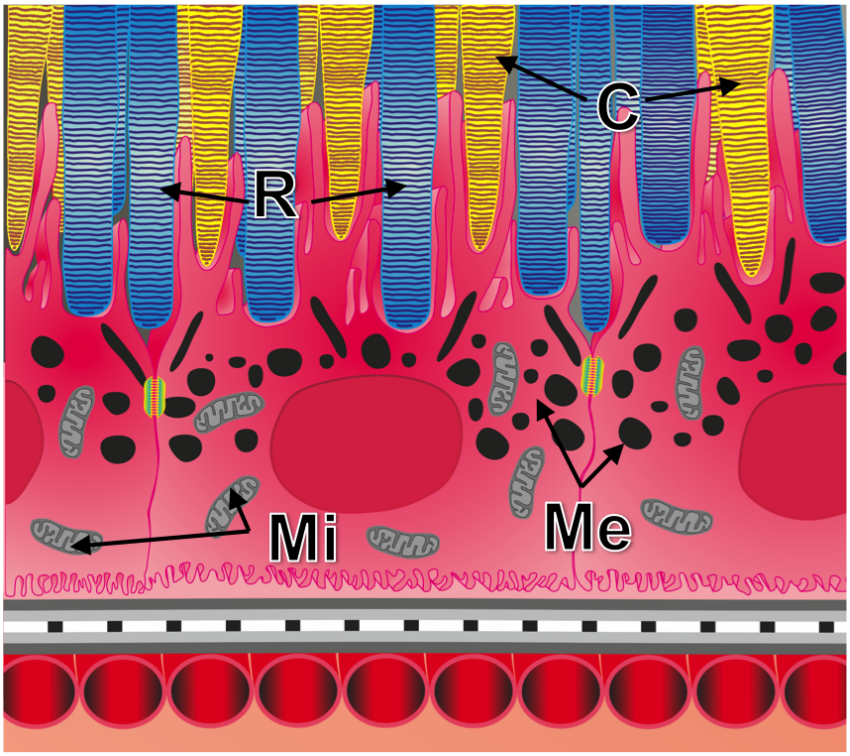

Figure 3.1: RPE Cell structure and Organelle Distribution

RPE apical microvilli have a close structural interaction with the outer segments of the rods (R – shown in blue) and Cones (C – shown in yellow). Melanosomes (Me) are predominantly located in the apical and mid-portion of the cells. Most of the mitochondria (Mi) are located near the basolateral side of the cell.

3.1.1.2 Distribution of Organelles

Melanosomes, the organelle responsible for synthesis, storage and transport of melanin, are predominantly located in the apical and mid-portion of the cell,[143] while the majority of the mitochondria are located near the basolateral side[7].

3.1.1.3 Membrane protein distribution

In the dark, there is an intense and continuous flux of Na+ within the photoreceptors, from the outer segment to the inner segment via the connecting cilium. This is balanced by the efflux of K+ from the inner segments, thereby reducing the polarisation of the photoreceptor plasma membrane. A high Na+ photoreceptor environment is required to support this process and is achieved because there is a Na-K-ATPase located in the apical region of the RPE cell.

The RPE transports fluid from the subretinal space, and this is achieved because of the Cystoid Fibrosis Transmembrane Conductance Regulator (CFTR). CFTR is a chloride transporter that is usually found in the apical region of epithelial cells and is the abnormal protein in patients with cystic fibrosis. In the RPE, CFTR is basally located, and provides the driving force for secondary fluid transport, thereby creating a negative hydrostatic pressure within the subretinal space, which is essential in ensuring that the neurosensory retina remains attached to the RPE.

Lehmann *et al.* have noted that RPE cells show an unconventional distribution of membrane proteins, and a number of proteins that are located basolaterally in other epithelia are expressed apically or in a non-polar fashion in RPE cells.[144] Conversely, CFTR is located apically in other epithelia but is located basally in the RPE. Table 3.1 compares the conventional epithelial localisation of various membrane proteins with the localisation in RPE.

Plasma membrane protein	Purpose	RPE localisation	Conventional epithelial localisation	Model
MCT1 (monocarboxylate transporter 1)	Removal of lactate generated by neurosensory retina	Apical	Basolateral	Cultured hfRPE *Ex-vivo* adult rat eyes
Na+K+-ATPase (sodium-potassium-adenosine triphosphatase pump)	Maintain high interphotoreceptor [Na+] for phototransduction	Apical	Basolateral	Cultured hfRPE Native adult rat eyes
NCAM (Neural cell adhesion molecule)	Regulate adhesive contacts with photoreceptors	Apical	Basolateral	Native developing and adult rat eyes
EMMPRIN/CD147 (Extracellular matrix metalloproteinase inducer)	Induce matrix metalloproteinases; remodelling and maintenance of interphotoreceptor matrix	Apical	Basolateral	Cultured hfRPE Native and ex-vivo adult rat eyes
JAM-C (Junctional Adhesion Molecule C)	Junctional adhesion molecule	Apical / tight junctions	Basolateral / tight junctions	Cultured hfRPE Native adult mouse eyes
CAR (Coxsackie-Adenovirus Receptor)	Cell adhesion molecule	Non polar	Basolateral	Cultured hfRPE; ARPE-19
TfR (Transferrin receptor)	Iron transport by transcytosis	Non polar	Basolateral	ARPE-19
CFTR (Cystic fibrosis transmembrane conductance regulator)	Chloride transporter (facilitating secondary fluid transport)	Basolateral / non polar	Apical	Native hfRPE

Table 3.1: A comparison of the conventional epithelial localisation of various membrane proteins with the localisation in RPE.

Several proteins that are normally present in the basolateral membrane of conventional epithelia have been identified in the apical regions of RPE cells. The converse is true for only one membrane protein, CFTR, which is located in the apical membrane of conventional epithelia but shows a basolateral distribution in RPE cells. Table adapted from Lehman *et al.*[144]

3.1.1.4 Secreted growth factors

The RPE preferentially secretes a number of proteins from its apical surface, including hyaluronan, matrix metalloproteinase-2 (MMP-2), tissue inhibitor of metalloproteinase-1 (TIMP-1), Interphotoreceptor matrix Retinoid Binding Protein (IRBP), SPACR (sialoprotein associated with cones and rods - also known as IPM150) and SPACRCAN (sialoproteoglycan associated with cones and rods – also known as IPM200).[145] These are all associated with the formation, maintenance and turnover of the interphotoreceptor matrix, and have clinical relevance because they can be associated with ocular disease. Choroidal neovascularisation (CNV), the abnormal growth of new blood vessels in the sub-RPE space, is the pathogenic process in neovascular AMD. CNV stimulates the formation of MMP-2 which itself is angiogenic and therefore potentiates disease. Mutations in TIMP-1 are associated with necrotising scleritis, a severe sight-threatening inflammatory condition of the sclera.[145]

3.1.1.4.1 Pigment Epithelium-Derived Factor (PEDF)

Pigment Epithelium-Derived Factor (PEDF) is a soluble extracellular protein that was discovered as a product of cultured RPE cells from human foetal eyes,[146] but was subsequently found to be secreted from a wide variety of tissues in the body, including adipose, brain, spinal cord, plasma, bone, prostate, pancreas, heart, liver and lung.[147]

PEDF secretion from the RPE is polarised, and it is preferentially secreted from the apical membrane. Biochemical and immunohistochemical studies have identified PEDF in washes of the interphotoreceptor matrix, vitreous, and aqueous of several mammalian species.[148] PEDF is a member of the Serpin superfamily of ***se***rine ***p***rotease ***in***hibitors and it has two main roles:

(a) it is neurotrophic, allowing the survival and differentiation of photoreceptors and other neurons within the retina

(b) PEDF is antiangiogenic, and can inhibit neovascularisation in both the posterior segment (vitreous, retina) and in the cornea.

3.1.1.4.2 Vascular Endothelial Growth Factor (VEGF)

Vascular Endothelial Growth Factor (VEGF), originally known as Vascular Permeability Factor (VPF) was first identified in 1983 by Senger *et al.*[149] although the existence of a "blood vessel growth stimulating factor" was postulated as early as 1939 following historical observations that tumour growth is associated with increased vascularity.[150] VEGF is highly angiogenic and can be regarded conceptually as the antithesis of PEDF. Although VEGF has physiological roles in blood vessels development during embryological development, after injury, or to bypass blocked vessels, overexpression of VEGF is well recognised in the pathophysiology of disease. In 1989 Ferrara made the first anti-VEGF antibody whilst working at Genentech.[151] In mammals there are five subtypes of VEGF, shown in Table 3.2. VEGF-A has multiple isoforms that result rom alternative mRNA splicing of a single 8-exon *VEGFA* gene. The resulting isoforms can be divided into two groups depending on the terminal exon (exon 8) splice site. Isoforms that result from the proximal splice site (denoted VEGFxxx) are expressed during angiogenesis, while isoforms from the distal splice site (VEGFxxxb) are anti-angiogenic.[152]

Isoform	Biological effects
VEGF-A	Angiogenesis • Mitosis and migration of endothelial cells • Increased matrix metalloproteinase activity • Creation of fenestrations and blood vessel lumens Chemotactic for macrophages and polymorphonuclear leucocytes Vasodilation, by nitric oxide release
VEGF-B	Embryonic myocardial angiogenesis; Inflammatory angiogenesis
VEGF-C	Lymphangiogenesis without angiogenesis
VEGF-D	Lymphangiogenesis with angiogenesis, particularly in embryogenesis
VEGF-E	VEGF homologues produced by Orf viruses
PlGF	Angiogenesis during ischaemia, inflammation, wound healing, cancer
VEGF-F	Identified in snake venom

Table 3.2: Isoforms of Vascular Endothelial Growth Factor (VEGF) and their biological effects.

Placental growth factor (PlGF) was first discovered in the placenta, as implied by the name, but is also included in the VEGF family, which comprises seven secreted glycoproteins. However, VEGF-E and VEGF-F are not expressed in mammals.

VEGF is produced constitutively by human RPE cells, and is preferentially secreted from the basal membrane.[153] Increased VEGF production is associated with a variety of retinal disorders and over the last ten years, anti-VEGF injections into the vitreous have been used in the treatment of several retinal disorders including neovascular age related macular degeneration,[154] diabetic macular oedema,[155] and macular oedema secondary to retinal vein occlusion.[156] However VEGF is also essential for the survival

and maintenance of functional morphology of the choriocapillaris.[153] This is consistent with findings of the CATT study, a large clinical trial showing that geographic atrophy occurs in up to one fifth of patients receiving regular intravitreal anti-VEGF drugs for neovascular AMD.[35]

3.1.1.5 Mechanism of RPE Polarisation

The mechanisms in which RPE cells polarise is not yet fully understood, but can be categorised into intracellular, extracellular, and intercellular.

1. *Intracellular* – The maturation of the apical surface and the development of long apical microvilli appear to be highly dependent on the presence of a protein called Ezrin, which, with its associated proteins radixin and moesin, make up the ERM family, all of which may play a role in the visual cycle.[7] The polar distribution of these proteins is achieved by preferential transcytosis trafficking form the Golgi to the apical membrane, together with suppression of basolateral sorting mechanisms.

2. *Extracellular* – Receptors interacting with extracellular signalling molecules such as integrins and cadherins also appear to play a role in achieving apical to basolateral polarity.

3. *Intercellular* – The formation of tight junctions between RPE cells appears to be important in promoting polarisation. Therefore the polarisation of RPE cells is intrinsically linked to the formation of an RPE monolayer with tight junctions, which is vital for its function as the second blood retinal barrier.

3.1.2 The RPE as a barrier

There are two barriers between the retina and the bloodstream. The inner blood-retinal barrier is made of the endothelial cells of the retinal vasculature. The RPE forms the outer blood-retinal barrier, and separates the outer neurosensory retina from the choriocapillaris. The cornerstone of any epithelial barrier is the tight junction, which limit diffusion through the paracellular spaces between cells in the monolayer. Although tight junctions in some tissues, such as in the epithelium of the urinary bladder, completely block the paracellular path, physiologists have long since recognised that tight junctions in many epithelia are semipermeable, semiselective, and tissue specific.[157] Tight junctions define the boundary between the apical and basolateral membranes, and actively participate in the intracellular trafficking of proteins to the appropriate surface.[158]

Three stages of tight junction formation have been suggested. Rudimentary tight junctions allow the RPE to form a leaky barrier but also permit partial polarisation of membrane proteins. The intermediate stage of tight junction development is associated with the maturation of both the junctional complex and the cytoskeleton, further enhancing cell polarisation. The final stage is characterised with an increase in number and branching of tight junctional strands, allowing the formation of a tight epithelium and a blood retinal barrier. Based on studies of chick RPE, mature tight junctions are composed of ZO-1 (zonula occludens-1), occludin, and claudins 1, 2, 5 and 12 (see Strauss for review).[7]

The appearance of RPE cells in culture differs depending on whether the cells are confluent and functioning as a monolayer (i.e. functioning as a tissue) or whether they are simply isolated pockets of cells. This difference in appearance is shown in Figure 3.2.

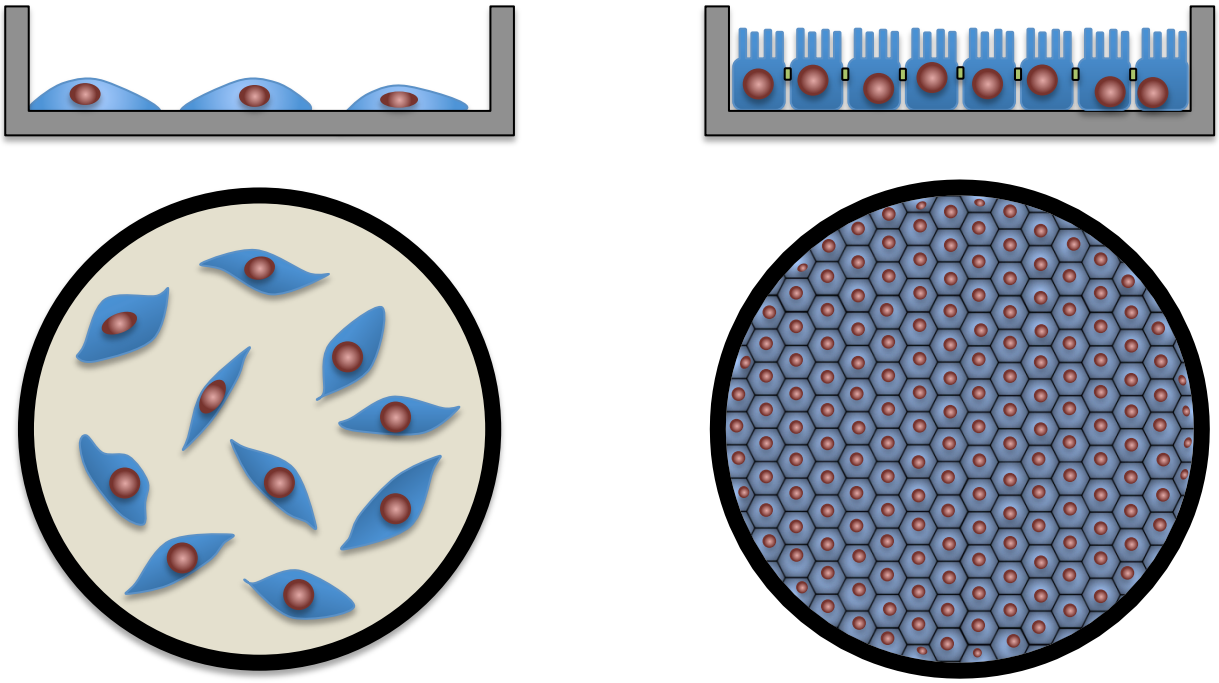

Figure 3.2: Subconfluent vs. confluent RPE cells.

Subconfluent RPE cells are spindle shaped and do not demonstrate the normal structural and functional characteristics of RPE cells *in vivo* (Top left, Bottom Left). With time, ARPE-19 cells become confluent, develop tight junctions and become polarised, allowing the formation of apical microvilli (Top Right, Bottom Right). Adapted from Pfeffer *et al.* (2014).[159]

3.1.2.1 Techniques for studying barrier and polarisation

The methodology required for the study of RPE polarisation is similar to that required for the study of RPE barrier function. For these studies, the culture of epithelial cells on plastic or glass surfaces, either in a tissue culture flask or in tissue culture wells, is not suitable, because when the epithelial cells form fully differentiated tight junctions, the basolateral membrane does not have access to the tissue culture media which may in turn restrict the uptake of key nutrients via transporters polarised to the basolateral membrane. This predicament is easily solved by seeding RPE cells on to a permeable polycarbonate, polyester or collagen-coated polytetrafluoroethylene (PTFE).[160] These materials differ in their thickness, pore size, and optical properties, but all allow the formation of a polarised RPE monolayer. Such permeable supports (often simply referred to as Transwells ® [Corning, USA]) allow cell culture in media designed to

resemble the apical and basal environments of *in vivo* epithelium, as shown in Figure 3.3.

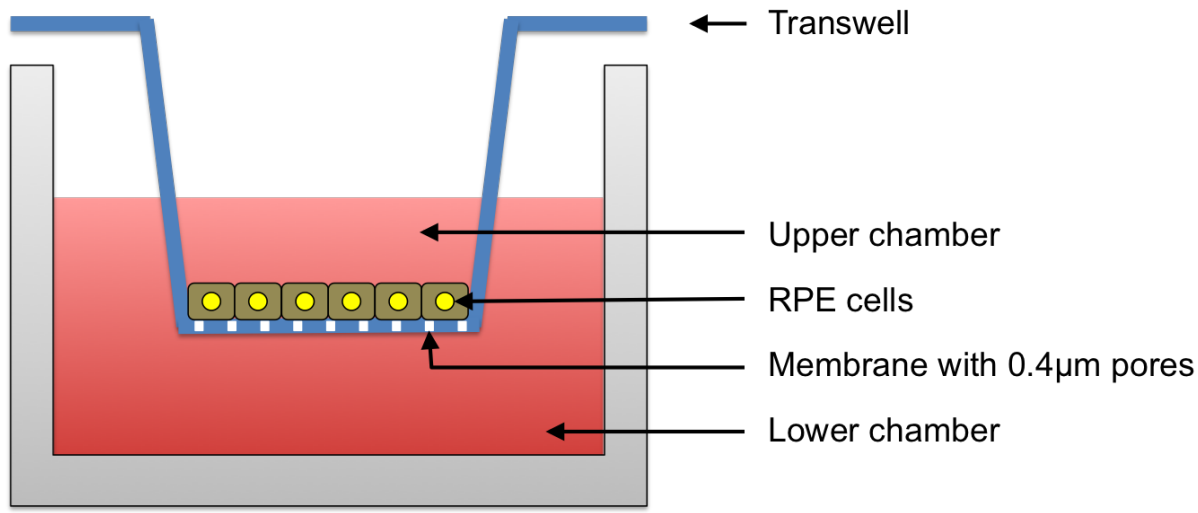

Figure 3.3: Transwells ® [Corning, USA]) allow cell culture in media designed to resemble the apical and basal environments of *in vivo* epithelium.

Transwells allow easy sampling of tissue culture medium from the upper and lower chambers for measurement of protein concentrations, and also facilitate assessment of the transepithelial electrical resistance (TEER).

Polarisation can be studied by assessing the upper and lower compartments for concentrations of secreted protein, or by assessing the monolayer either for the steady state localisation of plasma membrane proteins, or by assessing polarised membrane protein delivery.[144]

Barrier function is usually assessed by the measurement of TEER. This method models the epithelial monolayer as a circuit of parallel resistors composed of individual transcellular and paracellular elements (see Figure 3.4), where each of these elements can be regarded as a circuit of resistors in series,[161] such that:

$$R_{transcellular} = R_{apical\ membrane} + R_{basal\ membrane}$$

$$R_{paracellular} = R_{tight\ junction} + R_{lateral\ intercellular\ space}$$

and

$$1/R_{total} = 1/R_{transcellular} + 1/R_{paracellular}$$

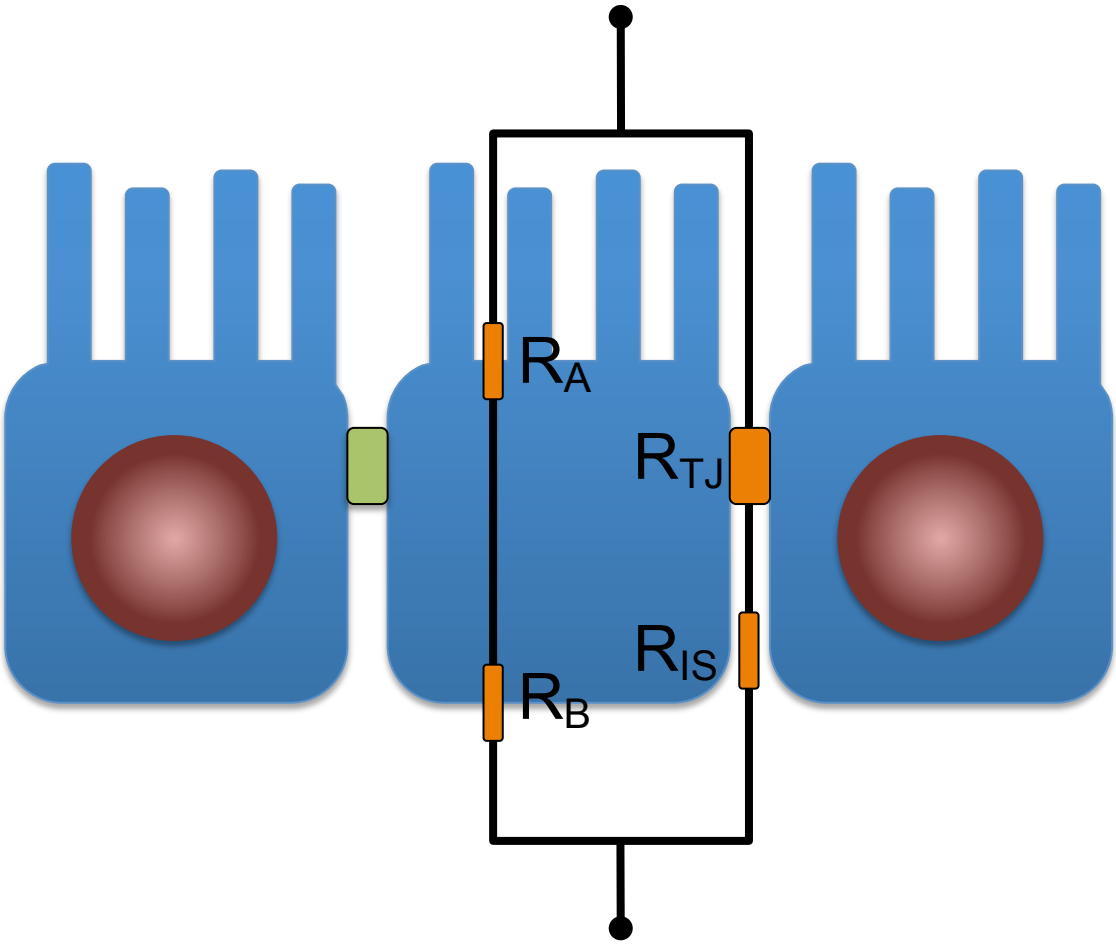

Figure 3.4: Components of Transepithelial Electrical Resistance.

Transepithelial electrical resistance measurements are based on the notion that the epithelial monolayer can be regarded as a circuit of parallel resistors composed of individual transcellular and paracellular elements. The transcellular electrical resistance is the sum of the resistance across the apical membrane (R_A) and the resistance across the basal membrane (R_B). Similarly, the electrical resistance of the paracellular pathway is the sum of the resistance across the intercellular tight junction (R_{TJ}) and the lateral intercellular space (R_{IS}), although the latter is rarely significantly physiologically. Adapted from Anderson and Van Itallie (2009).[161]

It is often mistakenly assumed that the transepithelial resistance represents the resistance of the ion current across the tight junction, but the equation above demonstrates that this can only be true when the paracellular junction is relatively leaky

and the transcellular resistance is significantly higher than the paracellular resistance. The TEER is dominated by the element with the lowest resistance. The lateral intercellular space (R_{IS}) could in theory contribute to resistance in series with the tight junction, but there is little evidence that this is physiologically significant.[161]

The Epithelial Voltohmmeter (EVOM2, World Precision Instruments, Sarasota, Florida USA) allows the measurement of resistance across epithelial layers. Although it has several well-recognised limitations, this device is in widespread use and is convenient for measuring resistance in cultured epithelium without breaching sterility, thereby allowing the sequential monitoring of TEER.[162]

3.1.3 Cellular models of RPE polarisation and barrier function

3.1.3.1 Cell culture techniques

Ideally, cell culture conditions should mimic *in vivo* epithelial properties. Therefore the culture of epithelial cells in plastic flasks is not ideal, and certainly not suitable for the assessment of barrier function and/or polarisation, because the formation of tight junctions precludes access of the tissue culture media to the basolateral membrane. This is likely to reduce the epithelial uptake of key nutrients that are normally transported via membrane proteins that are polarised to the basolateral membrane of the cell.

Transwell (Corning, USA) is a proprietary product that allows cell culture on a permeable support with microporous membranes. Suspension of cells in this way affords independent access, for both the cell layer and the researcher, to separate apical and basolateral chambers of tissue culture media. Cellular functions such as transport, absorption, and secretion can be studied using this system. It allows polarised cells to feed basolaterally, which may better mimic the natural state, and there is some suggestion that greater cell differentiation can be achieved as a result.[160]

There are three types of Transwell membrane, each with different thickness, pore size and optical properties. Of note, two of these materials, namely polyethylene terephthalate (PET, also known as polyester) and polytetrafluoroethylene (PTFE), have been proposed as cellular scaffolds for RPE transplantation.[86, 127]

3.1.3.2 *In vitro* RPE models

Primary RPE cells, from various species, have been commonly used for *in vitro* RPE culture, and have been shown to retain key elements of RPE function including photoreceptor outer segment phagocytosis and transport retinoids.[159, 163] However human eyes can be difficult to obtain for primary culture, may exhibit physiological differences between donors and often need purification to establish a uniform population of cells.

An immortalised cell line is a population of cells that are all derived from a single cell, and therefore consisting of identical genetic make up. Although these cells would not normally proliferate indefinitely *in vivo*, genetic mutation causes cells to avoid normal senescence and therefore continually divide for prolonged periods in cell culture.

There are several RPE cell lines available, both for human cells and for other species. Cell lines can spontaneously occur, or can be created by transformation of a primary culture with an oncogene or viral proteins.

RPE-J is a cell line that was created by infecting primary rat RPE culture with the temperature sensitive SV40 virus. RPE-J cells demonstrate many typical features of RPE cells, including the production of melanosomes, but the polarity of some membrane proteins, including N-CAM (Neural Cell Adhesion Molecule) and Na+K+-ATPase (sodium-potassium-adenosine triphosphatase pump) differs from the *in vivo* polarisation. BPEI-1 is a spontaneously arising RPE cell line derived from Long Evans rats.

There are two human RPE cell lines: D407 and ARPE-19. Both cell lines occurred due to spontaneous transformation. ARPE-19, first described by Dunn *et al.,*[77] is a commercially available cell line that expresses RPE-specific proteins such as CRALBP and RPE65, and demonstrates barrier function measurable by transepithelial resistance.

3.1.4 Measurement of VEGF and PEDF using Sandwich ELISA

Enzyme-linked immunosorbent assay (ELISA) is a tool for the detection and quantification of specific antigens or antibodies in a given sample. It is widely used not only in biomedical research but also as an industrial quality control tool, and as a diagnostic tool in clinical medicine.[164] For example, the home pregnancy test uses the Sandwich ELISA technique.[165]

The principle of ELISA, sometimes referred to as an enzyme immunoassay (EIA), is derived from the radioimmunoassay (RIA), which was first described by Rosalyn Yalow and Solomon Berson in 1960. Yalow used the technique to measure endogenous plasma insulin, and was awarded the Nobel Prize in 1977. RIA was developed to detect and measure small quantities of biological molecules, but because of safety concerns associated with the use of radioactivity, RIA has now been completely replaced with ELISA.

The basic principle of ELISA relies on specific binding between an antigen and its antibody. Using a 96-well microtitre plate, the antigen in any given sample is immobilised and bound to the surface of the well. The antigen is subsequently allowed to bind to its specific antibody, which itself is detected by a secondary, enzyme coupled antibody. A chromogenic substrate for the enzyme yields a visible colour change or fluorescence, indicating the presence (and quantity) of antigen.

Technically, if the primary antibody was conjugated to an enzyme, the secondary antibody would be unnecessary, but the use of a secondary antibody conjugate avoids the expensive process of creating enzyme linked antibodies for every antigen to be detected.

Immobilisation of the antigen is important so that after incubation, any excess unbound antibody can be washed off but bound antibody will remain in the well. The main disadvantage of traditional 'indirect' ELISA is that the method of antigen immobilisation is not specific, and other proteins in the sample competitively bind to the well, thereby lowering the quantity of antigen that is immobilised. The sandwich ELISA technique overcomes this, by using a 'capture' antibody that is unique to the specific test antigen, to select it out of the sample. The principle of Sandwich ELISA is shown in Figure 3.5.

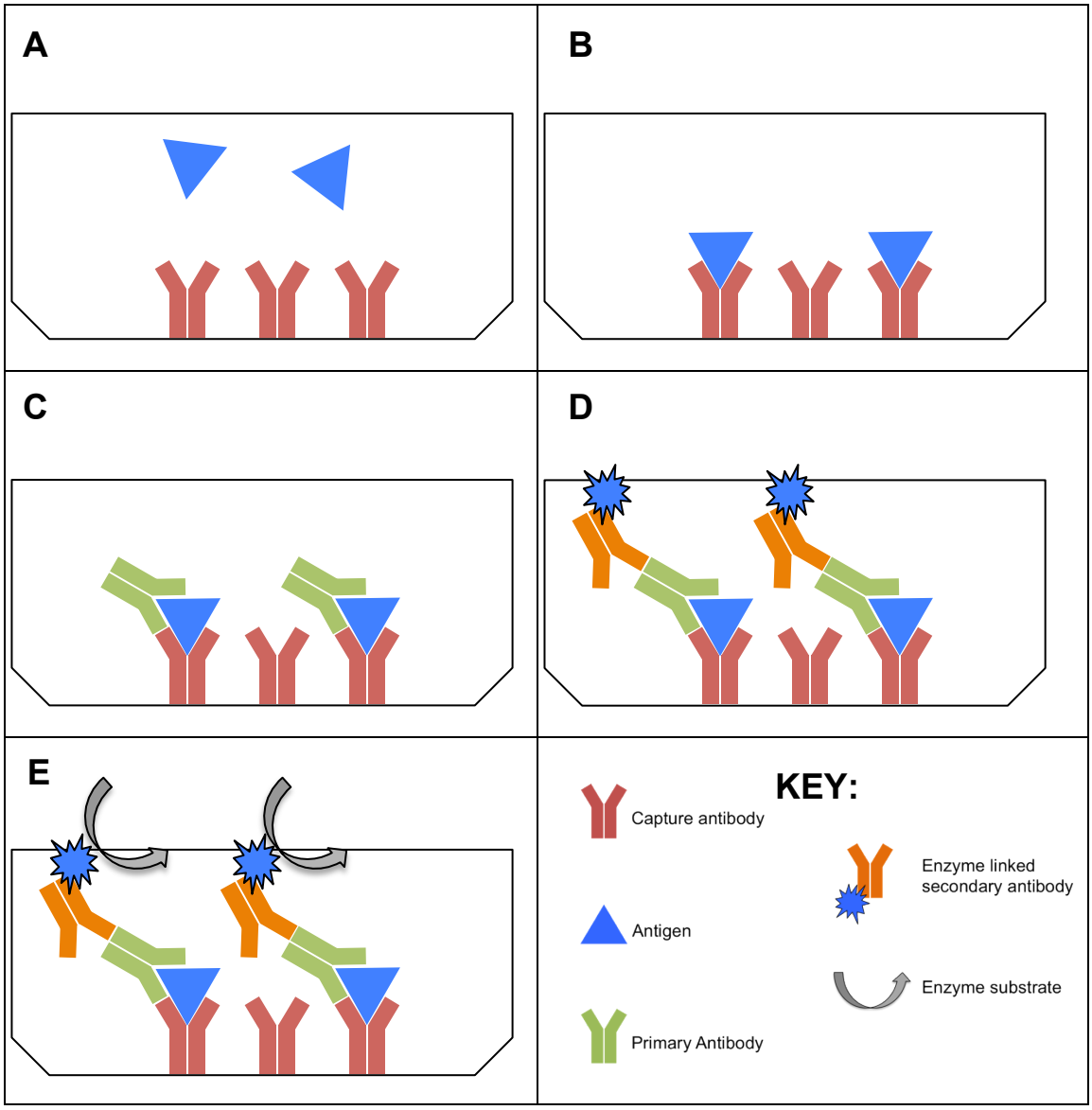

Figure 3.5: Principle of Sandwich ELISA.

In Sandwich ELISA, nonspecific binding sites are initially blocked using bovine serum albumin. The sample is then added to the plate (A), the antigen is immobilised by the capture antibody (B), and the addition of a specific primary antibody leads to a 'sandwiching' of the antigen (C). The enzyme linked secondary antibody is applied, and this binds to the Fc portion of the primary antibody (D). Unbound antibody-enzyme conjugate is washed away, the enzyme substrate is added (E), and the colour change (or fluorescence) is quantified. Use of the purified specific antibody to immobilise the antigen eliminates the need for antigen purification before the assay is performed. Adapted from Gan *et al.* (2013)[164]

3.2 Aims and Objectives

The two aims of this chapter were to assess whether the RPE cells growing on the 60:40 P(MMA-co-PEGM-succinimidyl carbonate) copolymer will (a) form a polarised monolayer of cells and (b) form intercellular tight junctions to allow the RPE layer to function as a barrier. The formation of intercellular junctions is intrinsically linked to the formation of a polarised monolayer, and these two features are therefore studied in conjunction in this chapter.

These experiments were conducted with both ARPE-19 cells and primary rabbit RPE cells. ARPE-19 cells have been used extensively in Professor Lotery laboratory in Southampton in recent years. However since the ultimate aim of this project was to develop a cell-seeded scaffold for surgical implantation in an animal model, primary rabbit RPE was seeded on to the polymer surface with the aim of transplanting these samples into rabbit eyes.

Objectives of this experiment were:

- Culture ARPE-19 cells in Transwells, and assess the degree of polarisation by measuring VEGF and PEDF concentrations in the upper and lower chambers of the Transwells.

- Compare the degree of polarisation of ARPE-19 cells growing on polymer ARPE-cells growing on the transwell insert without polymer.

- Determine the transepithelial electrical resistance of ARPE-19 cells cultured on polymer in the transwells.

- Determine the degree of polarisation and the transepithelial electrical resistance of primary rabbit RPE cells cultured on polymer or on the transwell insert without polymer.

3.3 Methods

3.3.1 Preparation of Transwells

Two 24-well culture plates (Corning, USA) were used to support 35 clear polyester (PET) Transwell inserts of 6.5mm diameter and 0.4μm pore size. Laminin (0.5 mg/ml) (Invitrogen, Paisley, UK) coatings, made in PBS, of 200μl per well were used for 30/35 of the Transwell inserts, left to dry for four hours in a tissue culture hood under sterile conditions, and then washed three times with phosphate buffered saline (PBS 1X)

The Transwell inserts were arranged in the following configuration:

Plate 1

Row A (5 wells)	Transwell insert only (no laminin coating, no cells)
Row B (5 wells)	Transwell insert + laminin coating (no cells)
Row C (5 wells)	Transwell insert + laminin coating + Primary Rabbit RPE cells
Row D (5 wells)	Transwell insert + laminin coating + ARPE-19 cells

Plate 2

Row E (5 wells)	Transwell insert + laminin coating + polymer (no cells)
Row F (5 wells)	Transwell insert + laminin coating + polymer + primary Rabbit RPE cells
Row G (5 wells)	Transwell insert + laminin coating + polymer + ARPE-19 cells

3.3.2 Preparation of polymer

A pre-cut template was used to create fifteen 6.5mm diameter discs from an electrospun 60:40 P(MMA-co-PEGM-succinimidyl carbonate) copolymer scaffold sheet. Each polymer disc was of the correct size to completely cover the membrane at the base of each transwell insert. Polymer discs were UV-irradiated overnight, and washed three times with phosphate buffered saline (PBS) before use. These discs were placed in rows E, F, and G of the transwell plate.

3.3.3 Preparation of ARPE-19 cells

ARPE-19 cells (passage 21) (American Tissue Culture Collection [ATCC] Manassas, VA] were seeded directly on to the laminin-coated porous membrane of the transwell inserts (row D) or on to the polymer disc that had been placed on top of the membrane (row G). A cell seeding density of 25,000 cells in 2µl was used, because previous experiments (data not included) had established that this was sufficient to ensure confluent RPE cells at 5 days.

ARPE media, consisting of:

- 196ml of Dulbecco's Modified Eagle Medium (DMEM) with 25mM glucose, 1.0mM pyruvate and 0.04mM phenol red (Life Technologies, catalogue number 11995)
- 2mls of foetal bovine serum (Sigma-Aldrich)
- 2ml of antibiotic/antifungal (10,000 U/mL penicillin G, 10 mg/mL streptomycin sulphate, and 25 mg/mL amphotericin B; Sigma-Aldrich)

Human ARPE-19 cells were maintained in an incubator (Nuaire NU5510E Serial # 142811022311) at 37°C under humidified atmosphere with 5% CO_2 in culture medium. Culture medium was changed every 72 h.

3.3.4 Preparation of Primary Rabbit RPE cells

Primary rabbit RPE was isolated from a 3 month old Murex half lop rabbit (Pettingill Technology Ltd, Oxford, UK). The animal was euthanised with an intravenous dose of pentobarbitone (100mg/kg) and the eye was enucleated. Following conjunctival peritomy, the four rectus muscles were identified and cut, and the optic nerve was then divided transversely, freeing the globe from the orbit. A circumferential incision 1 mm from the limbus was used to dissect and remove first the anterior segment (i.e. cornea, anterior chamber and iris) and then the crystalline lens, as shown in Figure 3.6.

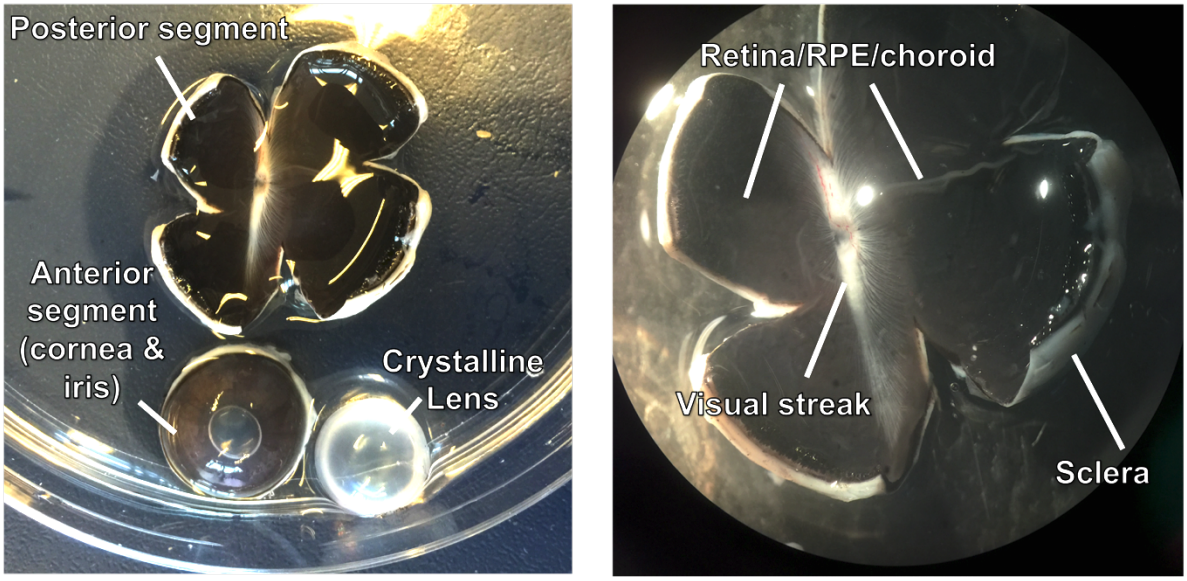

Figure 3.6: Rabbit eye dissection to harvest primary rabbit RPE cells for culture.

LEFT: Following conjunctival peritomy, the four rectus muscles were identified and cut, and the optic nerve was then divided transversely, freeing the globe from the orbit. A circumferential incision 1 mm from the limbus was used to dissect and remove first the anterior segment (i.e. cornea, anterior chamber and iris) and then the crystalline lens.

RIGHT: The posterior segment was cut in a petalloid fashion before peeling the neurosensory retina away from the RPE.

The posterior segment was cut in a petalloid fashion. The neurosensory retina, together with vitreous, were peeled from the underlying RPE. Initial attempts to mechanically peel the RPE as a sheet from the underlying BrM and choroid were unsuccessful and resulted in significant damage to the RPE sheet, so this technique was abandoned. Instead, enzymatic RPE dissection was performed by filling the posterior eye cup with Dispase (concentration**) for 30 minutes before petalloid dissection. Dispase was washed off with primary rabbit RPE media (Dispase allowed a more reliable and consistent method for harvesting primary rabbit RPE as a cell sheet.

Primary rabbit RPE cells were maintained at 37°C under humidified atmosphere with 5% CO_2 in culture medium comprising of Minimum Essential Medium (MEM) α (Life Technologies/ Invitrogen Catalogue Number 22571-020), 5% foetal calf serum (GE Lifesciences, Buckinghamshire, UK), 1% non-essential amino acids (Sigma-Aldrich,

UK), 1% B27 (Invitrogen, catalogue number 17504044), and 1% antibiotic-antimycotic solution (10,000 U/mL penicillin G, 10 mg/mL streptomycin sulphate, and 25 mg/mL amphotericin B; Sigma-Aldrich, UK). Culture medium was changed every 72 h.

Primary rabbit RPE cells (passage 1) were then seeded directly on to the laminin-coated porous membrane of the transwell inserts (row C) or on to the polymer disc that had been placed on top of the Transwell membrane (row F). A cell seeding density of 25,000 cells in 2µl was used.

3.3.5 Immunocytochemistry of human and rabbit RPE cells

Immunocytochemistry of human RPE (ARPE-19) and primary rabbit RPE cells was performed by fixation of cells with 4% PFA in an 8-well chamber slide. For blockage of non-specific binding sites, 250µl of 5% (50µl/ml) donkey blocking serum in PBS-T (PBS with 0.3% Triton). After incubation for 30 minutes at rt, the blocking serum was aspirated and 250µl of the primary antibody (1:100 ZO-1, Invitrogen, 33-9100; and 1:250 Phalloidin-tetramethylrhodamine B isothiocyanate, P1951, Sigma Aldrich), made up in PBS-T with 5% blocking serum, was applied in each well. After incubation overnight at 4°C, the cells were washed twice with PBS for 5 minutes, and the secondary antibody, an Alexa Fluor 488-conjugate (1:500 in PBS-T without any blocking serum) was applied. The plate was kept dark, by wrapping in aluminium foil, and incubated at rt for 2 hours. Following two further five minute washes with PBS, 250 µl of 4′,6-diamidino-2-phenylindole (DAPI) (5µg/ml in distilled water) was applied and incubated for only 6 minutes. The DAPI was then aspirated, cells were washed twice with PBS, and a coverslip was mounted prior to imaging. Samples were imaged using a Leica DM IRBE microscope (Leica Microsystems UK Ltd, Milton Keynes, England), using a digital camera and controller (Model C4742-96-12G04, Hamatsu Photonics KK, Japan), Volocity Software v4 (Improvision 2007, Coventry, UK) on an iMac7.1 (Mac OS 10.4.11, Apple Inc, Cupertino, California, USA).

3.3.6 VEGF Sandwich ELISA

The Human VEGF ELISA Kit (Invitrogen KHG 0111) was used to determine the presence and quantity of VEGF secreted in the apical and basal chambers of each Transwell. The media was completely aspirated from the upper chamber and the lower chamber of each Transwell, and replaced with fresh media (250µl and 500µl for upper

and lower chambers respectively). Rather than discarding the used media, it was instead placed in individual Eppendorf tubes and stored at -80ºC.

The kit was used according to the manufacturer's instructions. Care was taken to ensure that the microtitre plate and all reagents were at room temperature (rt) before use. Apart from "blank" wells, 50µl of Incubation Buffer and 100µl of Standard Diluent Buffer were added to each well in the plate. A standard curve was generated using serial dilutions of highly purified Human VEGF, and 100µl of each standard was used. For samples of tissue culture media from the upper and lower chambers of the Transwell, 50µl of sample was diluted 1:1 with an equal volume of diluent buffer. Two different samples from each condition were used for testing, and each sample was tested in duplicate.

Samples and standards were incubated for two hours at rt. The plates were then washed thoroughly four times with the wash buffer provided in the kit.

- 100µl of biotinylated Human VEGF (Biotin Conjugate) was added to each well, incubated at rt for a further hour, and then washed thoroughly four times with the wash buffer provided in the kit.
- 100µl of Streptavidin-Horseradish Peroxidase (HRP), an enzyme-linked antibody, was added to each well and incubated at rt for 30 minutes, followed by four washes.
- 100µl of stabilised chromogen was added to each well, and incubated at rt for 30 minutes in the dark but not wrapped in aluminium foil, as per the manufacturer's instructions
- 100µl of Stop Solution was added to each well to halt the reaction.
- Absorbance of samples was measured on a FLUOstar Optima microplate reader (BMG Labtech) with a test wavelength of 490 nm.

The maximum value on the standard curve was 1500pg/ml, but beyond this point, the VEGF concentration-absorbance relationship becomes non-linear and the standard curve cannot simply be extrapolated. Therefore any samples that generated concentrations greater than 1500pg/ml were diluted with standard diluent buffer, reanalysed using the microplate reader such that the reading would fall within the limits of the standard curve. The correct concentration was then calculated using the appropriate dilution factor.

3.3.7 PEDF Sandwich ELISA

The Human PEDF ELISA Kit (Biovendor RD191114200R) was used to determine the presence and quantity of PEDF secreted in the apical and basal chambers of each Transwell. The use of this kit for testing PEDF concentrations in cell culture media is well established.[166] The same media samples that were aspirated from the upper chamber and the lower chamber of each Transwell and used for detection of VEGF, as outlined in the previous section, were also used for the detection of PEDF.

The kit was used according to the manufacturer's instructions. Care was taken to ensure that the microtitre plate and all reagents were at rt before use. Each sample was diluted 8000x with dilution buffer, by two sequential dilutions, immediately prior to the assay. A standard curve was generated using serial dilutions of highly purified Human PEDF and 100µl of each standard was used. Apart from "blank" wells, 100µl of each sample or standard was applied into each well. All samples were tested in duplicate.

Samples and standards were incubated for one hour at rt, shaking at 300rpm on an orbital microplate shaker. The plates were then washed thoroughly five times with a wash solution (0.35ml per well), and inverted against a paper towel to remove as much residual fluid as possible.

- 100µl of biotin-labelled Human PEDF was added to each well, incubated for a further hour while shaken at 300rpm on the orbital microplate shaker, and then washed thoroughly five times with the wash solution provided.
- 100µl of Streptavidin-Horseradish Peroxidase (HRP) conjugate, an enzyme-linked antibody used, was added to each well and incubated for one hour while shaken at 300rpm on the orbital microplate shaker, and then washed thoroughly five times.
- 100µl of substrate solution was added to each well, the plate was wrapped in aluminium foil, and incubated in the dark for 5 minutes at room temperature, without shaking.
- 100µl of Stop Solution was added to each well to halt the reaction.
- Absorbance of samples was measured on a FLUOstar Optima microplate reader (BMG Labtech) with a test wavelength of 450 nm.

3.3.8 Transepithelial Electrical Resistance (TEER)

The Epithelial Voltohmmeter (EVOM2, World Precision Instruments, Sarasota, Florida USA) allows the measurement of resistance across epithelial layers. This device connects to the STX2 stick electrode which incorporates a pair of probes, each 4mm wide and 1mm thick. The lengths of the probes are unequal, such that the longer electrode can be placed into the lower chamber of the transwell, while the shorter probe is positioned in the upper chamber. The design of the probes is such that when the longer probe rests on the bottom surface of the transwell, the shorter probe will not be able to touch the cell layer being tested. The experimental apparatus is shown diagrammatically in Figure 3.7.

It is well recognised that TEER measurements will be affected by several factors including variance of angle of probe insertion, depth of electrode probe immersion, temperature, and freshness of the tissue culture media. To minimise fluctuations for all measurements, the following precautions were taken during measurement

- Considerable care was taken to ensure that the probe was directly vertical at the time of measurement.

- The STX2 electrode was immersed to the point at which the longer probe was touching the bottom surface of the lower chamber. Care was taken to ensure that the longer probe was just touching the bottom surface and not under any pressure to cause the probe to flex.

- All measurements were taken in the morning, and were taken just before changing the tissue culture media. For all measurements, the STX2 probe was first immersed in 70% alcohol to sterilise the probe, then into sterile water, and then immersed in the appropriate tissue culture media (either ARPE-19 or primary rabbit RPE media), until the readings stabilised. The probe was inserted into each well and once the TEER reading became stable, the resistance value was noted. Measurements were taken in triplicate, and the probe was then moved directly into the next well in the same row. At the end of the row, the elecrodes were placed back into 70% ethanol, then water, and then into the tissue culture media, before the next set of readings was taken.

- Time points were chosen at 1 3 and 8 weeks were chosen, based on findings of Stanzel *et al.* that TEER increases between these time points before stabilises.

3.3.9 Statistical Analysis

The independent t-test was used to compare each cell type growing on either polymer or on the Transwell insert. The paired t-test was used to compare apical and basal secretion of VEGF or PEDF from any given Transwell. For TEER, paired t-tests were used to assess changes between week 1 and week 3, and week 3 and week 8. A p-value of <0.05 was considered statistically significant.

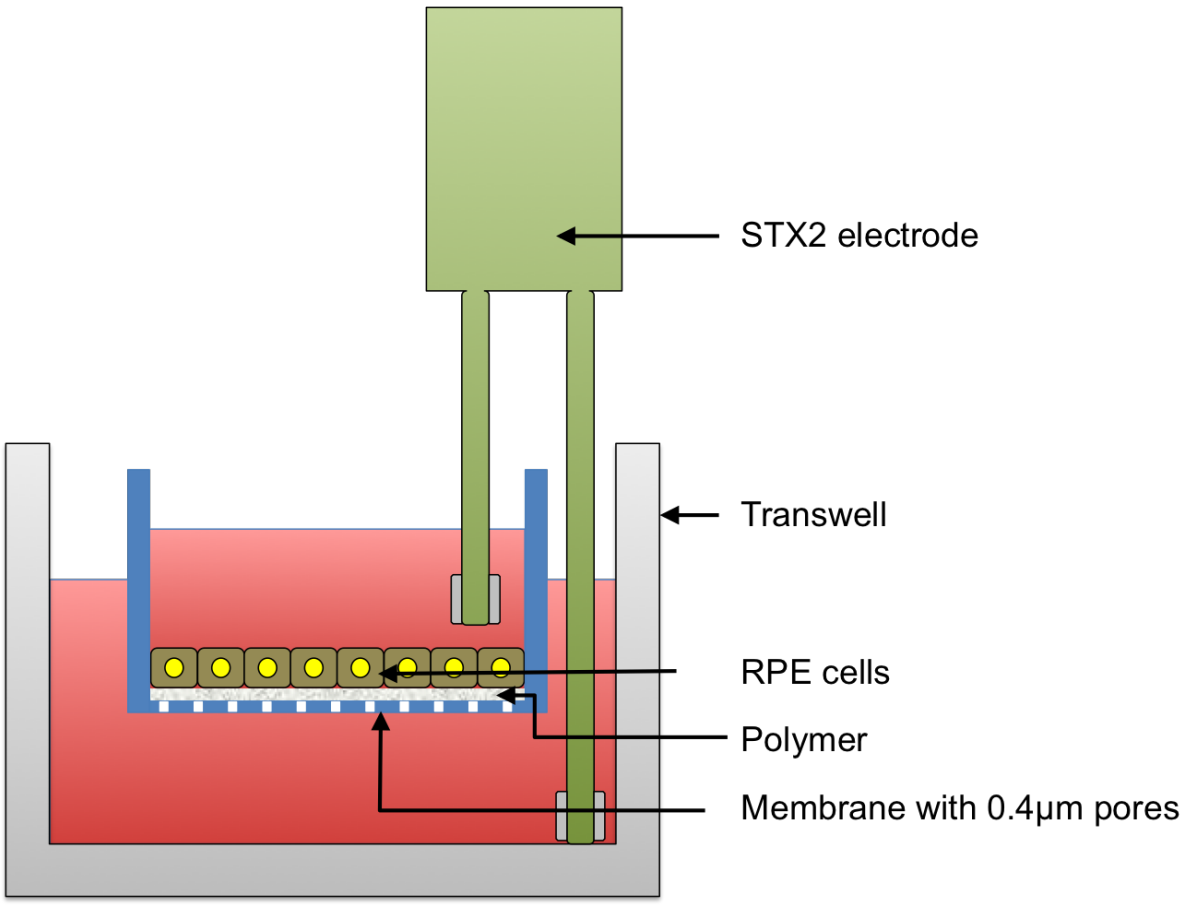

Figure 3.7: Method for measuring transepithelial electrical resistance using the EVOM2 (electrovoltohmmeter) and the STX2 electrode.

Measurements can be dependent on angular orientation of the probe, and all measurements were therefore taken with the probe directly vertical. The STX2 electrode was immersed until the longer probe was just touching the bottom surface of the lower chamber. Care was taken to ensure that the probe was not under any pressure to cause the probe to flex. The tip of shorter probe was immersed in the media but did not touch the cell layer. All measurements were taken in triplicate.

Transepithelial resistance was calculated using the formula:

$$R_{tissue} = R_{total} - R_{blank\ membrane}$$

where $R_{blank\ membrane}$ = resistance measurement across a Transwell without cells

To evaluate the individual effects of the Transwell membrane, the laminins coating, and the presence of polymer, three types of “blank” well were used:

- Row A (Transwell alone),
- Row B (Transwell + Laminin), and
- Row E (Transwell + Laminin + Polymer).

The blank with the lowest measurable resistance was used as the baseline for all the other measurements.

3.4 Results

3.4.1 Immunocytochemistry of Human and Rabbit RPE Cells

Staining with DAPI and phalloidin is shown below in Figure 3.8 and Figure 3.9. Neither the ARPE-19 cells nor the primary rabbit RPE cells showed any stained for ZO-1.

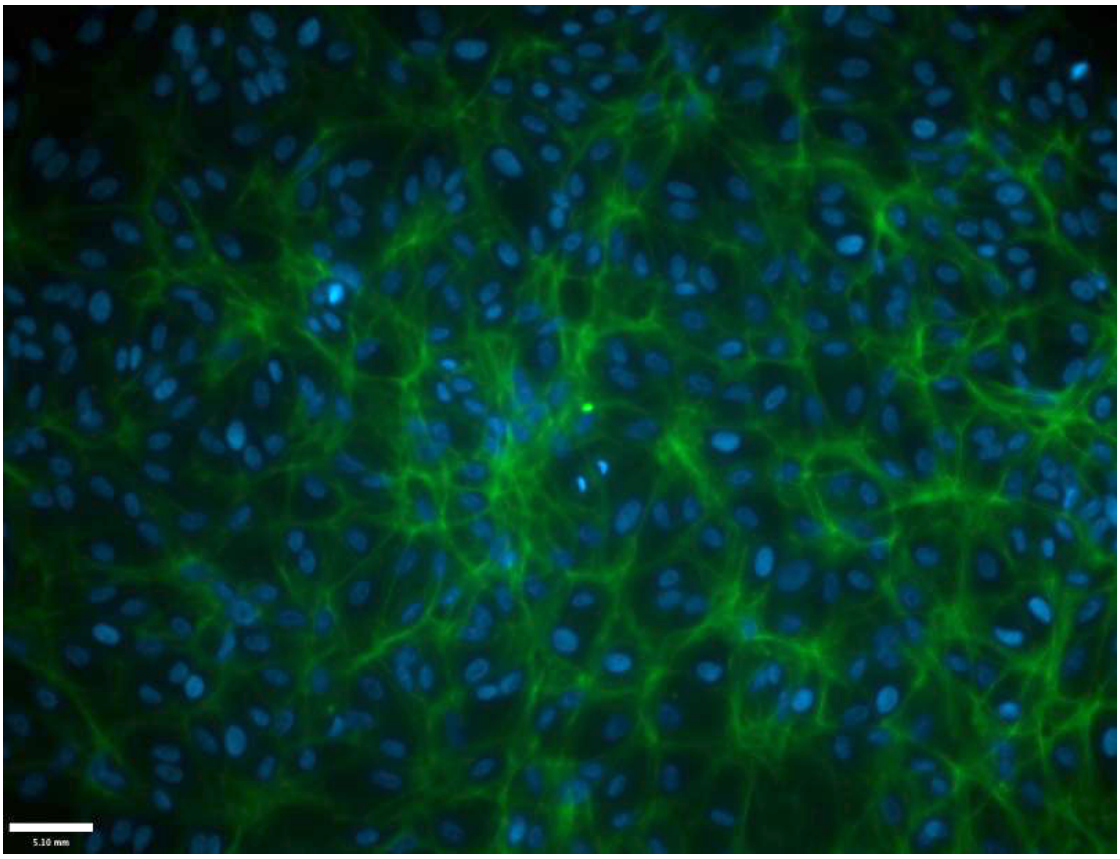

Figure 3.8: ARPE-19 cells stained with DAPI (blue) and Phalloidin (green)

The cells show the hexagonal morphology typical of RPE cells. In some areas it appears as if there are multiple nuclei within each RPE cell. Although a small proportion (3%)of human RPE cells are known to be binucleate,[167] a more likely explanation is that the phalloidin staining is incomplete. A further possibility is that the ARPE-19 cells have developed multiple layers, but this is unlikely because all of the nuclei are in focus, suggesting that they are in the same focal plane.

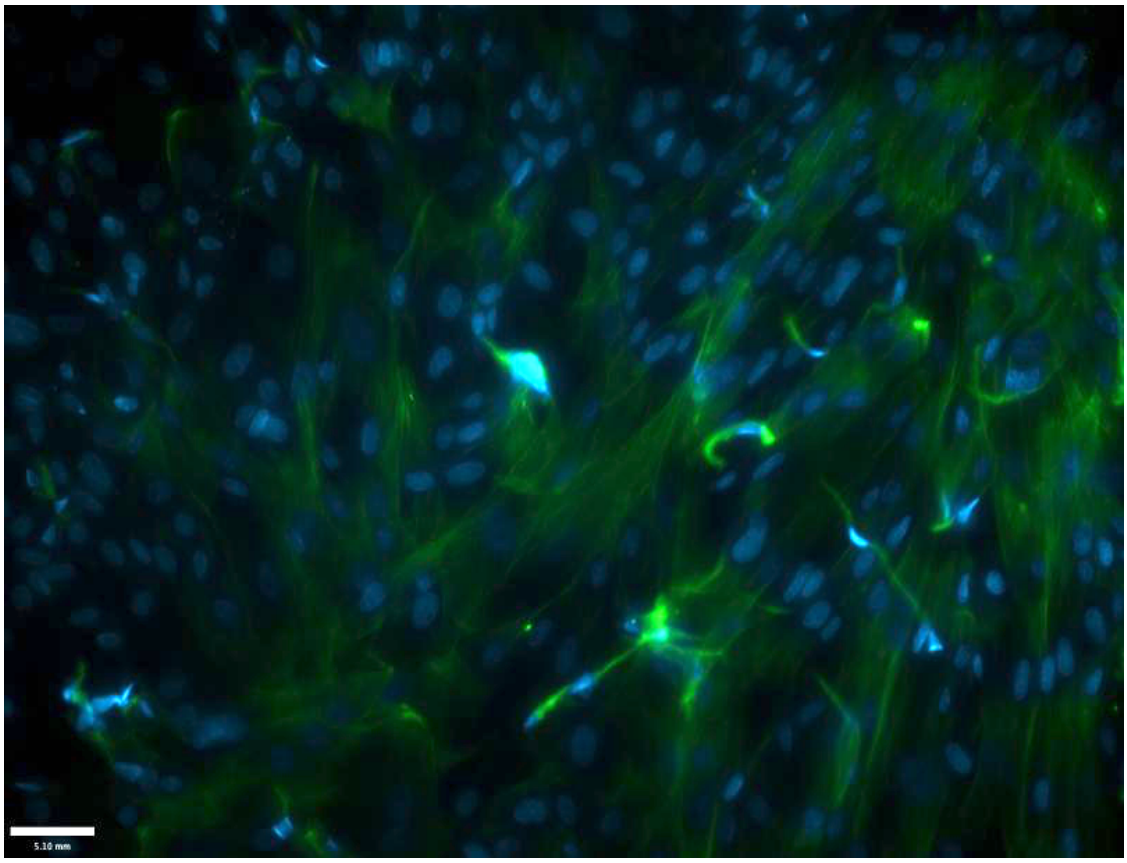

Figure 3.9: Primary rabbit RPE cells stained with DAPI (nuclei = blue) and Phalloidin (actin filaments = green).

The hexagonal morphology is less obvious in the primary RPE cells than in ARPE-19 cells. The actin filaments appear to orientated more in parallel than in the ARPE-19 cells, and this could account for the tangential contractile force observed in the primary rabbit RPE monolayers, as described in section 5.3.1.4. Most rabbit RPE cells are binucleate (Ts'o *et al.,*[167] as quoted by Samuelson.[168])

3.4.2 PEDF assay

A standard curve, shown in Figure 3.10, was used to interpolate the measurements of PEDF concentration in the samples.

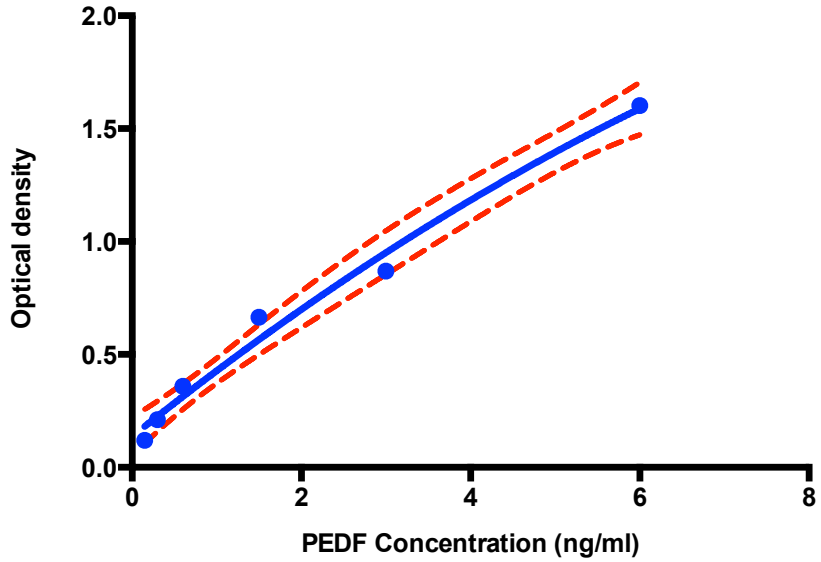

Figure 3.10: Standard curve for PEDF Sandwich ELISA assay.

Blue line shows line of best fit, red dotted lines shows standard deviation. This curve was generated by measuring the optical density at 450nm of known concentrations of human PEDF. These values were thereby used to interpolate the PEDF concentrations of samples taken from the apical and basal chambers of the Transwells in the tissue culture plate.

Higher PEDF concentrations were detected with ARPE-19 cells than with primary rabbit RPE cells at all time points, as shown in Figure 3.11.

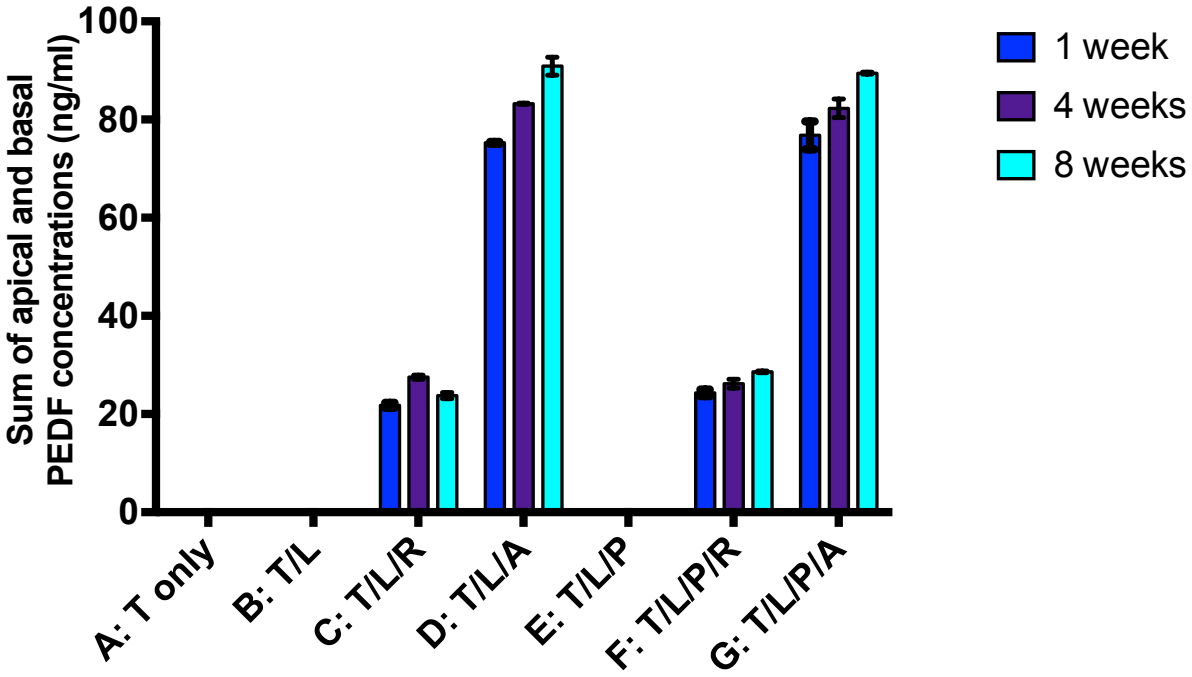

Figure 3.11: Mean PEDF concentrations measured in the Transwells for ARPE-19 cells and Primary rabbit RPE cells, either with or without polymer.

Abbreviations: T=Transwell; L=Laminin; P=P(MMA-co-PEGM-succinimidyl carbonate); R=Primary Rabbit RPE cells; A=ARPE-19 cells. (error bars=SEM)

Note that there is no PEDF detected in A, B, or E and this is expected because none of these wells have any cells. ARPE-19 cells produce more PEDF (as detected on a human PEDF ELISA assay) than primary rabbit RPE cells (mean 82.98, SD 6.29 vs. mean 25.36, SD 2.50 respectively, $p<0.001$). Comparing C and F, there is a similar amount of total PEDF produced by rabbit RPE cells at any given time point irrespective of whether the cells are growing on the polymer (mean 26.36, SD 2.04) or on the Transwell membrane (mean 24.35, SD 2.67) ($p=0.172$). Similarly, comparing D and G, there is a similar amount of total PEDF produced by ARPE-19 cells at any given time point whether the cells are growing on polymer (mean 82.85 SD 6.07) or not (mean 83.12, SD 7.08), ($p=0.943$).

Both rabbit RPE cells and ARPE-19 cells produce similar PEDF concentrations in the apical and basal chambers of the Transwell at all time points

Figure 3.12, Figure 3.13 and Figure 3.14 respectively show apical and basal PEDF concentrations at one week, four weeks and eight weeks after seeding. Figure 3.15 compares PEDF concentrations (as an average across all time points) in the apical and basal chambers of the Transwells.

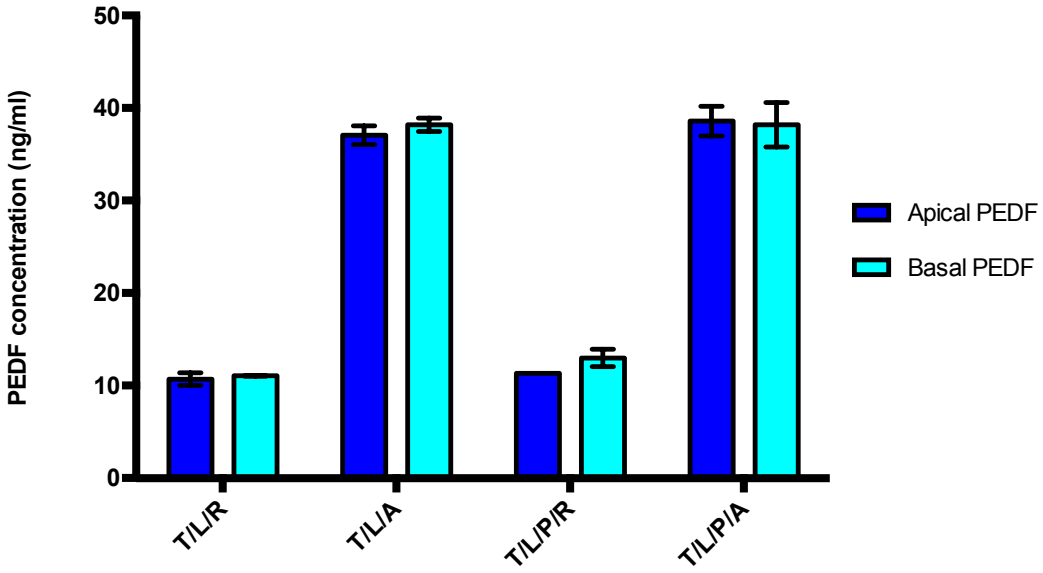

Figure 3.12: Mean PEDF concentrations measured in the apical and basal chambers of the Transwells for ARPE-19 cells and primary rabbit RPE cells, either with or without polymer, one week after seeding.

Abbreviations: T=Transwell; L=Laminin; P=P(MMA-co-PEGM-succinimidyl carbonate); R=Primary Rabbit RPE cells; A=ARPE-19 cells. (error bars=SEM)

One week after seeding, there was no discernable polarisation of PEDF secretion, with similar concentrations measured in the apical and basal chambers for both the ARPE-19 cells (respectively: with polymer, mean 38.59 vs. 38.19, p=0.604; without polymer 37.07 vs. 38.20, p=0.531) and the primary rabbit RPE cells (with polymer, mean 11.33 vs. 13.00, p=0.67; without polymer 10.70 vs 11.07, p=0.568). Similar concentrations of PEDF were detected from ARPE-19 cells irrespective of whether the cells were growing on polymer or not (mean apical concentrations 41.95 SD 4.02 with polymer, 40.75 SD 3.35 without polymer, p=0.588; mean basal concentrations 40.90 SD 2.48 with polymer, 42.37, SD 3.83 without polymer, p=0.451). Rabbit RPE cells produced less detectable PEDF, but concentrations were similar irrespective of whether the cells were growing on polymer (mean apical concentrations 13.05 SD 1.65 with polymer, 11.69 SD 0.90 without polymer, p=0.117; mean basal concentrations 13.32 SD 0.84 with polymer, 12.66, SD 2.14 without polymer, p=0.506). The pattern shown in the graph above was similar to that seen at 4 weeks (see Figure 3.13) and 8 weeks (see Figure 3.14).

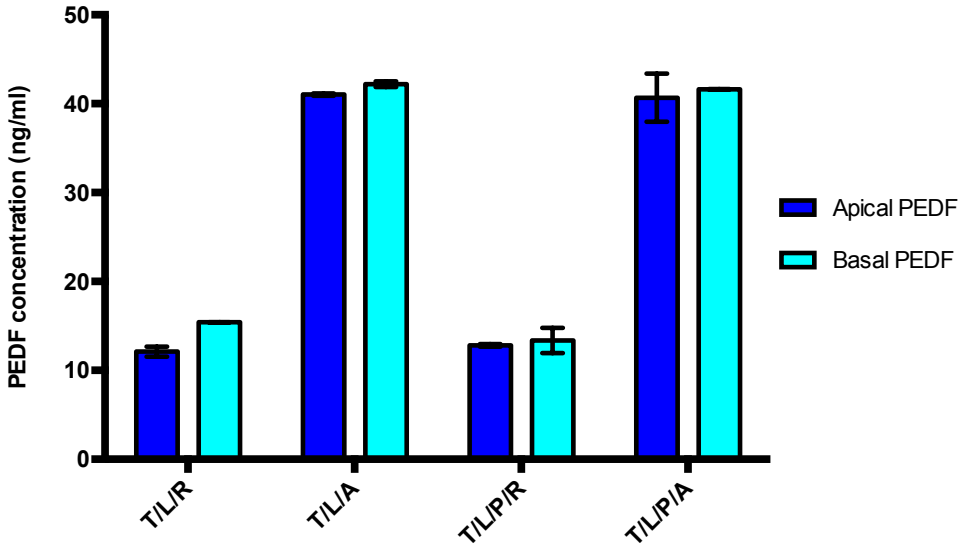

Figure 3.13: Mean PEDF concentrations measured in the apical and basal chambers of the Transwells for ARPE-19 cells and primary rabbit RPE cells, either with or without polymer, four weeks after seeding.

Abbreviations: T=Transwell; L=Laminin; P=P(MMA-co-PEGM-succinimidyl carbonate); R=Primary Rabbit RPE cells; A=ARPE-19 cells. (error bars=SEM)

At four weeks after seeding, there was still no discernable polarisation of PEDF secretion, with similar concentrations measured in apical and basal chambers for both ARPE-19 cells (apical vs. basal: with polymer, mean 40.67 vs. 41.63, p=0.707; without polymer 41.03 vs. 42.19, p=0.172) and primary rabbit RPE cells (apical vs. basal: with polymer, mean 12.82 vs. 13.36, p=0.710; without polymer 12.11 vs. 15.40, p=0.074). Similar concentrations of PEDF were detected from ARPE-19 cells irrespective of whether cells were growing on polymer or not (mean apical concentrations 40.67 SD 2.70 with polymer, 41.03 SD 0.14 without polymer, p=0.883; mean basal concentrations 41.63 SD 0.028 with polymer, 42.19 SD 0.315 without polymer, p=0.237). Rabbit RPE produced less detectable PEDF than ARPE-19 cells (mean 27.51 SD 0.585 vs. mean 83.22 SD 0.174, p=0.02), but concentrations were similar irrespective of whether cells were growing on polymer (mean apical concentrations 12.82 SD 0.147 with polymer, 12.11 SD 0.563 without polymer, p=0.312; mean basal concentrations 13.36 SD 1.41 with polymer, 15.40 SD 0.215 without polymer, p=0.290). The pattern shown in the graph above was similar to that seen at 1 week (see Figure 3.12) and 8 weeks (see Figure 3.14).

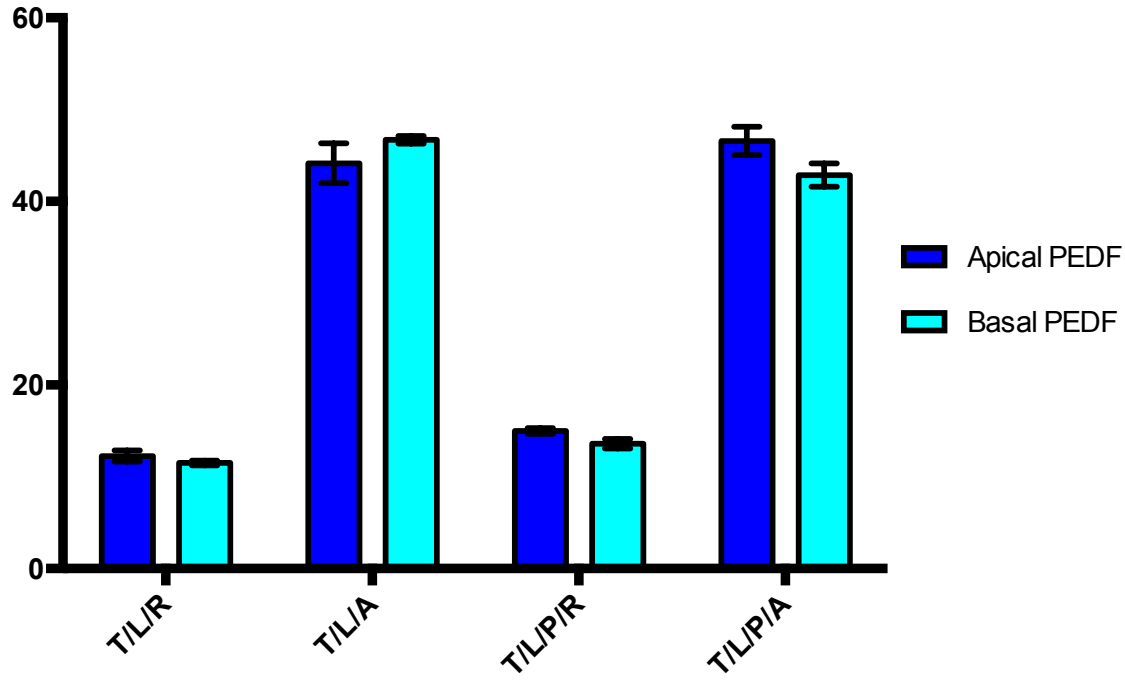

Figure 3.14: Mean PEDF concentrations measured in the apical and basal chambers of the Transwells for ARPE-19 cells and primary rabbit RPE cells, either with or without polymer, eight weeks after seeding.

Abbreviations: T=Transwell; L=Laminin; P=P(MMA-co-PEGM-succinimidyl carbonate); R=Primary Rabbit RPE cells; A=ARPE-19 cells. (error bars=SEM)

At eight weeks after seeding, the amounts and distribution of secreted PEDF were similar to those found at one week (Figure 3.12) and four weeks (Figure 3.13), with no discernable polarisation of PEDF secretion. Similar PEDF concentrations were measured in the apical and basal chambers for both the ARPE-19 cells (apical vs. basal: with polymer, mean 46.58 vs. 42.87, p=0.314; without polymer 44.16 vs. 46.72, p=0.286) and the primary rabbit RPE cells, (apical vs. basal: with polymer, mean 14.99 vs. 13.59, p=0.252; without polymer mean 12.26 vs. 11.51, p=0.206) irrespective of whether the cells were growing on polymer or not. Rabbit RPE cells produced less detectable PEDF than ARPE-19 cells (mean 26.18, SD 2.83 vs. 90.16 SD 1.72; p<0.001).

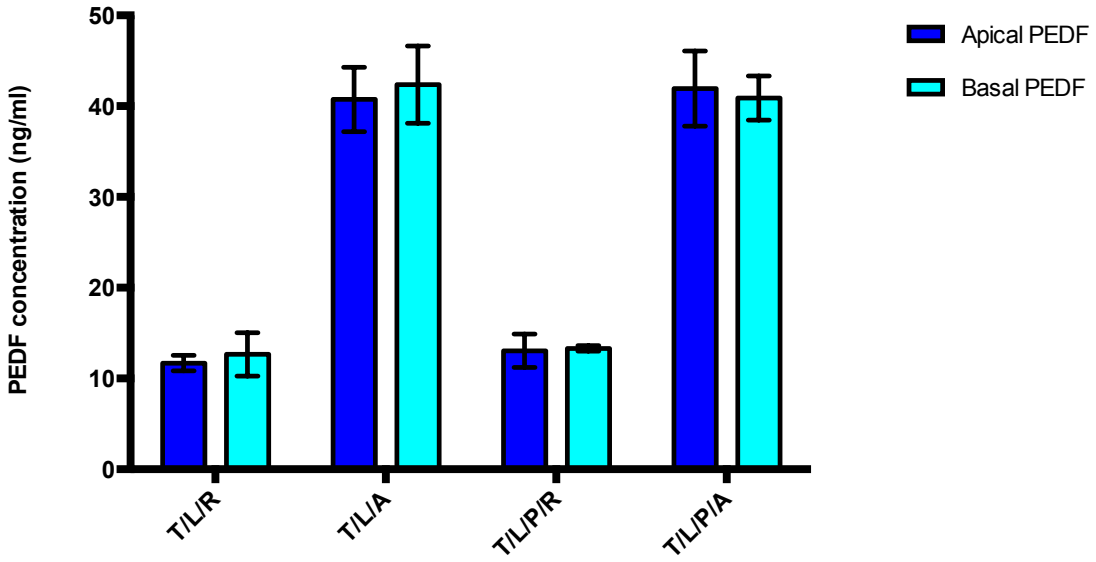

Figure 3.15: Bar chart comparing PEDF concentrations (average of all time points) in the apical and basal chambers of the Transwells.

Abbreviations: T=Transwell; L=Laminin; P=P(MMA-co-PEGM-succinimidyl carbonate); R=Primary Rabbit RPE cells; A=ARPE-19 cells. Error bars indicate standard deviation.

ARPE-19 cells produced more PEDF than primary rabbit RPE cells (mean 82.98 SD 6.29 vs. 25.36 SD 2.50, $p<0.001$). There was no difference in the concentrations measured in the apical and basal chambers of the Transwell for rabbit RPE, irrespective of whether the cells were growing on the polymer scaffold or not (rabbit RPE with polymer 13.05 apical vs. 13.32 basal, $p=0.705$; rabbit RPE without polymer, 11.69 apical vs. 12.66 basal, $p=0.270$). For ARPE-19 on polymer, there was no difference in PEDF concentrations between the apical and basal chambers (41.95 apical vs. 40.90 basal $p=0.40$), but without polymer there was a small difference between the apical and basal chambers (mean apical 40.75 SD 3.35 vs. mean basal 42.37 SD 3.83, $p=0.032$).

3.4.3 VEGF Assay

A standard curve, shown in Figure 3.16, was used to interpolate the measurements of VEGF concentration in the samples. Figure 3.17 shows mean VEGF concentrations measured in the Transwells for ARPE-19 cells and primary rabbit RPE cells, either with or without polymer. Figures 3.18, 3.19 and 3.20 respectively show apical and basal VEGF concentrations at one week, four weeks and eight weeks after seeding. Figure 3.21 compares VEGF concentrations (as an average across all time points) in the apical and basal chambers of the Transwells. Figure 3.22 shows the degree of polarisation of both VEGF and PEDF secretion by rabbit RPE and ARPE-19 cells, with and without polymer, at all time points.

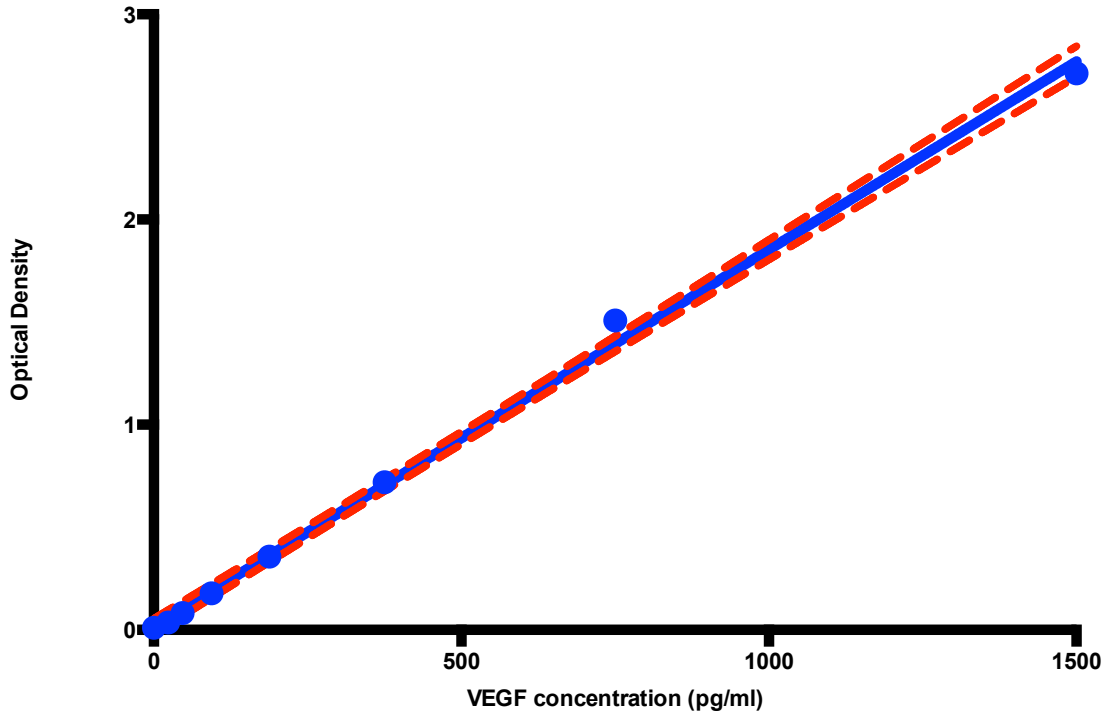

Figure 3.16: Standard 'curve' for VEGF Sandwich ELISA assay.

Blue line shows line of best fit, red dotted lines shows standard deviation. This curve was generated using optical density measurements at 450nm of known concentrations of human VEGF, and thereby used to interpolate the VEGF concentrations of samples taken from the apical and basal chambers of the Transwells in the tissue culture plate.

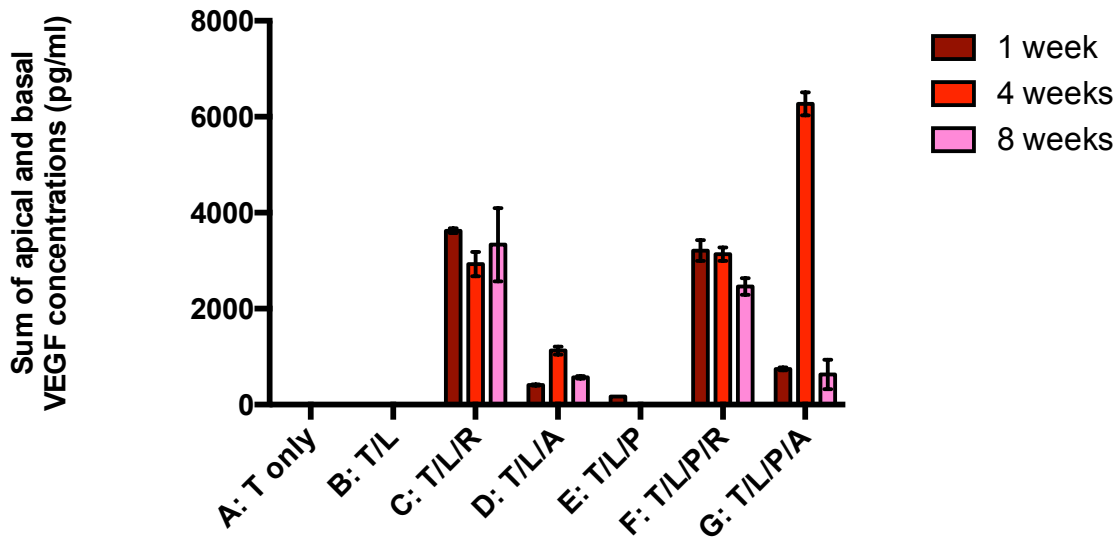

Figure 3.17: Mean VEGF concentrations measured in the Transwells for ARPE-19 cells and primary rabbit RPE cells, either with or without polymer.

Abbreviations: T=Transwell; L=Laminin; P=P(MMA-co-PEGM-succinimidyl carbonate); R=Primary Rabbit RPE cells; A=ARPE-19 cells. (error bars=SEM)

Note that there is no VEGF detected in A, or B, and sample E has virtually no measurable VEGF. These wells had no cells and no VEGF would be expected in any of these samples. Overall, rabbit cells produced more VEGF than ARPE-19 cells (respectively, mean 3117.42, SD 526.7 vs. mean 1626.20, SD 2187.28, p=0.04). Comparing C with D, it appears that the ARPE-19 cells produce less VEGF than the primary rabbit RPE cells (mean 703 SD 340 vs. mean 3298 SD 598, p<0.01, as detected on a human VEGF ELISA assay). Comparing C and F, there is a similar amount of total VEGF produced by rabbit RPE cells at any given time point irrespective of whether the cells are growing on the polymer (mean 2938 SD 418) or on the Transwell membrane (mean 3296 SD 598) (p=0.260). Comparing D and G, VEGF production is low after 1 week, but peaks at week 4, and then declines by week 8. At week 1, there is more VEGF produced by ARPE-19 cells on polymer than without polymer (746 SD 349 vs. 411 SD 418; p=0.03). At week 8, there is a similar amount of total VEGF produced by ARPE-19 cells whether the cells are growing on polymer or not (mean 632, SD 433 vs. mean 571, SD 35, p=0.876). At week 4, VEGF production by ARPE-19 cells growing on the polymer is

almost 6-fold that of ARPE-19 cells growing on the Transwell inserts (mean 6268, SD 341 vs. mean 1127, SD 115, p=0.017).

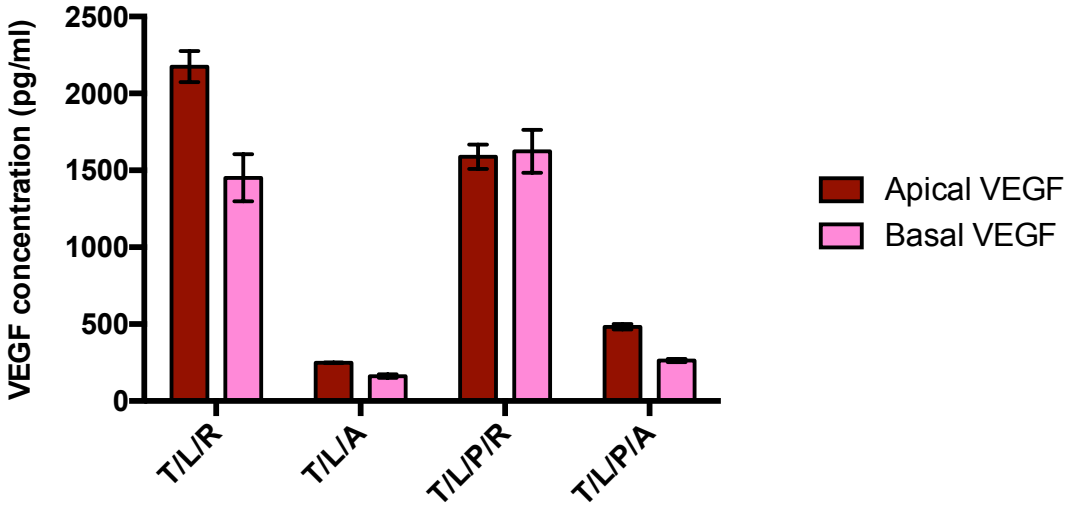

Figure 3.18: Mean VEGF concentrations measured in the apical and basal chambers of the Transwells for ARPE-19 cells and primary rabbit RPE cells, either with or without polymer, one week after seeding.

Abbreviations: T=Transwell; L=Laminin; P=P(MMA-co-PEGM-succinimidyl carbonate); R=Primary Rabbit RPE cells; A=ARPE-19 cells. (error bars=SEM)

Higher VEGF concentrations were detected with rabbit RPE cells (mean 3419, SD 301) than with ARPE-19 cells (mean 579, SD 195). For rabbit RPE cells growing on the Transwell insert, there seemed to be a trend for higher VEGF concentrations to be found in the apical chamber than in the basal chamber but this was not statistically significant (apical vs. basal: mean 2174 SD 142 vs. mean 1451, SD 216, p=0.215). There was no significant difference between apical and basal VEGF concentrations for rabbit RPE cells growing on the polymer. VEGF secretion was polarised to the apical chamber for ARPE-19 cells on the polymer (mean apical 483, SD 25 vs. mean basal 264, SD 14, p=0.022), but this did not reach statistical significance for ARPE-19 cells growing on the Transwell insert (mean apical 249, SD 2.89 vs. mean basal 162, SD 15, p=0.065).

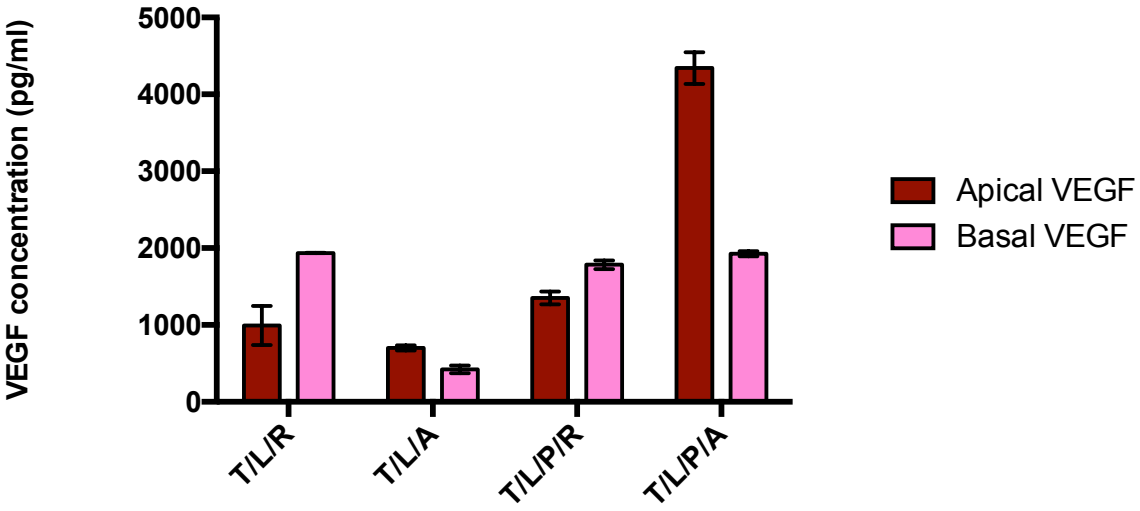

Figure 3.19: Mean VEGF concentrations measured in the apical and basal chambers of the Transwells for ARPE-19 cells and primary rabbit RPE cells, either with or without polymer, four weeks after seeding.

Abbreviations: T=Transwell; L=Laminin; P=P(MMA-co-PEGM-succinimidyl carbonate); R=Primary Rabbit RPE cells; A=ARPE-19 cells. (error bars=SEM)

For rabbit RPE cells, VEGF secretion was polarised to the basal chamber with polymer (mean apical VEGF 1354, SD118, mean basal VEGF 1785 SD 79, p=0.04) but not without the polymer (mean apical 992 SD 358; mean basal 1937 SD 3.3). For ARPE-19 cells, VEGF secretion was polarised in the opposite direction, to the apical chamber (with polymer, mean apical VEGF 4342, SD293 vs. mean basal VEGF 1927 SD 49, p=0.045; without polymer, mean apical VEGF 704 SD 47, mean basal VEGF 423 SD 69, p=0.035). Although at one week after seeding, higher VEGF concentrations were detected with rabbit RPE cells than with ARPE-19 cells (see Figure 3.18), this was not the case at 4 weeks (total VEGF in rabbit RPE and ARPE-19 respectively: 3034 vs 3698, p=0.686), with extremely high VEGF concentrations detected from ARPE-19 cells growing on the polymer.

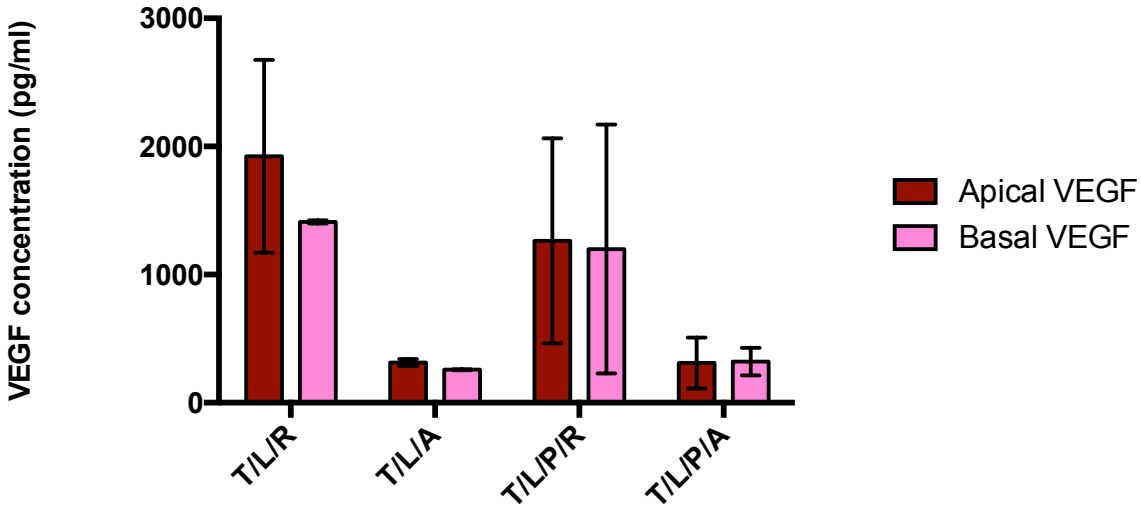

Figure 3.20: Mean VEGF concentrations measured in the apical and basal chambers of the Transwells for ARPE-19 cells and primary rabbit RPE cells, either with or without polymer, eight weeks after seeding. *(error bars=SEM)*

Abbreviations: T=Transwell; L=Laminin; P=P(MMA-co-PEGM-succinimidyl carbonate); R=Primary Rabbit RPE cells; A=ARPE-19 cells.

The results at eight weeks were similar to those seen at one week after seeding (see Figure 3.18). Higher VEGF concentrations were detected with rabbit RPE cells than with ARPE-19 cells (mean VEGF was respectively 2899 vs. 602, p=0.008). No polarisation of VEGF secretion was demonstrable for rabbit RPE cells growing on the Transwell insert (apical mean 1264 vs. basal mean 1199, p=0.977) or for rabbit RPE cells growing on the polymer (apical mean 1923 vs. basal mean 1411, p=0.615).

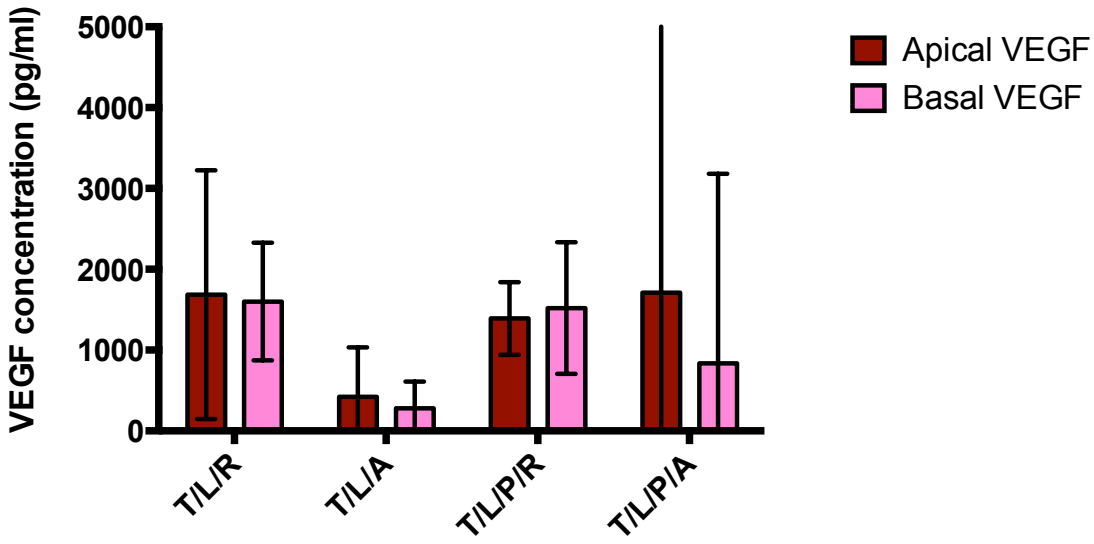

Figure 3.21: Mean VEGF concentrations measured in the apical and basal chambers of the Transwells for ARPE-19 cells and primary rabbit RPE cells, either with or without polymer, across all time points.

Abbreviations: T=Transwell; L=Laminin; P=P(MMA-co-PEGM-succinimidyl carbonate); R=Primary Rabbit RPE cells; A=ARPE-19 cells. Error bars indicate standard deviation.

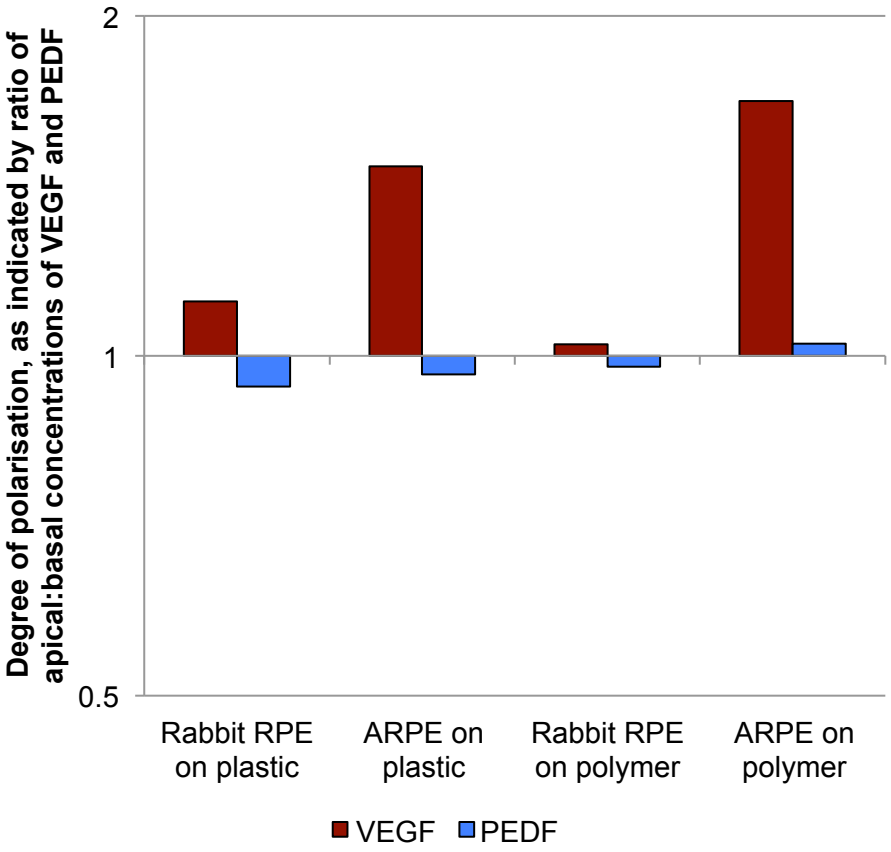

Figure 3.22: Degree of polarisation of VEGF and PEDF secretion by rabbit RPE and ARPE-19 cells, with and without polymer, at all time points.

This graph indicates the degree of polarisation, as measured by the apical:basal ratio of VEGF and PEDF respectively. The x- and y- axes intersect at 1, indicating that when the apical:basal ratio is 1, there is no polarisation. Ratios >1 or <1 indicate apical and basal polarisation respectively. The y-axis is a logarithmic scale to ensure that bars are the same size irrespective of whether the polarisation is apical or basal. For ARPE-19 cells growing on the transwell membrane there is a statistically significant difference between the apical and basal concentrations of both VEGF and PEDF i.e. the cells seem to be polarised. However, for ARPE-19 cells growing on polymer, and for rabbit RPE cells either on polymer or on the Transwell insert, there was no statistically significant difference between apical and basal concentrations.

3.4.4 Transepithelial Electrical Resistance (TEER)

Three types of "blank" well were used: Row A (Transwell alone), Row B (Transwell + Laminin), and Row E (Transwell + Laminin + Polymer). The electrical resistance across the Transwell with media (but no cells) was similar to that of a laminin-coated Transwell without cells (see Figure 3.23, A and B respectively). However, the presence of a polymer disc on the surface of the laminin-coated Transwell (Row E) reduced the measurable resistance by almost 20 Ohms. Therefore the mean measurable resistance between the apical and basal chambers of Row E was used as the 'blank' resistance and all other conditions were evaluated relative to this.

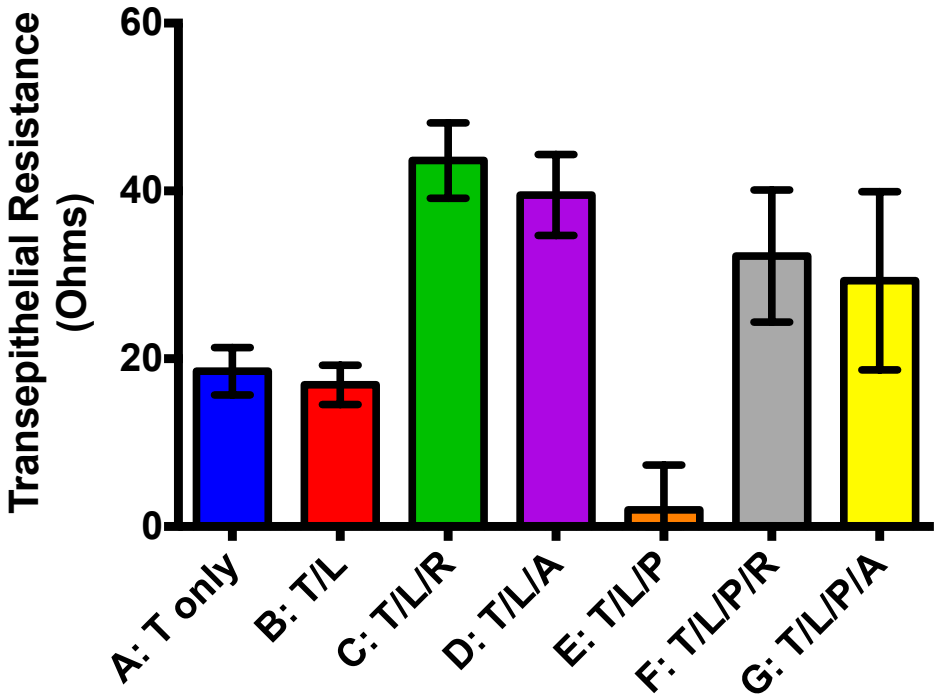

Figure 3.23: Transepithelial Electrical Resistance Measurements of ARPE-19 and primary rabbit RPE cells, with and without polymer.

Abbreviations: T=Transwell; L=Laminin; P=P(MMA-co-PEGM-succinimidyl carbonate); R=Primary Rabbit RPE cells; A=ARPE-19 cells. (error bars=SEM)

Three types of "blank" well were used: Row A (Transwell alone), Row B (Transwell + Laminin), and Row E (Transwell + Laminin + Polymer). Row E had the lowest measurable resistance and was therefore used as the baseline for all other measurements. Presence of the polymer reduced the

resistance even in a blank well. Rabbit RPE had the highest TEER (Row C), and ARPE-19 cells without polymer (Row D) had a similar but slightly lower TEER. Cells growing on polymer (F and G) had a lower TEER than cells without polymer (C and D), with ARPE-19 cells having a similar but slightly lower TEER than the rabbit RPE cells.

TEER measurements were taken 1 week, 3 weeks and 8 weeks after seeding. The time course of the TEER measurements is shown in Figure 3.24.

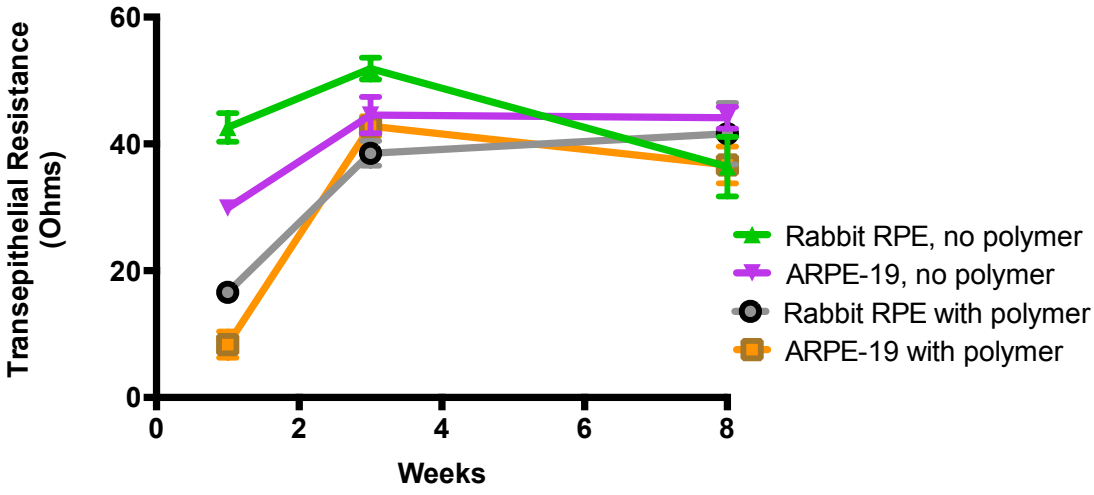

Figure 3.24: Time course for TEER development.

For both ARPE-19 cells and rabbit RPE cells, TEER increased between 1 week and 3 weeks and this change was statistically significant ($p \leq 0.002$ for each of the four conditions). Between 3 weeks and 8 weeks, there was no statistically significant change for ARPE-19 cells growing on the Transwell insert or for rabbit RPE cells growing on the polymer. However, for rabbit RPE cells growing on the Transwell insert, there was a statistically significant decrease in TEER between week 3 (51.9 Ohms) and week 8 (36.4 Ohms) ($p=0.012$). There was also a statistically significant reduction in TEER for ARPE-19 cells growing on the polymer between week 3 (mean 42.8, SD 6.1) and week 8 (mean 36.7, SD 11.3) ($p=0.010$).

3.5 Discussion

Polarisation of the RPE is intrinsically associated with the formation of intercellular tight junctions. Without the epithelium functioning as a tight monolayer, polarisation cannot occur and the results of the TEER studies and the polarisation studies should therefore be evaluated in conjunction.

It is well established that often TEER measurements are taken at ambient temperature and that this overestimates the true electrical resistance in the body. Since the readings were taken in a tissue culture hood and each set of readings took some time, it is very likely that the true resistance in the body is much lower than that measured in this study. The purpose of this experiment was to compare TEER readings of the cells growing on the polymer, with cells growing on the transwell insert alone. There are sufficient controls to allow useful data from this experiment.

The TEER studies demonstrate that when growing on Transwell inserts, both the rabbit RPE cells and the ARPE-19 cells form an electrically resistant barrier. This supports, but does not definitively prove, the hypothesis that the cells form a monolayer with tight junctions. However, while immunohistochemistry confirmed the presence of a sheet of hexagonal shaped cells, no tight junctions could be detected using antibodies against ZO-1 despite numerous attempts at immunohistochemical detection of intercellular cell junctions. Although there are no reports of ZO-1 detected in rabbit RPE cells, ZO-1 has been observed in ARPE-19, and can indicate the presence not only of tight junctions but also of adherens junctions. However, it is well-recognised that variations in cell culture conditions and media lead to considerable heterogeneity in the apical junctional complex in ARPE-19 cells,[169] and the absence of ZO-1 staining does not exclude the presence of intercellular junctions, but may indicate lack of maturation of the junction.

It was interesting to note that the presence of the polymer in a Transwell with no cells produced a lower electrical resistance than an otherwise blank Transwell. Potential reasons for this may be that the polymer improves the electrical conductance of the Transwell insert, or alternatively it may simply be that the thickness of the polymer allows the shorter probe to be closer to a physical surface, thereby reducing the electrical resistance. In our experiments, TEER was not affected by coating of the Transwell insert with Laminin; this finding has been replicated by other groups.[162] The manufacturers of EVOM2 indicate that the background resistance is not related to the

membrane of the transwell insert, and occurs mainly due to the small gap between the bottom of the cell culture insert and the bottom of the cell culture plate.

Although the cells growing on the polymer showed a slightly reduced TEER compared to cells growing on the transwell inserts, there was clear evidence of an electrically resistant barrier, as shown in Figure 3.23. The time course for the formation of this barrier was similar regardless of the cell type or the cell scaffold, as shown in Figure 3.24. Although tight junctions have not been directly demonstrated, the presence of tight junctions, even if immature, can be inferred by the TEER.

The polarisation studies could not demonstrate any polarisation at all for PEDF secretion. However it is reassuring that PEDF secretion from cells growing on the polymer was no different to cells on the Transwell insert. The VEGF secretion is more difficult to interpret. For ARPE-19 cells, the degree of polarisation (i.e. ratio of apical VEGF to basal VEGF) was higher when the cells were grown on the polymer rather than on the Transwell insert, yet this difference was only statistically significant for the cells on the Transwell, but not for cells on the polymer. This trend supports the hypothesis that RPE cells growing on the polymer are polarised, and taken in conjunction with the TEER experiments, but further experiments are needed, especially for VEGF secretion, to confirm that the polymer facilitates polarisation and is therefore a useful substrate for RPE transplantation.

There are several interesting observations that warrant discussion. The first is that physiologically, PEDF is thought to be polarised to the apical membrane, and VEGF is polarised to the basal membrane. However, the results above suggest that *in vitro*, PEDF does not show polarisation and that for ARPE-19 cells, VEGF is polarised to the apical, rather than basal, membrane. This 'reversal' of VEGF secretion is a feature specific to ARPE-19 cells. Ablonczy *et al.* compared TEER, protein secretion and cellular morphology of ARPE-19 cells and foetal human RPE (fhRPE) cells and also noted that while fhRPE cells secreted VEGF basally, ARPE-19 VEGF secretion was apical rather than basal. The apical:basal ratio determined by Ablonczy *et al.* was similar to that found in our experiments.[170]

The TEER of the ARPE-19 cells in our experiments was also similar to that identified by Ablonczy *et al*.[170] Notably, while ARPE-19 cells produce an electrical resistance of approximately 40Ωcm^2, fhRPE cells produce 400Ωcm^2.[170] Despite their name, tight

junctions are in fact semi-permeable and semi-selective. While the permeability is controlled by proteins such as occludin, the selectivity is determined by the expression of a unique subset of proteins known as claudins.[162] Intercellular tight junctions between ARPE-19 cells are known to remain rudimentary and although they express the minor claudins, the major human claudin, claudin-19, is not expressed.[159] The other human RPE cell line, D407, shows no tight junctions or any biologically significant TEER. Some groups express a preference for freshly-isolated explants of human RPE, rather than the use of cultured cells, for modelling human RPE barrier function and polarisation. However, although this may be the gold standard this is impractical because of difficulties with obtaining fresh RPE tissue. Although human RPE cell lines are limited in their use as a barrier model, for the purposes of these experiments the ARPE-19 cells nevertheless provide useful information, by allowing comparison between cells growing on polymer and cells without polymer. Ideally, the Endohm electrodes would have been used for TEER measurements in ARPE-19 cells, but our laboratory did not have this facility. Endohm electrodes are not subject to positioning artifacts, and their lower background resistance makes them useful for monolayers that have rudimentary tight junctions that therefore a relatively low TEER.

The one finding that remains unexplained is the massive increase in VEGF production in both the apical and basal chambers of ARPE-19 cells on polymer at 4 weeks. The VEGF production then returns to more normal levels at 8 weeks. It would be tempting to attribute this to an aberrant reading but the samples were measured in duplicate and then averaged, but on review of the original data, both samples (taken from separate wells) showed similarly high VEGF production for the apical and basal chambers. This could be accounted for by an increase in cell number at the 4 week time point, but if this is the case then it is unclear why the cell number would then fall again at the 8 week time point.

Primary rabbit RPE was used in these experiments with the ultimate aim of implanting rabbit RPE-seeded polymer into the subretinal space of a different rabbit. It was thought that this allograft approach would avoid the intense inflammatory reaction that would be expected from xenotransplantation of human RPE cells into the rabbit subretinal space. It became clear quite early in the experiments that implantation of rabbit RPE-seeded polymer would be unfeasible, because the rabbit RPE cell sheet was extremely contractile. This was not visible at 1 week after seeding, but by 4 weeks, four out of five rabbit RPE-polymers had folded in half. In retrospect, photographic evidence of this would have been useful. This is presumably due to

transformation of the RPE cells into myofibroblasts, similar to the process that occurs in proliferative vitreoretinopathy. Gentle attempts to tease the polymer apart with the pipette tip during media changes were unsuccessful. However, this observation alone was helpful, because it explains why there was no significant polarisation of rabbit RPE on the polymer, and demonstrated that rabbit RPE is not a suitable cell type for implantation in a rabbit model, unless the mechanical strength of the polymer can be improved to ensure that the polymer does not buckle under the contractile force of the RPE monolayer.

3.6 Conclusions

- VEGF secretion was polarised to the apical chamber for ARPE-19 cells growing on the Transwell insert. For cells growing on the polymer, there was no statistical difference between the mean VEGF concentration in the apical and basal chambers.

- There was no discernable polarisation in PEDF secretion for rabbit cells or for ARPE-19 cells, irrespective of whether the cells were growing on polymer or on the transwell membrane.

- Presence of intercellular junctions could not be demonstrated for ARPE-19 cells or primary rabbit cells with immunocytochemistry staining with ZO-1.

- For both ARPE-19 cells and rabbit RPE cells, TEER increased between 1 week and 3 weeks and then reached a plateau. This was true for cells growing on the Transwell insert and also for those growing on the polymer. This supports the hypothesis that the polymer can allow RPE cells to form intercellular junctions.

- - -

Chapter 4: SURGICAL INSTRUMENTATION

> "It is difficult to predict the future of retinal epithelial cell transplantation…The major challenge that must be met, in order to bring this method to bear on human retinal disease, lies in the microsurgical technology needed to operate in the subretinal space."
>
> [Gouras and Lopez, 1989] [171]

4.1 Surgical Instrumentation

Pars plana vitrectomy is a safe, well-established and commonly performed surgical procedure that allows surgical access to the retina.[172] Physiologically, the subretinal space is a potential space rather than a true space. Surgical delivery of RPE cells first requires creation of a 'bleb' within the subretinal space, usually with balanced salt solution. Some authors have suggested that bleb collapse can be prevented by the use of subretinal viscoelastic injection. The need for removal of the residual RPE bed remains undetermined but this has been studied by several investigators.[99, 101, 138] An incision into the bleb allows delivery of RPE cells into the subretinal space. Each of these stages (bleb maintenance, residual RPE bed removal, RPE delivery – see Figure 4.1) requires specific micro-instrumentation. This chapter reviews the literature so far on surgical instrumentation for subretinal surgery, and outlines some key experiments that we have performed.

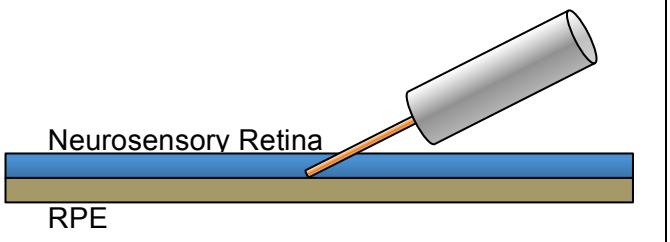

Creation of subretinal bleb

41 gauge tip cannula on 20-gauge instrument used to inject balanced salt solution between retina and RPE

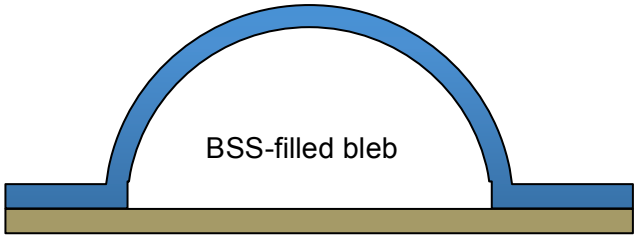

Neurosensory retina shown in blue. RPE (including basement membrane) shown in brown.

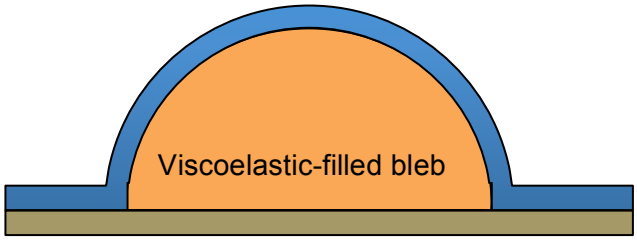

Viscoelastic

Bleb can be filled with viscoelastic to prevent collapse

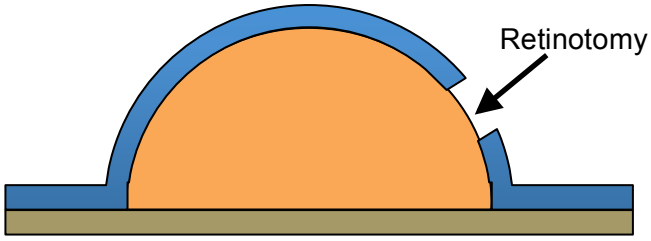

Bleb incision

Bleb is incised, creating a retinotomy that allows insertion of a cell-seeded polymer through an injector

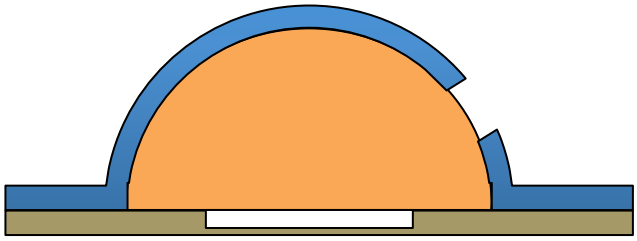

Debridement of host RPE

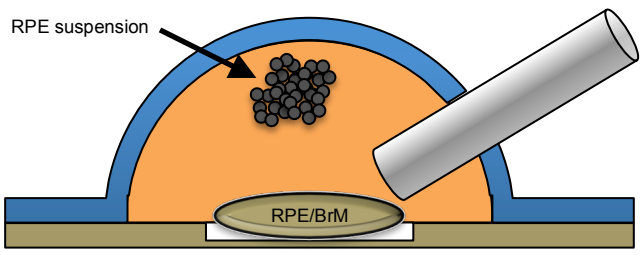

Injection of an RPE cell suspension *or* a cell-seeded BrM substitute

The delivery device must not damage the polymer or the cells during delivery

Figure 4.1: Instrumentation required during stages of subretinal surgery

4.1.1 Ophthalmic Viscoelastic Device (OVD)

Ophthalmic Viscoelastic Devices (OVDs) are transparent gel-like substances that are used routinely to maintain the stability of the eye during cataract surgery.[173, 174] Viscosity, which can be defined as resistance to flow, is determined by the molecular weight and concentration of the OVD. OVDs have properties of both fluids and solids. However, many OVDs are non-Newtonian fluids and therefore demonstrate the phenomenon of pseudoplasticity, which refers to the change in viscosity at different shear rates. Therefore an OVD with high pseudoplasticity has the properties of a solid when at rest, but during injection through a narrow gauge cannula, the OVD behaves as a fluid. In addition to viscosity, OVDs are elastic and therefore return to their original shape after deformation. The elasticity of an OVD allows their use as a space maintainer and affords protection of the ocular tissues from ultrasound energy and fluid irrigation during cataract surgery. The pseudoplasticity allows rapid delivery and removal of these agents during surgery. OVDs are chemical compounds but are classified as medical devices rather than as drugs.[173]

OVDs have been classified by Arshinoff according to both viscosity and by a measurement of cohesion (cohesion-dispersion index (CDI)).[173, 175] Highly viscous OVDs tend to be more cohesive, and can induce and sustain pressure. Low viscosity OVDs are useful in partitioning spaces within the eye. A small number of OVDs are known as viscoadaptive because they have properties of both cohesion and dispersion.

OVDs are not routinely used intraocularly during vitreoretinal surgery. Methylcellulose is effective in allowing lubrication of the cornea during retinal surgery, obviating the need for frequent corneal irrigation from a surgical assistant. El Rayes & Elborgy have described the use of a viscoelastic, Perlane, a long acting hyaluronic acid, as a suprachoroidal “spacer”, to allow a surgical cannula to pass between the choroid and the sclera for suprachoroidal buckling.[176] Veritti *et al.* used a dispersive viscoelastic during macular hole surgery to protect the RPE from the toxicity of indocyanine green, an intraocular dye. However the authors found that retained viscoelastic in three patients caused the surgery to fail.[177]

There have been few *in vitro* studies on the effects of viscoelastic on RPE cells. Fernandez-Vigo *et al.* investigated the use of HPMC as a vitreous substitute in rabbit eyes.[178] They concluded that HPMC would be a poor vitreous substitute, because it

mixes readily with intraocular fluids rather than creating a barrier at retinal breaks to prevent retinal detachment. However, it was notable that these authors found no adverse effect of HPMC on cultures of primary human RPE cell, with density and RPE confluence maintained even after 24 days in culture.[178]

After creation of the subretinal bleb with balanced salt solution, some manipulation of the bleb is required. Fluid irrigation into the eye, in combination with incision into the bleb to allow RPE-BrM delivery, can lead to rapid loss of BSS from the subretinal space into the vitreous cavity, thereby causing bleb collapse. Stanzel *et al*. have experienced spontaneous flattening of the bleb during surgery in a rabbit model of RPE transplantation, and have proposed that immediately after bleb creation with balanced salt solution, ophthalmic viscoelastic devices (OVDs) can be used to maintain the subretinal space even after it has been incised. Stanzel *et al* noted that the use of >0.25% hyaluronate prevented bleb collapse, but 0.1% hyaluronate or balanced salt solution did not prevent bleb collapse.[138]

The ideal OVD for the subretinal space remains undetermined. A bleb created with a 41g cannula will not collapse because the retinal opening created to inject balanced salt solution into the subretinal space is small and self-sealing. However, incision into the bleb is required to allow RPE cell delivery, either as a suspension or as a patch graft, and once the incision is made, the bleb can collapse because of the intraocular pressure generated by the intraocular fluid infusion.

4.1.2 Removing residual RPE

A number of investigators have used animal models to determine the effects of removing the residual RPE prior to transplantation. Lopez *et al.* used a diamond dusted needle but subsequent histological examination revealed numerous inadvertent breaks in BrM, resulting in cellular proliferation from the choroid into the subretinal space.[101] This group therefore reverted to removing host RPE with the force of the subretinal fluid injection. However this is also not ideal because the RPE is not removed; the investigators observed that RPE remained attached to the underside of the neurosensory retina, thereby creating a different plane of separation. Following

transplantation the host RPE lies between the transplanted cells and the photoreceptors.

Wongpichedchai *et al.* used 100µl of 0.02% ethylenediaminetetraacetic acid (EDTA) to create subretinal blebs in rabbits. The EDTA was then aspirated, bringing RPE cells with it. These cells were of sufficient number to achieve *in vitro* culture.[99]

Stanzel *et al.* have recently reported use of a 0.1mm prolene loop to facilitate RPE removal. In a rabbit model, an area of 2.5mm x 1.5mm was treated with a single forward and backward stroke. This area was later found to be 70% devoid of RPE cells, although a few miniscule BrM lacerations and choriocapillaris blood clots also occurred. A thinner, more flexible prolene loop was less effective, as was a 0.1mm metal wire which also caused intraoperative subretinal haemorrhage.[138]

4.1.3 Delivery of RPE cells

4.1.3.1 Delivery of an RPE cell suspension

In their seminal experiments with the RCS rat, Li & Turner used a blunt needle to deliver a suspension of RPE cells into the subretinal space, via a trans-sclero-choroidal route.[48] Lopez *et al.* performed surgery in rabbits and were able to pass a glass cannula with an internal diameter of 100µm through the pars plana, and then create a small subretinal bleb via a retinotomy.[101] The diameter of their glass cannula is similar to that of the 41-gauge cannula that is used in modern surgery for formation of a localised retinal detachment during vitrectomy.

Similar to the methods of Lopez *et al*., Gouras and coauthors used a glass cannula to deliver RPE cells into the subretinal space in patients with dry AMD.[75] They used the cannula to deliver either a cell suspension or a patch transplant of cultured human foetal RPE. While their attempts to inject an RPE cell suspension were largely successful, they were dissatisfied with the subretinal patch graft technique. The 0.6mm diameter circular graft would fold in the subretinal space, and on histological examination the outer nuclear layer tended to be thinner over the folded RPE graft than when the photoreceptors were adjacent to a single (unfolded) RPE layer. Gouras *et al.* did not use a BrM substitute and were simply cutting a circular patch of an RPE

monolayer grown in tissue culture.[75] The use of a BrM substitute would not only improve the chances of preventing photoreceptor degeneration but has the added advantage of providing some stability and rigidity to the graft.

Wongpichedchai *et al.* compared internal and external approaches of RPE transplantation in rabbits, and identified differing challenges.[99] For the external approach, disinsertion of a rectus muscle was necessary to access the posterior pole. For the internal approach, a micropipette with an internal diameter of just 60μm, drawn from glass, was used to induce a subretinal bleb. The micropipette was advanced vertically through the pars plana incision, to avoid trauma to the large crystalline lens in the rabbit eye. To ensure precise placement of the tip, and controlled injection of the RPE cell suspension, an electronic injection microsyringe manipulator was utilised. This ensured that at the point of the retinotomy, the cells were injected no more than 200μm deep to the inner retinal surface, and were injected at a constant controlled rate.[99] Similarly, Weichel used a manual oil-hydraulic microinjection pump to achieve controlled subretinal infusions of RPE cells.[102]

4.1.3.2 Delivery of a patch graft

Maaijwee *et al.* have done considerable work investigating different types of instrumentation for use with grafts of RPE-BrM-partial thickness choroid.[179] The group compared traditional grasping forceps with an aspiration-reflux cannula manufactured by DORC, similar in design to the instrument utilised by Thumann *et al*., but found that the main difficulty with both methods was ensuring release of the graft once the tip of the instrument was in the subretinal space.[179] To combat the friction between the graft and the carrier platform of the aspiration-reflux instrument, Maaijwee *et al.* performed several laboratory experiments demonstrating that the ability to make the instrument vibrate, utilising either the linear motor of a loudspeaker, or the vibration function of a mobile phone, would allow successful dislodgement of the graft.[179] These techniques are yet to be used in clinical or surgical practice. The same group have investigated the use of a microscale thermal tissue gripper which utilises heat induced attachment and detachment of the graft.[180] Using chicken meat for experimental purposes, success rates exceeding 90% for graft attachment/detachment were observed. Due to the small contact area of the instrument with the tissue, visible tissue damage was limited to only 0.005mm^2.

Thumann *et al.* used a custom made device to deliver an RPE cell sheet.[63] The device consists of a perforated carrier platform, attached to a syringe which exerts a vacuum on the under surface of the graft, thereby preventing it from becoming dislodged. The platform is then covered by a second cannula, protecting the RPE cells from damage or dislodgement when introduced into the eye. Once the instrument tip was in the subretinal space, the second cannula was pulled back and a small amount of pressure was placed on the syringe plunger, allowing release of the graft. A modified version of the instrument had a tip angled at 45 degrees to allow easy access to the subretinal space. Thumann *et al.* were able to ensure consistent delivery of the cell sheet, without rolling or folding, and simply used micro tweezers to ensure satisfactory positioning.[63]

Stanzel *et al.* have described a custom-made implant shooter instrument to deliver polyester membrane inserts, some of which were gelatin covered, to facilitate implant loading and delivery. The investigators performed pars plana vitrectomy and induced a subretinal bleb with a 41-gauge needle, and utilised a novel infusion cannula with two side ports, to reduce the stream of fluid over the subretinal bleb, thereby avoiding collapse of the bleb or uncontrolled tearing of the retinotomy.[181] Despite elegant demonstration of delivery into the appropriate anatomical space, implantation of polyester implants without RPE cells resulted in development of a multi-layered fibrocellular scar tissue, and almost complete atrophy of photoreceptors overlying the implant, with evidence of intraretinal cyst formation on OCT scanning. This may have occurred because of the mechanical separation of photoreceptors from the RPE by the implant. Similar atrophic changes have been observed after subretinal implantation of artificial retina chips and it was hypothesised that a more permeable carrier may result in a better preserved outer retinal architecture.[181] Implantation into rabbit eyes of the polyester carrier with RPE derived from human embryonic stem cells resulted in 95% survival at four weeks.[128]

4.2 Aims and Objectives

There were two main aims of this chapter. The first was determine the effect of various viscoelastic substances on RPE cells in vitro. The second aim was to develop a surgical instrument that potentially allowed delivery of an RPE monolayer, growing on a segment of polymer, into the subretinal space, with a view to using the instrument to performing surgery in rabbit eyes.

Objectives of these experiments were:

- Culture ARPE-19 cells in Transwells, expose the cells to a number of different types of viscoelastic of varying viscosity and cohesiveness, and assess the degree of cell death, as measured by a Lactose Dehydrogenase (LDH) assay.

- Develop a surgical instrument and assess its success in being able to eject a polymer successfully, without damage.

- Assess the degree of RPE cell death caused by loading and ejection of the RPE-seeded polymer from the surgical instrument.

4.3 Methods

4.3.1 RPE cell culture

Human ARPE-19 cells [American Tissue Culture Collection (ATCC) Manassas, VA] were maintained at 37°C under humidified atmosphere with 5% CO_2 in culture medium comprising 1:1 (vol/vol) mixture of DMEM:F12 supplemented with 1mM sodium pyruvate and 25mM D-glucose (Life Technologies/Invitrogen). This was additionally supplemented with 1% antibiotic-antimycotic solution (10,000 units/ml Penicillin G, 10mg/ml streptomycin sulphate, 25mg/ml amphotericin B [Sigma-Aldrich]) and 1% foetal bovine serum (FBS) [ATCC]. Culture medium was changed every 72 hours

4.3.2 Effect of Viscoelastic on RPE cells in culture

4.3.2.1 Ophthalmic Viscoelastic Devices (OVD)

Three OVDs that are commonly used in ophthalmic surgery were evaluated. The three agents, 1.0% hyaluronic acid (Healon; Abbott Medical Optics, Illinois, USA), 1.4% hyaluronic acid (Healon GV Abbott Medical Optics, Illinois, USA) and 2% hydroxypropylmethylcellulose (HPMC, Moorfields Pharmaceuticals, London) were chosen because they varied in viscosity and cohesiveness. ARPE-19 cells were seeded on Corning Transwell polyester membrane inserts (Sigma-Aldrich, UK) at a cell density of 25,000 cells in 500µl. When the cells reached confluence, 100µl of viscoelastic was injected onto the surface of the top chamber of the transwell. For the control wells, 100µl of tissue culture media was used. Every 72 hours, media was collected from the lower chamber for cytotoxicity assay, and replaced with 750µl of fresh media. No media changes were performed in the upper chamber.

A second plate, containing primary rabbit RPE rather than ARPE-19, was also used. Primary rabbit cells were seeded at the identical cell density (25,000 cells in 500µl). A third plate, containing media and viscoelastic only, without cells, was used as the control. All experiments were performed in triplicate.

4.3.2.2 Cytotoxicity assay

Lactate dehydrogenase (LDH) is an enzyme present in the cytosol of animals, plants and prokaryotes. It is used in the clinical setting as a surrogate for tissue breakdown, and several disorders, including haemolysis and cancer, are associated with a high LDH. *In vitro*, cell membrane damage leads to release of LDH into the tissue culture media. The released LDH can be quantified using a colorimetric assay (Cytotoxicity Detection Kit, Roche), which uses a coupled enzymatic reaction. First, released LDH catalyses the conversion of lactate to pyruvate via reduction of NAD+ to NADH. Second, diaphorase uses NADH to reduce a tetrazolium salt (INT) (2-(4-iodophenyl)-3-(4-nitrophenyl)-5-phenyl-2H-tetrazolium chloride) to a red formazan product. The level of formazan formation is directly proportional to the amount of released LDH in the tissue culture media. The formazan dye is water-soluble and shows a broad absorption maximum at around 500nm. The tetrazolium salt INT shows no significant absorption at these wavelengths.

The protocol for the LDH assay was as described in the manufacturer's instructions. Briefly, 100µl of tissue culture media from the bottom chamber of each well was added to 100µl of the LDH reagent, and incubated in the dark for 30 minutes at room temperature. Positive controls were produced by adding 100µl of 1M Hydrochloric acid (HCl) to RPE cells in a transwell. Negative controls included three wells each containing 200µl of LDH solution, and three wells each containing 100µl LDH solution and 100µl of tissue culture media. Absorbance of samples was measured on a FLUOstar Optima microplate reader (BMG Labtech) with a test wavelength of 490 nm.

The initial experiment was unsuccessful because the standard tissue culture media was used. This contains phenol red, a pH indicator that turns progressively yellow in acidic conditions. This had two deleterious effects on the experiment. Firstly, the absorbance of the red formazan dye could not be detected because of the background absorbance of the phenol red.[182] Secondly, the positive controls were yellow and therefore had very little absorbance.

The experiment was repeated using phenol red free tissue culture media. This experiment also produced meaningless results, because the standard RPE media used contains pyruvate. However pyruvate was an intermediate product of the LDH reaction,[182] and therefore the experiment was conducted a third time using phenol-red

free, pyruvate-free media. On this occasion, the positive controls still produced 500nm absorbance lower than most of the samples. The positive controls were repeated separately using 9% Triton X-100 (Thermo Fisher Scientific, NH, USA) rather than HCL. Triton acts to lyse the cells.[182]

Cytotoxicity was calculated as:

$$\text{Cytotoxicity (\%)} = \frac{\text{Sample absorbance – Negative control}}{\text{Positive control – Negative control}}$$

4.3.3 Design and Assessment of RPE/Polymer Injector

4.3.3.1 Injector Design

At the commencement of this project, there was no commercially available instrument for the subretinal delivery of an RPE-cell seeded substrate. In light of this, considerable thought was given to the development of an injector. Although several microprecision engineering companies and one ophthalmic surgical instrument manufacturer were approached and showed interest in collaboration, the design and manufacture of a prototype device was eventually executed in-house, by the workshop in the Department of Chemistry, Highfield Campus, University of Southampton. This prototype device will herein be referred to as "POLARIS" (***POL***ymer ***A***nd ***R***PE cell ***I***njector ***S***outhampton), an acronym that was coined in June 2013.

A disposable vitreoretinal 20-gauge end-gripping membrane forceps (DORC, Netherlands) was used as a basis for the dimensions of the novel instrument. Aspects of instrument design that were considered:

- **Instrument Tip -**
    - to enter the subretinal space and then deliver the RPE/polymer parallel to the RPE, the tip of the instrument would need to be angled.
- **Handle -**
    - it was essential that the instrument could be operated by the surgeon single-handedly, because during 3-port pars plana vitrectomy, the other

hand is required to hold the fibre-optic light pipe and therefore not available to press the plunger.

- **Design -**
  - results from the diffusion experiments (see section 2.4) had demonstrated that the polymer was very fragile and using the hydraulic force from a column of fluid (e.g. balanced salt solution) would likely result in polymer damage. Therefore an actuator would be required to push on the edge of the polymer sheet without causing it to crumble, while avoiding contact the RPE monolayer on the surface of the polymer.
- **Polymer piece -**
  - a large polymer piece would enable a larger area of transplantation. Although we initially considered folding the polymer, similar to the folding of an intraocular lens used in cataract surgery, there was considerable risk for the integrity of the RPE monolayer. If the polymer was folded inwards, the RPE cells may have been in contact with each other during the injection process and it was unclear whether this would adversely affect their function. If the polymer was folded outwards then it was considered more likely that the cells would slough off during delivery. Not only would this reduce the number of cells transplanted, but it may also lead to RPE proliferation on the retinal surface, which could lead to proliferative vitreoretinopathy,[183] a scarring process that can lead to recurrent retinal detachment.
  - eventually, it was decided that partial folding of the polymer (similar to a taco) would be the ideal solution, allowing delivery of the polymer but minimising contact of the cell monolayer with itself or with any part of the instrument.
  - to ensure that the polymer was delivered in the correct orientation, it was considered that the eventual polymer should be an asymmetric shape, so that it would be obvious if the polymer had been delivered upside down into the subretinal space.
- **Gauge -**
  - Modern pars plana vitrectomy in human patients utilises 23-gauge (0.64mm outer diameter) or 25-gauge (0.51mm outer diameter) instruments. Some surgeons are even using 27-gauge (0.41mm) instruments. However, the cost of smaller instruments in the context of

RPE transplantation is that the area of RPE/BrM that can be transplanted is also smaller.

- For the purposes of this project, 20-gauge (0.9mm) pars plana vitrectomy instruments were used. Therefore the gauge of the POLARIS instrument tip was engineered to be 1.0mm. This is slightly wider than 20-gauge and would require enlargement of the scleral opening. If proof of principle was demonstrated with a surgical delivery device, a 23-gauge tip could then be developed.

POLARIS Mark I was developed in February 2013, but failed to fully eject the polymer. POLARIS Mark II, with an extended actuator to allow full polymer ejection, was developed in April 2013. In October 2013, the Bonn-Shooter instrument developed by Dr Boris Stanzel in Bonn was made available to us as a special purchase from Geuder. This enabled us to perform a direct comparison of the POLARIS and Bonn-Shooter instruments.

4.3.3.2 Preparation of Polymer

Both unfunctionalised and functionalised polymer were tested in preliminary studies. However, unfunctionalised polymer was extremely friable, and had a tendency to float away or to adhere to itself. In contrast, functionalised polymers were much more robust and seemed to have at least some "memory". All subsequent experiments were conducted with functionalised polymer fibre.

Sheets of the functionalised polymer scaffolds were sterilised with ultraviolet light for 12 hours. Under aseptic conditions, a 2mm skin biopsy punch was used to create identical polymer segments, which were rinsed three times with PBS. All samples were then flooded with culture medium and allowed to equilibrate for 0 min at 37°C before seeding. Cells were seeded at a density of 2.5×10^4 per well. Cell-seeding density was established from previous experiments (data not shown).

For comparisons with the Bonn-Shooter instrument, a standardised polymer size and shape was achieved by using a compressed 2mm skin biopsy punch to produce an oval polymer segment. Although a separate graft punch was purchased with the Bonn-

Shooter instrument, we found that a compressed skin biopsy punch was sharper and more effective at achieving polymer with clean cut edges.

4.3.4 TUNEL assay

Apoptosis, also known as programmed cell death, is a physiological phenomenon common to all eukaryotic cells. Apoptosis, sometimes described in lay terms as "cell suicide", occurs when cells are no longer required or when there is significant cellular damage. Apoptotic cells fragment into membrane-bound bodies which can be easily phagocytosed by macrophages, without generating an immune response. This is in stark contrast to necrosis, in which cell death leads to loss of cell membrane integrity, cell lysis, and a local inflammatory reaction.

The process of loading and ejecting a cell-seeded polymer into the subretinal space could cause damage to cellular layer, and cells could:

- detach from the fibre due to the trauma of the polymer being handled and then ejected (DETACHED)
- remain attached to the polymer but sustain sufficient cell damage to lead to apoptosis (APOPTOTIC)
- remain attached to the fibre but are damaged/dead and therefore fail to proliferate (NON-PROLIFERATIVE)
- remain attached to the polymer, healthy and viable, and continue to proliferate (VIABLE)

A cytotoxicity assay, such as the LDH assay, would not necessarily be a useful measure because most of the cells that die and undergo cell lysis will be mechanically removed from the polymer. An assay was used to determine what proportion of the cells remaining on the polymer were apoptotic.

The TUNEL assay (DeadEnd™ Fluorometric TUNEL System, Promega) is an assay to determine the presence of cells that have an activated apoptotic pathway. During apoptosis, endogenous endonucleases cleave the DNA of apoptotic cells into DNA fragments, each of 180-200 base pairs in length. The DeadEnd™ Fluorometric TUNEL System measures the fragmented DNA of apoptotic cells by catalytically incorporating

fluorescein-12-dUTP at 3'-OH DNA ends using the Recombinant enzyme Terminal Deoxynucleotidyl Transferase (rTdT). This enzyme forms a polymeric tail using the principle of the TUNEL (TdT-mediated dUTP Nick-End Labeling) assay. The fluorescein-12-dUTP-labeled DNA can then be directly by fluorescence microscopy (green). Propidium iodide staining is used to assess the total number of cells. Propidium iodide was used to stain all cells (both apoptotic and non-apoptotic) red. Fluorescein-12-dUTP incorporation results in localised green fluorescence within the nucleus of apoptotic cells only. The proportion of cells showing evidence of apoptosis was calculated.

The protocol for the TUNEL assay was as described in the manufacturer's instructions. Cells were fixed removing tissue culture media and replacing it with 4% paraformaldehyde in PBS (pH 7.4) for 30 minutes at 4ºC. The cells were then washed twice in fresh PBS, for 5 minutes each, at room temperature. Cells were permeabilised by immersion in 0.2% Triton X-100 solution in PBS for 5 minutes, followed by 2 washes in fresh PBS at room temperature for 5 minutes each. The cells were then covered in 100µl of Equilibration Buffer for 10 minutes, and during this period the Nucleotide Mix and rTDT incubation buffer was prepared, kept on ice and protected from light. The equilibration buffer was removed and 50µl of Nucleotide Mix/rTDT incubation buffer was placed in each well. After this step the cells were protected from light by wrapping the tissue culture plate in aluminium foil and incubated at 37ºC for 60 minutes. The reaction was terminated by immersion in 2X saline-sodium citrate (SSC) for 15 minutes at room temperature. Three washes with PBS at room temperature for 5 minutes each, were performed to remove any unincorporated fluorescein-12-dUTP. Propidium iodide diluted in PBS to 1µg/ml was added to each polymer segment and left for 15 minutes at room temperature. Samples were washed three times with deionised water for 5 minutes at room temperature.

Fluorescence microscopy was used to analyse the samples. Fluorescein fluoresces green (excitation 490nm, emission 520nm) and propidium iodide is viewed as red (excitation 535nm, emission 620nm).

One-way ANOVA was used to compare the apoptotic cell death following ejection from the Southampton Injector (POLARIS) and the Geuder Injector (Bonn-Shooter), compared to unejected controls. A p-value <0.05 was considered statistically significant.

4.4 Results

4.4.1 Viscoelastic experiment

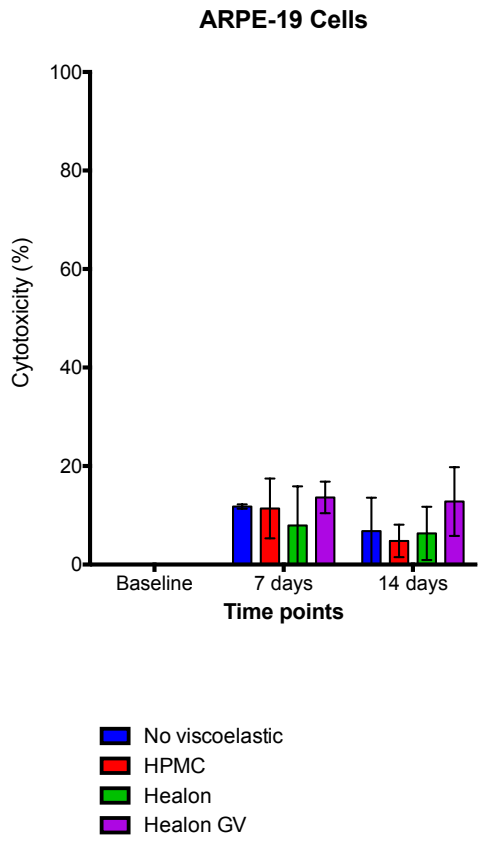

Figure 4.2: Cytotoxicity of cohesive and dispersive ophthalmic viscoelastic devices to RPE cells

ARPE-19 cells show no increased cytotoxicity from application of viscoelastic to the upper chamber of the Transwell. Baseline cytotoxicity was less than 20%.

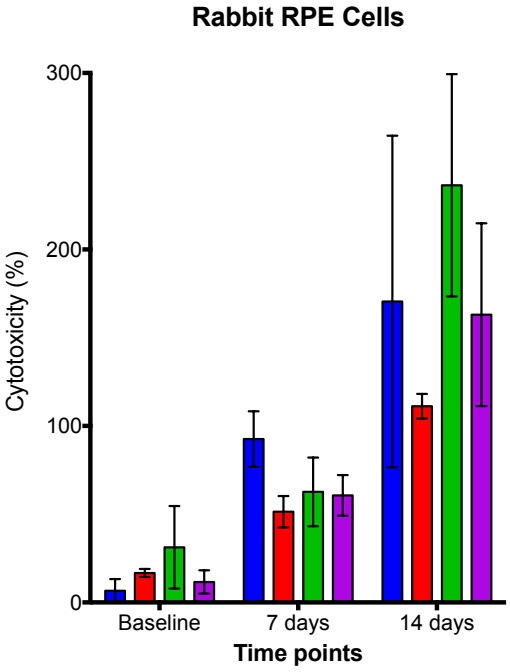

For primary rabbit RPE cells, there was increasing cell death with time. There was no discernable difference between viscoelastic or media. No primary RPE cells were available as a positive control, and therefore ARPE-19 positive controls were used to calculate cytotoxicity. This accounts for the "300% cytotoxicity" observed.

4.4.2 Evaluation of POLARIS Injector

POLARIS Mark I, shown in Figure 4.3, failed to successfully eject the polymer (see Figure 4.4). POLARIS Mark II was more successful, as shown in Figure 4.5 and Figure 4.6.

4.4.2.1 POLARIS Mark I

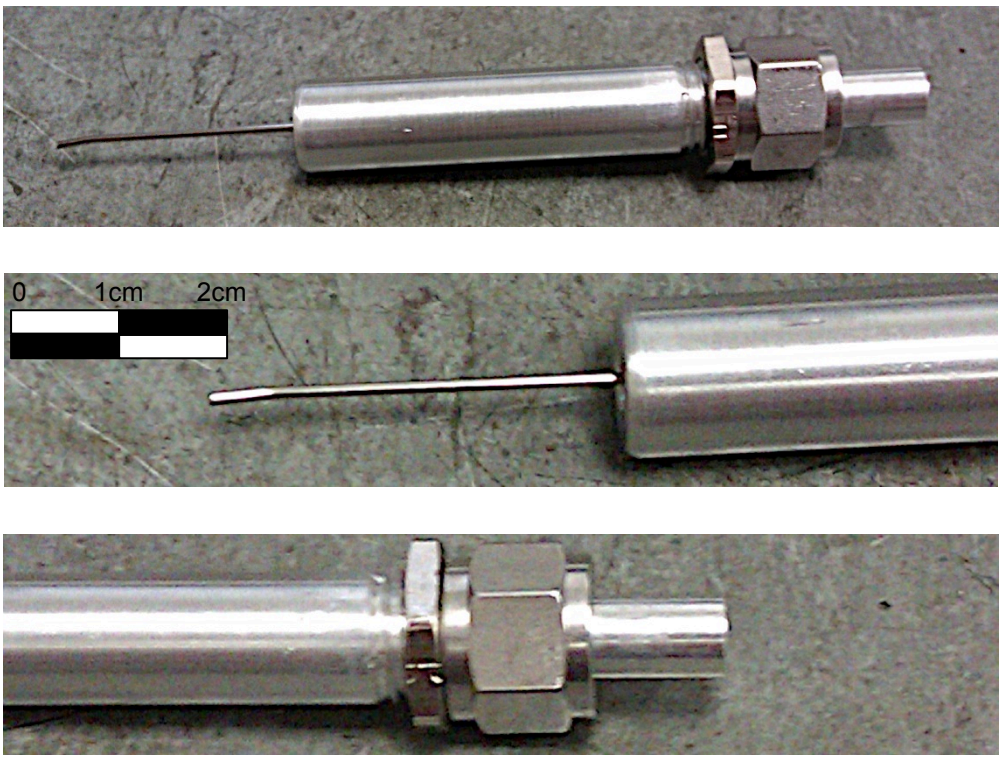

Figure 4.3: Photographs of the **POL**ymer **A**nd **R**PE **I**njector from **S**outhampton (POLARIS), Mark I.

The tip had an outer diameter of 1mm (slightly larger than 20-gauge), and was angled to allow easier access to the subretinal space. The polymer was delivered by depression of the button at the top of the instrument, which allows the actuator to advance. The instrument can be operated with one hand, which is an important consideration for instruments used in retinal surgery.

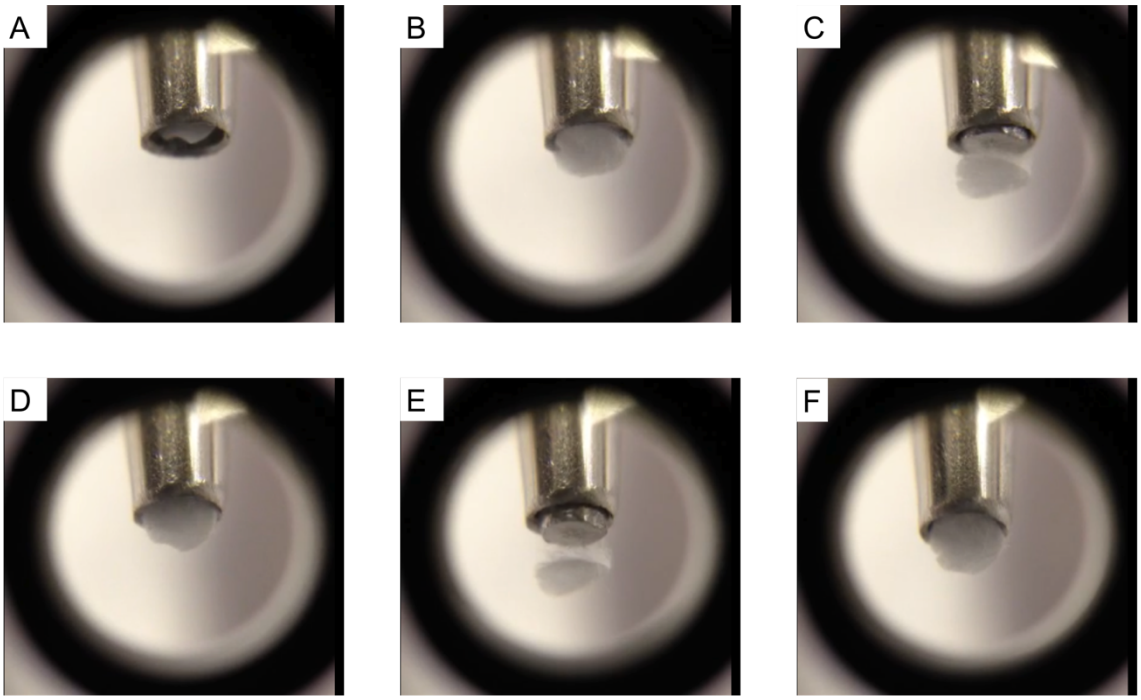

Figure 4.4: Photographs showing failed ejection of a polymer (without cells) from POLARIS Mark I.

POLARIS Mark I had a 1mm tip. In A, the 1mm diameter polymer disc is held within the instrument barrel. Note the slight damage to the polymer edge caused by toothed forceps during loading of the polymer into the instrument tip. Although initial ejection was normal (B), the polymer was not successfully deployed despite full extension of the actuator (C), because one of the polymer fibres is caught between the actuator and the instrument barrel. The actuator was retracted but the polymer then remained partially within the instrument tip (D). Further attempts to eject the polymer, by repeated depression and then release of the button, are unsuccessful (E,F). Images taken with an iPhone 5 (Apple, Cupertino, California, USA) with microscope attachment (Foxnovo, Las Vegas, Nevada, USA).

4.4.2.2 POLARIS Mark II

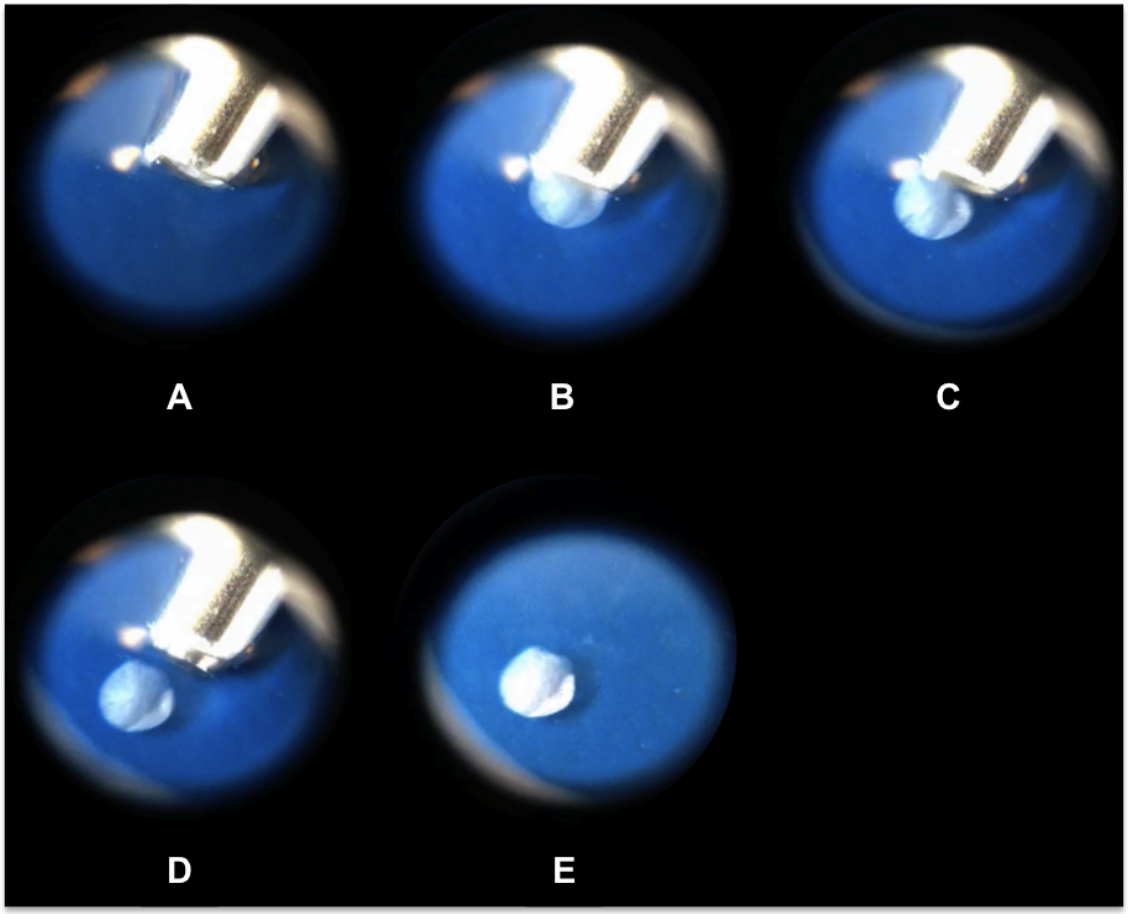

Figure 4.5: Photograph panel showing successful ejection of polymer (without cells) from POLARIS Mark II.

POLARIS Mark II had a wider tip, allowing a larger polymer disc to be delivered. The diameter of the polymer was 2mm. The tip of the actuator was modified to allow it to extend further out of the instrument barrel. This allowed consistently successful polymer ejection.

4.4.2.3 Polymer and Cell survival after POLARIS II ejection

The structural integrity of the polymer discs remained completely intact after ejection from POLARIS Mark II, as shown in Figure 4.6. To evaluate cell survival and viability, a TUNEL assay was performed, and the results of this are shown in Figure 4.7.

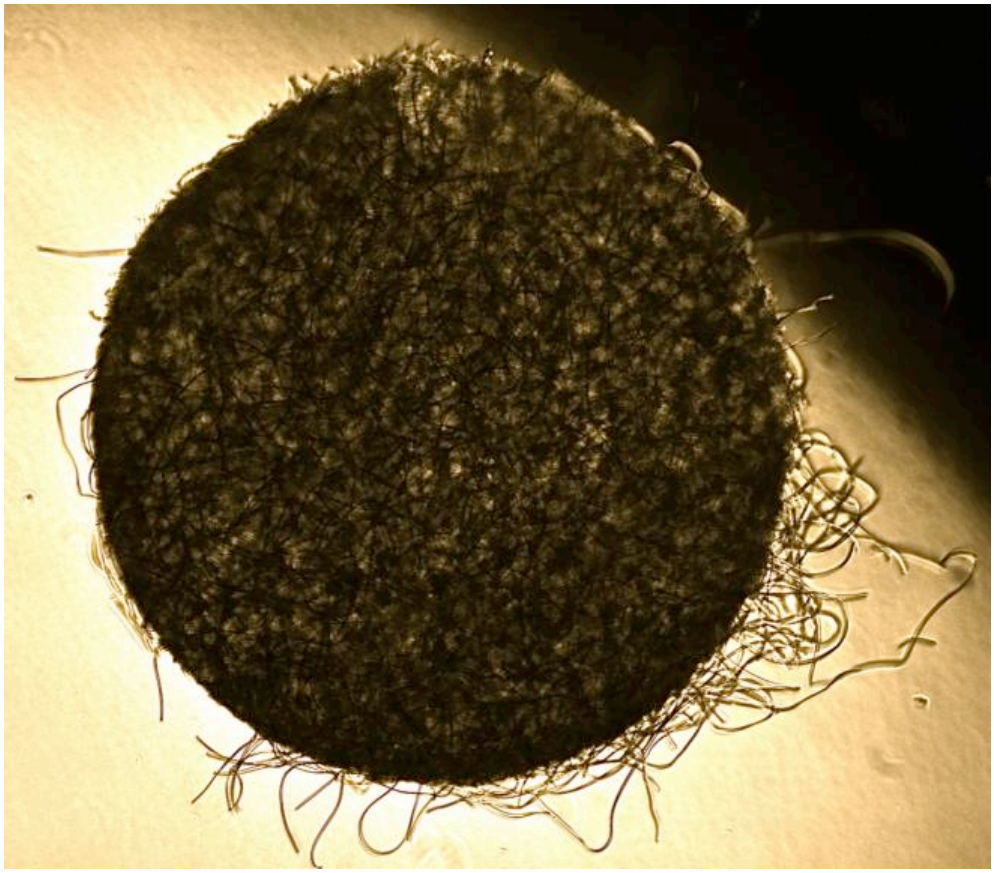

Figure 4.6: Image demonstrating that structural integrity of the 2mm diameter polymer disc was maintained even after ejection from POLARIS Mark II.

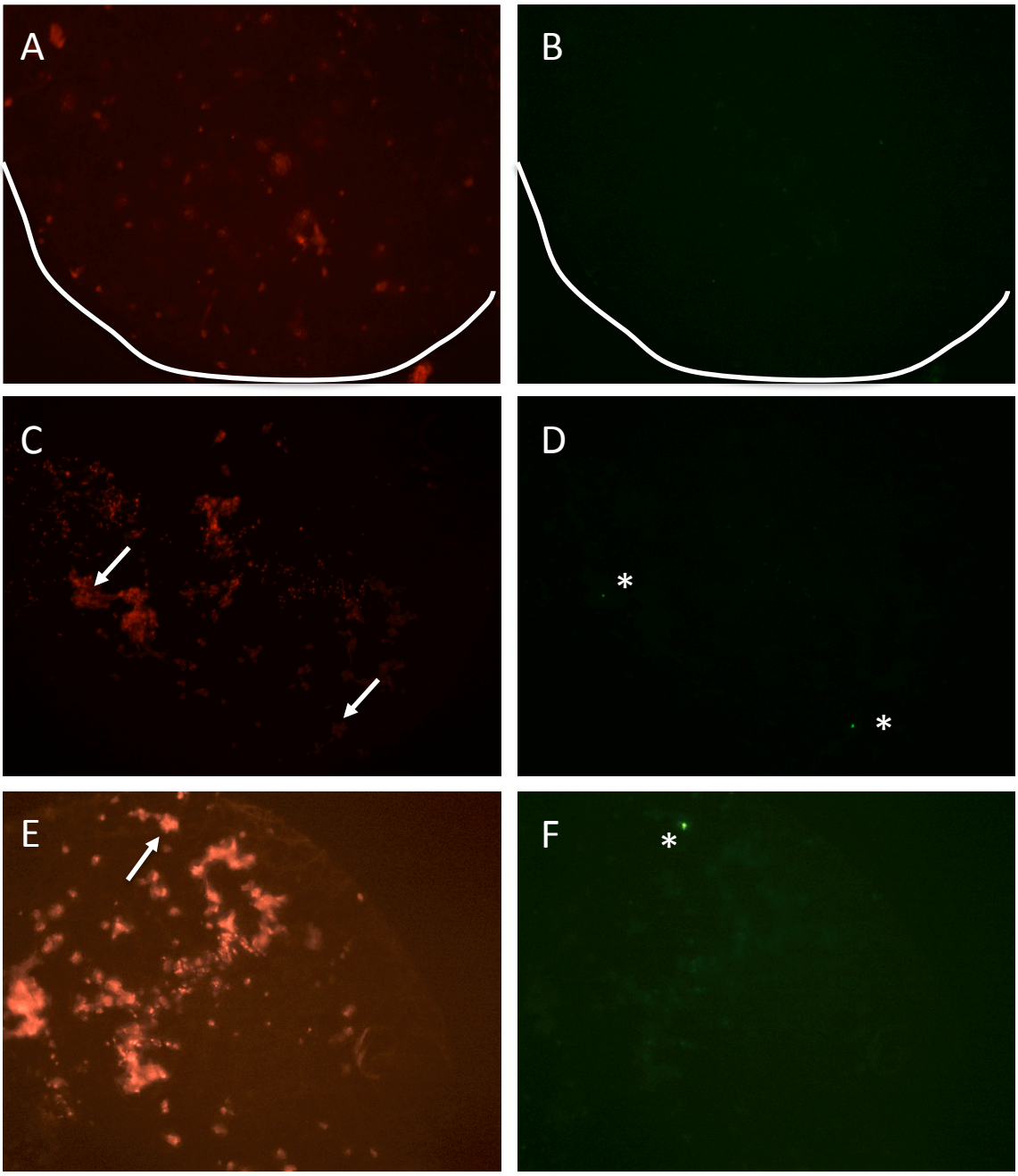

Figure 4.7: TUNEL assay of polymer ejected from POLARIS Mark II.

*Outline of the polymer has been drawn in figures A and B. Green fluorescent apoptotic cells are marked with * in images D and F. Arrows in C and E indicate the cell that was apoptotic.*

The TUNEL assay allows identification of apoptotic cells, and quantification of the number of apoptotic cells relative to the total number of cells on the polymer. Polymer discs of 2mm diameter were seeded with ARPE-19 cells.

Two polymer discs were used as controls, and instead of being loaded into the POLARIS device, were simply transferred from one well to another with toothed forceps. Six remaining polymer discs were loaded into POLARIS II and then ejected into a well with fresh PBS. The cells were then fixed and stained with propidium iodide (PI). Photographs above show results from one control polymer (A, B) and two ejected polymers (C,D, and E,F). Figures B, D, and F show exactly the same polymer as in A, C, and E respectively, but show only the apoptotic cells, which fluoresce green. In the control i.e. unejected polymer (A), there was no apoptosis (note there is no green fluorescence in B). In the ejected polymer discs (C, E), there was only minimal apoptosis relative to the number of cells on the polymer (D, F). Note that the polymer fibres also stain with PI (A, C, E).

Overall, the unejected polymers showed less apoptosis (mean 1.7%, range 1.0% - 32.5%) than polymers that had been ejected from POLARIS II (mean apoptotic cell loss 18.6%, range 11.8%-19.9%). However it was noted that the cell coverage on the polymer was not complete on any of the polymer discs, but because it was not possible to visualise the cells while they were growing on the polymer (NB the ARPE-19 cells were not pigmented), it was impossible to determine whether the poor coverage after fixation was because some of the cells had been completely removed from the polymer or whether it was the baseline number of cells was inadequate. The experiment therefore needed to be repeated, but at this point the opportunity arose to purchase the Bonn-Shooter instrument (Geuder, Heidelberg, Germany). This patented instrument has previously been used for subretinal implantation of RPE-seeded polymers into rabbit eyes by Stanzel *et al*.[181]

4.4.3 Comparison between POLARIS II & Bonn-Shooter instruments

POLARIS Mark II and the Bonn Shooter instrument were compared with respect to polymer integrity and cell viability following ejection.

Following the previous experiment (see previous section), the size of the polymer discs was modified. Although POLARIS II is capable to delivering a 2mm polymer graft, the Bonn Shooter instrument can only delivery a 2mm x 1mm polymer segment. Therefore a standardised polymer size of 2mm x 1mm was used for both instruments.

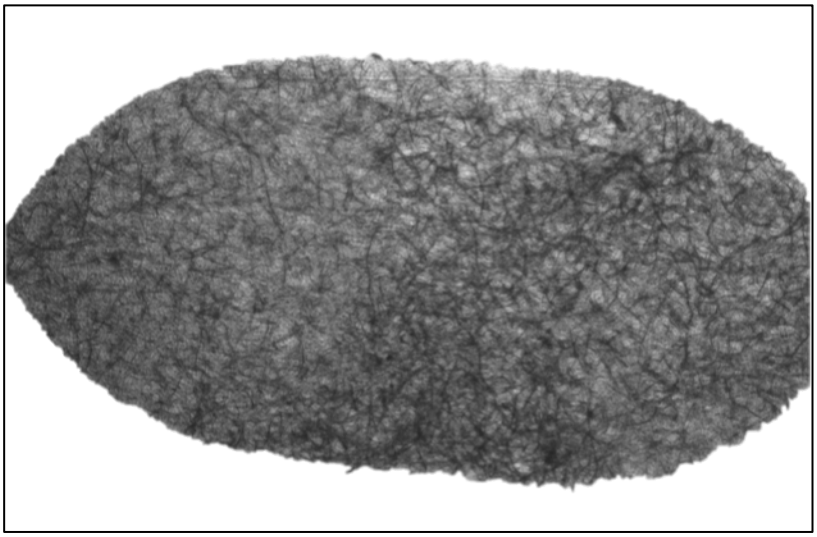

Figure 4.8: A bullet-shaped polymer segment, measuring 2mm x 1mm

The results of qualitative testing of polymer integrity after ejection are shown in Table 4.1 and Figure 4.9. Cell viability results are shown in Figures 4.10 and 4.11.

	Intact Polymer	Damaged Polymer
POLARIS Mark II (n=6)	6	0
Bonn-Shooter (n=6)	5	1
Unejected control (n=6)	5	1

Table 4.1. Table comparing frequency of polymer damage after ejection of polymer from surgical instruments (POLARIS Mark II, or Bonn-Shooter) vs. control.

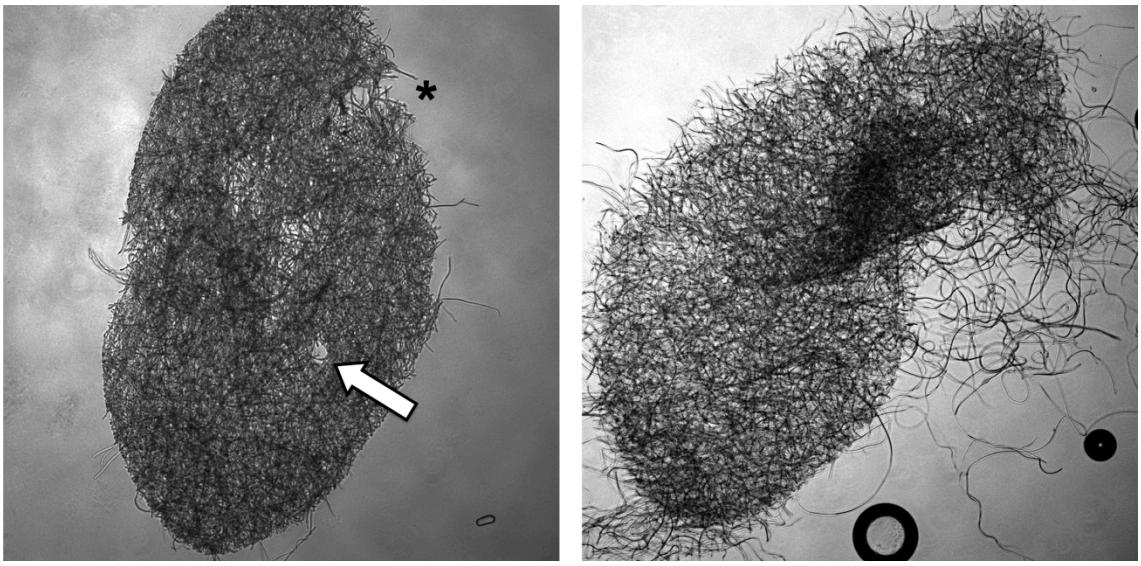

Figure 4.9: Polymer damage following ejection from surgical instruments

LEFT: One polymer in the control group showed evidence of a central hole (see arrow) and damage to the polymer edge (marked by *). This damage was attributed to the effect of handling the polymer with forceps.

RIGHT: One patch was severely distorted following ejection from the Bonn-Shooter instrument, despite uneventful loading of the polymer into the instrument tip. Notably, none of the patches ejected from POLARIS Mark II were damaged. The small circles in the bottom right of the picture are air bubbles.

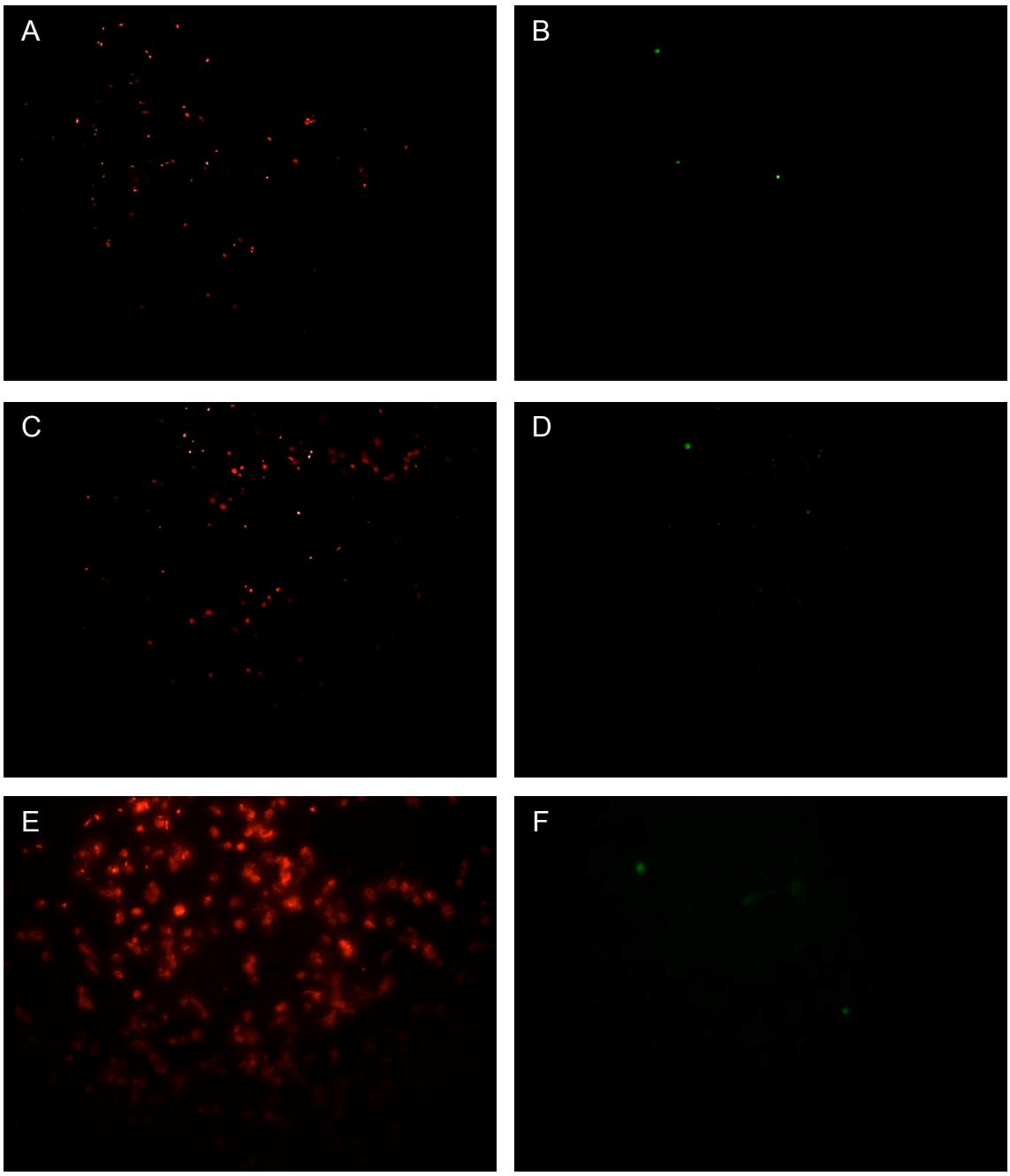

Figure 4.10: Photographs showing cells remaining on polymer immediately after ejection from the Bonn-Shooter and POLARIS instruments.

Left photographs (red) show total number of cells. The control polymer (A), was transferred from one well to another and then fixed immediately. Ejected polymers were fixed immediately after ejection from the Bonn-Shooter instrument (C) and the POLARIS II device (E). Right photographs

show apoptotic cells from the control polymer (B), and the polymers ejected from the Bonn-shooter (D) and the POLARIS II (F), which fluoresce green. The panel of photographs shows that very few cells are apoptotic.

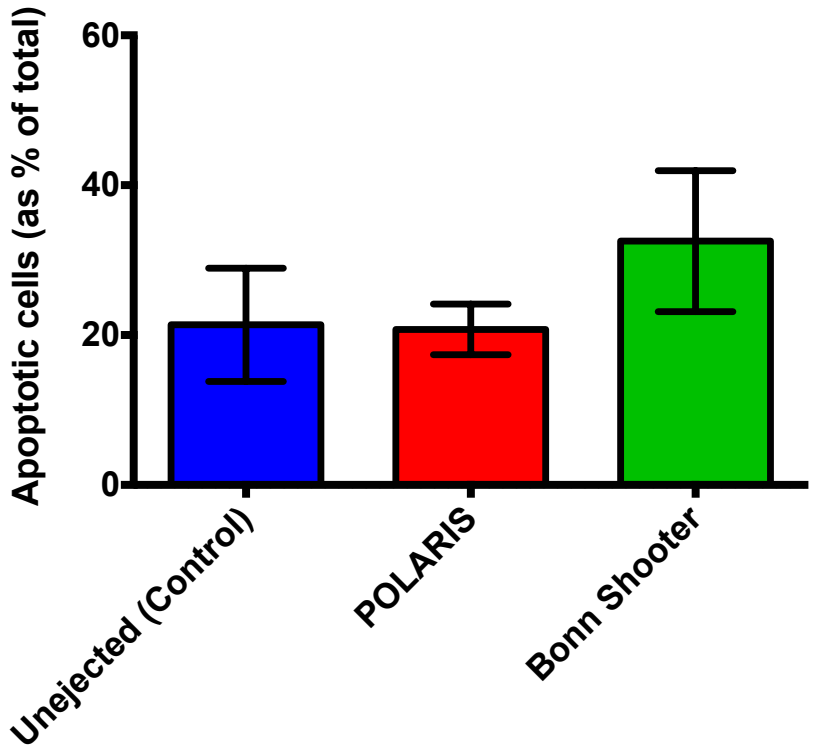

Figure 4.11: Apoptotic cell death following ejection from the Southampton Injector (POLARIS) and the Geuder Injector (Bonn-Shooter), compared to unejected controls.

Bar chart and error bars indicate mean and SEM respectively. There was no statistical difference in the apoptotic cell death between POLARIS (21%) and the unejected controls (21%). The Bonn-Shooter showed a trend for a higher rate of apoptotic cell death (33%) but this was not statistically significant. The control samples showed considerable variation in the degree of apoptotic cell death.

4.5 Discussion

These results confirm that when ARPE-19 cells *in vitro* are exposed to OVDs of varying viscosity and cohesiveness, the rate of cell death is unchanged from controls. This provides the option for use of viscoelastic within the subretinal space, to prevent bleb collapse during insertion of the RPE/BrM graft. While the experiments above have shown that OVDs are not toxic to the RPE, any viscoelastic in the subretinal space will also be in contact with the photoreceptors, and I have not performed any experiments to determine photoreceptor toxicity. It is possible that the presence of viscoelastic may delay the full reattachment of the retina once the RPE/BrM graft is in situ and this could theoretically have consequences for visual recovery. The true effect of viscoelastic can therefore only be tested in an *in vivo* model.

The unusual results yielded from the LDH assay of primary rabbit RPE cells exposed to viscoelastic warrants some discussion. Firstly, the cell death noted in the samples was three-hold that of cell death in the positive control. This is a reflection of the lack of an adequate positive control. Because of difficulties with this experiment, it needed to be repeated three times, each with different conditions. By the time the third experiment was conducted, no rabbit RPE cells were available for use as a positive control, and therefore ARPE-19 cells, treated with ARPE-19 media and Triton, were used instead. This is an obvious experimental flaw. In spite of this, it is interesting to note that while the ARPE-19 cell death was similar at 7 and 14 days, the primary rabbit RPE cell death increased between 7 and 14 days. This may indicate a true effect of viscoelastic toxicity but the considerable variation between samples precludes any definitive conclusions.

The design of the injector was my first task when I embarked upon this project and with only two revisions the design of the injector seems remarkably robust. Only after designing this instrument did I gain access to the Bonn-Shooter. One particular design feature is common to the POLARIS instrument, the Bonn Shooter, and the injector designed by Lyndon da Cruz and Pete Coffey for the London Project to Cure Blindness[184]: the apical cells surface is in contact with the injector or any other surface, and the RPE/BrM graft is kept flat, rather than curved or folded, at all times. Successful injection relies on the actuator pushing on the edge of the polymer, which itself needs to be sufficiently strong to prevent crumpling during the injection process.

During the course of this project, Gareth Ward, my fellow doctoral student and resident polymer chemist within the Lotery laboratory, has been successfully working on the refinement of the constituent design of the polymer to make it mechanically stronger and robust. This new design is being patented and therefore details of this are beyond the scope of this thesis.

The results support the use of the injector as a potential delivery device for a RPE cell –seeded polymer. The POLARIS device is able to deliver a much larger polymer disc than the Bonn-Shooter device and the size of the RPE-BrM graft has significant implications. Larger grafts allow a large number of cells to be delivered, and a wider area of retinal rescue, thereby bestowing a larger visual field for the patient. Larger grafts have a smaller edge-to-area ratio, and since it is likely that most of the cell loss occurs at the edge of the polymer where it is in contact with the injector, a larger graft may result in lower rates of cell loss. However, implantation of a larger graft needs both a larger sclerotomy and a wider retinotomy, and surgical difficulties in achieving this may ultimately limit graft size.

4.6 Conclusions

- For ARPE-19 cells exposed *in vitro* to OVDs of varying viscosity and cohesiveness, the rate of cell death is unchanged from controls.

- This provides the option for use of viscoelastic within the subretinal space, to prevent bleb collapse during insertion of the RPE/BrM graft.

- There was no statistical difference in apoptotic cell death following ejection of RPE cell-seeded polymer from POLARIS (21%) compared to unejected controls (21%). The Bonn-Shooter showed a trend for a higher rate of apoptotic cell death (33%) but this was not statistically significant.

- The results support the use of the POLARIS injector as a potential delivery device for a RPE cell–seeded polymer.

Chapter 5: SURGICAL TECHNIQUES

"Out, vile jelly! Where is thy lustre now?"

- Duke of Cornwall renders the Earl of Gloucester blind by removing vitreous. In King Lear Act III, Scene VII, by *William Shakespeare*

5.1 Introduction

The first description of RPE transplantation was by Gouras *et al.*, who transplanted cultured 3H thymidine labelled human RPE cells on to denuded BrM in owl monkeys.[100] The investigators used an open-sky technique: the cornea was removed, and the globe was open for the duration of the procedure. As a result, the investigators experienced difficulties reattaching the neurosensory retina.[100] Following modification of the technique to a closed-eye method, consisting of pars plana vitrectomy, retinotomy and delivery of cells through a pipette, early spontaneous retinal reattachment was achieved.[101] In both of these studies, donor RPE cells successfully attached to BrM and some phagocytosis of photoreceptor outer segments could be demonstrated.

Following this, a number of investigators have continued to use an internal transvitreal approach, involving pars plana vitrectomy, whilst others favour an external approach involving dissection of posterior sclera and trans-sclero-choroidal subretinal injection of RPE cells. The external approach was first described in the human eye in 1975 by Peyman *et al.*, who performed a scleral-chorioretinal biopsy in a patient with suspected malignant melanoma.[97] Choroidal haemorrhage was avoided by extensive diathermy but moderate vitreous loss occurred through the wound. This technique was subsequently adapted for RPE harvesting in pigs[98] and rabbits.[99] However, several investigators have utilised an internal approach in humans, consisting of pars plana vitrectomy, surgical excision of subfoveal CNV, followed by translocation of dissociated RPE cells[59] or an RPE/BrM/choroid graft,[55-57] either free or pedicled.

The external approach is preferable in animal studies, especially in rodents, where the globe is small, the lens is large, and there is no true vitreous cavity to operate within (see Figure 5.4).[185] However this technique not only requires rupture of BrM but also

causes choroidal trauma, leading to the risk of severe intraocular or suprachoroidal haemorrhage, and may possibly lead to inflammation and immune responses that would not occur with the transvitreal approach. In larger eyes, the internal surgical approach is considerably easier. Wongpichedchai *et al.* compared the external vs. internal approaches in rabbits, and noted that although similar results were achieved, access to the posterior pole using the external approach was difficult, and required disinsertion of a rectus muscle.[99] In contrast, pars plana vitrectomy is a commonly performed procedure in the developed world, with an estimated 100,000 procedures performed in the USA each year,[186] and around 20,000 in the UK (see Figure 4.1).[187] Therefore, the internal approach may be more appropriate for the human eye, allowing use of existing surgical skills, experience and instrumentation.

5.1.1 Pars Plana Vitrectomy

In Shakespeare's work *King Lear*, removal of the vitreous (referred to as the "vile jelly") was associated with rendering an eye blind. It was only in 1863 that Von Graefe performed vitreous surgery with the aim of improving vision.[188] However, until the development of pars plana vitrectomy over a hundred years later by Machemer *et al*.[189], vitreous surgery was usually performed through the anterior segment and involved removal of the cornea, in a so-called 'open-sky' approach.

Figure 5.2 and 5.3 illustrate the initial steps of a 'modern' pars plana vitrectomy (PPV). PPV, usually referred to simply as 'vitrectomy', was first described in 1971 by Machemer *et al*.[189] This technique allowed surgery to the retina using an internal approach using a truly closed system. This not only allowed maintenance of the intraocular pressure, thereby preventing globe collapse intraoperatively, but also obviated the need for removal of the cornea and the lens. The surgical wound of a pars plana vitrectomy was smaller, so there was less iatrogenic trauma, and the time required to suture the wound closed was also considerably shorter than with the open-sky approach.

Machemer developed the vitrectomy instrument by attempting to remove egg white from an egg, without the shell disintegrating. Machemer *et al.* described the use of a 17-gauge (1.5mm diameter) instrument that aspirated and cut vitreous, and also infused saline into the eye to replace the vitreous that had been removed.[189] This approach was modified in 1974 by O'Malley and Heintz, who separated the infusion

and aspiration lines, and also introduced a third port to allow the introduction of a light source.[190] Although there have been considerable advances in instrumentation, with 23-gauge, 25-gauge and more recently 27-gauge instruments available,[188] the three port pars plana vitrectomy (TPPPV) approach that was developed by O'Malley and Heintz remains relatively unchanged.

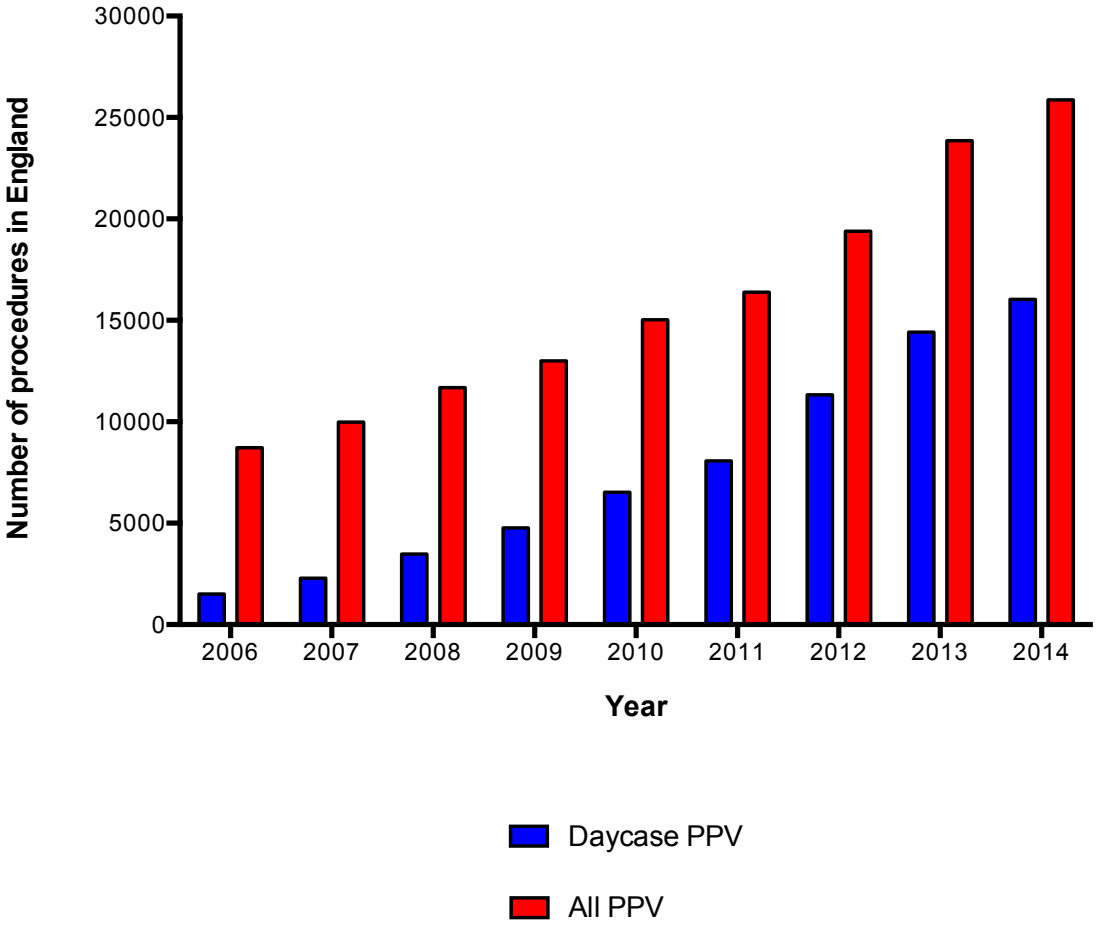

Figure 5.1: Number of pars plana vitrectomies performed in England, 2006-2014.

The number of pars plana vitrectomies being performed is increasing. The reasons for this are unclear and although it is possible that the prevalence of retinal disease may be increasing, a more likely explanation is that the threshold for surgery is becoming lower, mainly because of advances in surgical technology that allow the procedure to be performed more safely. The procedure is usually well tolerated under local anaesthetic, and the

majority of procedures are now performed as day-case operations (i.e. the patient is not required to stay overnight in hospital). Chart created using data from Hospital Episode Statistics (HES).

It is well recognised that opacification of the crystalline lens, known as cataract, is much more common after vitrectomy, although the exact mechanism of this remains unknown. In human patients, cataract formation occurs in 74% of patients within three years of vitrectomy surgery.[191]

In many macular conditions, it is important to remove the vitreous because the vitreoretinal interface is the cause of the pathology. However, macular surgery without the need for vitrectomy has been described, although this is not common practice. A small number of studies have shown that surgical removal of epiretinal membrane peel can be performed without removing vitreous, although the authors acknowledge that in some patients, complete removal of the epiretinal membrane could not be achieved without vitrectomy.[192, 193] The main drive for non-vitrectomising macular surgery is to avoid the development of post-vitrectomy cataract. However, cataract formation is common in elderly eyes without any other pathology and modern cataract surgery is highly successful. It is therefore widely accepted that for patients with macular pathology that require surgical intervention, the advantages of vitrectomy, such as removing vitreous cavity opacities, allowing space in the vitreous cavity for tamponade, and removing vitreous traction, outweigh the fairly minor disadvantage of post-vitrectomy cataract formation. Complete removal of the vitreous is essential in the treatment of proliferative vitreoretinopathy (PVR), since the vitreous can be regarded as a collection pool for growth factors and inflammatory mediators.[194] This may be of relevance for the treatment of AMD, a disease that is known to be partly inflammatory in origin.

Diagnostic	• Vitreous +/- chorioretinal biopsy for • Bacterial or fungal infection • Neoplasia
Non resolving vitreous opacity	• Vitreous haemorrhage • Vitreous debris from previous intraocular inflammation • Floaters from posterior vitreous detachment
Retinal detachment	• Retinal detachments associated with posterior vitreous detachment and vitreoretinal traction • Proliferative vitreoretinopathy • Giant retinal tears • Posterior breaks e.g. macular holes
Diseases of the vitreomacular interface	• Epiretinal membranes • Macular holes • Vitreomacular traction • Submacular haemorrhage
Trauma	• Penetrating injuries • Intraocular foreign body
Proliferative vitreoretinopathies	• Proliferative diabetic retinopathy • Retinal vein occlusion • Sickle cell retinopathy • Eales' disease • Retinopathy of prematurity

Table 5.1: Indications for pars plana vitrectomy surgery.

This is not an exhaustive list, but gives an indication of the wide variety of applications of vitrectomy surgery.

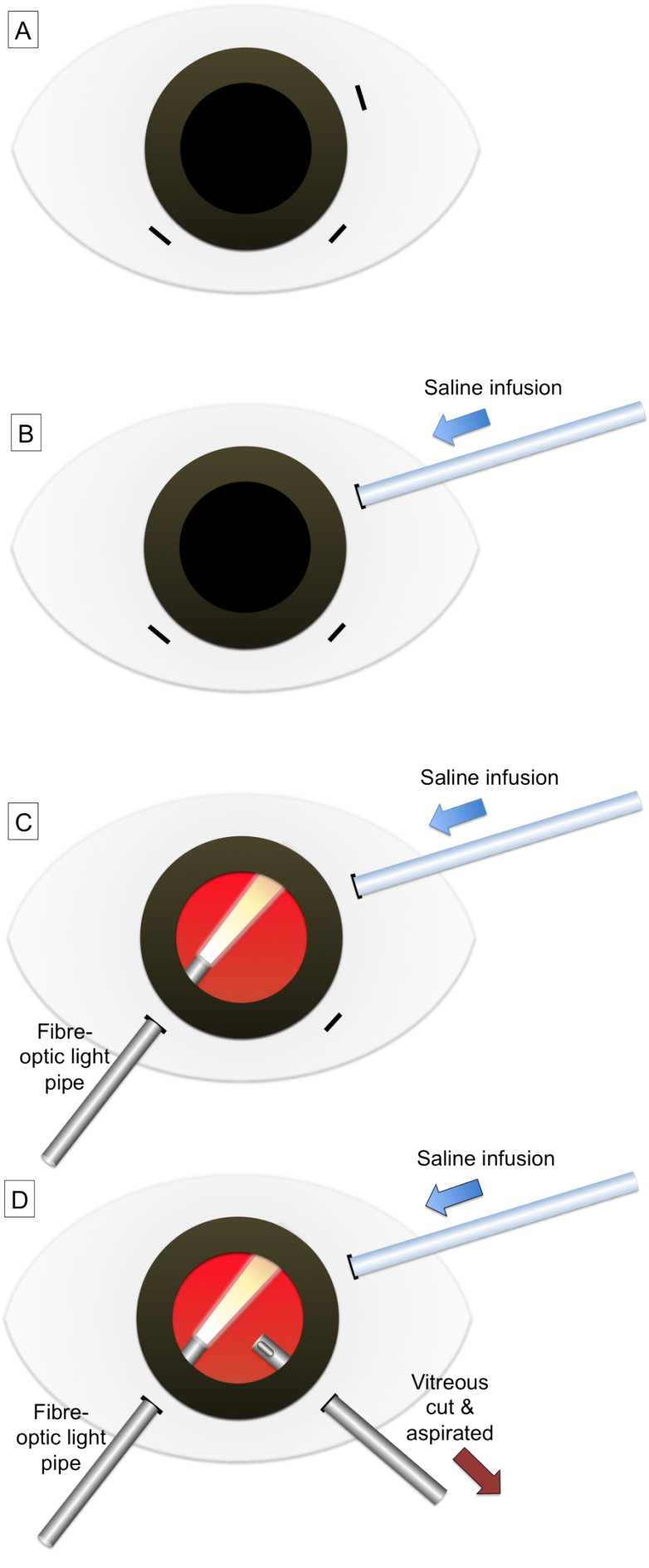
A
B
Saline infusion
C
Saline infusion
Fibre-
optic light
pipe
D
Saline infusion
Vitreous
cut &
aspirated
Fibre-
optic light
pipe

Figure 5.2: Initial steps of pars plana vitrectomy.

A: Three circumferential incisions are made through the sclera and the pars plana. In a human eye, this is 3.5-4.0mm from the limbus (the edge of the cornea). The position of these sclerotomies allows insertion of instruments between the crystalline lens and the retina, without damaging either structure. The width of the incisions is dictated by the size of the instruments available. Typical instrument sizes are 20-, 23- and 25-gauge. Note that 20 gauge instruments are larger than 25-gauge instruments.

B: An infusion line is inserted into one of the sclerotomies, to allow an infusion of balanced saline solution into the eye during the procedure, preventing globe collapse. For 20-gauge systems, it may be necessary to suture the infusion line to the sclera to ensure it does not become displaced.

C: A fibre-optic light “pipe”, connected to a light source, is introduced into the second sclerotomy. This allows reflection of light from the fundus, leading to the “red-reflex”.

D: The third sclerotomy is used for the introduction of a vitreous cutter, also known as a vitrector. The surgical microscope cannot focus beyond the posterior surface of the crystalline lens and to view the retina it is therefore necessary to use an additional optical viewing system, such as a contact lens (not shown).

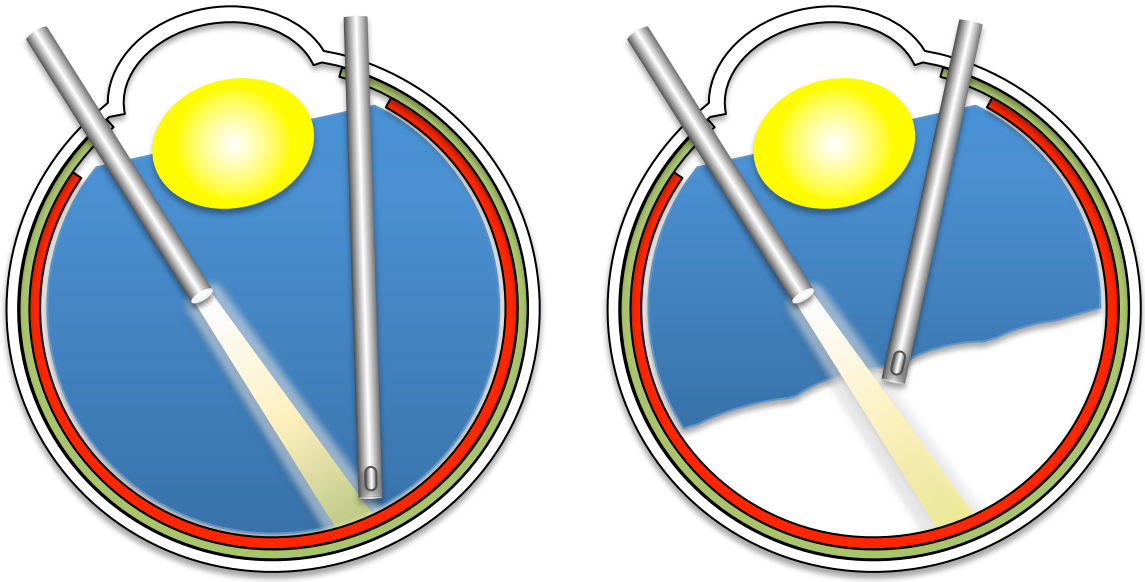

Figure 5.3: Cross-sectional illustrations showing the method for surgical inducing posterior vitreous detachment (PVD) in a human eye.

Once it has been confirmed that the infusion cannula is in the correct position and the tip is within the vitreous cavity, it is safe to allow flow into the eye. The retinal viewing system can then put in place and the light pipe and the vitreous cutter are inserted into the eye. The first step in vitrectomy is induction of the posterior vitreous detachment. This involves using the vitrector to exert a very high vacuum (e.g. 600mmHg) at the posterior pole (LEFT), allowing vitreous strands to enter the port. The instrument is then moved anteriorly allow separation between the posterior surface of the vitreous (the posterior hyaloid membrane) and the inner surface of the retina. The vitreous (blue) can then be removed with the vitrector, without risk of damage to the retina. The space created between the vitreous and retina is filled instantly with balanced saline solution from the infusion cannula (RIGHT).

5.1.2 Animal Models for Ocular Surgery

Almost every major medical advance has depended on the use of animals during research, development and testing. Examples include the development of antibiotics, anaesthetics, subcutaneous insulin, organ transplants, and joint replacement surgery.[195]

Despite this, animal research remains an area of great controversy and ethical debate. The principles of the three 'R's – Replacement, Reduction, Refinement – were developed over 50 years ago as a framework for scientists conducting human animal research.[196] These principles have subsequently become incorporated in national and international legislation. In the United Kingdom, animal research is regulated by an Act of Parliament. The Animal (Scientific Procedures) Act (often referred to as ASPA) was passed in 1986, and modified in 2012.

Our research group, and indeed the University of Southampton, is firmly committed to implementation of the 3Rs, and they are outlined briefly here.

Replacement – Animals protected under ASPA include all living vertebrates (except humans), and cephalopods such as octopus, squid and cuttlefish. Every effort should be made to avoid or replace the use of these protected animals. Instead, the use of mathematical or computer models, cell lines, invertebrates such as Drosophila or nemade worms, or even human volunteers may be more appropriate.

Reduction – When animals are used, methods to minimise the number of animals used per experiment should be employed. This can be achieved by improved experimental design, sharing data and resources, and using imaging technology to allow longitudinal studies in the same animals. However, it should also be noted that the use of too few animals may be detrimental to the validity of the experiment.

Refinement – Every effort should be made to ensure that the pain, suffering, distress and harm experienced by animals is minimised. This applies to all aspects of their care, including their housing, use of appropriate anaesthetic and analgesic, and minimising stress by allowing rabbits to become familiar with the researchers and even with certain procedures such as imaging.

During the course of this project, every effort has been made to develop *in vitro* experiments to minimise the use of animal research. Indeed this is reflected in the thesis – only one of the four experimental chapters involve *in vivo* work. However, to develop novel surgical techniques and to determine the effect of surgery and RPE transplantation on ocular tissues, as opposed to cells, animal work is essential.

There is a rich history of animal use in ocular research, including the evaluation of intraocular lens implants for cataract surgery, and the use of anti-VEGF agents that are now in widespread clinical use to treat AMD. The correct choice of animal species is obviously crucial, and is dependent on the type of experiment.

5.1.3 Comparative Ocular Anatomy

Dubielzig has emphasised the importance of knowledge of comparative ocular anatomy to ensure that the correct species is chosen to answer the experimental question.[197] The body of experience in the scientific literature on the species of choice is also of importance.

The primary determinant for the choice of species for experimental surgery is the size of the eye, for reasons shown in Figure 5.4 and Figure 5.5. It is useful for the animal eye to be similar to that of human eyes, so that any surgical procedures developed during animal experimentation can be directly translated to patients.

	Axial length (mm)	Corneal thickness (mm)	Anterior chamber depth (mm)	Lens thickness (mm)	Vitreous chamber depth (mm)	Reference
Human	**23.92**	**0.55**	**3.05**	**4.0**	**16.32**	Deering, 2005[198]
Cat	**22.3**	**0.68**	**4.52**	**8.5**	**8.13**	Vakkur & Bishop, 1963[199]
Pig	**21.64**	**0.98**	**2.47**	**7.4**	**10.79**	Sanchez 2010[200]
Dog	**20.8**	**0.64**	**4.29**	**7.85**	**10.02**	Mutti, 1999[201]
Rabbit	**18.1**	**0.4**	**2.9**	**7.9**	**6.2**	Hughes, 1972[202]
Monkey	**17.92**	**0.55**	**3.24**	**2.98**	**11.3**	LaPuerta, 1995[203]
Rat	**5.98**	**0.25**	**0.87**	**3.87**	**1.51**	Massof & Chang, 1972[204]
Mouse	**3.37**	**?**	**≈0.5**	**≈2.2**	**0.59**	Remtulla & Hallett, 1985[185]

Table 5.2: Ocular anatomy of animals used for experimental surgery.

The human eye has the longest axial length, cats dogs and monkeys have deeper anterior chambers than humans. Although mice and rats are widely used in medical research, the dimensions of small rodent eyes, as shown above and illustrated in Figure 5.4, makes them unsuitable as animal models for experimental vitreoretinal surgery.

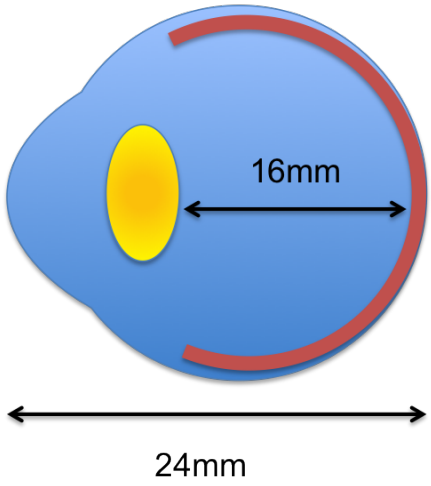

Human Eye

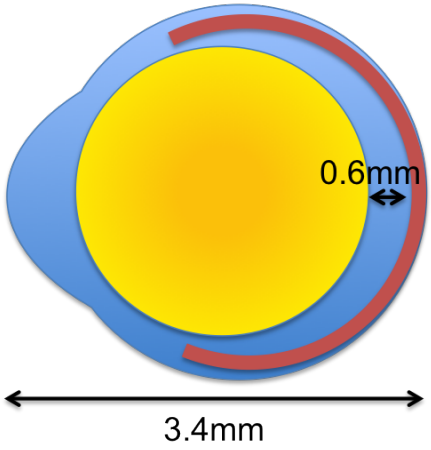

Mouse Eye

Figure 5.4: Schematic eyes for human and mouse

Human eyes are large and have a biconvex crystalline lens. The vitreous cavity depth allows surgical manipulation of instruments within the eye. Small eyes need to refract light over a shorter distance and therefore need a crystalline lens with a high dioptric power. Mouse and rat eyes are unsuitable for vitreoretinal surgery not only because the eyes are so small but also because the large spherical lens occupies most of the space within the globe. The vitreous cavity in the mouse eye is smaller than the diameter of most vitreoretinal instruments, and an epiretinal approach to RPE transplantation following pars plana vitrectomy would be impossible.

Common species used for experimental retinal surgery include cats[205, 206], dogs[207], pigs[208], rabbits[128, 138, 181, 209-217] and monkeys[218]. Among mammals, the fovea is found only in simian primates, making monkeys ideal for retinal studies. The size of the monkey eye, and particularly the depth of the vitreous cavity, would easily allow manipulation of vitreoretinal instruments. However the use of non-human primates brings cost implications and significant ethical concerns,[219] and potentially health concerns because of the risk of disease transmission between animal and the researcher. As an alternative, pig eyes are widely regarded as being similar to human eyes[200, 220-222]. The greatest difficulty with vitreoretinal surgery in pigs is that the globe is enophthalmic within the orbit, because of the presence of the retractor bulbi, an extraocular muscle that is not present in humans.[200] Pigs, like many animals, have a nictitating membrane, posterior muscle insertion, fragile conjunctiva and thick sclera compared to human eyes.[221] Perhaps most importantly, full size adult pigs are expensive to purchase, difficult to keep, and since a full size adult pig can weigh up to 350kg, these animals can be difficult to anaesthetise, examine or move within the laboratory. Our animal research facility has no experience with pigs.

Cat eyes are the most frequently used animal model for research in visual prosthesis research.[223] Cats have a rod-dominated retina that has a dual vascular supply, much like the human retina. The outer retina is supplied by the choroidal circulation and an intraretinal vasculature supplies the inner retina. Although feline retinal anatomy has similarities to humans, feline vitrectomy is technically challenging because the globe is deep-set within the orbit, and access to the sclera is limited.[205] Studies of subretinal electronic implants in cat eyes have previously required removal of the frontal process of the zygomatic bone to allow access to the globe.[224, 225] At the very least, a lateral canthotomy is necessary.[205] Significant intraoperative haemorrhage from vessels in the pars plana is a well-described complication of feline vitrectomy, and is sometimes uncontrollable despite the judicious use of thermocautery.[226]

It was observed in the early 1970s that the rabbit retina can spontaneously degenerate in experimental models of retinal detachment.[227] Subsequently, Faude *et al.* created experimental retinal detachments in rabbit eyes, and used subretinal viscoelastic to prevent the detachment from spontaneously resolving.[228] After 21 days histological examination revealed widespread and multi-layered degeneration of the rabbit retina. Although the rabbit retina is not suitable for experimental models of retinal detachment,

several groups have used lapine vitrectomy for the purposes of RPE transplantation, where the area and duration of detached neurosensory retina is limited.[128, 138, 181, 210, 211, 213-216] Rabbits are docile, easy to handle, and relatively inexpensive (compared to the pig), which explains why they are the most commonly used laboratory animal for comparative ophthalmology.[229] Furthermore, our animal facility has extensive experience with housing them. Therefore we chose to use the rabbit as an experimental model for vitrectomy and subretinal implantation of RPE cells.

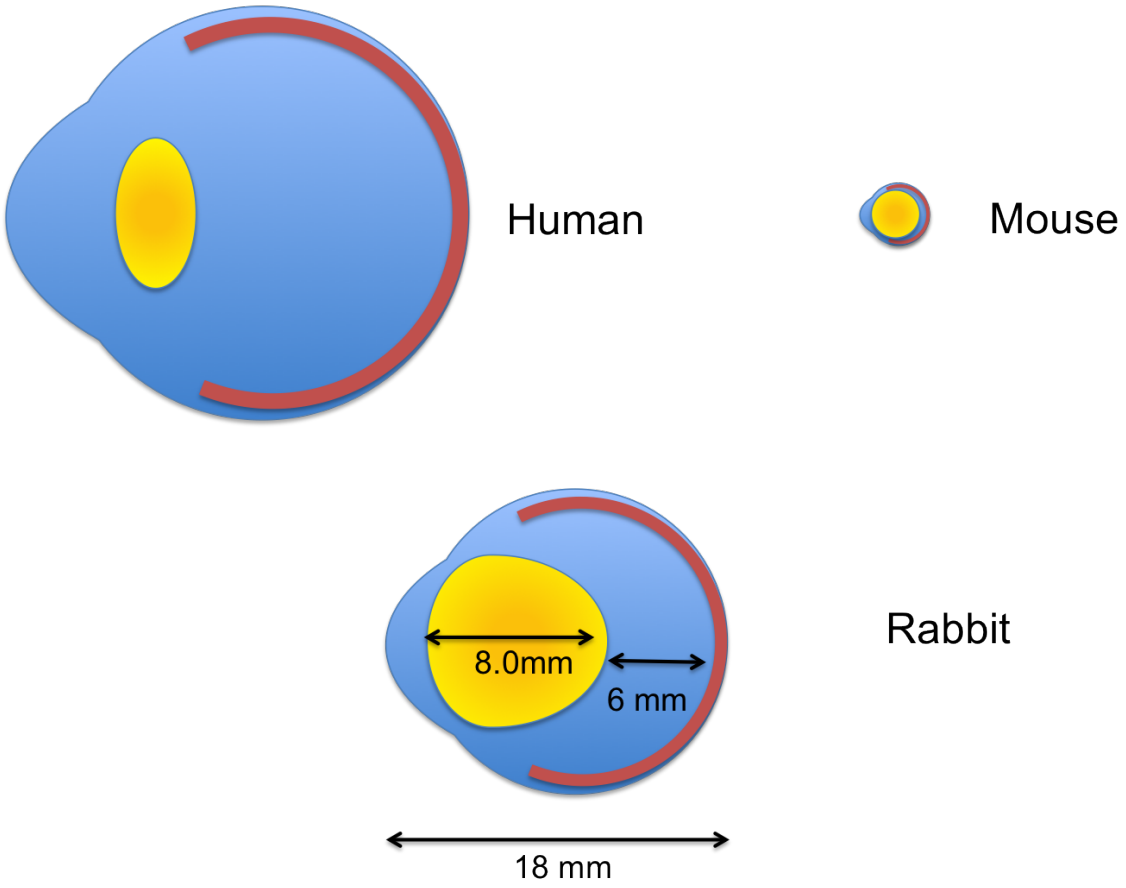

Figure 5.5: Schematic eyes of the human, mouse and rabbit.

The rabbit eye is only slightly smaller than a human adult eye, and there is sufficient space within the vitreous cavity to allow pars plana vitrectomy and creation of a subretinal bleb. While the rabbit lens is larger than a human lens, intraoperative lens touch can be avoided with careful surgery. The rabbit eye is therefore an excellent model for RPE transplantation techniques.

5.1.4 Surgical Anatomy of the Rabbit Eye

This section is not an exhaustive description of the anatomy of the rabbit eye, but discusses only the anatomical differences from the human eye that are relevant to the vitreoretinal surgeon performing experimental lapine vitrectomy. Figure 5.6 shows a close up photograph of a rabbit eye.

5.1.4.1 Orbital, adnexal and ocular surface anatomy

In addition to the six extraocular muscles found in humans (superior rectus, inferior rectus, medial rectus, lateral rectus, superior oblique, inferior oblique), the rabbit also possesses an active retractor bulbi. This muscle arises from the apex of the orbit, runs within the muscle cone enveloping the optic nerve, and inserts into the posterior sclera. Its primary function is to retract the globe into the orbit.[229]

The nictitating membrane is a transparent or translucent third eyelid that moves horizontally across the ocular surface to moisten and protect the cornea, while still maintaining visibility, particularly when the globe is retracted into the orbit. In humans, the plica semilunaris can be regarded as homologous. Harder's gland, present in rabbits but not in humans, is located on the nasal side of the orbit and functions to lubricate the nictitating membrane.[229]

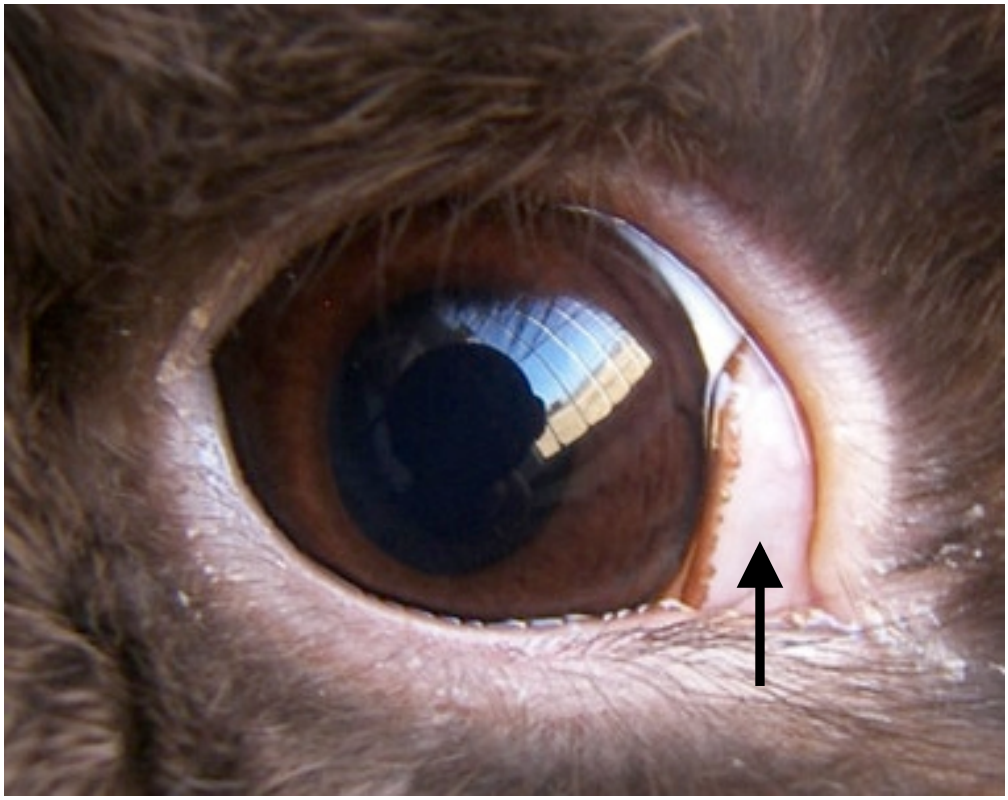

Figure 5.6: The nictitating membrane of the rabbit eye

The nictitating membrane (marked by arrow), also known as the third eyelid, is located nasally and moves horizontally to allow lubrication of the ocular surface while still permitting some vision. It is homologous to the plica semilunaris in humans. It poses potential difficulty for the surgeon because it obstructs access to the nasal sclera and cannot be easily retracted with a standard lid speculum.

There is a single nasolacrimal punctum in the rabbit and a duct with a convoluted passage through the lacrimal and frontal bones, passing close to the roots of the molar and incisor teeth. Although seemingly irrelevant to the vitreoretinal surgeon, the importance of this for the current project will become apparent in the Results section of this chapter (see section 5.4).

The rabbit's retrobulbar venous plexus, not present in humans, can be avoided by performing a conjunctival peritomy prior to enucleation. In veterinary practice, avoidance of the plexus is important, to prevent catastrophic bleeding in live rabbits undergoing enucleation.[230] For research purposes, enucleation was only undertaken after the rabbit was sacrificed, and therefore inadvertent rupture of the plexus was of little consequence.

5.1.4.2 Pars plana anatomy of the rabbit eye

The pars plana is approximately 4mm wide in human eyes, and this has allowed the development of the pars plana approach for vitrectomy surgery. Instruments can be inserted 3-4mm from the limbus without damaging the lens or the retina. In comparison, rabbits have a very narrow ciliary region, which is thought to contribute to a wider field of vision and is achieved because the ciliary processes arise directly from the posterior surface of the iris.[231] Confusingly, many researchers performing vitrectomy in rabbits use the term "pars plana vitrectomy" even though the existence of the pars plana in the rabbit eye is disputed. Funk has studied the anatomy of the rabbit pars plana,[232] but some authors maintain that there is no true pars plana at all,[233] while others suggest that there is while a pars plana may exist, it is small (only 0.5mm wide) and only present on the temporal side of the globe.[231] As a result of this dispute, it is difficult to ascertain how far from the limbus any incisions should be made. Notably, intravitreal injections are usually given 1mm posterior to the limbus in rabbit eyes.[234]

Scleral thickness in rabbit eyes is around 0.5mm near the limbus and then becomes thinner more posteriorly.[229] Scleral thickness and water content is thought to be similar in rabbits and humans.[235]

5.1.4.3 Retinal anatomy of the rabbit eye

Four patterns of retinal vasculature have been described: holangiotic, merangiotic, paurangiotic, and anangiotic.[168] Most mammals, including humans, mice and rats, possess the holangiotic pattern, in which there is an intraretinal circulation that extends from the optic nerve to the retinal periphery. The elephant, rhinoceros, horse, and marsupial family exhibit the paurangiotic pattern, in which the blood vessels occur only in the peripapillary region (i.e. around the optic disc). Some species, including birds and bats, have no vasculature at all within the neurosensory retina.[168]

Rabbits, hares and pika are members of the taxonomic order lagomorpha, which are most closely related to rodents than any other mammal. Despite this, these animals exhibit the merangiotic pattern, in which blood vessels are restricted to only one region of the retina (see Figure 5.7). The vessels arise from the optic disc and run in a horizontal band, temporally and nasally, confluent with the medullated nerve fibres.[168]

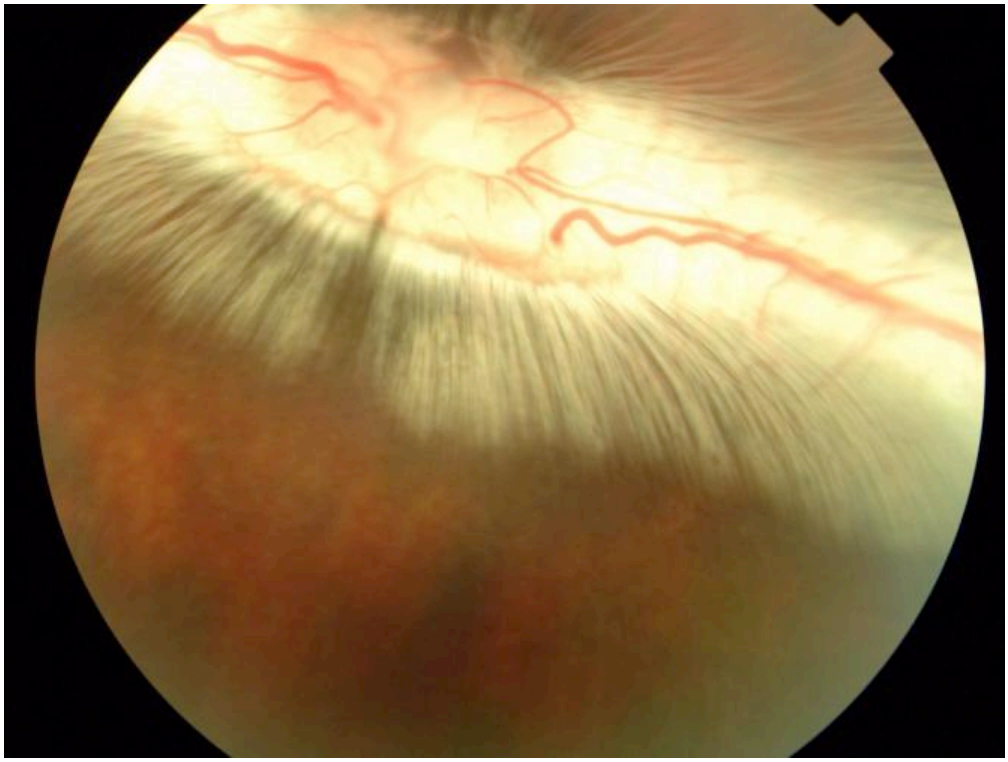

Figure 5.7: Photograph of the rabbit retina.

Rabbits have an optic disc from which the vessels and the medullated nerve fibres emanate horizontally. Note that the medullary ray is positioned in the centre of the retina but is approximately 1/3 from the superior retina periphery. The retina inferior to the medullary ray is therefore the most suitable locus for experimental retinal surgery. The fundus has an orange-red colour, similar to the human eye, due to reflection of light from the choroidal vessels. (Photograph taken with the Topcon Retinal Camera TRC-50DX).

The fovea, consisting only of cone photoreceptors and characterised by the complete absence of rods, is present in eyes of simian primates (including humans), reptiles, birds and fish. Most birds have two foveae in each eye, one to provide monocular peripheral vision and the other to provide stereoscopic central vision. Instead of the fovea, rabbits and other non-primate mammals have an area centralis, sometimes referred to as the visual streak. This is the region of the retina with the greatest concentration of ganglion cells and usually the greatest cone density also.[168] Cone density within the rabbit visual streak is 18,000/mm^2, compared to 7000/mm^2 in the dorsal (i.e. superior) retina and 10,000-12,000/mm^2 in the ventral (i.e. inferior) retina.[236]

In histological studies, rabbit RPE is almost always found in contact with the inner most layer of the choroid, known as the lamina vitrea, so called because it appears as a thin, homogenous, unbroken glass-like membrane.[237] The lamina vitrea was first described by Bruch in his 1844 doctoral thesis,[136] and therefore in humans it is referred to as BrM. Importantly, the rabbit does not possess a tapetum lucidum. The tapetum is a highly reflective layer within the medium-sized vessel layer of the choroid, just external to the choriocapillaris, which allows light that has passed through the retina to be reflected back to restimulate the photoreceptors. In animals that possess the tapetum, RPE cells are devoid of pigment in this area. Therefore, although access to the globe may be difficult in the rabbit eye, for RPE research, the rabbit is an ideal model.

5.2 Aims and Objectives

The aim of this chapter was to identify, optimise and evaluate surgical techniques to deliver polymer, with and without cells, into the subretinal space of the rabbit eye.

The main objectives of this experiment:

- Develop a method for delivering polymer into the subretinal space

- Use histological techniques to determine the relative effects of surgical trauma (i.e. vitrectomy and creation of a subretinal bleb), polymer insertion (vitrectomy, bleb, polymer), and RPE transplantation (vitrectomy, bleb, polymer & cells)

- Assess imaging methods to determine if these can be utilised for monitoring transplanted eyes.

5.3 Methods

5.3.1 In vivo transplantation experiments in rabbits

The purpose of this chapter was to develop novel surgical methods to allow RPE transplantation on a BrM substitute. Therefore, the surgical technique used was constantly being optimised.

5.3.1.1 Animal handling

Twenty-six murex half-lop pigmented laboratory rabbits (Pettingill Technology, Oxford, UK) of 3.5kg to 4.5kg were utilised for these experiments. All of the procedures were performed in a purpose-built large animal operating room within the Biomedical Research Facility at the University of Southampton. Animals were kept in floor pens in groups of three, in a temperature-regulated room, with free access to food and water. After surgery, animals were kept in individual cages.

All members of the research team had received training in animal handling and each researcher had a personal licence (PIL) granted by the Animals in Science Regulation Unit at the Home Office. All experiments were conducted in accordance with the project licence (PPL 30/2843), granted by the Home Office to Professor Andrew Lotery.

Researchers wore surgical scrubs, a 3M face mask, and a hair cover. Hands were disinfected with chlorhexidine or povidone iodine prior to wearing sterile surgical gloves.

5.3.1.2 Anaesthetic

Rabbits were weighed to ensure correct anaesthetic dosing. Prior to anaesthesia, all rabbits received a pre-medication intramuscular injection of 1mg/kg acepromazine (ACP 10mg/ml, Centaur Services, Somerset, UK), into the hind leg. The animal was left in a quiet dark room for 10 minutes, which allowed the animal to become calm and docile and reduced the total anaesthetic dose required during surgery.

The rabbits were anaesthetised with a mixture of 35mg/kg ketamine hydrochloride (Ketaset 100mg/ml, Centaur Services, Somerset, UK) and 5mg/kg xylazine hydrochloride (Rompun 20mg/ml, Centaur Services, Somerset, UK). The right pupil of each animal was dilated with 1% atropine and 2.5% phenylephrine.

5.3.1.3 Surgical Technique

A standard pars plana vitrectomy technique was attempted in all rabbits. In preparation, Jenny Scott and I visited the Institute of Ophthalmology, London, in October 2013 to observe Hari Jayaram and David Charteris performing rabbit vitrectomy. In October 2014 we visited Boris Stanzel in Bonn to help further refine certain aspects of our technique. Even before this project started, I had already performed 500 pars plana vitrectomies in human eyes.

Every aspect of this technique was varied and optimised in an attempt to find the best method for delivering polymer into the subretinal space. In particular, the following factors were addressed:

- Surgical access
- Size of incisions (20-gauge vs. 23-gauge)
- Need for and technique of performing lensectomy at the time of vitrectomy
- Method for inducing posterior vitreous detachment
- Method for creating and incising bleb
- Prevention of bleb collapse using air and/or viscoelastic
- Efficacy of the polymer injector in vitro to inject polymer, both with and without cells

5.3.1.4 Polymer preparation

Sheets of the functionalised polymer scaffolds were sterilised with ultraviolet light for 12 hours. Under aseptic conditions, a compressed 2mm skin biopsy punch was used to create identical polymer segments that were oval in shape, and therefore suitable for loading into the Bonn-Shooter injector. All samples were then flooded with culture medium and allowed to equilibrate for 0 min at 37°C before seeding.

The original intention when this project began was for polymer to be seeded with primary rabbit RPE cells prior to implantation. However, these polymer samples began to curl from the tangential contractile force of the RPE monolayer. At the time, we were unable to produce in our own laboratory RPE cells that had been derived from either ESC or iPS. However Professor Lotery has a longstanding collaboration with Professor Majlinda (Linda) Lako in Newcastle, who conducts ESC-RPE research. Therefore, we collaborated with the University of Newcastle to obtain Embryonic Stem Cell (ESC) derived-RPE seeded polymer fibres. Sheets of polymer scaffold were sent by courier to Newcastle, and Valeria Chichagova, a PhD student in Professor Lako's laboratory, seeded ESC-RPE and cultured the cells for 130 days (see Figure 5.16). The cell-seeded scaffolds were brought to Southampton 8 hours before implantation and kept in an incubator (Nuaire NU5510E Serial # 142811022311) at 37 degrees prior to implantation.

5.3.2 Histological Examination

5.3.2.1 Paraformaldehyde fixation and frozen sections

Initially, eyes were fixed in 50mls of 4% PFA immediately after enucleation. After 24 hours, 25mls of the PFA was replaced with an equal volume of 30% sucrose. A further 24 hours later, all of the liquid was discarded and replaced with 30% sucrose for cryoprotection for at least 24 hours. Eyes were embedded in optical cutting temperature (OCT) media (R. Lamb, East Sussex, UK) and then cryosectioned at 15μm at a temperature of -22°C.

5.3.2.2 Haematoxylin and eosin (H&E)

H&E staining was performed as follows:

- Tissue washed 3 times x 10 mins in PBS
- Stained with Harris' haematoxylin for 15 secs.
- Washed in running tap water for 2 minutes
- Stained with eosin for 2 minutes.
- Washed in running tap water for 10 seconds.

- Dehydrated in increasing concentrations of alcohol (70%, 80%, 90%, 95%) before mounting and coverslip.

5.3.2.3 Davidson's fixative solution and paraffin sectioning

Davidson's fixative solution was made using the following constituents:

- 30ml of 100% ethanol
- 20ml of 10% Neutral Buffered Formalin (Sigma-Aldrich)
- 10ml Glacial Acetic Acid (Sigma-Aldrich)
- 30ml Distilled water

All paraffin sectioning was kindly performed by the Jenny Norman and Helen Rigden of the Biomedical Imaging Unit.

5.3.2.4 Optimising Histological Sectioning using Porcine Eyes

Twenty-four porcine eyes were obtained from the local butcher (Uptons of Bassett Ltd, Southampton, UK). Eyes were fixed in either 4% PFA for 36 hours (12 eyes), or Davidson's fixative solution for 24 hours (12 eyes), and then underwent paraffin embedding.

To potentially improve intraocular fixation, a 2mm aperture was made in the cornea (keratotomy) with a tissue biopsy punch (Kai, Northumbrian Medical Supplies, UK) either before fixation (6 eyes), after fixation but before processing (6 eyes), or after processing but before embedding in paraffin (6 eyes). Six eyes were processed without a keratotomy being made.

Fixative	Hole
PFA 36 hours	No hole
PFA 36 hours	Pre-fixation
PFA 36 hours	Post-fixation
PFA 36 hours	Post-processing
Davidsons 24 hours	No hole
Davidsons 24 hours	Pre-fixation
Davidsons 24 hours	Post-fixation
Davidsons 24 hours	Post-processing

Table 5.3: Table showing the different types of fixative tested and points at which keratotomy was created in porcine eyes, to try to improve histological processing and preserve tissue architecture.

It subsequently was clear that Davidson's fixative preserved the tissue architecture more than PFA, and that a hole made after fixation but before processing produced the best histological results.

5.3.2.5 Optimising Histological Sectioning using Lapine eyes

Further studies of 9 lapine eyes were made but with different sized tissue biopsy punches, with the keratotomy made after fixation but before processing, as follows:

Fixative	Keratotomy
Davidsons 24 hours	2mm post-fixation keratotomy
Davidsons 24 hours	6mm post-fixation keratotomy
Davidsons 24 hours	8mm post-fixation keratotomy

Table 5.4: Table showing the different sizes of keratotomy that were tested in lapine eyes, to optimise histological sectioning.

5.3.2.6 Perfusion Fixation of Lapine Eyes

To my knowledge, there is no published technique for perfusion fixation of rabbit eyes. Below is the method that we used, and has been adapted from the methods of Boris Stanzel that Jenny Scott and I observed during a visit to Bonn, Germany. I am grateful to Dr Neil Smyth BVSc PhD, for his expertise in performing the neck dissections when we performed these experiments. Figure 5.8 shows the principle of perfusion fixation, and Figure 5.9 shows photographs taken during these experiments.

Rabbits were anaesthetised with ketamine and xylazine as previously described (see section 5.3.1.2). The animals were positioned with their ventral surface exposed, and a midline incision was made in the neck after fur had been removed with clippers. With blunt dissection, carotid arteries and jugular veins on each side were identified, and a 2/0 silk suture was loosely tied around each vessel. The carotid artery that had better surgical exposure was cannulated with a sterile 22-gauge (blue) intravenous cannula. Once the cannula was secured with a suture, infusion of 0.9% NaCl into the cerebral circulation via the cannulated carotid artery began. The remaining three vessels were quickly ligated with 2/0 silk suture, and the jugular veins were cut on the cerebral side of the suture. Normal saline was infused until the fluid flowing from the jugular veins was clear, and the infusion was then switched from saline to 3% gluteraldehyde (kindly donated by Anton Page, Biomedical Imaging Unit, Southampton). A total of 500mls of gluteraldehyde was infusion, or until the head of the rabbit was fixed (subjectively assessed by the malleability of the ear). To enucleate the globe, it was necessary to first excise the eyelids to widen the palpebral aperture. Enucleated globes were kept in gluteraldehyde for 24 hours.

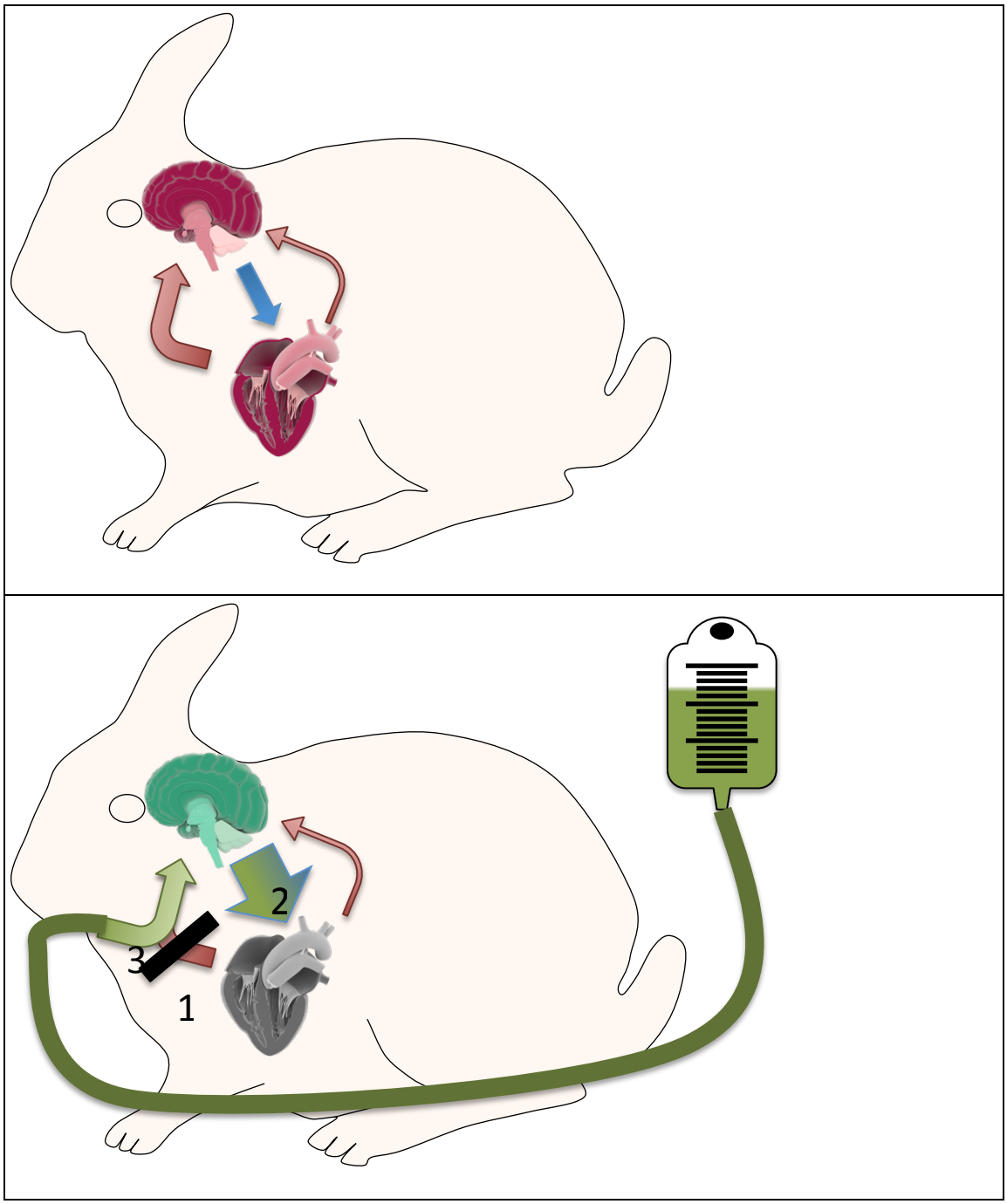

Figure 5.8: Schematic showing perfusion fixation

In a normal rabbit (top picture), the arterial cerebral circulation consists of both an anterior circulation (carotid arteries – thick red arrow) and a posterior circulation (basilar artery – thin red arrow) that anastomose in the

Circle of Willis. Venous drainage occurs via the internal jugular veins (blue arrow).

For perfusion fixation (bottom picture), the anterior circulation is ligated with a 2/0 silk suture (1), the jugular veins are cut (2) to increase outflow and reduce the resistance to inflow, and the anterior circulation is then perfused with saline via a 22 gauge intravenous cannula. The technique does not interrupt the posterior arterial circulation via the basilar artery because of the technical difficulties of doing this. As a result, perfusion of pure saline (and later fixative, shown in green for the sake of illustration) into the cerebral circulation is impossible. However as the infusion begins, a lethal dose of pentobarbital is injected into the mediastinum, and this causes cardiac arrest within a few minutes.

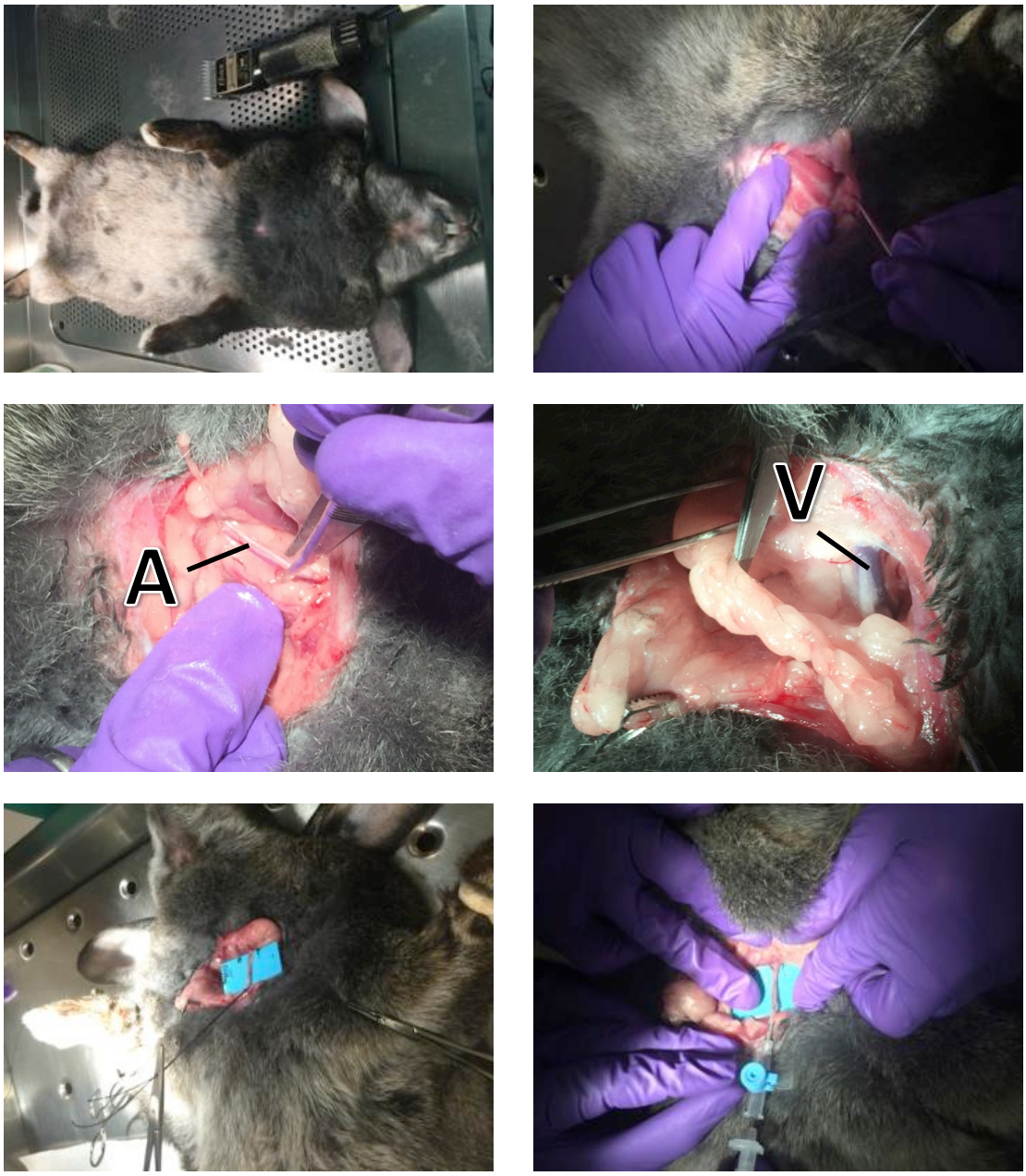

Figure 5.9: Photographs of Perfusion Fixation

Top Left: The rabbit is positioned on its back and the neck is shaved with clippers. Top Right: Midline incision and blunt dissection is used to identify the vessels. Middle Left: Carotid artery on each side is identified and a 2/0 silk suture is tied loosely around each. Middle Right: Internal jugular veins on each side are identified. Bottom Left and Right: We found that a piece of card placed beneath the artery facilitated cannulation, and allowed early detection of arterial dissection/rupture at the time of cannulation.

5.3.3 Optical Coherence Tomography of Rabbit Eyes

Optical Coherence Tomography (OCT) scans were taken of rabbit eyes using the Zeiss OCT Stratus 3000. The rabbits were anaesthetised with a mixture of 35mg/kg ketamine hydrochloride (Ketaset 100mg/ml, Centaur Services, Somerset, UK) and 5mg/kg xylazine hydrochloride (Rompun 20mg/ml, Centaur Services, Somerset, UK). The right pupil of each animal was dilated with 1% atropine and 2.5% phenylephrine.

Scans were taken with the rabbit lying on the lap of a researcher, such that the side of the rabbit faced the OCT scanner. No contact lens was used but the scanner was adjusted to the maximum hypermetropic correction (+12 dioptres) to account for the short axial length of the rabbit eye (relative to a human eye). The cornea was lubricated with HPMC (Moorfields Pharmaceuticals, London).

Intraoperative scans were attempted with perflurocarbon liquid *in situ*, to obtain scans of the polymer in the subretinal space.

5.4 Results

5.4.1 Surgical Technique

Below is an outline of the final optimised method of achieving RPE transplantation in rabbits. Some discussion regarding the evolution of this surgical technique is included in this section.

5.4.1.1 Pre-operative saline injection

An intravitreal injection of 0.9% saline in 0.05ml is given 2-3 days before vitrectomy. This is conducted under general anaesthesia under sterile conditions, with a speculum but without a surgical drape. The eye is cleaned with povidone iodine and the injection is administered 3mm from the temporal limbus. Although the eye would often become very hard, no anterior chamber paracentesis was attempted because the anterior chamber in rabbits is very shallow and the risk of complications e.g. iris trauma, corneal trauma, inadvertent lens capsule touch, was therefore considerable.

The practice of intravitreal saline injection was adopted only for the later experiments. In early experiments we were unable to surgically induce posterior vitreous detachment, as is usually possible in human eyes. No investigator had described successful PVD induction in rabbits in the literature. In September 2014 we discovered that Boris Stanzel from Bonn, Germany has been able to achieve surgical PVD induction in the rabbit eye using a 25G vitrectomy probe. Despite attempting to reproduce his technique we were still unable to surgically induce PVD. From October 2014 we have been administering “pars plana” intravitreal 0.9% saline injection (0.05ml). This practice was based on observations in human eyes that the mechanical effect of saline injection into the vitreous cavity can induce PVD within 28 days.[238]

5.4.1.2 Animal Positioning and Surgical Access

Figure 5.10 shows photographs showing the preparatory stages of surgery. We initially used a travel pillow to try and optimise the animal position, to ensure that the cornea was facing directly upwards towards the microscope.

Figure 5.10: Photographs showing preparation before vitrectomy surgery

The eyelashes and fur close to the eyelids was cut with scissors (top left photograph). The ocular surface was then irrigated vigorously with balanced salt solution, to remove remnants of fur/eyelashes (top right). Masking tape was and blue towel was then placed strategically to cover the whisker (bottom left).

After anaesthesia, the rabbit was positioned on its side, with the head raised on a travel pillow to allow access to the globe and to prevent the abdominal contents from impinging on the lung fields. A sterile field was established around the experimental eye. Care was taken to avoid touching the whiskers with the adhesive part of the surgical drape.

During the first procedure, a paediatric Barraquer speculum was used to retract the eyelids, but it was difficult to retract the nictitating membrane, which impinged on the nasal limbus. This issue was resolved after the second rabbit, by performing a wide peritomy (superior 180 degrees rather than only the superior 90 degrees) and by using an adult speculum. The Lang speculum was generally more useful than the Barraquer speculum (see Figure 5.11). Topical adrenaline 1:1000, and topical povidone iodine were administered.

A self-retaining Dehaan infusion cannula was placed 1.5mm from the limbus at the 12 o'clock position. Balanced salt solution was used as the irrigation fluid. Corneal hydration was maintained with topical hydroxypropylmethylcellulose (HPMC).

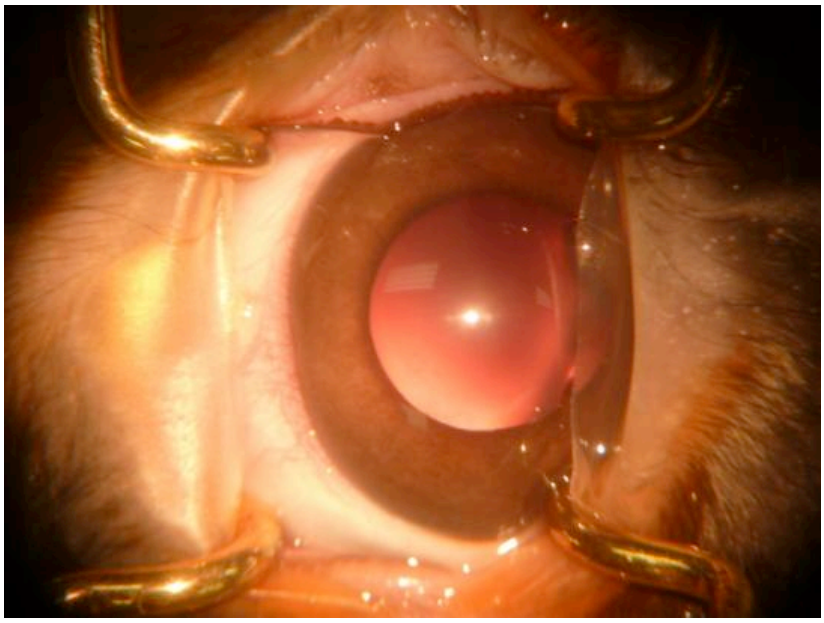

Figure 5.11: Photograph showing the Lang speculum

This rigid speculum allowed slightly greater lid retraction than the Barraquer speculum, allowing more sclera to be exposed for the scleral incisions to be made.

In subsequent experiments, two thin, blunt, flat instruments (measuring callipers for intravitreal injections are ideal) were used to proptose the eye from the orbit (see Figures 5.12 and 5.13). This was an effective method for improving scleral exposure and incisions were therefore made 3.5-4.0mm from the limbus rather than 1.5mm.

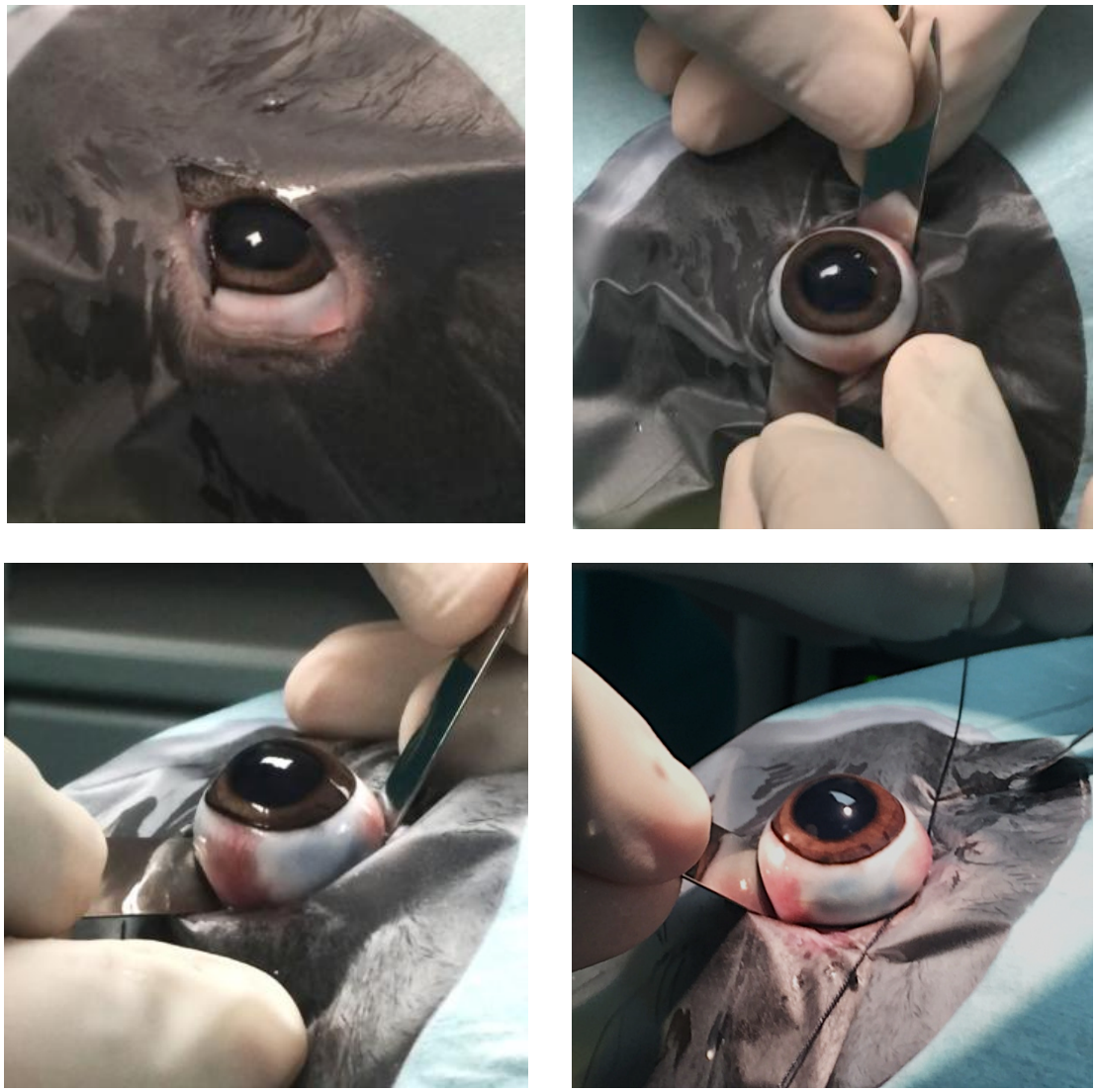

Figure 5.12: Photographs showing technique for globe proptosis

An ellipsoid excision from the plastic area of the drape was made to allow sufficient space for the globe to be prolapsed (top left photograph). Two wide, flat, blunt metal instruments were placed above and below the globe, and the globe was prolapsed out of the orbit (top right; side view shown in bottom left photograph). A 2/0 silk suture was passed around the globe muscle cone and tied with a single throw around the retrobulbar muscle cone. No speculum was required.

Figure 5.13: Photograph showing scleral ischaemia in a proptosed rabbit eye.

Scleral ischaemia (seen as the black area in above photograph) was observed to occur if the silk suture around the base of the globe was tied too tight. Loosening of the suture lead to immediate reperfusion of the sclera, which returned to its normal colour.

5.4.1.3 Incisions

Prior to discovering that the eye can be proptosed for ocular surgery, access to the sclerotomies was particularly difficult due to the anatomical considerations. The presence of a contact lens to view the retina further obstructed easy access to the sclerostomies. Leakage of irrigating fluid, and in some cases vitreous incarceration, was noted upon removal of the instruments.

Initial experiments used 20G incisions, placed 1-2mm from the limbus. In an attempt to reduce leakage from these sclerostomies, we attempted 23G vitrectomy with the use of trocars and self-retaining valved cannulae (see Figure 5.14).

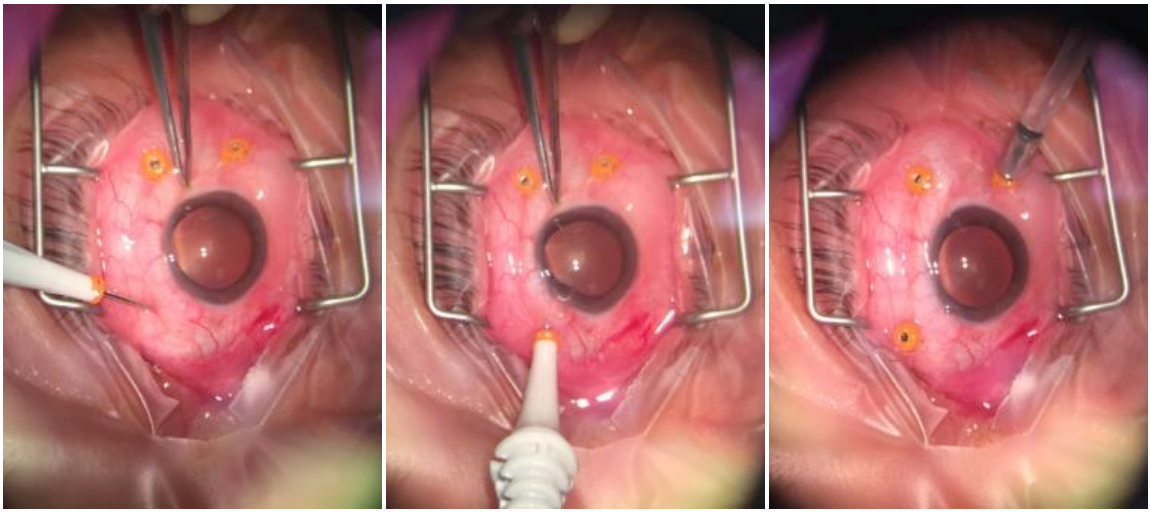

Figure 5.14: Photograph panel showing method for insertion of self-retaining 23-gauge cannulae in a human eye

A trocar, with the cannula (orange), already mounted, is inserted tangentially into the sclera (LEFT). The angle of the incision is then changed, allowing creation of a long, oblique and therefore self-sealing sclerotomy track (CENTRE). The cannula is retained between the scleral fibres once the trochar is removed (RIGHT). The infusion can simply placed into one of the cannulae without the need for be inserted

Trocars are medical devices consisting of a hollow cannula, an 'obturator' which can be made of metal or plastic, and a seal. Trocars are routine used in laparascopic surgery to function as portals for the subsequent placement of different instruments. Similarly, valved trocars used for vitrectomy surgery allow creation of sclerostomies without leakage. This strategy, although useful in human vitrectomy surgery, was unsuccessful during the rabbit vitrectomies because there was evidently some scleral expansion due to the infusion maintained during the procedure. This scleral elasticity led to expansion of the globe, leakage of fluid from between the scleral fibres, and gradual extrusion of the cannula during the procedure. Reinsertion of the extruded cannulae into a now hypotonous eye was difficult and hazardous. The use of 23-gauge cannulae was therefore abandoned.

To minimise leakage of intraocular fluid intraoperatively, the superonasal sclerotomy was made with a 23-gauge incision. An infusion port with flange was sutured to

prevent inadvertent withdrawal. The main sclerotomy, used for vitrectomy, and insertion of the subretinal polymer, was made with a 20-gauge incision.

Following discovery that the eye can be prolapsed from the orbit, all incisions were made at 3.5mm from the limbus rather than 1.5-2.0mm from the limbus.

5.4.1.4 Lensectomy

Early experiments involved pars plana lensectomy. This was necessary because the incisions were close to the limbus and without lensectomy, iatrogenic cataract secondary to lens touch was a common occurrence. Rabbit lenses were observed to be extremely touch and were difficult to remove with the vitreous cutter alone. We therefore had to procure a fragmatome, to allow the use of ultrasound energy to fracture and emulsify the lens. The lens fragments could then be removed.

Following discovery that the eye could be proptosed, lensectomy was no longer performed.

5.4.1.5 Vitrectomy

Posterior vitreous detachment could only be induced if intravitreal saline had been injected 2-3 days before vitrectomy. Posterior vitreous detachment was induced over the inferior retina and extended up to the visual streak. No attempt was made to separate the vitreous over the superior retina. Care was taken to remove the vitreous above the visual streak (see Figure 5.15 A). Posterior vitreous detachment was quite obvious and there was no need for vitreous staining with Kenalog (triamcinolone acetate), as has been described by others.[181] Before rabbit 19, vitrectomy was performed using a contact lens to visualise the retina. After rabbit 19, a disposable BIOM (Stat One Services, Sutton Coldfield, UK) was used, and this was found to be preferable because it allowed visualisation of a wider field of retina.

5.4.1.6 Bleb formation

Blebs could be consistently fashioned using a 20-gauge instrument with a 41-gauge tip (DORC, Netherlands) (see Figure 5.15 B). It was helpful to shorten the tip of the cannula by approximately a third of its length. Creating the retinotomy using an MVR blade led to an uncontrolled and often stellate incision. We therefore adopted the technique favoured by Boris Stanzel (personal communication, 2014) of using the points of the blades of horizontal-cutting delamination scissors to enter the bleb, and then cutting. Viscoelastic, particularly HPMC, was useful in maintaining the bleb. During injection of HPMC, subretinal air was inadvertently injected into one bleb, and this was also found to be an effective method of preventing bleb collapse (see Figure 5.15 D).

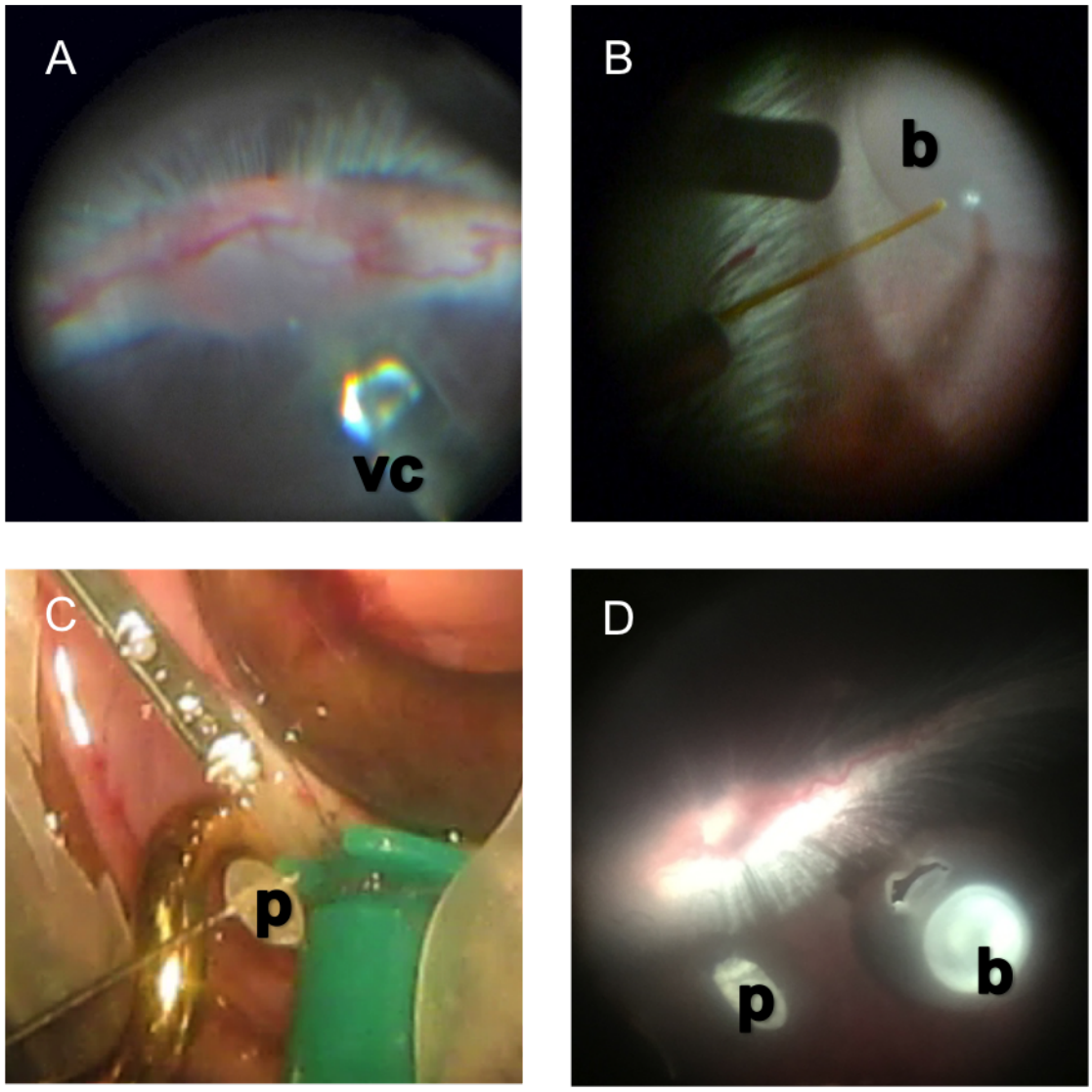

Figure 5.15: Photographs illustrating stages in vitrectomy and subretinal implantation of polymer.

The vitreous cutter (vc) is used to first separate the posterior hyaloid membrane from the retinal surface. (A) The vitreous was then removed. Care was taken to vitrectomise over the visual streak. The posterior vitreous separation only occurred in the inferior retina and no attempt was made to induce vitreous separation in the superior retina. (A) Once the vitreous was removed, a 41-gauge cannula was used to inject balanced salt solution into the subretinal space, creating a bleb (b), shown in photo B. Simultaneously, a surgical assistant was loading the polymer (p) into the injector. This was best achieved by balancing the polymer on the tip of a

needle. (C). The retinotomy was then created in the bleb and the polymer was injected into the subretinal space. Photograph D shows an eye that has had two blebs created. A polymer has already been injected into one bleb, which collapsed spontaneously after polymer insertion. The other bleb is being maintained by an air bubble.

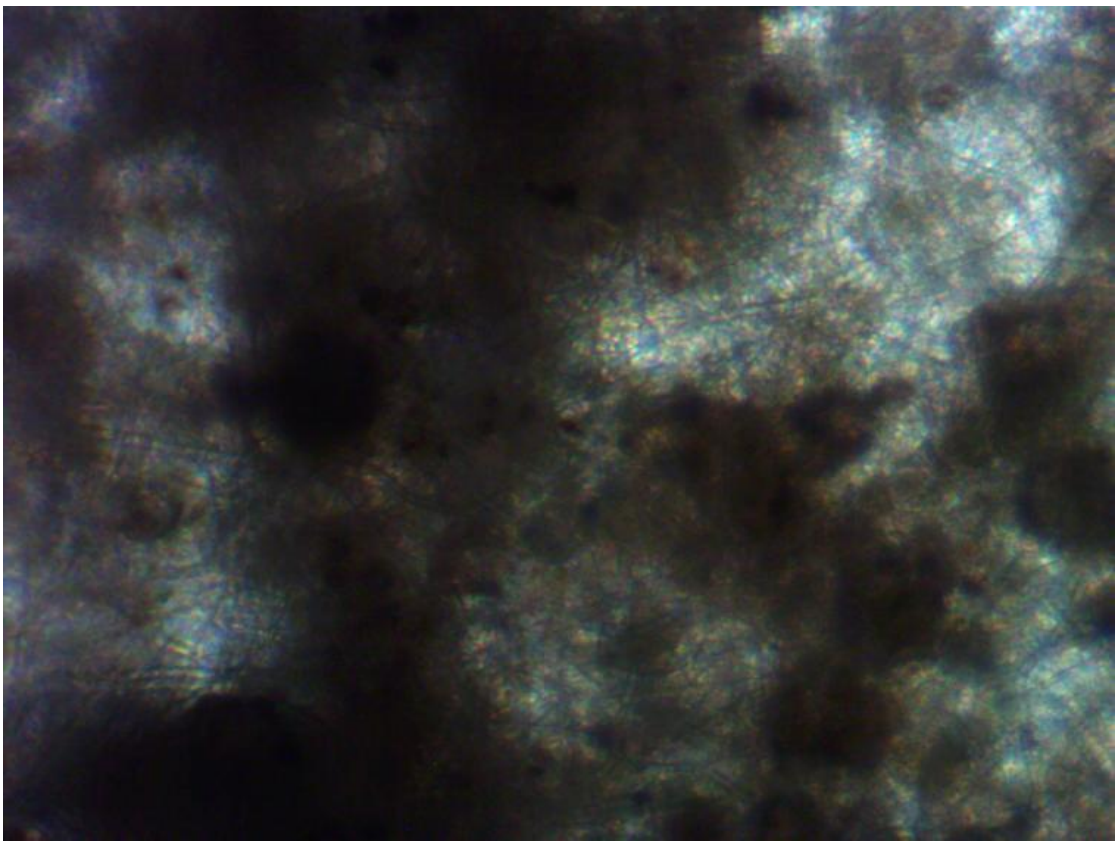

Figure 5.16: Light micrograph (10x) showing ESC-derived RPE monolayer on a 4mm disc of polymer, day 25 *in vitro*.

Note that the RPE pigmentation is uneven microscopically, even though the cells had formed an electrically resistant monolayer in vitro (Valeria Chichagova, Personal Communication, 2015). Image courtesy of Valeria Chichagova, University of Newcastle.

Table 5.5 shows the results of all the rabbit vitrectomy procedures performed during the course of this research.

Number	Code	Experiment date	Weight	Anaesthetic details	Aim of procedure	Anaesthetic success?	Surgical success?	Saline Pre-op?	Proptosis	Gauge	Lensectomy	Polymer?	Cells?	Post-op examination
1	B1R1	13/11/13	3	A/K/R	Vitreolensectomy + bleb + cull	Yes	No	No	No	20	Vitrector	No	No	N/A
2	B1R2	20/11/13	Didn't weigh	A/K/R	Vitreolensectomy + bleb + cull	No	No	No	No	20	Vitrector	No	No	N/A
3	B1R3	27/11/13	2.8	A/K/R	Vitreolensectomy + bleb + cull	Yes	Yes	No	No	20	Vitrector	No	No	N/A
4	B1R4	03/12/13	3.2	A/K/R	Vitreolensectomy + bleb + cull	Yes	Yes	No	No	20	Vitrector	No	No	N/A
5	B1R5	18/12/13	3.1	A/K/R	Vitreolensectomy + bleb + cull	Yes	No	No	No	20	Vitrector	No	No	N/A
6	B1R6	18/12/13	3.2	A/K/R	Vitreolensectomy + bleb + cull	Yes	No	No	No	20	Vitrector	No	No	N/A
7	B2R1	29/01/14	3.8	A/K/R	Vitreolensectomy + bleb	Yes	Yes	No	No	20	Frag	No	No	d1: no fundal view
8	B2R2	11/02/14	3.7	A/R/K/R	Vitreolensectomy + bleb	Yes	Yes	No	No	20	Frag	No	No	d1 - minimal haem, hypotony

Number	Code	Experiment date	Weight	Anaesthetic details	Aim of procedure	Anaesthetic success?	Surgical success?	Saline Pre-op?	Proptosis	Gauge	Lensectomy	Polymer?	Cells?	Post-op examination
9	B2R3	11/03/14	?	A/R/K/R	Vitreolensectomy + bleb	Yes	No	No	No	20	Frag	No	No	d1: plasmoid aqueous,. 19/3/14: ?endophthalmitis,
10	B2R4	25/03/14	?	A/R/K/R	Vitreolensectomy + bleb	Yes	Yes	No	No	20	Frag	No	No	d1: corneal oedema 2/4/14: inflammatory mass inferior retina, flat retina, ?atrophic area in bleb
11	B2R5	25/03/14	?	A/R only	died during anaesthesia	No	N/A	No	No	N/A	N/A	N/A	N/A	N/A
12	B2R6	Necrotising enterocolitis	Did not use	Did not use	Did not use	Did not use	Did not use	Did not use	Did not use	Did not use	Did not use	Did not use	Did not use	Did not use
13	B3R1	03/06/14	?	A/R/K/R	Vitreolensectomy + bleb + polymer	Yes	Yes	No	No	23	Frag	Yes	No	D1 - vitreous haemorrhage

Number	Code	Experiment date	Weight	Anaesthetic details	Aim of procedure	Anaesthetic success?	Surgical success?	Saline Pre-op?	Proptosis	Gauge	Lensectomy	Polymer?	Cells?	Post-op examination
14	B3R2	17/06/14	4.2	A/R/K/R	Vitrectomy + bleb + polymer	Yes	No	No	No	23	No	Yes	No	Lens touch. D1 - dense cataract, no fundal view
15	B3R3	27/06/14	4.5	A/R/K/R	Vitrectomy + bleb + polymer	Yes	Yes	No	No	23	No	Yes	No	D1 - comfortable, no red reflex, no view, round pupil
16	B3R4	01/07/14	???	A/R/K/R	Vitrectomy + bleb + polymer	Yes	Yes	No	No	23	No	Yes	No	Cataract
17	B3R5	04/09/14	5.3	A/R/K/R	Vitreolensectomy + bleb + polymer	No	No	No	No	23	Frag	Yes	No	Rabbit woke, moved, total RD
18	B3R6	25/09/14	5.9	A/R/K/R	Vitrectomy + PVD + bleb + polymer	Yes	No	No	No	23	Yes	Yes	No	Lens touch
19	B4R1	08/12/14	4.5	A/R/K/R	Vitrectomy + PVD + bleb, no polymer	Yes	Yes	No	Yes	23	No	No	No	Cataract
20	B4R2	08/12/14	?	A/R/K/R	Vitrectomy + PVD + bleb, no polymer	Yes	Yes	No	Yes	23	No	No	No	Cataract
21	B4R3	22/01/15	?	A/R/K/R	Vitrectomy + PVD + bleb + polymer	Yes	No	19/01/15	Yes	23	No	Yes	No	Intraoperative RD: culled

Number	Code	Experiment date	Weight (kg)	Anaesthetic details	Aim of procedure	Anaesthetic success?	Surgical success?	Saline Pre-op?	Proptosis	Gauge	Lensectomy	Polymer?	Cells?	Post-op examination
22	B4R4	21/01/15	?	A/R/K/R	Vitrectomy + PVD + bleb + polymer	Yes	Yes	19/01/15	Yes	23	No	Yes	No	Cataract
23	B4R5	23/01/15	?	A/R/K/R	Vitrectomy + PVD + bleb + polymer	Yes	Yes	21/01/15	Yes	23	No	Yes	ESC-RPE	Died post op
24	B4R6	18/07/15	5.5	A/R/K/R	died during anaesthesia	No	N/A	22/01/15	N/A	23	N/A	N/A	No	N/A
25	B5R1	07/08/15	6.5	A/R/K/R	Vitrectomy + PVD + bleb + polymer + cells	Yes	Yes	Yes	Yes	23	No	PG4	ESC-RPE	Posterior subcapsular cataract
26	B5R2	07/08/15	?	A/R/K/R	Vitrectomy + PVD + bleb + polymer + cells	Yes	No	Yes	Yes	23	No	PG4	ESC-RPE	N/A

Table 5.5. Details of all rabbit vitrectomy procedures performed.

Number indicates study number. Code is Batch number and rabbit number within batch i.e. B5R2 is rabbit 2 within batch 5. Anaesthetic details: A=acetopromazine; R=Rompun half dose, K=Ketamine; A/K/R indicates rabbit received acetopromazine followed by full dose ketamine and rompun. PG4=polymer generation IV.

-

5.4.2 Optimisation of Histology

Although the initial intention had been to fix all the operated rabbit eyes with 4% PFA, and then obtain histological specimens by cryosectioning, it became apparent from the first seven eyes that this was not possible. Massive tissue distortion occurring during the cryosectioning process led to collection of specimens unrecognisable as retina (figures not shown). Therefore, a number of experiments were performed to try to optimise the histological fixation (see Figures 5.17, 5.18, 5.19, 5.20, 5.21, 5.22 and 5.23)

5.4.2.1 Fixation with 4% paraformaldehyde vs. Davidson's fixative

An experiment using pig eyes was used to compare paraformaldehyde fixation with Davidson's fixation. The results of these are shown in Figure 5.17 and Figure 5.18, demonstrating that the best tissue processing is achieved with Davidson's fixative rather than PFA, and that a keratotomy made after histological processing allowed greatest preservation of the tissue.

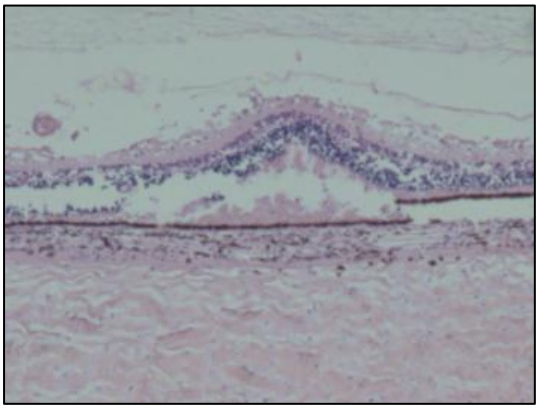

PFA, 36 hours - no aperture

Tissue architecture abnormal, RPE disruption, degradation of intraretinal layers

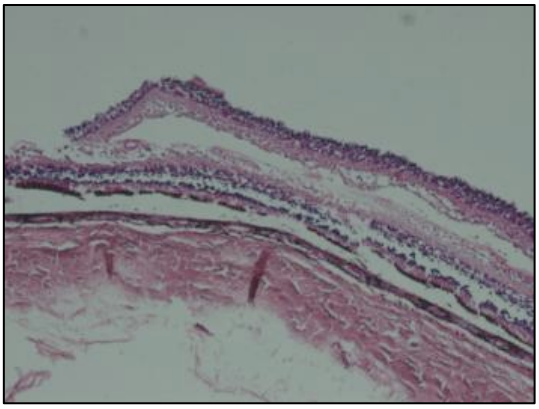

PFA, 36 hours - pre-fixation 2mm aperture

Separation between and within layers of the retina

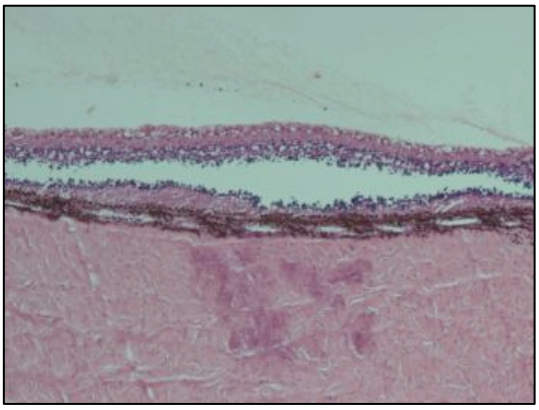

PFA 36 hours – post-fixation 2mm aperture

Cleave within the outer nuclear layer of the retina

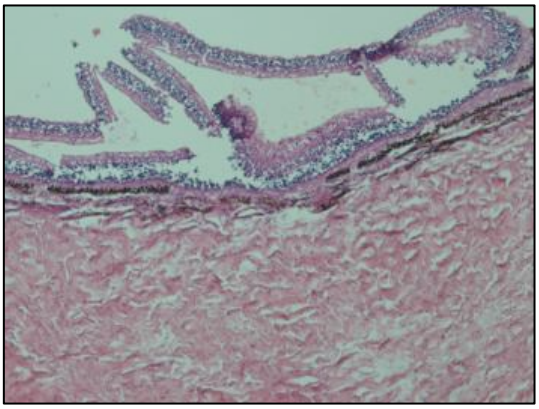

PFA 36 hours - post processing 2mm aperture

Disorganised, fractured retina

Figure 5.17: Histological results after fixation with 4% paraformaldehyde.

PFA created marked tissue distortion or disorganisation, irrespective of when the corneal aperture was created. Samples that had a corneal aperture after processing had the most disorganised appearances.

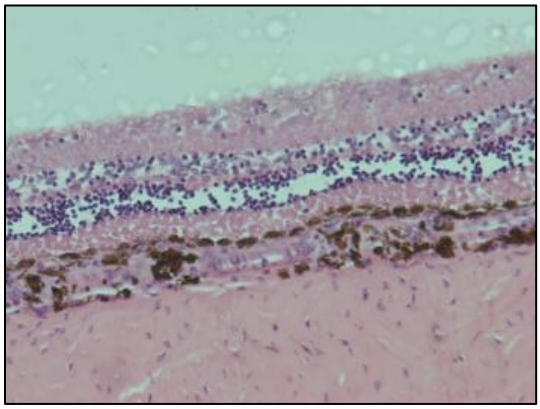

Davidson's 24 hours – 2mm aperture before fixation

Note the cleavage within the outer nuclear layer

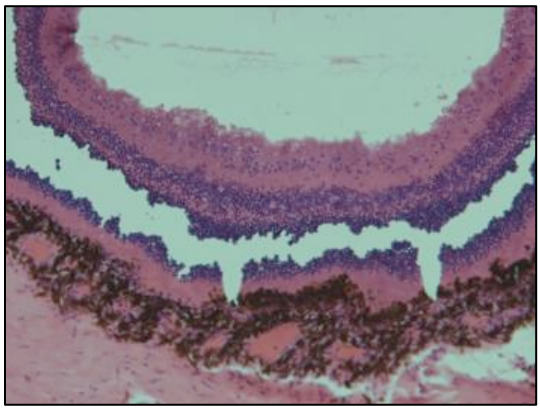

Davidson's 24 hours – 2mm aperture after fixation

Cleavage and degradation of the outer nuclear layer and the photoreceptors

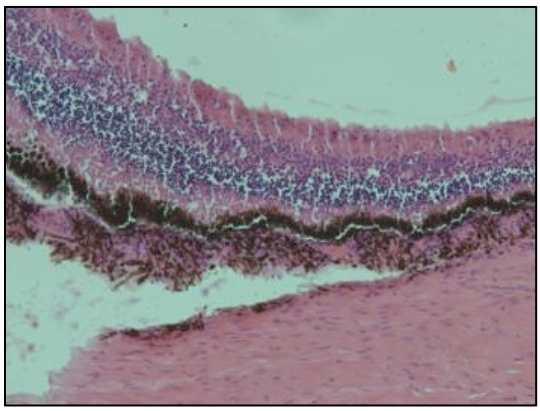

Davidson's 24 hours – 2mm aperture after processing

Intact retina, localised retinal detachment in some areas (not shown in this figure). Artefactual separation of the choroid from the sclera is noted in this figure.

Figure 5.18: Histological results after fixation with Davidson's fixative

Davidson's fixative was better than PFA for preservation of retinal architecture. The outer nuclear layer appeared to be a site of cleave in multiple samples. There was considerable success with fixation with Davidson's fixative and a 2mm aperture made in the cornea after processing. This was in stark contrast to the findings of PFA, where the post-processing hole led to the most disorganised tissue.

5.4.2.2 Duration of Fixative and Size of Keratotomy

The previous experiment (see Figure 5.18: Histological results after fixation with Davidson's fixative) determined that Davidson's fixative was more effective than PFA for retinal tissue preservation, especially when a corneal aperture was made with a biopsy punch after histological processing. A subsequent experiment was performed to determine the effect of variations in duration of fixation with Davidson's (24h vs. 48h) and the size of the post-processing aperture made (2mm vs. 6mm vs. 8mm).

The results, shown in Figure 5.19, suggest that 24h of fixation followed by a 6mm post-processing aperture is the most appropriate course of action.

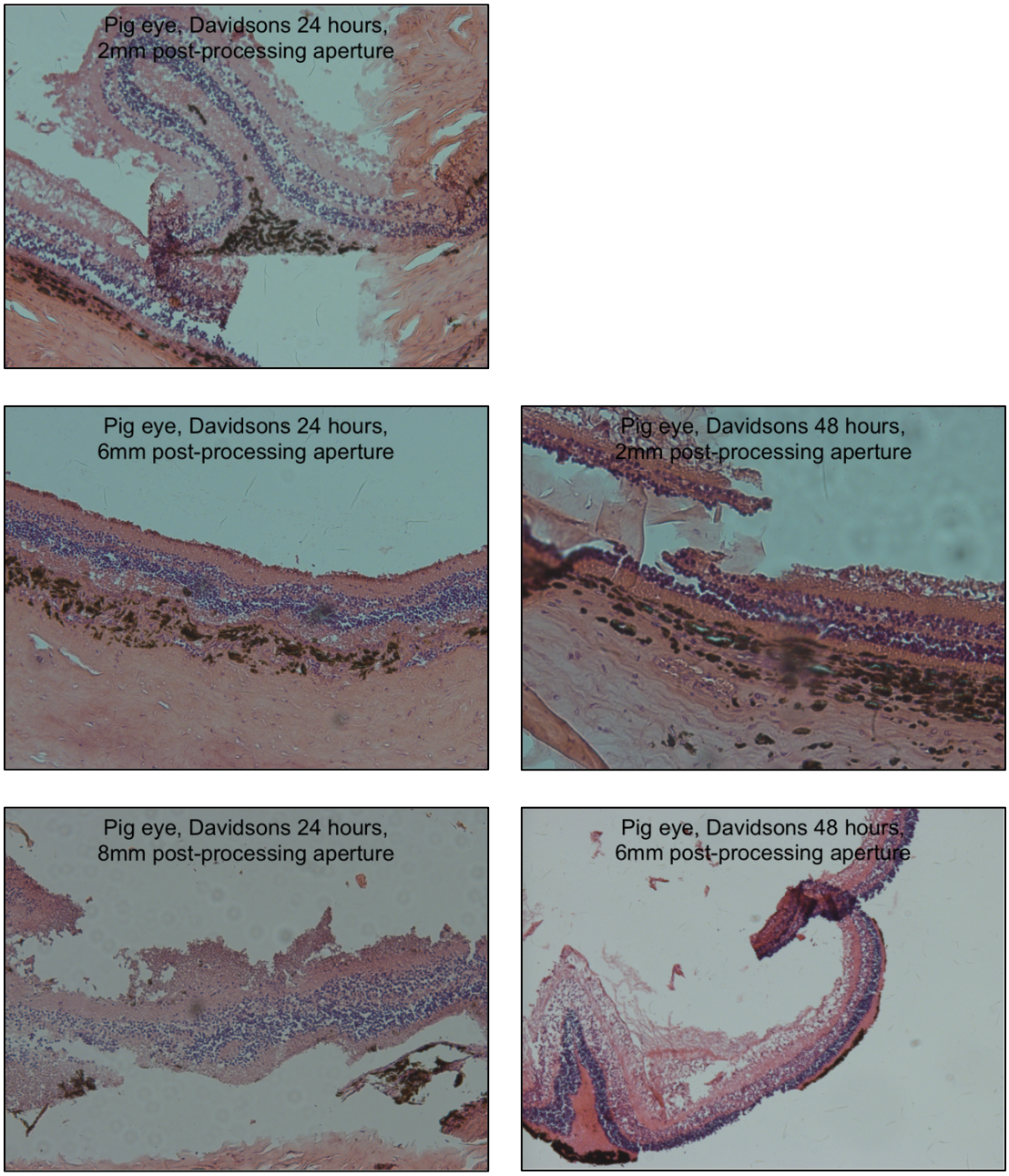

Figure 5.19: Histological results after fixation for either 24h or 48h with Davidson's fixative

5.4.2.3 Histology of Rabbit Eyes

Following the previous experiments that were performed in pig eyes, all subsequent histological specimens of rabbit eyes was performed with 24h Davidson's fixation, and a 6mm keratotomy was made after histological processing but before paraffin embedding. The results of histological processing of normal rabbit eyes are shown herein.

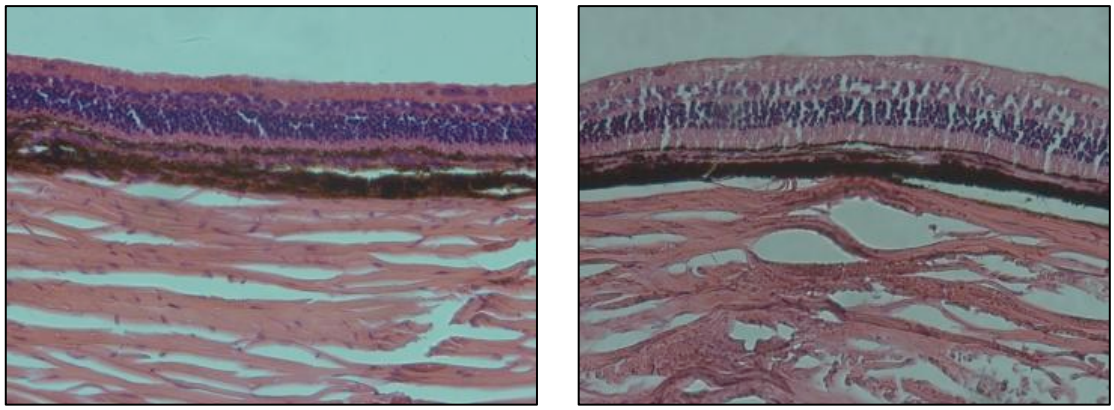

Figure 5.20: Histology of normal rabbit eyes (Davidson's fixative, 6mm post-processing aperture, H&E stain)

The individual layers of the retina, including the photoreceptors, and the outer and inner nuclear layers, can be clearly identified within these samples. The retinal pigment epithelium is completely intact, although there is some artefactual separation between the RPE and choroid. This validates the use of Davidson's and wax paraffin embedding as a useful technique for histology in rabbit eyes.

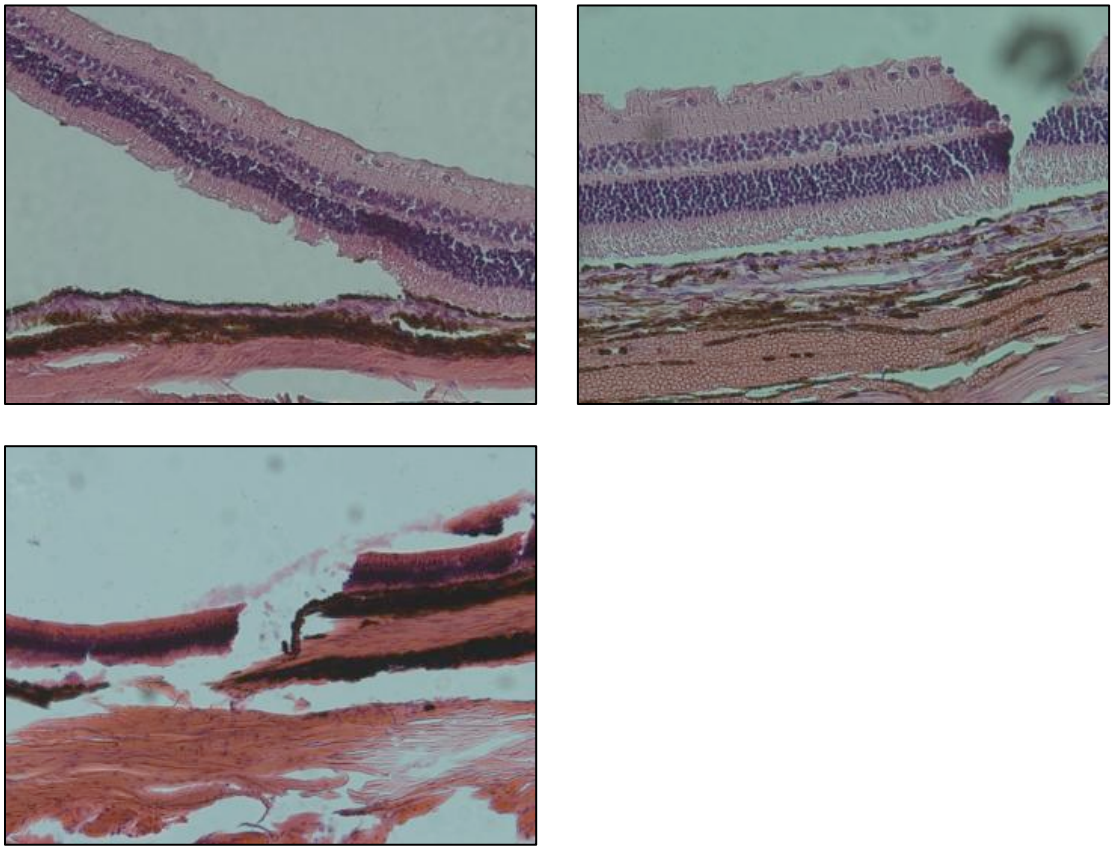

Figure 5.21: Examples of histological artefact in normal rabbit eyes.

Top left: Artefactual retinal detachment is a common finding even in normal rabbit eyes undergoing histology. Interestingly, Davidson's can prevent artefactual retinal detachment in histological samples of all animal species except the rabbit.[239] As noted in the top left figure, the retina has detached from the RPE but there is also some loss of the photoreceptor layer.

Top right: Some samples had numerous full thickness retinal breaks.

Bottom left: In other samples, the retina, choroid and sclera had all been fractured by the histological processing.

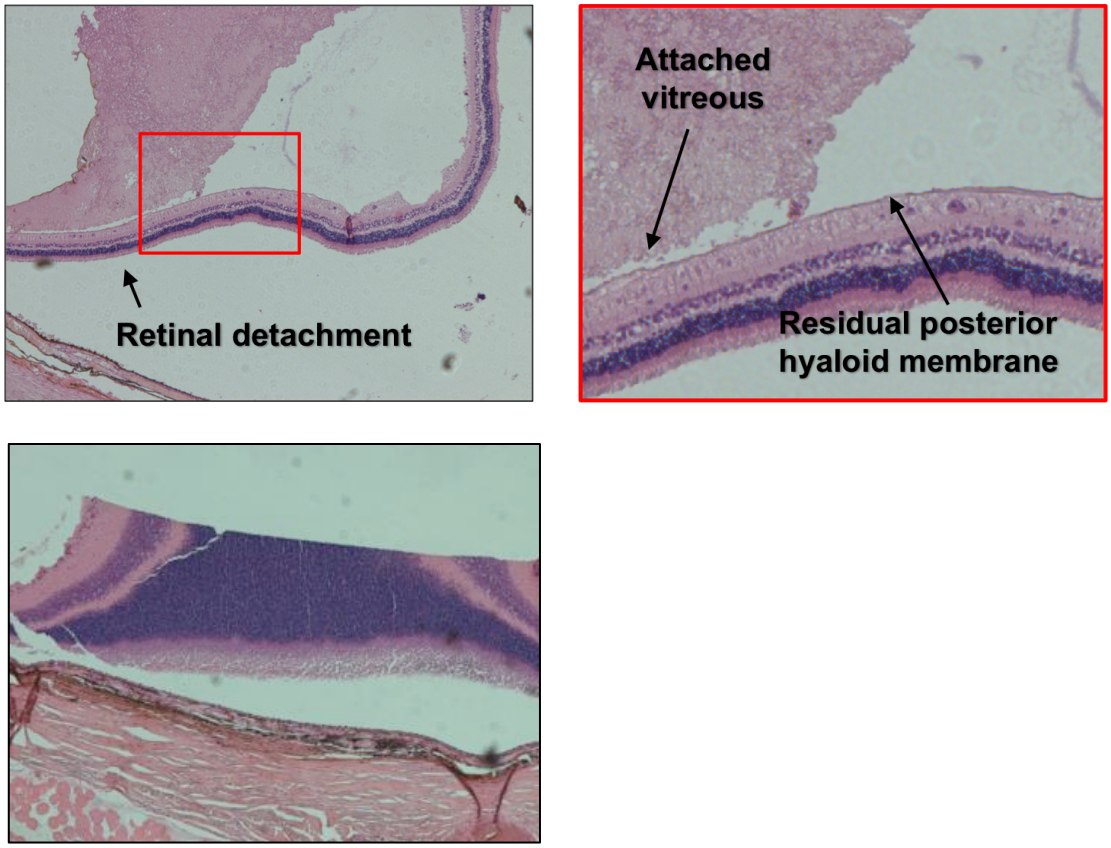

Figure 5.22: Examples of the retinal distortion that can occur following vitrectomy and submacular polymer implantation.

The top left figure shows retinal detachment due to residual attached vitreous (rabbit eye, no PVD induced, vitrectomised, subretinal polymer). The area within the red triangle is shown at higher magnification in the top right figure. The posterior hyaloid membrane has not been fully separated from the retina and this may be a cause for the retinal detachment in this case. The bottom left picture shows massive expansion of the outer nuclear layer due to mechanical stretch, presumably due to vitreoretinal traction. The posterior hyaloid membrane and the inner retina has been lost from the slide.

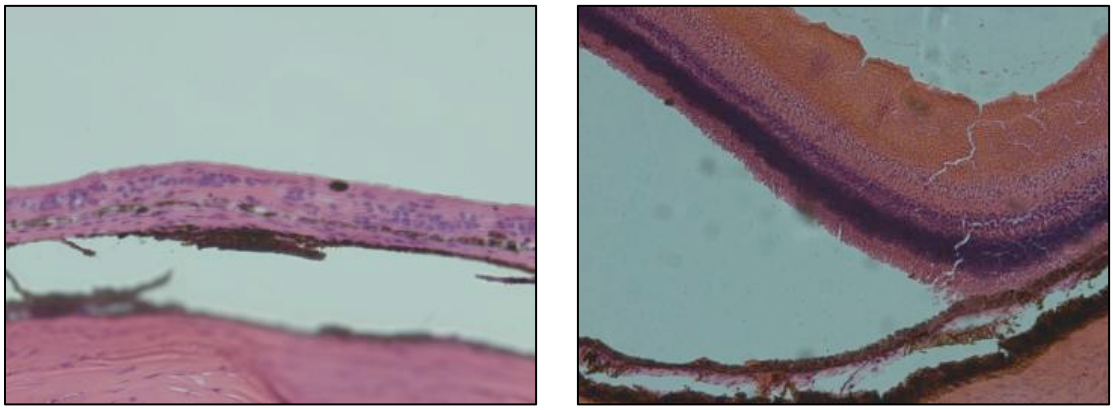

Figure 5.23: Examples of histological results from rabbit eyes that had undergone vitrectomy surgery and subretinal implantation.

These samples show retinal detachment, but the cleavage plane is uneven and in some areas the RPE remains attached to the undersurface of the neurosensory retina. The samples were taken from the central retina of rabbit eyes receiving subretinal polymer implantation (without cells). It is possible that these photographs show the bleb created by the 41-gauge cannula, to allow polymer implantation. Alternatively, these retinal detachments may simply be an artefact of histological processing, as noted in Figure 5.21.

5.4.2.4 Histological processing of polymer

As shown in Figure 5.23, in rabbit eyes that had received subretinal polymer, the polymer could not be identified. The results of histological processing of the polymer alone are shown below.

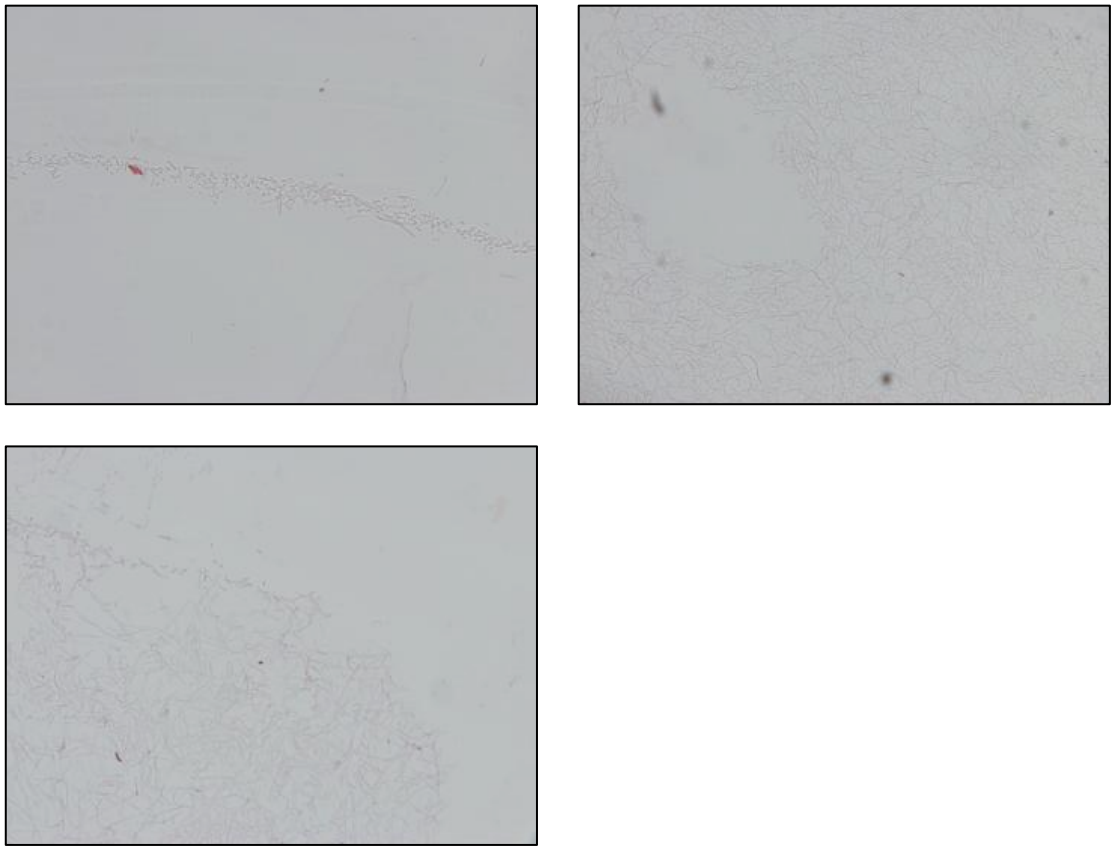

Figure 5.24: Photographs of polymer that has been exposed to Davidson's fixative and then undergone histological processing.

The polymer is barely visible with H&E stain (top left) and when viewed *en-face* (top right, bottom left) degradation of the polymer was evident both at the edges and within the centre.

In an attempt to improve the identification of the polymer, Verhoeff's staining of polymer alone, and rabbit retina alone, was attempted.

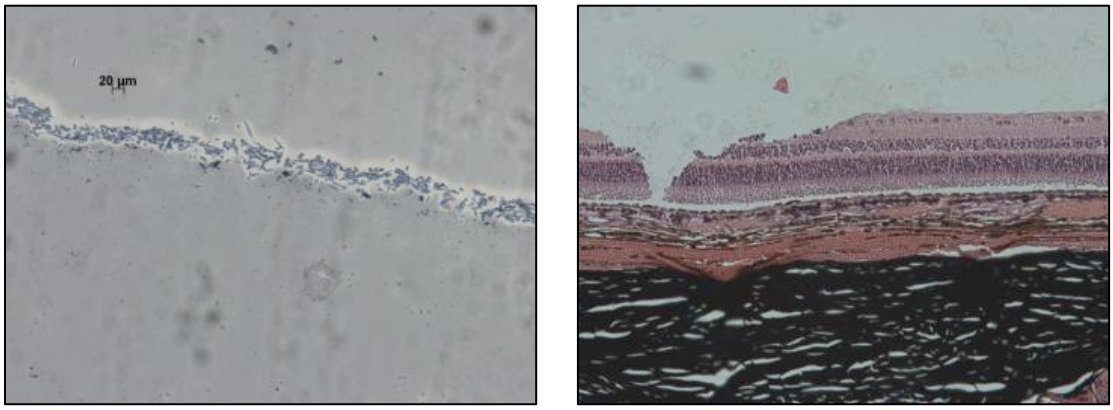

Figure 5.25: Verhoeff's staining of polymer and retina

Verhoeff's stain was effective at staining the polymer blue (left). Despite this, the polymer was not visible in samples of retina that had received subretinal polymer (right)

5.4.2.5 Histological result of polymer in the subretinal space

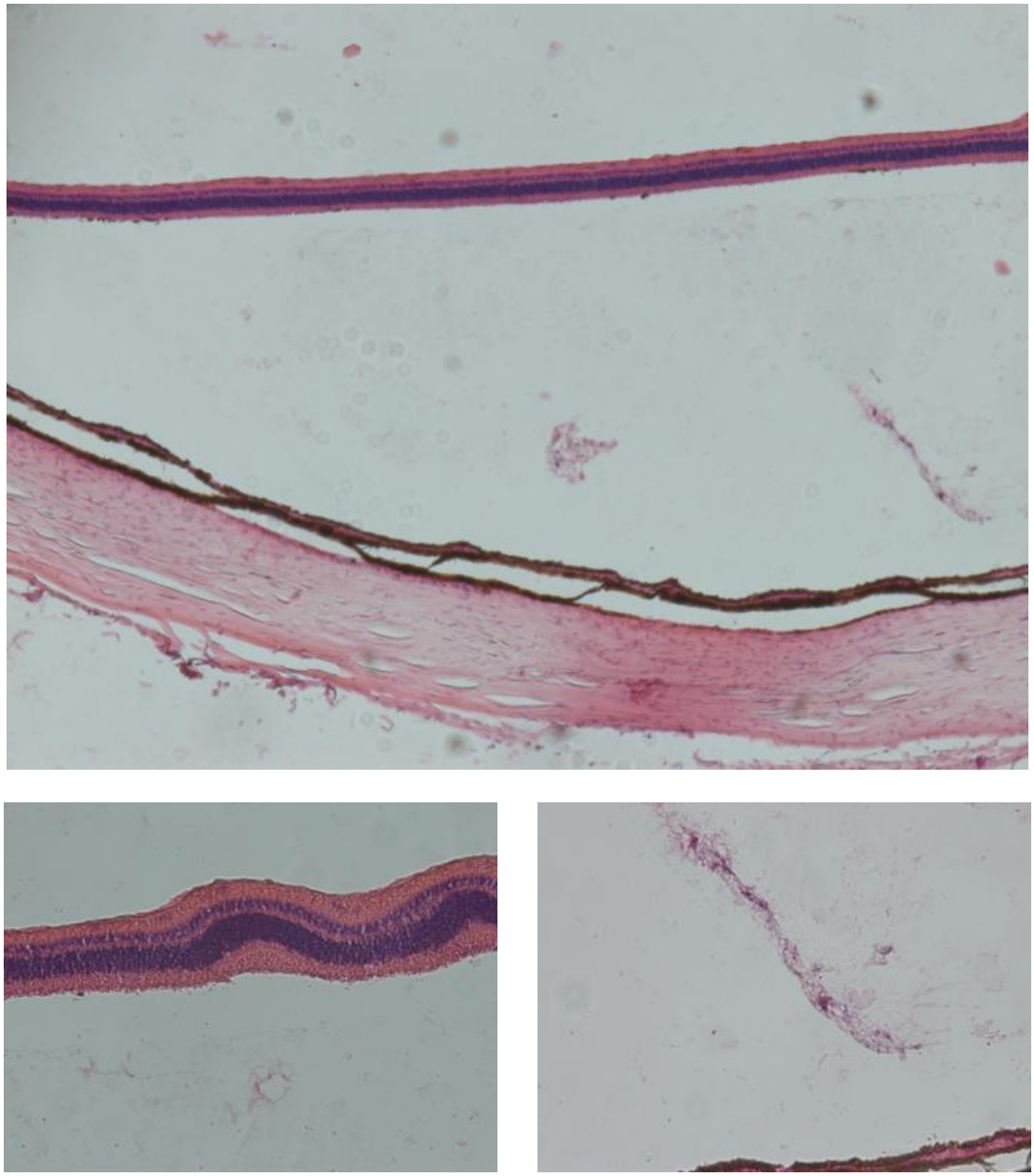

Figure 5.26: Single example of polymer detection in the subretinal space

This sample, taken from rabbit 13, shows material in the subretinal space which could possibly indicate the presence of polymer. The retina is detached and the distance between the retina and the RPE (top figure) is far greater than that observed in the artefactual retinal detachments in Figure 5.21. The retinal architecture is intact (bottom left) and the polymer shows variegated staining due to the presence of some cellular material (bottom right).

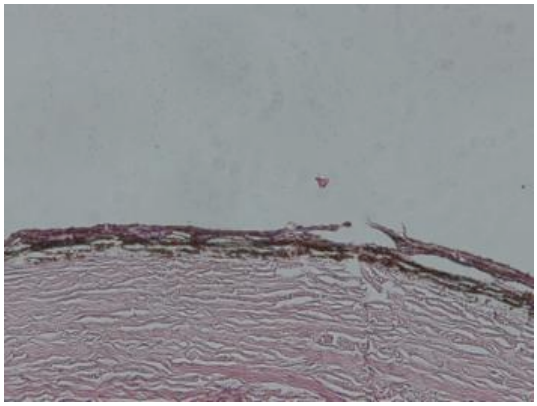

Figure 5.27: Results of perfusion-fixation with 4% PFA.

The RPE was identified but the retina could not be found within the sample.

5.4.3 OCT of Rabbit Eyes

OCT scans of health rabbit eyes, conducted under general anaesthesia, are shown in Figure 5.28.

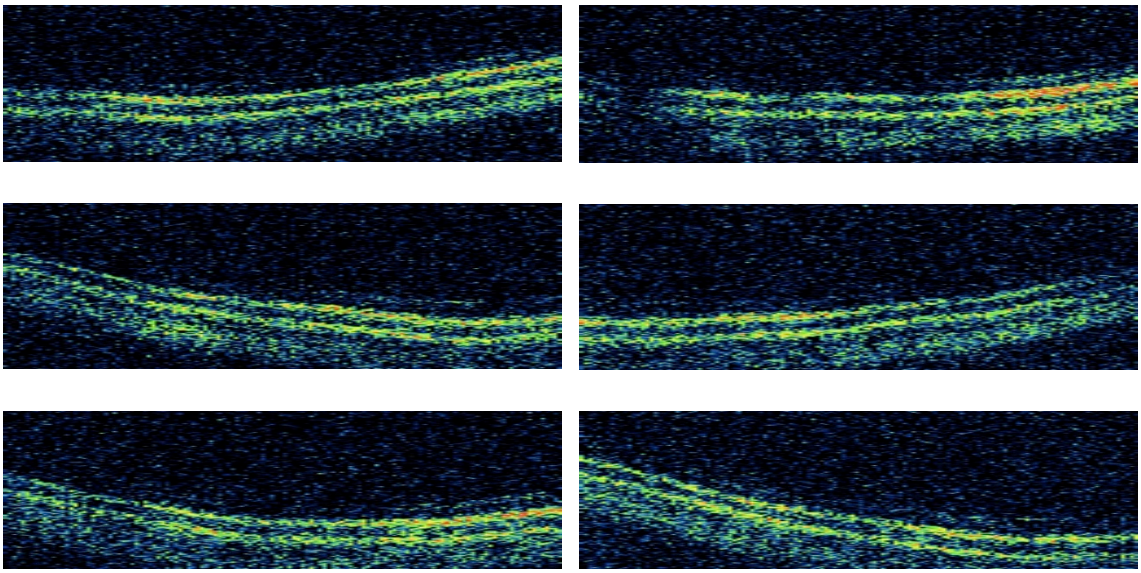

Figure 5.28: Examples of Rabbit OCT scan using the Zeiss Stratus OCT

These scans were taken in a healthy eye before any surgery was undertaken. Despite numerous attempts, it was not possible to take any OCT scans showing the polymer in situ, either because of difficulties with positioning, media opacity, but most commonly because the polymer was not placed in the exact centre of the retina. The scanning head of the Zeiss Stratus OCT scanner is fixed to detect the central retina and cannot be directed to other areas of interest in the ocular fundus.

5.5 Discussion

The aims of the experiments in this part of the thesis were to ensure surgical delivery of the polymer into the subretinal space, and then to evaluate the effect of the polymer, using histology and/or *in vivo imaging.*

Surgical delivery of the polymer was challenging, partly because of the limitations of the rabbit anatomy, and because of my own surgical learning curve. By the time the final rabbit experiment was performed, the surgical technique had been honed and the polymer, with or without cells, could be consistently delivered. Despite the benefits of the rabbit model, there are certain aspects of rabbit anatomy that warrant discussion here, because of the limits that they place on surgical outcome.

The rabbit has small lung fields and during experimental procedures, the risk of anaesthetic death is well recognised. In this series of 26 rabbits, anaesthetic failure occurred in four rabbits; of these, two rabbits died during the anaesthetic, while the remaining two rabbits (rabbits 2 and 17) were not sufficiently anaesthetised and therefore woke up during the procedure. Rabbit 2 had been given the incorrect dose and this occurred because of (my) human error. Rabbit 17 was given the correct dose but still moved unexpectedly and without warning during the vitrectomy, leading to a total retinal detachment and the need for immediate cull, as per the conditions of our animal project licence.

Rabbits 1-6 were culled immediately after surgery, as planned, because I was still on the learning curve for performing these procedures. Indeed the difficulties during these initial procedures all arose from human error, as a result of trying something new. For example, rabbit 2 was given the incorrect dose of anaesthetic. For these rabbits, the lensectomy was performed using the vitrector because I did not have a fragmatome available. It became clear that the vitrector was inadequate because, surprisingly, the rabbit crystalline lens is much tougher than the human crystalline lens. As a result, lensectomy was generally unsuccessful and simply led to more intraoperative complications.

Rabbits 1-13 all underwent vitreolensectomy. The rationale for this was that by performing planned lensectomy, there would be more space available to perform the vitrectomy. Otherwise, lensectomy would only be performed in the event of

intraoperative lens touch and this would introduce unwanted heterogeneity into the surgical procedures. Lensectomy with fragmatome was reasonably straightforward to perform but postoperatively the eyes were very inflamed and vitreous haze precluded any clear view of the retina on the first postoperative day.

One rabbit of 26 (rabbit 9) developed suspected endophthalmitis. This rabbit underwent vitreolensectomy but unlike the other rabbits, had a plasmoid aqueous and a hypopyon. Although it is possible that this was simply a severe inflammatory reaction, postoperative endophthalmitis was suspected and the animal was culled. Rabbits have a long nasolacrimal duct that passes close to the dental roots, and therefore rabbits are very prone to eye infections. The eye was too disordered to provide any histological specimens.

Surgical success was dramatically improved by three factors, all of which happened at around a similar time in the project. Firstly, I discovered that the globe could be completely proptosed from the orbit. Although details of this have not been explicitly described in the literature, this technique/finding is not new and has been alluded to vaguely by other researchers performing rabbit vitrectomy.[228] Globe proptosis, performed from Rabbit 19 onwards, revolutionised our ability to perform safe rabbit vitrectomy because it overcame many of the difficulties that we had had with positioning of the animal and placing the speculum within the eyelids, especially to attempt to retract the nictitating membrane. Proptosis dramatically improved the surgical access and as a result lensectomy was no longer required.

The second factor that improved our surgical experiments was the use of the disposable BIOM, rather than a contact lens, to visualise the retina intraoperatively. Not only did this widen the surgical field but it also avoided the hindrance of the contact lens, which inevitably slipped from the central cornea and would obstruct access to the sclerotomies.

The third factor is novel and has not been described previously in the literature, and relates to the induction of posterior vitreous detachment. Our finding that the use of intravitreal saline 48 hours before vitrectomy facilitated posterior vitreous detachment is particularly significant for researchers using the rabbit vitrectomy model. Central vitrectomy, with failure to remove the posterior hyaloid membrane from the inner retinal surface, has long been thought to lead to giant retinal tears in human eyes,[240] and the massive tissue distortion that occurred in rabbit eyes before our use of pre-operative

intravitreal saline technique is shown in Figure 5.22. Although Stanzel is able to induce posterior vitreous detachment in rabbits without using preoperative intravitreal injections, I was not able do this. [241] This may reflect differences in our surgical technique, particularly in the gauge of the vitrectomy instruments, but may even be affected by the strain of rabbit used.

Despite these three 'advances' in the development of the rabbit surgery model, the problems that they solve are unique to rabbits and do not occur in humans. In humans, combined phacovitrectomy is straightforward and no more complicated than vitrectomy alone, and induction of PVD in human eyes is routine at the time of vitrectomy, without the need for any preoperative intravitreal injection. And of course there is certainly no need to proptose the human eye from the orbit, because even with small eyes, access is usually more than adequate. Therefore, while the experiments above may not have directly translatable consequences for human surgery, they do allow better characterisation of the rabbit model, and making rabbit vitrectomy a useful procedure for the evaluation of regenerative cellular therapies.

It was interesting to observe, quite by accident, the ability of subretinal air to maintain the bleb. Although much effort had been taken in Chapter 4 to evaluate the effect of viscoelastic on RPE cells, the injection of a small bubble of air may be an alternative. One potential disadvantage is that during surgical 'flattening' of the bleb, the air will escape very rapidly and this may in turn cause retinal trauma.

It would have been useful to be able to evaluate the polymer *in vivo* with OCT. Unfortunately we did not have an OCT device that was adequate for rabbits, and could not detect the polymer in the subretinal space, even intraoperatively, with our OCT scanner. Newer OCT scanners, such as the Spectralis (Heidelberg Engineering, Heidelberg, Germany) or the Envisu preclinical SDOCT (Bioptigen, North Carolina, USA) allow more rapid image acquisition and image-guided OCT slices and either of these devices would have been useful in monitoring the effect of the polymer, with and without cells, *in vivo.* A recently described software algorithm that allows automated objective analysis of vitreous inflammation based on Spectralis OCT scans may have potential use for the assessment of the inflammatory sequelae of polymer implantation, particularly if xenograft RPE cells are used.[242]

The histological processing of the samples remain a challenge. Although we modified our fixation and histological technique from PFA and cryosectioning to Davidson's fixative and paraffin sectioning, the artefactual changes in normal non-vitrectomised eyes are considerable. It is therefore impossible to determine with any degree of certainty what the relative effects are of surgical trauma vs. polymer vs. cellular implantation, since retinal detachment, photoreceptor loss, outer nuclear layer cleavage, and fracture of the retina/choroid/sclera can occur during histological processing even in normal eyes. Our attempts to perform perfusion fixation have not yielded promising results so far. The most challenging obstacle is that the polymer seems to degrade during histological processing. My colleague Gareth Ward is continuing to find new methods for detecting polymer, and is currently investigating the use of Raman Spectroscopy to detect the presence of the unique 'signature' produced by the polymer in eyes that have undergone vitrectomy and polymer implantation. The results of these studies are eagerly awaited but are beyond the scope of this thesis.

5.6 Conclusions

- Intravitreal injection of saline 48h before pars plana vitrectomy facilitates surgical induction of posterior vitreous detachment in the rabbit eye.

- Globe proptosis is a useful manoeuvre to improve surgical access during rabbit vitrectomy.

- Combined vitrectomy and lensectomy causes a marked inflammatory reaction and this may confound the observed effects of experimental subretinal implantation of polymer +/- RPE cells.

- Histological processing of the rabbit eye is best achieved with Davidson's fixative and wax-paraffin sectioning artefactual tissue destruction during processing is common. It is therefore impossible to determine whether tissue destruction is the effect of surgical trauma, polymer, cellular transplantation, or artefact.

- Perfusion fixation may be preferable as a method of obtaining histological specimens in rabbit eyes.

- *In vivo* imaging with OCT is likely to be the optimal method for assessment of the effects of subretinal implantation, and this is most likely to be achieved high resolution spectral domain technology that allows image-guided OCT.

–

Chapter 6: CONCLUSIONS & FUTURE WORK

"The best way to predict the future is to invent it."

Alan Kay

The aim of this thesis was to evaluate the 60:40 P(MMA-co-PEGM-succinimidyl carbonate) co-polymer as a potential artificial BrM, to potentially allow RPE transplantation. The seven objectives of the thesis were aimed at determining whether the co-polymer meets the criteria of an ideal BrM substitute:

- supports acquisition and/or maintain the RPE phenotype
- allows for fluid transport, i.e. with porosity comparable to juvenile BrM
- enables easy surgical manipulation
- well tolerated in the subretinal space
- biodegrades or integrates over time

The results have shown that the RPE layer on the polymer surface exhibits measurable electrical resistance but the results did not show clear evidence of ARPE-19 polarisation on the polymer. Immunohistochemical evidence of ZO-1 could not be demonstrated even in ARPE-19 cells growing in wells. A novel surgical device has been developed to allow implantation of the polymer into the subretinal space, and this device has been shown to produce no apoptotic cell death compared to controls, and may have a more favourable cell safety profile compared to the Bonn-shooter instrument. I have shown that OVDs are non-toxic to RPE cells and these may be a potential adjunct for subretinal surgery during RPE transplantation. I have demonstrated that with specific surgical manoeuvres, the difficulties of the rabbit vitrectomy can be overcome, and polymer can be consistently implanted into the subretinal space.

During these studies I have been unable to demonstrate the effect of the polymer, with or without cells, on the neurosensory retina, not have I been able to determine what happens to the polymer over time. Improved histology is vital for determining the effects of the polymer and/or cells with respect to inflammation/immune response and photoreceptor dysfunction. Our histological techniques were initially based on the techniques used by Hari Jayaram at the Institute of Ophthalmology. We subsequently

modified our techniques based on advice from Boris Stanzel in Bonn. Despite considerable efforts to optimise the histological sectioning, the results remain unsatisfactory. In retrospect it would have been prudent to outsource the histological sectioning to the Institute of Ophthalmology, rather than try to perform this in-house. While Raman Spectroscopy is useful for enucleated eyes in the laboratory setting, it is likely that better *in vivo* imaging, with high definition spectral domain OCT, is the more useful technology, because it can be used in the clinical setting in addition to the laboratory.

The pathological changes in BrM are key features in the development of AMD, yet at present we have no method for assessing the structure or function of BrM *in vivo*. Even using high resolution OCT, BrM merges with, and is indistinguishable from, the RPE on the cross-sectional image. The ability to image and functionally assess BrM in a consistent way would carry a number of advantages. Firstly it would enable us to phenotype and risk-stratify our AMD patients more effectively and reliably. The ability to assess *in vivo* the hydraulic conductivity of BrM would provide invaluable information, especially if this conductivity could be localised within the fundus. The rate of decline of hydraulic conductivity could be correlated with other known clinical features of AMD. All of these factors would enable us to identify patients who are at high risk of visual loss, yet who do not exhibit signs of neurosensory retinal dysfunction or photoreceptor loss. RPE transplantation will ultimately be a preventative treatment, yet the invasive nature of the surgery, which involves surgically induced retinal detachment at the fovea, must be justifiable based on reliable prognostic data. Early detection of reversible change within the BrM and RPE disease may provide the opportunity for some other therapy, obviating the need for a major surgical procedure such as RPE transplantation.

In addition to AMD, functional assessment of BrM may help our understanding of other diseases. For example, laser treatment to the macula is well known to be an effective treatment for macular oedema due to diabetes or branch retinal vein occlusion yet the mechanism of this remains uncertain. Although the received wisdom is that laser treatment stimulates the RPE, I cannot help but wonder whether the laser is in fact changing BrM, rather than the RPE, in a way that facilitates the removal of intraretinal fluid by the RPE into the choroid.

All scientific literature, including this thesis, is conventionally structured into an introduction, methods, results and discussion. This can be misleading because it would have us believe that scientific experiments are conducted in a linear fashion. This project has demonstrated that the true experimental course is far more tortuous. Early failures lead to changes in the method, and as projects progress, the new availability of equipment, expertise, funding, technical assistance, combined with advances reported by other research groups, can result in rapid changes in experimental design. One aim of this project was to determine surgical methods for RPE transplantation but the lack of histological data has not allowed this. However, instead the experiments have allowed us to optimise and characterise the use of the rabbit vitrectomy model, which I hope will be of use not only to the Lotery group but also to researchers from other groups.

This work has primarily used ARPE-19 cells, but cell lines have limitations. For many years preceding the start of this project, the consensus has been that iPSC-derived cell therapy appeared to be the most promising technology because they allow patient-specific treatment. This is the ultimate form of personalised medicine. While the London Project to Cure Blindness was using ESC-derived RPE, the RIKEN trial, based in Japan, was the first trial in the world to use iPSC. However, there have been several interesting developments in recent months. The RIKEN trial was suspended after the first patient, because six mutations were identified in the iPSC-RPE due to be transplanted into the second patient. The observation that these six genetic changes, were not present in the patient's somatic cells, has led to more questions than answers. How and when did these mutations arise? Are they preventable? This has resulted in some regulatory changes in Japan for the use of iPSC-derived cell therapies. The RIKEN trial resumed in June 2016 but the iPSC used will be provided by Kyoto University's Center for iPS Cell Research and Application (CiRA) and transplanted at the Osaka University Hospital and Kobe City Medical Center General Hospital. Therefore the iPSC-derived RPE will not be personalised for individual patients but they will be HLA-matched to reduce the risk of rejection.

The Lotery lab are now developing iPSC-derived RPE and it would be useful to test the polarisation and transepithelial resistance of these cells on the polymer surface. Immunohistochemical confirmation of RPE markers such as RPE-65, cytokeratin and CRALBP would be required to demonstrate that the cells derived from the iPSC maintains their phenotype as RPE cells.

Much of the limitation in the field of RPE transplantation arises ffrom the surgical complexities and complications. Professor Rob MacLaren at Oxford has recently used a robotic system to perform retinal surgery. The first procedure was performed in late 2016 and involved removal of an epiretinal membrane. This procedure is a routine vitreoretinal procedure that is usually performed manually, and the use of the robotic system in this case has probably not enhanced the patient's treatment. However it does indeed demonstrate the potential capabilities of robotic systems for intraocular surgical procedures that require precision beyond the physiological limits of the human surgeon's hand. It may be that nanorobotic systems, using robots that are 0.1-10μm in size, would enable individual RPE cells to be delivered into the subretinal space with minimally invasive approach, potentially avoiding the need for detaching the macula from the underlying RPE.

The pathogenesis of AMD is thought to initiate from the RPE and BrM. Accordingly, this current project has focussed only on RPE and BrM transplantation. However, the role of the choroid in the pathophysiology of the RPE still remains uncertain. Successful 'proof-of-principle' experiments such as macular translocation and autologous RPE-BrM-choroid grafts both involve transplantation of the RPE, BrM *and* choroid. Therefore, perhaps the choroid needs to be transplanted in conjunction with BrM and the RPE.

Cell biology techniques will continue to improve, as will the ability to convert ESC and iPS cells *in vitro* not only into a single RPE layer, but potentially into a multi-layered retina comprising of neurosensory retina, RPE and choroid suitable for transplantation. Human ESC have already been used to produce a self forming optic cup in a 3D *in vitro* culture system.[243] Transplantation of multi-layered structures would be facilitated by improved surgical technique to ensure more precise placement.

For the first time in five decades, diabetic retinopathy is not the commonest cause of visual impairment in the working age population. Instead, inherited eye diseases, particularly outer retinal degenerations such as Stargardt disease and Retinitis Pigmentosa, are the commonest causes of visual loss in this age group.[244] Although this thesis has focussed on AMD, it is feasible that RPE transplantation, with or without

photoreceptor transplantation, may have a role in the treatment of these inherited retinal degenerations.

For inherited retinal degenerations, the use of CRISPR/Cas9 technology could allow targeted genome editing, thereby allowing the transplantation of iPS cells, with all of the advantages that this brings, including the lack of an immune response, yet elegantly avoids the pitfall of transplanting cells with genetic abnormalities.

The polymer evaluated in this thesis holds considerable promise in its current state, yet modification to the polymer may enhance its potential. A variation of the composition of the polymer, which makes the polymer stronger and robust, is currently under evaluation. The size of the polymer sheet transplanted determines the area of photoreceptor rescue but larger sheets require wider incisions that in turn confer greater surgical risk. An alternative is for multiple small polymer sheets to provide a sufficient area of photoreceptor rescue to preserve central visual field. However, it is much more difficult to manipulate multiple small polymer segments in the subretinal space than a single large sheet. A recent video shown by the RIKEN group at ARVO 2016 showed that transplantation of a small RPE cell sheet without an underlying scaffold, while potentially successful in an *in vitro* setting, results in a delicate and extremely mobile tissue which can easily flip upside-down during insertion into the subretinal space.

Our reliance on the 60:40 P(MMA-co-PEGM-succinimidyl carbonate) co-polymer was based on experiments conducted by Andrew Treharne, a previous PhD student in Chemistry, well before I joined the research group. Based on a series of sequential experiments over many years, our laboratory has pursued the most promising line at each stage. However it is possible that with the advances in 3D printing technology in recent years, the approach to an ideal artificial BrM may be completely different. With current technology, it may even be feasible to print a pentilaminar structure, made of exactly the same acellular materials as juvenile human BrM. This would completely avoid the need for an

Further potential modifications of the polymer include the use of drug-elution technology. The slow release of a low-dose immunosuppressant could prevent cell rejection and reduce the risk of macular oedema and other inflammatory complications of surgery.

RPE transplantation is most likely to be effective in eyes that have abnormal RPE but relative normal photoreceptors. The identification of suitable candidates for this therapy is crucial, and is likely to rely on further advances in imaging including autofluorescence and adaptive optics.

Much will be learnt from the patients undergoing treatment in the London Project to Cure Blindness, which uses ESC-derived RPE on a scaffold, and the RIKEN trial of iPS-derived RPE without the use of a scaffold. The difference in immune response will be helpful in determining the importance of iPSC technology over ESC or HLA-matched RPE tissue banks. Even if a florid immune reaction is avoided, it is still possible that the cells will be under attack from microglial cells within the retina. This entire thesis is based on the premise that RPE transplantation is unsuccessful unless a cellular scaffold is used as an artificial BrM, yet the RIKEN trial does not use a scaffold. Observations and findings in these patients will be helpful at determining where the focus of laboratory research into RPE transplantation should be for the coming years.

- - -

Appendix

Reprint of:

Alexander P, Thomson HA, Luff AJ, Lotery AJ.

Retinal pigment epithelium transplantation: concepts, challenges, and future prospects.

Eye (Lond) 2015 Aug;29(8):992-1002. doi: 10.1038/eye.2015.89.
Epub 2015 Jun 5.

Eye (2015), 1–11

www.nature.com/eye

REVIEW

Retinal pigment epithelium transplantation: concepts, challenges, and future prospects

P Alexander, HAJ Thomson, AJ Luff and AJ Lotery

Abstract

The retinal pigment epithelium (RPE) is a single layer of cells that supports the light-sensitive photoreceptor cells that are essential for retinal function. Age-related macular degeneration (AMD) is a leading cause of visual impairment, and the primary pathogenic mechanism is thought to arise in the RPE layer. RPE cell structure and function are well understood, the cells are readily sustainable in laboratory culture and, unlike other cell types within the retina, RPE cells do not require synaptic connections to perform their role. These factors, together with the relative ease of outer retinal imaging, make RPE cells an attractive target for cell transplantation compared with other cell types in the retina or central nervous system. Seminal experiments in rats with an inherited RPE dystrophy have demonstrated that RPE transplantation can prevent photoreceptor loss and maintain visual function. This review provides an update on the progress made so far on RPE transplantation in human eyes, outlines potential sources of donor cells, and describes the technical and surgical challenges faced by the transplanting surgeon. Recent advances in the understanding of pluripotent stem cells, combined with novel surgical instrumentation, hold considerable promise, and support the concept of RPE transplantation as a regenerative strategy in AMD.

Eye advance online publication, 5 June 2015; doi:10.1038/eye.2015.89

Introduction

Age-related macular degeneration (AMD) is the leading cause of visual impairment in the developed world.[1] The prevalence increases with age and AMD affects up to one third of those aged over 75 years.[2] Recent advances in anti-Vascular Endothelial Growth Factor (anti-VEGF) therapy for AMD have revolutionised the management of neovascular AMD (nvAMD).[3,4] However, initial enthusiasm for this therapy has been dampened by the realisation that up to one fifth of patients treated for nvAMD will develop geographic atrophy,[5] resulting in visual impairment due to loss of photoreceptor cells. Therefore, therapy to combat the development of dry AMD as well as nvAMD is needed.

At present there is no effective treatment for dry AMD, which is the more prevalent form of the disease.[6] As the primary pathogenic process in AMD appears to occur within the complex of the retinal pigment epithelium (RPE), Bruch's Membrane (BrM), and choriocapillaris, a logical approach would be to repair the RPE via either transplantation or translocation of RPE cells.

The RPE consists of a monolayer of highly specialised cuboidal cells that lie between BrM and the outer neurosensory retina (see Figure 1). When viewed from above the cells appear hexagonal, and are joined together by tight junctions (zonulae occludentes), which block the free passage of ions and water. The RPE is therefore the second site of the blood retinal barrier, the first site being the capillary endothelium of the retinal vessels. The most important function of the RPE is the regeneration of bleached opsins, which occurs in the RPE cell cytosol. The RPE has a number of other essential roles including phagocytosis, transepithelial transport, secretion of growth factors, absorption of light, and protection against photo-oxidation.[7]

The polarity of the RPE cell is essential for ion transport. The intercellular tight junctions establish a strong barrier between the subretinal space and the choroid, such that paracellular resistance is 10 times higher than transcellular resistance.[8,9] The high metabolic activity of the photoreceptors leads to the generation of a large amount of water and the intraocular pressure

Clinical Neurosciences Research Group, Clinical and Experimental Sciences, Faculty of Medicine, University of Southampton, University Hospital Southampton, Southampton, UK

Correspondence: Professor AJ Lotery, Professor of Ophthalmology, Director Clinical Neurosciences Research Group, Clinical Neurosciences Research Group, Clinical and Experimental Sciences, Faculty of Medicine, University of Southampton, South Lab and Path Block, Mailpoint 806, Level D, University Hospital Southampton, Southampton SO16 6YD, UK
Tel: +44 (0)23 8120 5049; Fax: +44 (0)709 212 5081.
E-mail: a.j.lotery@soton.ac.uk

Received: 10 November 2014
Accepted in revised form: 14 April 2015

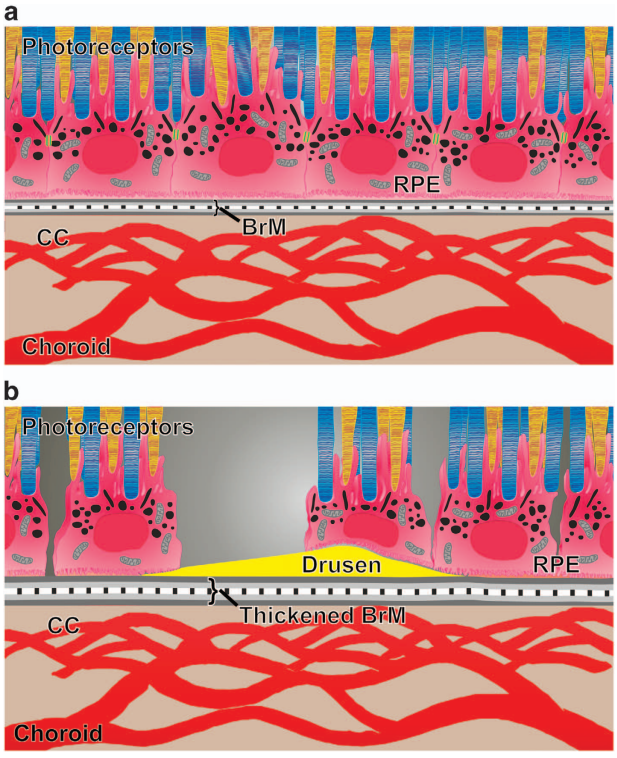

Figure 1 (a) Healthy RPE: healthy RPE exists as a polarised monolayer with tight junctions (green). Melanin is located in the apical cytoplasm and acts to absorb scattered light, thereby improving the optical quality of the eye. Microvilli on the apical RPE membrane interdigitate with the photoreceptors (rods shown in blue; cones shown in yellow). Microvilli allow phagocytosis of the shed photoreceptor outer segments and recycling of the visual pigments. The tight junctions ensure that the RPE can maintain its function as the outer blood retinal barrier. Bruch's membrane (BrM) is a pentilaminar structure; the innermost layer of BrM is formed by the basement membrane of the RPE. The outer layer of BrM is formed by the basement membrane of the choriocapillaris (CC). Breaches of BrM lead to growth of choroidal vessels into the sub-RPE and subretinal space, known as choroidal neovascularisation. (b) RPE degeneration in AMD: BrM is thickened, impairing diffusion between the choriocapillaris and the neurosensory retina. Drusen are clinically visible deposits that occur beneath the RPE. RPE cell death occurs, and there is loss of tight junctions between the remaining RPE cells, resulting in a discontinuous cell layer. These changes all lead to secondary photoreceptor cell loss, resulting in visual impairment.

causes a net flow of water through the retina from the vitreous.[7] By transporting ions and water from its apical side to its basolateral surface, the RPE cell ensures the removal of water from the subretinal space but also establishes an adhesive force between the retina and the RPE.[7]

When considering the RPE as a layer, rather than individual cells, it is evident that the ability to perform its many functions is reliant on two factors. First, the RPE layer must be a confluent monolayer, with intercellular tight junctions. Second, the cells must be polarised. Both of these factors are therefore reliant on the RPE basement membrane, which itself forms the innermost layer of BrM, an acellular structure first described in 1844 but characterised in detail in 1961 by Hogan.[10] BrM has five distinct layers: RPE basement membrane; inner collagenous layer; elastin layer; outer collagenous layer; and the basement membrane of the choriocapillaris. BrM has three main functions: to regulate diffusion between RPE and choroid; to provide physical support for RPE adhesion, migration and, possibly, differentiation; and to create a barrier between retina and choroid, thereby preventing cellular migration from one tissue to the other. During the development of RPE transplantation techniques, the importance of BrM has perhaps been overlooked, which may account for the limited success thus far.

RPE transplantation

Human RPE cells were first isolated and characterised over 30 years ago.[11–13] RPE cell structure and function are well understood, the cells are readily sustainable in culture under laboratory conditions, and unlike other cell types within the retina, RPE cells do not require synaptic connections to perform their role. These factors, together with the relative ease of imaging with ophthalmoscopy and optical coherence tomography (OCT) scanning, make RPE cells an attractive target for cell transplantation compared with other cell types in the retina or central nervous system. Compared with other forms of cell replacement therapy, the number of cells required for a given lesion site is relatively small.[14] RPE replacement would prevent secondary photoreceptor degeneration, thereby preserving visual function.

Seminal experiments by Li and Turner[15] used the Royal College of Surgeons (RCS) rat, an animal model of retinal dystrophy, to demonstrate proof of principle of RPE transplantation. The inherited retinal degeneration within the RCS rat was first discovered in 1938 but it was only in 1962 that Dowling and Sidman[16] discovered an accumulation of outer segments on electron microscopy, suggesting abnormal phagocytosis by the RPE. In 2000, D'Cruz *et al*[17] discovered that the RCS strain had a defect in the *merTK* gene and is therefore unable to produce RPE cells that phagocytose shed rod outer segments; this results in photoreceptor death and degeneration of the neurosensory retina within 2 months. However, Li and Turner[15] demonstrated that subretinal injection of healthy RPE cells allows preservation of the outer nuclear, outer plexiform, and photoreceptor layers. Since then, successful RPE transplantation has also been demonstrated in RPE65 knockout mice that are unable to isomerise all-*trans*-retinal to 11-*cis*-retinal.[18]

Surgical strategies to allow RPE transplantation in humans arose primarily from the absence of effective treatments for nvAMD prior to the development of

anti-VEGF intravitreal injections. Submacular surgery aimed to remove the subfoveal choroidal neovascular membrane (CNV) and any associated haemorrhage, and the first randomised controlled trial to evaluate this technique, the Submacular Surgery Trial, was initiated in 1998. However the visual outcomes were poor and this disappointing result was attributed to mechanical removal of the RPE at the time of CNV excision.[19] Since then, three approaches to RPE transplantation have been attempted:

- Macular translocation
- Autologous RPE-Choroid Patch graft
- Subretinal injection of a suspension of autologous RPE cells

Macular translocation

Macular translocation is a procedure in which the neurosensory retina is surgically detached, rotated, and reattached so that the macula, and in particular the fovea, is repositioned from an area of diseased RPE to an area of healthy RPE.[20] Therefore, although the RPE itself is not moved, macular translocation surgery can be regarded as a functional RPE transplantation. This procedure can confer long-term visual stability, and in a significant proportion of patients leads to an improvement in both visual acuity[21] and quality of life.[22] Of interest, in a series of seven patients undergoing macular translocation for nonexudative AMD, new geographic atrophy was reported in the new subfoveal RPE of one patient.[23] All patients undergoing macular translocation require further surgery to reposition extraocular muscles to prevent intractable torsional diplopia and the large retinotomies can have significant complications including retinal detachment, proliferative vitreoretinopathy (PVR), macular pucker, and macular hole.[21] Owing to the high rate of complications, macular translocation surgery has been abandoned by clinicians.

Autologous RPE-choroid patch graft

Numerous investigators have attempted autologous RPE sheet transplantation, with the aim of using healthy peripheral RPE, on a bed of BrM and partial thickness choroid, and moving the multilayered patch graft to the submacular space. Peyman *et al* were the first to describe this technique, and report two patients who underwent vitrectomy and CNV excision, combined with RPE transplantation. Visual acuity improved in the patient that received an autologous pedicle RPE graft, while the patient that received RPE and BrM transplant from an enucleated donor eye did not improve.[24] Stanga *et al* operated on six patients, and performed vitrectomy and CNV excision with translocation of RPE/BrM from the paramacular area to the subfoveal space. Using a small retinotomy, they fashioned a free RPE/choroid graft in five patients and a pedicled RPE/choroid graft in one patient, followed by air fluid exchange, and face down posturing. Four of the six patients could detect a fixation target projected onto the fovea overlying the translocated RPE, although none of the patients showed any improvement in visual acuity. Three out of six patients experienced significant complications, including subretinal bleeding, PVR-related total retinal detachment, and insertion of an upside-down RPE graft.[25] Later studies used grafts from the mid peripheral retina, rather than from the edge of the macular RPE defect.

Van Meurs *et al* also used an internal approach in six patients undergoing subfoveal CNV excision with transplantation of a full thickness patch of RPE and choroid from under the peripheral retina, to the subfoveal space, to cover the excision site.[26] Four of the six patients showed improvement in visual acuity but this technique still carries with it a significant risk of intraocular haemorrhage, retinal detachment, and PVR. Van Meurs' group recently published the long-term outcomes of 133 patients who underwent CNV excision followed by autologous RPE-Choroid grafting. The postoperative PVR rate in this cohort was 10%. The visual acuity outcomes overall were modest but four years after surgery, 5% of patients had Best Corrected Visual Acuity [BCVA] better than 20/40.[27]

Submacular injection of RPE cell suspension

In a series of 14 eyes, Binder *et al* performed pars plana vitrectomy, and created a retinotomy nasal to the optic disc to allow formation of a subretinal bleb. Using a blunt instrument, RPE cells from this area were mobilised, aspirated into a micropipette, and then transplanted over an RPE defect in the macula,[28] but the dissociated RPE cells were unable to attach to the damaged BrM under the fovea. However, RPE cells from the extramacular site in the peripheral retina were able to restore RPE continuity, because of their ability to divide and adhere to undamaged BrM. This observation suggests that it is the damaged host BrM that is the limiting factor for adherence of isolated cells, and not the age of the RPE donor cells. Furthermore, *in vitro* studies have shown that embryonic RPE cells can adhere to normal, but not aged, BrM from post-mortem specimens.[29] These age-related changes in BrM also represent one of the critical differences between human subjects and laboratory animals in which many of the successes of RPE transplantation experiments have been reported, because the latter are generally young and have a healthy BrM.[15,30,31]

The inference from these findings is that successful RPE transplantation for AMD must take replacement of BrM into consideration.[32]

Surgical challenges to RPE transplantation

In his editorial, Gouras and Lopez[33] noted that the greatest challenge in human RPE cell transplantation lies in the microsurgical technology to enable subretinal surgery. This review will evaluate the challenges facing by the vitreoretinal surgeon and will address four main areas:

- Choice of approach: external (transchoroidal) *vs* internal (transvitreal)
- Sources of donor RPE cells
- Types of surgical instrumentation
- Prevention and control of PVR and recurrent retinal detachment

Surgical approach: external *vs* internal

The first description of RPE transplantation was by Gouras *et al*, who transplanted cultured ^{3}H thymidine-labelled human RPE cells on to denuded BrM in owl monkeys.[34] The investigators used an open-sky technique: the cornea was removed, and the globe was open for the duration of the procedure. As a result, the investigators experienced difficulties reattaching the neurosensory retina.[34] Following modification of the technique to a closed-eye method, consisting of pars plana vitrectomy, retinotomy, and delivery of cells through a pipette, early spontaneous retinal reattachment was achieved.[35] In both of these studies, donor RPE cells successfully attached to BrM and some phagocytosis of photoreceptor outer segments could be demonstrated. Following this, a number of investigators have continued to use an internal transvitreal approach, involving pars plana vitrectomy, whereas others favour an external approach involving dissection of posterior sclera and transsclerochoroidal subretinal injection of RPE cells. The external approach was first described in the human eye in 1975 by Peyman *et al*,[36] who performed a scleral–chorioretinal biopsy in a patient with suspected malignant melanoma. Choroidal haemorrhage was avoided by extensive diathermy but moderate vitreous loss occurred through the wound. This technique was subsequently adapted for RPE collecting in pigs[37] and rabbits.[38] However, several investigators have utilised an internal approach in humans, consisting of pars plana vitrectomy, surgical excision of subfoveal CNV, followed by translocation of dissociated RPE cells[28] or an RPE/BrM/choroid graft,[24–26] either free or pedicled.

The external approach is preferable in animal studies, especially in rodents, where the globe is small, the lens is large, and there is no true vitreous cavity to operate within (see Figure 2).[39] However this technique not only requires rupture of BrM but also causes choroidal trauma, leading to the risk of severe intraocular or suprachoroidal haemorrhage, and may possibly lead to inflammation and immune responses that would not occur with the transvitreal approach. In larger eyes, the internal surgical approach is considerably easier. Wongpichedchai *et al*[38] compared the external *vs* internal approaches in rabbits, and noted that although similar results were achieved, access to the posterior pole using the external approach was difficult, and required disinsertion of a rectus muscle. In contrast, pars plana vitrectomy is a commonly performed procedure in the developed world, with an estimated 100 000 procedures performed in the USA each year,[40] and around 20 000 in the UK.[41] Therefore, the internal approach may be more appropriate for the human eye, allowing use of existing surgical skills, experience and instrumentation.

Sources of cells

Although the aim of cell transplantation is to restore RPE function and prevent photoreceptor loss, the transplanted cells do not necessarily need to be RPE cells. Subretinal injection of iris pigment epithelial (IPE) cells,[42] Schwann cells,[43] human central nervous system stem cells,[44] and umbilical cord cells[45] all facilitate photoreceptor rescue in the RCS rat. Transplanted cells may be primary cells that have been collected immediately before transplantation, or can instead be cultured *in vitro* prior to transplantation. Alternatively, a transformed RPE cell line such as ARPE-19 or h1RPE-7 can be used, although these tend to be utilised only for experimental purposes because of the risk of teratoma formation *in vivo*. From the point of view of the transplanting surgeon, the original source of the cell is not as important as the technical aspects of collecting and delivery. Therefore, many types of cell sources can be used to produce a pure cell culture *in vitro*, but to the vitreoretinal surgeon what is more pertinent is whether the cells are to be transplanted as a cell sheet or as a suspension. From the surgical point of view, cell sources can be divided into three types:

- Autologous RPE cells (discussed in the previous section)
- Autologous IPE cells
- *In vitro* cultured allogenic cells

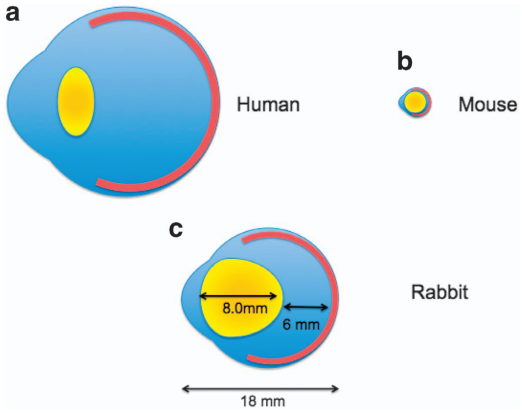

Figure 2 (a-c): Schematic diagrams of (a) human eye (b) mouse eye and (c) rabbit eye (shown to scale). Retinal surgery in the human eye is facilitated by the large vitreous cavity. Following surgical pars plana vitrectomy, a subretinal bleb can be created with a 41-gauge cannula, to create a space for the transplanted RPE. The mouse eye (b) is an unsuitable experimental model not only because the eye is so small (axial length approx. 3 mm) but also because the lens is large and spherical and occupies most of the space within the globe. The vitreous cavity in the mouse eye is small and an epiretinal approach to RPE transplantation following pars plana vitrectomy is impossible. In contrast, the rabbit eye (c) is only slightly smaller than a human adult eye, and there is sufficient space within the vitreous cavity to allow pars plana vitrectomy and induction of a subretinal bleb. While the rabbit lens is larger than a human lens, intraoperative lens touch can be avoided with careful surgery. The rabbit eye is therefore an excellent model for RPE transplantation techniques.

Autologous IPE cells

IPE cells are a source for autologous cell transplantation because they are similar to RPE cells but are much easier to collect.[46] Surgical iridectomy is a relatively straightforward procedure and iridectomy specimens have been successfully used to produce dissociated IPE cells that can be propagated in culture.[47]

RPE and IPE cells are derived from the same embryonic cell line, and both cell types have apical/basal polarisation, microvilli, and tight junctions that serve as a barrier to regulate the passage of ions and small molecules and to restrict diffusion of membrane lipids and proteins. Importantly, RPE and IPE tight junctions are morphologically similar. IPE cells can survive for up to 20 weeks in the subretinal space of rabbits[48,49] and *in vivo* phagocytosis of photoreceptor outer segments of RCS rats has also been demonstrated.[50]

Gene expression in IPE cells differs from that of RPE cells. Gene expression for intra- and extracellular retinal binding proteins, which are essential for metabolism of the visual pigments, is lower in IPE cells than RPE cells.[51] *In vitro*, IPE cells are able to phagocytose photoreceptor outer segments but are less able to degrade them compared with RPE cells.[52] The level of expression of mRNA of VEGF is also lower in IPE cells than in RPE cells,[53] but it has been suggested that this may in fact make IPE cells more suitable than RPE cells for subretinal transplantation, especially in cases of exudative AMD where presence of VEGF can stimulate recurrence of CNV.[46] It is not know to what degree IPE cells acquire RPE properties when transplanted into the subretinal space in patients with AMD. However, Abe *et al* report 56 AMD patients who underwent pars plana, vitrectomy, CNV excision, IPE transplantation into the subretinal space, and gas tamponade. Despite an initial deterioration in visual acuity, there was a long-term logMAR visual acuity improvement, with at least 2 years follow-up in all patients (1.26 *vs* 1.48, $P=0.02$). Four of the 56 developed surgical complications including rhegmatogenous retinal detachment (three patients) and vasculitis (one patient).[46]

Ex vivo cell sheet expansion prior to transplantation

For nonautologous transplants, donor RPE cells can be removed from an enucleated eye cup either by using trypsin digestion for the collection of a cell suspension, or alternatively, dispase can be used to separate the basement membrane from the RPE monolayer, thereby allowing harvest of an intact RPE cell sheet.[20] Authors who have utilised foetal human RPE cells have cultured the cells *in vitro* prior to surgical injection. Gouras *et al*[54] excised a 0.6-mm RPE monolayer patch from foetal human RPE cells cultured *in vitro*, and by aspiration into a glass pipette were able to deliver the patch into the subretinal space. Primary cell cultures have a limited lifespan because after a number of population doublings (known as the Hayflick limit), cells undergo senescence and stop dividing. This is beneficial because while the cells retain viability there is very little risk of non-regulated growth.[55]

Transformed RPE cells can be defined as cell lines that have either spontaneously or deliberately acquired genetic modifications that lead to a state of unregulated growth. They are useful in cell culture because they show long-term stability *in vitro*. RPE cell transformations can occur spontaneously, such as with the ARPE19 and the D407 cell lines,[56,57] but may also be genetically engineered for example, H1RPE7.[58] RPE cells can also be genetically modified to alter some other aspect of their behaviour, so that they either express a marker (eg. Green Fluorescent Protein (GFP)-labelled RPE) or modify gene expression. However, after repeated passage it has been established that these adult human cell lines can dedifferentiate and lose their morphology and RPE gene expression, and express neuronal cell markers instead.[59,60]

Pluripotent stem cells

The use of stem cell technology holds promise as a novel source of cells for transplantation in AMD and other degenerative diseases. Stem cells are able to self-renew indefinitely, while maintaining a stable undifferentiated state, but are pluripotent and can, therefore, differentiate into any cell type in the body (except into placental cells).[61] Human embryonic stem cells (hESCs) can be isolated from the inner cell mass of the human blastocyst at approximately five days post fertilisation. These cells can then be maintained indefinitely under defined conditions *in vitro*, as pluripotent cells, and, when required, can be differentiated into RPE cells.[62] Using hESC-derived RPE, Lu *et al* have demonstrated photoreceptor rescue and sustained cell function in the RCS rat. The first use of hESC-derived RPE cells in human patients was described by Schwartz *et al*, in one patient with Stargardt's macular dystrophy and another with dry AMD.[63] Initial results show no significant improvement in visual function, but do suggest a good safety profile. The use of hESC for RPE transplantation not only entails ethical obstacles, but also carries a risk of immune rejection, especially, as surgical trauma is likely to compromise the blood retinal barrier and the immune privilege status of the subretinal space.

The difficulties associated with hESC can be overcome with the use of induced pluripotent stem cells (iPSCs). This technology was first described in 2006 by Yamanaka, who was awarded the 2012 Nobel Prize for his work.[64] This technique uses viral vectors to insert four key genes into the DNA of any mature somatic cell, which then causes reprogramming of the cell into a stem cell capable of producing any cell lineage of the three germ layers.

The intrinsic attraction of iPSC technology is not only the avoidance of the ethical issues of using embryonic cells, but also that iPSC-derived cell transplantation would obviate the need for continual immunosuppression. In a model scenario, tissue would be obtained from a somatic cell of the patient with AMD, the cells would be reprogrammed to a pluripotent state, and then differentiated into RPE cells and expanded *in vitro*, prior to transplantation. Autologous transplantation of iPS-derived RPE cells, without any artificial scaffold, into a nonhuman primate showed no immune rejection or tumour formation. However, the immunogenicity of iPSC has not been well studied and while they certainly have an advantage over ESC, there is some evidence that iPSC derivatives can induce T-cell-dependent immune responses even in genetically identical organisms.[65]

Rather than simply being used as a regenerative source, the use of iPSCs in combination with gene therapy may enrich their therapeutic potential. Autologous iPSCs could be screened for common genetic mutations that could then be corrected *in vitro* by gene therapy. Cells would then be differentiated into RPE cells before surgical transplantation. Assuming that sufficient photoreceptors remained functionally intact, this could allow a disease-free phenotype to be maintained, but this tandem technique relies on complete elimination of any diseased host cells prior to transplantation.[66]

A significant concern associated with the use of iPSC technology is the risk of tumorigenicity. The four key genes used by Yamanaka all code for transcription factors: c-Myc, Sox2, Oct4, and Klf4. Of these, c-Myc is known to be an oncogene and the remaining factors have been implicated in tumorigenicity. Yu *et al* have demonstrated that a different combination of transcription factors—Oct4, Sox2, Lin28, and Nanog—can also induce pluripotency in human somatic cells, but Nanog is also known to be expressed in some tumours, and can promote breast cancer tumorigenesis and metastasis.[67] The iPSC technology uses viral DNA that could incorporate itself into the genome of the somatic cell and potentially cause harm. However, an approach that uses nonintegrating adenoviruses, could avert the cancer risks of iPSCs, and no tumours have been observed in mice derived from integration-free iPSCs up to 20 weeks of age.[68] However, exclusion of these oncogenic factors has a significant and detrimental effect on reprogramming efficiency and it is unknown whether reprogramming itself may lead to tumorigenesis.[69,70]

In 2014, Obokata reported that strong external stimuli, such as a transient low-pH stressor, can generate pluripotent stem cells without the need for transcription factor integration into the genome, has generated much excitement and controversy. This cellular reprogramming, known as stimulus-triggered acquisition of pluripotency (STAP), has not been reproduced despite fervent attempts by several other groups[71,72] and the original paper has since been retracted.[73] The observation by the original authors that STAP cell technology only seems to work on freshly collected cells from the early postnatal period suggests that this technology, even if reproducible, is unlikely to be of major benefit, and would certainly preclude its use for patients with AMD.

Surgical instrumentation

Removing residual RPE

A number of investigators have used animal models to determine the effects of removing the residual RPE prior to transplantation. Lopez *et al* used a diamond dusted needle but subsequent histological examination revealed numerous inadvertent breaks in BrM, resulting in cellular proliferation from the choroid into the subretinal space.[35]

This group therefore reverted to removing host RPE with the force of the subretinal fluid injection. However, this is also not ideal because the RPE is not removed, it simply remains attached to the underside of the neurosensory retina, thereby creating a different plane of separation. Following transplantation the host RPE lies between the transplanted cells and the photoreceptors.

Wongpichedchai *et al* used 100 μl of 0.02% ethylenediaminetetraacetic acid (EDTA) to create subretinal blebs in rabbits. The EDTA was then aspirated, bringing RPE cells with it. These cells were of sufficient number to achieve *in vitro* culture.[38]

Stanzel *et al* have recently reported use of a 0.1 mm prolene loop to facilitate RPE removal. In a rabbit model, an area of 2.5 mm × 1.5 mm was treated with a single forward and backward stroke. This area was later found to be 70% devoid of RPE cells, although a few miniscule BrM lacerations and choriocapillaris blood clots also occurred. A thinner, more flexible prolene loop was less effective, as was a 0.1 mm metal wire, which also caused intraoperative subretinal haemorrhage.[74]

Delivery of an RPE cell suspension

In their seminal experiments with the RCS rat, Li and Turner used a blunt needle to deliver a suspension of RPE cells into the subretinal space, via a transsclerochoroidal route.[15] Lopez *et al* performed surgery in rabbits and were able to pass a glass cannula with an internal diameter of 100 μm through the pars plana, and then create a small subretinal bleb via a retinotomy.[35] The diameter of their glass cannula is similar to that of a 41-gauge needle, which is now used widely for formation of a localised retinal detachment during vitrectomy.

Similar to the methods of Lopez *et al*, Gouras and coauthors used a glass cannula to deliver RPE cells into the subretinal space in patients with dry AMD.[54] They used the cannula to deliver either a cell suspension, or to deliver a patch transplant of cultured human foetal RPE. Although their attempts to inject an RPE cell suspension were largely successful, they were dissatisfied with the subretinal patch graft technique. The 0.6-mm diameter circular graft would fold in the subretinal space, and on histological examination the outer nuclear layer tended to be thinner over the folded RPE graft than when the photoreceptors were adjacent to a single (unfolded) RPE layer. Gouras *et al* did not use a BrM substitute and were simply cutting a circular patch of an RPE monolayer grown in tissue culture. The use of a BrM substitute would not only improve the chances of preventing photoreceptor degeneration but has the added advantage of providing some stability and rigidity to the graft.

Wongpichedchai compared internal and external approaches of RPE transplantation in rabbits, and identified differing challenges. For the external approach disinsertion of a rectus muscle was necessary to access the posterior pole. For the internal approach, a micropipette with an internal diameter of just 60 μm, drawn from glass, was used to induce a subretinal bleb. The micropipette was advanced vertically through the pars plana incision, to avoid trauma to the large crystalline lens in the rabbit eye. To ensure precise placement of the tip, and controlled injection of the RPE cell suspension, an electronic injection microsyringe manipulator was utilised. This ensured that at the point of the retinotomy, the cells were injected no more than 200 μm deep to the inner retinal surface, and were injected at a constant controlled rate.[38] Similarly, Weichel used a manual oil-hydraulic microinjection pump to achieve controlled subretinal infusions of RPE cells.[75]

Delivery of a patch graft

Maaijwee *et al*[76] have done considerable work investigating different types of instrumentation for use with grafts of RPE-BrM-partial thickness choroid. The group compared traditional grasping forceps with an aspiration-reflux cannula manufactured by DORC, similar in design to the instrument utilised by Thumann *et al*, but found that the main difficulty with both methods was ensuring release of the graft once the tip of the instrument was in the subretinal space. To combat the friction between the graft and the carrier platform of the aspiration-reflux instrument, Maaijwee performed several laboratory experiments demonstrating that the ability to make the instrument vibrate, utilising either the linear motor of a loudspeaker, or the vibration function of a mobile phone, would allow successful dislodgement of the graft. These techniques are yet to be used in clinical or surgical practice. The same group have investigated the use of a microscale thermal tissue gripper which utilises heat induced attachment and detachment of the graft.[77] Using chicken meat for experimental purposes, a greater than 90% success rate for graft attachment/detachment was observed. Owing to the small contact area of the instrument with the tissue, visible tissue damage was limited to only 0.005 mm^2.

Thumann *et al* used a custom-made device to deliver an RPE cell sheet.[42] The device consists of a perforated carrier platform, attached to a syringe which exerts a vacuum on the under surface of the graft, thereby preventing it from becoming dislodged. The platform is then covered by a second cannula, protecting the RPE cells from damage or dislodgement when introduced into the eye. Once the instrument tip was in the subretinal space, the second cannula was pulled back and a small amount of pressure was placed on the syringe plunger, allowing release of the graft. A modified version of the instrument had a tip angled at 45 degrees to allow easy

access to the subretinal space. Thumann *et al* were able to ensure consistent delivery of the cell sheet, without rolling or folding, and simply used micro tweezers to ensure satisfactory positioning.[42]

Stanzel *et al* have described a custom-made implant shooter instrument to deliver polyester membrane inserts, some of which were gelatin covered, to facilitate implant loading and delivery. The investigators performed pars plana vitrectomy and induced a subretinal bleb with a 41-gauge needle, and utilised a novel infusion cannula with two side ports, to reduce the stream of fluid over the subretinal bleb, thereby avoiding collapse of the bleb or uncontrolled tearing of the retinotomy.[78] Despite elegant demonstration of delivery into the appropriate anatomical space, implantation of polyester implants without RPE cells resulted in development of a multilayered fibrocellular scar tissue, and almost complete atrophy of photoreceptors overlying the implant, with evidence of intraretinal cyst formation on OCT scanning. This may have occurred because of the mechanical separation of photoreceptors from the RPE by the implant. Similar atrophic changes have been observed after subretinal implantation of artificial retina chips and it was hypothesised that a more permeable carrier may result in a better preserved outer retinal architecture.[78] Implantation into rabbit eyes of the polyester carrier with RPE derived from human embryonic stem cells resulted in 95% survival at four weeks.[79]

Prevention and control of PVR

PVR is an inflammatory and fibrotic process that occurs in patients with retinal holes or tears. It is caused by the migration and proliferation of RPE cells, and RPE cells have been identified in formed PVR membranes.[80] The prospect of an iatrogenic, albeit localised, retinal detachment by creation of a retinotomy, followed by insertion of donor RPE cells on a scaffold, possibly preceded by debridement of the existing RPE, is likely to allow significant RPE migration into the vitreous cavity and subsequently on to the surface of the retina, leading to PVR membrane formation and contraction. PVR over the macula causes preretinal membrane formation. Contraction of this membrane can lead to visual distortion and visual loss. PVR over the peripheral retina can cause retinal traction and subsequent retinal detachment. At around 10%, the rate of PVR development is similar for patients undergoing injection of a subretinal RPE cell suspension[81] and patients receiving an RPE-choroid graft from within the macular area.[25] Harvesting a peripheral RPE-choroid graft seems to produce a slightly higher rate of PVR and potential reasons for this include release of RPE cells during peripheral harvesting, traumatic enlargement of the macular retinotomy for graft insertion, or continued release of RPE postoperatively from the bed of the donor site.[82] There is no demonstrable difference in PVR rate between superior and inferior donor sites, suggesting that there is no advantage from attempting to avoid the inflammatory aqueous milieu in the inferior retina that may not be in direct contact with tamponade.[82]

Although some authors report the use of pharmacological agents to prevent PVR development, none of these is used in routine clinical practice. The use of silicone oil as an intraocular tamponade has been well described in the prevention and control of PVR,[83] although a recent Cochrane review could find no major difference between silicone oil and C_3F_8 gas tamponade.[84]

Future prospects

There are a number of clinical trials already underway to evaluate the safety and efficacy of RPE cell transplantation for patients with AMD or other retinal degenerative disorders. Only one trial will use RPE cells derived from iPSC, and all other trials will use RPE cells that have been derived from hESCs. In addition to the challenges already described earlier, cells for transplantation need to meet strict standards of quality, quantity, consistency and safety, which in the UK are governed by the Good Manufacturing Practice (GMP) standard.

Ocata Therapeutics, formerly named Advanced Cell Technology, is a biotechnology company that provides ESC-derived RPE and is the sponsor of three separate Phase I/IIa trials to evaluate safety and tolerability of subretinal RPE transplantation in patients with one of three diseases: Advanced Dry AMD, Stargardt's Macular Dystrophy, and Myopic Macular Degeneration. In each of these trials, the study patients will undergo vitrectomy followed by subretinal injection of a cell suspension of RPE cells derived from ESC. The Advanced Dry AMD trial (ClinicalTrials.gov Identifier: NCT01344993) has recently reported its early findings. It recruited nine patients with dry AMD, and had three cohorts, each with three patients. Each cohort received a different number of transplanted RPE cells (50 000, 100 000 or 150 000). Of note, this trial did not attempt to replace BrM, nor does it deliver the transplanted RPE cells into the subretinal space as a polarised monolayer. This is only a safety/tolerability study, yet six of the nine patients showed a visual acuity improvement of at least 11 letters. The usefulness of RPE transplantation in patients in patients who already have poor vision owing to secondary photoreceptor atrophy is unclear. It is hoped that the subsequent Phase III trial will yield valuable information.

The London Project to Cure Blindness (ClinicalTrials.gov Identifier: NCT01691261) aims to utilise human ESC to derive RPE cell sheets, rather than a cell suspension. This cell sheet will be supported by an engineered scaffold, to assist delivery and survival in the subretinal space of patients with recent rapid visual decline.

Masayo Takahashi leads the Laboratory for Retinal Regeneration at the Riken Institute in Japan, which has generated human iPS-derived RPE cell sheets without the use of any artificial scaffolds. A study of transplantation of a 1.3 mm × 3 mm RPE cell sheet in human subjects with exudative age-related macular degeneration (JPRN-UMIN000011929) is underway, with the first patient receiving transplantation in September 2014. This study is of great interest not only because of the decision to avoid using an artificial scaffold to support the RPE cells, but also because this is the first ever human clinical trial to use iPS-derived cells. The outcomes of this trial are anxiously awaited.

Conflict of interest

The authors declare no conflict of interest.

Acknowledgements

We are grateful to Dr Miguel Velazquez and Mr Alan Morris for their assistance with the illustrations in this article. We acknowledge funding support from the Brian Mercer Charitable Trust and the Global Ophthalmology Awards Program from Bayer.

References

1 Ambati J, Ambati BK, Yoo SH, Ianchulev S, Adamis AP. Age-related macular degeneration: etiology, pathogenesis, and therapeutic strategies. *Surv Ophthalmol* 2003; **48**(3): 257–293.
2 Zarbin MA. Current concepts in the pathogenesis of age-related macular degeneration. *Arch Ophthalmol* 2004; **122**(4): 598–614.
3 Rosenfeld PJ, Brown DM, Heier JS, Boyer DS, Kaiser PK, Chung CY *et al.* Ranibizumab for neovascular age-related macular degeneration. *N Eng J Med* 2006; **355**(14): 1419–1431.
4 Brown DM, Michels M, Kaiser PK, Heier JS, Sy JP, Ianchulev T. Ranibizumab versus verteporfin photodynamic therapy for neovascular age-related macular degeneration: Two-year results of the ANCHOR study. *Ophthalmology* 2009; **116**(1): 57–65 e55.
5 Grunwald JE, Daniel E, Huang J, Ying GS, Maguire MG, Toth CA *et al.* Risk of geographic atrophy in the comparison of age-related macular degeneration treatments trials. *Ophthalmology* 2014; **121**(1): 150–161.
6 Velez-Montoya R, Oliver SC, Olson JL, Fine SL, Mandava N, Quiroz-Mercado H. Current knowledge and trends in age-related macular degeneration: today's and future treatments. *Retina* 2013; **33**(8): 1487–1502.
7 Strauss O. The retinal pigment epithelium in visual function. *Physiol Rev* 2005; **85**(3): 845–881.
8 Miller SS, Steinberg RH. Active transport of ions across frog retinal pigment epithelium. *Exp Eye Res* 1977; **25**(3): 235–248.
9 Miller SS, Steinberg RH. Passive ionic properties of frog retinal pigment epithelium. *J Membr Biol* 1977; **36**(4): 337–372.
10 Hogan MJ. Ultrastructure of the choroid. Its role in the pathogenesis of chorioretinal disease. *Trans Pac Coast Otoophthalmol Soc Annu Meet* 1961; **42**: 61–87.
11 Flood MT, Gouras P, Kjeldbye H. Growth characteristics and ultrastructure of human retinal pigment epithelium in vitro. *Invest Ophthalmol Vis Sci* 1980; **19**(11): 1309–1320.
12 Boulton ME, Marshall J, Mellerio J. Human retinal pigment epithelial cells in tissue culture: a means of studying inherited retinal diseases. *Birth Defects Orig Artic Ser* 1982; **18**(6): 101–118.
13 Hu DN, Del Monte MA, Liu S, Maumenee IH. Morphology, phagocytosis, and vitamin A metabolism of cultured human retinal pigment epithelium. *Birth Defects Orig Artic Ser* 1982; **18**(6): 67–79.
14 Mason C, Dunnill P. Quantities of cells used for regenerative medicine and some implications for clinicians and bioprocessors. *Regen Med* 2009; **4**(2): 153–157.
15 Li LX, Turner JE. Inherited retinal dystrophy in the RCS rat: prevention of photoreceptor degeneration by pigment epithelial cell transplantation. *Exp Eye Res* 1988; **47**(6): 911–917.
16 Dowling JE, Sidman RL. Inherited retinal dystrophy in the rat. *J Cell Biol* 1962; **14**: 73–109.
17 D'Cruz PM, Yasumura D, Weir J, Matthes MT, Abderrahim H, LaVail MM *et al.* Mutation of the receptor tyrosine kinase gene Mertk in the retinal dystrophic RCS rat. *Hum Mol Genet* 2000; **9**(4): 645–651.
18 Gouras P, Kong J, Tsang SH. Retinal degeneration and RPE transplantation in Rpe65(-/-) mice. *Invest Ophthalmol Vis Sci* 2002; **43**(10): 3307–3311.
19 Hawkins BS, Bressler NM, Miskala PH, Bressler SB, Holekamp NM, Marsh MJ *et al.* Surgery for subfoveal choroidal neovascularization in age-related macular degeneration: ophthalmic findings: SST report no. 11. *Ophthalmology* 2004; **111**(11): 1967–1980.
20 da Cruz L, Chen FK, Ahmado A, Greenwood J, Coffey P. RPE transplantation and its role in retinal disease. *Prog Retin Eye Res* 2007; **26**(6): 598–635.
21 Chen FK, Patel PJ, Uppal GS, Tufail A, Coffey PJ, Da Cruz L. Long-term outcomes following full macular translocation surgery in neovascular age-related macular degeneration. *Br J Ophthalmol* 2010; **94**(10): 1337–1343.
22 Cahill MT, Stinnett SS, Banks AD, Freedman SF, Toth CA. Quality of life after macular translocation with 360 degrees peripheral retinectomy for age-related macular degeneration. *Ophthalmology* 2005; **112**(1): 144–151.
23 Eckardt C, Eckardt U. Macular translocation in nonexudative age-related macular degeneration. *Retina* 2002; **22**(6): 786–794.
24 Peyman GA, Blinder KJ, Paris CL, Alturki W, Nelson NC Jr., Desai U. A technique for retinal pigment epithelium transplantation for age-related macular degeneration secondary to extensive subfoveal scarring. *Ophthalmic Surg* 1991; **22**(2): 102–108.
25 Stanga PE, Kychenthal A, Fitzke FW, Halfyard AS, Chan R, Bird AC *et al.* Retinal pigment epithelium translocation and central visual function in age related macular degeneration: preliminary results. *Int Ophthalmol* 2001; **23**(4-6): 297–307.

26 van Meurs JC, Van Den Biesen PR. Autologous retinal pigment epithelium and choroid translocation in patients with exudative age-related macular degeneration: short-term follow-up. *Am J Ophthalmol* 2003; **136**(4): 688–695.
27 van Zeeburg EJ, Maaijwee KJ, Missotten TO, Heimann H, van Meurs JC. A free retinal pigment epithelium-choroid graft in patients with exudative age-related macular degeneration: results up to 7 years. *Am J Ophthalmol* 2012; **153**(1): 120–127 e122.
28 Binder S, Stolba U, Krebs I, Kellner L, Jahn C, Feichtinger H *et al.* Transplantation of autologous retinal pigment epithelium in eyes with foveal neovascularization resulting from age-related macular degeneration: a pilot study. *Am J Ophthalmol* 2002; **133**(2): 215–225.
29 Gullapalli VK, Sugino IK, Van Patten Y, Shah S, Zarbin MA. Retinal pigment epithelium resurfacing of aged submacular human Bruch's membrane. *Trans Am Ophthalmol Soc* 2004; **102**: 123–138.
30 Carr AJ, Vugler AA, Hikita ST, Lawrence JM, Gias C, Chen LL *et al.* Protective effects of human iPS-derived retinal pigment epithelium cell transplantation in the retinal dystrophic rat. *PLoS One* 2009; **4**(12): e8152.
31 Girman SV, Wang S, Lund RD. Cortical visual functions can be preserved by subretinal RPE cell grafting in RCS rats. *Vision Res* 2003; **43**(17): 1817–1827.
32 Lee E, MacLaren RE. Sources of retinal pigment epithelium (RPE) for replacement therapy. *Br J Ophthalmol* 2011; **95**(4): 445–449.
33 Gouras P, Lopez R. Transplantation of retinal epithelial cells. *Invest Ophthalmol Vis Sci* 1989; **30**(8): 1681–1683.
34 Gouras P, Flood MT, Kjedbye H, Bilek MK, Eggers H. Transplantation of cultured human retinal epithelium to Bruch's membrane of the owl monkey's eye. *Curr Eye Res* 1985; **4**(3): 253–265.
35 Lopez R, Gouras P, Brittis M, Kjeldbye H. Transplantation of cultured rabbit retinal epithelium to rabbit retina using a closed-eye method. *Invest Ophthalmol Vis Sci* 1987; **28**(7): 1131–1137.
36 Peyman GA, Fishman GA, Sanders DR, Apple DJ, Vlchek JK. Biopsy of human scleral-chorioretinal tissue. *Invest Ophthalmol* 1975; **14**(9): 707–710.
37 Lane C, Boulton M, Marshall J. Transplantation of retinal pigment epithelium using a pars plana approach. *Eye (Lond)* 1989; **3**(Pt 1): 27–32.
38 Wongpichedchai S, Weiter JJ, Weber P, Dorey CK. Comparison of external and internal approaches for transplantation of autologous retinal pigment epithelium. *Invest Ophthalmol Vis Sci* 1992; **33**(12): 3341–3352.
39 Remtulla S, Hallett PE. A schematic eye for the mouse, and comparisons with the rat. *Vis Res* 1985; **25**(1): 21–31.
40 Stein JD, Zacks DN, Grossman D, Grabe H, Johnson MW, Sloan FA. Adverse events after pars plana vitrectomy among medicare beneficiaries. *Arch Ophthalmol* 2009; **127**(12): 1656–1663.
41 Admitted Patient Care - England. Hospital Episode Statistics. Available at http://www.hscic.gov.uk/searchcatalogue?productid=9161&topics=1%2fHospital+care%2fInpatient+admissions&sort=Relevance&size=10&page=1 - top.
42 Thumann G, Viethen A, Gaebler A, Walter P, Kaempf S, Johnen S *et al.* The in vitro and in vivo behaviour of retinal pigment epithelial cells cultured on ultrathin collagen membranes. *Biomaterials* 2009; **30**(3): 287–294.
43 Lawrence JM, Sauve Y, Keegan DJ, Coffey PJ, Hetherington L, Girman S *et al.* Schwann cell grafting into the retina of the dystrophic RCS rat limits functional deterioration. Royal College of Surgeons. *Invest Ophthalmol Vis Sci* 2000; **41**(2): 518–528.
44 McGill TJ, Cottam B, Lu B, Wang S, Girman S, Tian C *et al.* Transplantation of human central nervous system stem cells - neuroprotection in retinal degeneration. *Eur J Neurosci* 2012; **35**(3): 468–477.
45 Lund RD, Wang S, Lu B, Girman S, Holmes T, Sauve Y *et al.* Cells isolated from umbilical cord tissue rescue photoreceptors and visual functions in a rodent model of retinal disease. *Stem Cells* 2007; **25**(3): 602–611.
46 Abe T, Yoshida M, Yoshioka Y, Wakusawa R, Tokita-Ishikawa Y, Seto H *et al.* Iris pigment epithelial cell transplantation for degenerative retinal diseases. *Prog Retin Eye Res* 2007; **26**(3): 302–321.
47 Hu DN, McCormick SA, Ritch R. Isolation and culture of iris pigment epithelium from iridectomy specimens of eyes with and without exfoliation syndrome. *Arch Ophthalmol* 1997; **115**(1): 89–94.
48 Crafoord S, Geng L, Seregard S, Algvere PV. Experimental transplantation of autologous iris pigment epithelial cells to the subretinal space. *Acta Ophthalmol Scand* 2001; **79**(5): 509–514.
49 Crafoord S, Geng L, Seregard S, Algvere PV. Photoreceptor survival in transplantation of autologous iris pigment epithelial cells to the subretinal space. *Acta Ophthalmol Scand* 2002; **80**(4): 387–394.
50 Rezai KA, Kohen L, Wiedemann P, Heimann K. Iris pigment epithelium transplantation. *Graefes Arch Clin Exp Ophthalmol* 1997; **235**(9): 558–562.
51 Thumann G, Kociok N, Bartz-Schmidt KU, Esser P, Schraermeyer U, Heimann K. Detection of mRNA for proteins involved in retinol metabolism in iris pigment epithelium. *Graefes Arch Clin Exp Ophthalmol* 1999; **237**(12): 1046–1051.
52 Dintelmann TS, Heimann K, Kayatz P, Schraermeyer U. Comparative study of ROS degradation by IPE and RPE cells in vitro. *Graefes Arch Clin Exp Ophthalmol* 1999; **237**(10): 830–839.
53 Kociok N, Heppekausen H, Schraermeyer U, Esser P, Thumann G, Grisanti S *et al.* The mRNA expression of cytokines and their receptors in cultured iris pigment epithelial cells: a comparison with retinal pigment epithelial cells. *Exp Eye Res* 1998; **67**(2): 237–250.
54 Gouras P, Algvere P. Retinal cell transplantation in the macula: new techniques. *Vision Res* 1996; **36**(24): 4121–4125.
55 Hayflick L, Moorhead PS. The serial cultivation of human diploid cell strains. *Exp Cell Res* 1961; **25**: 585–621.
56 Dunn KC, Aotaki-Keen AE, Putkey FR, Hjelmeland LM. ARPE-19, a human retinal pigment epithelial cell line with differentiated properties. *Exp Eye Res* 1996; **62**(2): 155–169.
57 Davis AA, Bernstein PS, Bok D, Turner J, Nachtigal M, Hunt RC. A human retinal pigment epithelial cell line that retains epithelial characteristics after prolonged culture. *Invest Ophthalmol Vis Sci* 1995; **36**(5): 955–964.
58 Lund RD, Adamson P, Sauve Y, Keegan DJ, Girman SV, Wang S *et al.* Subretinal transplantation of genetically modified human cell lines attenuates loss of visual function in dystrophic rats. *Proc Natl Acad Sci USA* 2001; **98**(17): 9942–9947.
59 Alge CS, Suppmann S, Priglinger SG, Neubauer AS, May CA, Hauck S *et al.* Comparative proteome analysis of native differentiated and cultured dedifferentiated

human RPE cells. *Invest Ophthalmol Vis Sci* 2003; **44**(8): 3629–3641.
60 Vinores SA, Derevjanik NL, Mahlow J, Hackett SF, Haller JA, deJuan E *et al.* Class III beta-tubulin in human retinal pigment epithelial cells in culture and in epiretinal membranes. *Exp Eye Res* 1995; **60**(4): 385–400.
61 Thomson JA, Itskovitz-Eldor J, Shapiro SS, Waknitz MA, Swiergiel JJ, Marshall VS *et al.* Embryonic stem cell lines derived from human blastocysts. *Science* 1998; **282**(5391): 1145–1147.
62 Carr AJ, Smart MJ, Ramsden CM, Powner MB, da Cruz L, Coffey PJ. Development of human embryonic stem cell therapies for age-related macular degeneration. *Trends Neurosci* 2013; **36**(7): 385–395.
63 Schwartz SD, Hubschman JP, Heilwell G, Franco-Cardenas V, Pan CK, Ostrick RM *et al.* Embryonic stem cell trials for macular degeneration: a preliminary report. *Lancet* 2012; **379**(9817): 713–720.
64 Takahashi K, Yamanaka S. Induction of pluripotent stem cells from mouse embryonic and adult fibroblast cultures by defined factors. *Cell* 2006; **126**(4): 663–676.
65 Zhao T, Zhang ZN, Rong Z, Xu Y. Immunogenicity of induced pluripotent stem cells. *Nature* 2011; **474**(7350): 212–215.
66 Sancho-Martinez I, Li M, Izpisua Belmonte JC. Disease correction the iPSC way: advances in iPSC-based therapy. *Clin Pharmacol Ther* 2011; **89**(5): 746–749.
67 Yu J, Vodyanik MA, Smuga-Otto K, Antosiewicz-Bourget J, Frane JL, Tian S *et al.* Induced pluripotent stem cell lines derived from human somatic cells. *Science* 2007; **318**(5858): 1917–1920.
68 Stadtfeld M, Nagaya M, Utikal J, Weir G, Hochedlinger K. Induced pluripotent stem cells generated without viral integration. *Science* 2008; **322**(5903): 945–949.
69 Lu X, Zhao T. Clinical therapy using iPSCs: hopes and challenges. *Genomics Proteomics Bioinformatics* 2013; **11**(5): 294–298.
70 Okita K, Yamakawa T, Matsumura Y, Sato Y, Amano N, Watanabe A *et al.* An efficient nonviral method to generate integration-free human-induced pluripotent stem cells from cord blood and peripheral blood cells. *Stem Cells* 2013; **31**(3): 458–466.
71 Obokata H, Wakayama T, Sasai Y, Kojima K, Vacanti MP, Niwa H *et al.* Stimulus-triggered fate conversion of somatic cells into pluripotency. *Nature* 2014; **505**(7485): 641–647.
72 Obokata H, Sasai Y, Niwa H, Kadota M, Andrabi M, Takata N *et al.* Bidirectional developmental potential in reprogrammed cells with acquired pluripotency. *Nature* 2014; **505**(7485): 676–680.
73 Obokata H, Wakayama T, Sasai Y, Kojima K, Vacanti MP, Niwa H *et al.* Retraction: Stimulus-triggered fate conversion of somatic cells into pluripotency. *Nature* 2014; **511**(7507): 112.
74 Stanzel BV, Thieltges F, Liu Z, Braun N, Wongsawad W, Somboonthanakij S *et al.* Localized RPE removal with a loop instrument in rabbits. *Invest Ophthalmol Vis Sci* 2014; **55**(5): E-abstract 1179.
75 Weichel J, Valtink M, Engelmann K, Richard G. Use of an oil-hydraulic microinjection pump for subretinal infusions. *Ophthalmic Surg Lasers* 2002; **33**(4): 340–342.
76 Maaijwee K, Koolen T, Rosenbrand D, Jacobs E, Kleinheerenbrink S, Knulst A *et al.* Threshold Amplitude and Frequency for Ocular Tissue Release from a Vibrating Instrument: An Experimental Study. *Invest Ophthalmol Vis Sci* 2008; **49**(4): 1629–1632.
77 Knulst AJ, Maaijwee K, van Meurs JC, Wieringa PA, Breedveld P, Schutte S. Micro-scale thermal tissue gripper. *Minim Invasive Ther Allied Technol* 2009; **18**(1): 8–14.
78 Stanzel BV, Liu Z, Brinken R, Braun N, Holz FG, Eter N. Subretinal delivery of ultrathin rigid-elastic cell carriers using a metallic shooter instrument and biodegradable hydrogel encapsulation. *Invest Ophthalmol Vis Sci* 2012; **53**(1): 490–500.
79 Stanzel BV, Liu Z, Somboonthanakij S, Wongsawad W, Brinken R, Eter N *et al.* Human RPE Stem Cells Grown into Polarized RPE Monolayers on a Polyester Matrix Are Maintained after Grafting into Rabbit Subretinal Space. *Stem Cell Reports* 2014; **2**(1): 64–77.
80 Kirchhof B, Sorgente N. Pathogenesis of proliferative vitreoretinopathy. Modulation of retinal pigment epithelial cell functions by vitreous and macrophages. *Dev Ophthalmol* 1989; **16**: 1–53.
81 Del Priore LV, Kaplan HJ, Hornbeck R, Jones Z, Swinn M. Retinal pigment epithelial debridement as a model for the pathogenesis and treatment of macular degeneration. *Am J Ophthalmol* 1996; **122**(5): 629–643.
82 van Zeeburg EJ, Maaijwee K, van Meurs JC. There is no relation between the occurrence of proliferative vitreoretinopathy and the location of the donor site after transplantation of a free autologous retinal pigment epithelium-choroid graft. *Acta Ophthalmol* 2014; **92**(3): 228–231.
83 Alexander P, Prasad R, Ang A, Poulson AV, Scott JD, Snead MP. Prevention and control of proliferative vitreoretinopathy: primary retinal detachment surgery using silicone oil as a planned two-stage procedure in high-risk cases. *Eye (Lond)* 2008; **22**(6): 815–818.
84 Schwartz SG, Flynn HW Jr., Lee WH, Wang X. Tamponade in surgery for retinal detachment associated with proliferative vitreoretinopathy. *Cochrane Database Syst Rev* 2014; **2**: CD006126.

List of References

1. Research AfEaV. Attitudinal Survey of Minority Populations on Eye and VIsion Health Research. . Available at: http://www.arvo.org/AEVRsurvey/.

2. De Leo D, Hickey PA, Meneghel G, Cantor CH. Blindness, fear of sight loss, and suicide. *Psychosomatics* 1999; **40**(4)**:** 339-344.

3. Kroger RH, Biehlmaier O. Space-saving advantage of an inverted retina. *Vision research* 2009; **49**(18)**:** 2318-2321.

4. Gospe SM, 3rd, Baker SA, Arshavsky VY. Facilitative glucose transporter Glut1 is actively excluded from rod outer segments. *Journal of cell science* 2010; **123**(Pt 21)**:** 3639-3644.

5. Moran D, Softley R, Warrant EJ. The energetic cost of vision and the evolution of eyeless Mexican cavefish. *Science Advances* 2015.

6. Vesalius. In: Garrison D, Hast M (eds). An annotated translation of the 1543 and 1555 editions of Andreas Vesalius' De Humani Corporis Fabrica: http://vesalius.northwestern.edu/.

7. Strauss O. The retinal pigment epithelium in visual function. *Physiological reviews* 2005; **85**(3)**:** 845-881.

8. Curcio CA, Owsley C, Jackson GR. Spare the rods, save the cones in aging and age-related maculopathy. *Investigative ophthalmology & visual science* 2000; **41**(8)**:** 2015-2018.

9. Kefalov VJ. Rod and cone visual pigments and phototransduction through pharmacological, genetic, and physiological approaches. *The Journal of biological chemistry* 2012; **287**(3)**:** 1635-1641.

10. Hogan MJ. Ultrastructure of the choroid. Its role in the pathogenesis of chorioretinal disease. *Transactions of the Pacific Coast Oto-Ophthalmological Society annual meeting* 1961; **42:** 61-87.

11. Guymer RH, Bird A. Bruch's membrane, drusen and age-related macular degeneration. . The retinal pigment epithelium. . Oxford University Press: New York; 1998. pp 693-703.

12. Starita C, Hussain AA, Patmore A, Marshall J. Localization of the site of major resistance to fluid transport in Bruch's membrane. *Investigative ophthalmology & visual science* 1997; **38**(3)**:** 762-767.

13. Moore DJ, Hussain AA, Marshall J. Age-related variation in the hydraulic conductivity of Bruch's membrane. *Investigative ophthalmology & visual science* 1995; **36**(7)**:** 1290-1297.

14. Starita C, Hussain AA, Marshall J. Decreasing hydraulic conductivity of Bruch's membrane: relevance to photoreceptor survival and lipofuscinoses. *American journal of medical genetics* 1995; **57**(2)**:** 235-237.

15. Marshall GE, Konstas AG, Reid GG, Edwards JG, Lee WR. Type IV collagen and laminin in Bruch's membrane and basal linear deposit in the human macula. *The British journal of ophthalmology* 1992; **76**(10)**:** 607-614.

16. Fang IM, Yang CH, Yang CM, Chen MS. Overexpression of integrin alpha6 and beta4 enhances adhesion and proliferation of human retinal pigment epithelial cells on layers of porcine Bruch's membrane. *Experimental eye research* 2009; **88**(1)**:** 12-21.

17. Gullapalli VK, Sugino IK, Van Patten Y, Shah S, Zarbin MA. Retinal pigment epithelium resurfacing of aged submacular human Bruch's membrane. *Transactions of the American Ophthalmological Society* 2004; **102:** 123-137; discussion 137-128.

18. Binder S, Stanzel BV, Krebs I, Glittenberg C. Transplantation of the RPE in AMD. *Progress in retinal and eye research* 2007; **26**(5)**:** 516-554.

19. Crane IJ, Liversidge J. Mechanisms of leukocyte migration across the blood-retina barrier. *Seminars in immunopathology* 2008; **30**(2)**:** 165-177.

20. da Cruz L, Chen FK, Ahmado A, Greenwood J, Coffey P. RPE transplantation and its role in retinal disease. *Progress in retinal and eye research* 2007; **26**(6)**:** 598-635.

21. Thompson DA, Li Y, McHenry CL, Carlson TJ, Ding X, Sieving PA *et al.* Mutations in the gene encoding lecithin retinol acyltransferase are associated with early-onset severe retinal dystrophy. *Nature genetics* 2001; **28**(2)**:** 123-124.

22. Ruiz A, Kuehn MH, Andorf JL, Stone E, Hageman GS, Bok D. Genomic organization and mutation analysis of the gene encoding lecithin retinol acyltransferase in human retinal pigment epithelium. *Investigative ophthalmology & visual science* 2001; **42**(1)**:** 31-37.

23. Gu SM, Thompson DA, Srikumari CR, Lorenz B, Finckh U, Nicoletti A *et al.* Mutations in RPE65 cause autosomal recessive childhood-onset severe retinal dystrophy. *Nature genetics* 1997; **17**(2)**:** 194-197.

24. Veske A, Nilsson SE, Narfstrom K, Gal A. Retinal dystrophy of Swedish briard/briard-beagle dogs is due to a 4-bp deletion in RPE65. *Genomics* 1999; **57**(1)**:** 57-61.

25. D'Cruz PM, Yasumura D, Weir J, Matthes MT, Abderrahim H, LaVail MM *et al.* Mutation of the receptor tyrosine kinase gene Mertk in the retinal dystrophic RCS rat. *Human molecular genetics* 2000; **9**(4)**:** 645-651.

26. Marmorstein AD, Marmorstein LY, Rayborn M, Wang X, Hollyfield JG, Petrukhin K. Bestrophin, the product of the Best vitelliform macular dystrophy gene (VMD2), localizes to the basolateral plasma membrane of the retinal pigment epithelium. *Proceedings of the National Academy of Sciences of the United States of America* 2000; **97**(23)**:** 12758-12763.

27. Ambati J, Ambati BK, Yoo SH, Ianchulev S, Adamis AP. Age-related macular degeneration: etiology, pathogenesis, and therapeutic strategies. *Survey of ophthalmology* 2003; **48**(3)**:** 257-293.

28. Zarbin MA. Current concepts in the pathogenesis of age-related macular degeneration. *Archives of ophthalmology* 2004; **122**(4)**:** 598-614.

29. Miller JW. Age-related macular degeneration revisited--piecing the puzzle: the LXIX Edward Jackson memorial lecture. *American journal of ophthalmology* 2013; **155**(1)**:** 1-35 e13.

30. Keane PA, Patel PJ, Liakopoulos S, Heussen FM, Sadda SR, Tufail A. Evaluation of age-related macular degeneration with optical coherence tomography. *Survey of ophthalmology* 2012; **57**(5)**:** 389-414.

31. Bird AC, Bressler NM, Bressler SB, Chisholm IH, Coscas G, Davis MD *et al.* An international classification and grading system for age-related maculopathy and age-related macular degeneration. The International ARM Epidemiological Study Group. *Survey of ophthalmology* 1995; **39**(5)**:** 367-374.

32. Ferris FL, 3rd, Wilkinson CP, Bird A, Chakravarthy U, Chew E, Csaky K *et al.* Clinical classification of age-related macular degeneration. *Ophthalmology* 2013; **120**(4)**:** 844-851.

33. Rosenfeld PJ, Brown DM, Heier JS, Boyer DS, Kaiser PK, Chung CY *et al.* Ranibizumab for neovascular age-related macular degeneration. *The New England journal of medicine* 2006; **355**(14)**:** 1419-1431.

34. Brown DM, Michels M, Kaiser PK, Heier JS, Sy JP, Ianchulev T. Ranibizumab versus verteporfin photodynamic therapy for neovascular age-related macular degeneration: Two-year results of the ANCHOR study. *Ophthalmology* 2009; **116**(1)**:** 57-65 e55.

35. Grunwald JE, Daniel E, Huang J, Ying GS, Maguire MG, Toth CA *et al.* Risk of geographic atrophy in the comparison of age-related macular degeneration treatments trials. *Ophthalmology* 2014; **121**(1)**:** 150-161.

36. Velez-Montoya R, Oliver SC, Olson JL, Fine SL, Mandava N, Quiroz-Mercado H. Current knowledge and trends in age-related macular degeneration: today's and future treatments. *Retina (Philadelphia, Pa)* 2013; **33**(8)**:** 1487-1502.

37. Bainbridge JW, Smith AJ, Barker SS, Robbie S, Henderson R, Balaggan K *et al.* Effect of gene therapy on visual function in Leber's congenital amaurosis. *The New England journal of medicine* 2008; **358**(21)**:** 2231-2239.

38. MacLaren RE, Groppe M, Barnard AR, Cottriall CL, Tolmachova T, Seymour L *et al.* Retinal gene therapy in patients with choroideremia: initial findings from a phase 1/2 clinical trial. *The Lancet* 2014.

39. Sahni JN, Angi M, Irigoyen C, Semeraro F, Romano MR, Parmeggiani F. Therapeutic challenges to retinitis pigmentosa: from neuroprotection to gene therapy. *Current genomics* 2011; **12**(4)**:** 276-284.

40. Luo YH, da Cruz L. The Argus II Retinal Prosthesis System. *Progress in retinal and eye research* 2015.

41. Ho AC, Humayun MS, Dorn JD, da Cruz L, Dagnelie G, Handa J *et al.* Long-Term Results from an Epiretinal Prosthesis to Restore Sight to the Blind. *Ophthalmology* 2015; **122**(8)**:** 1547-1554.

42. SecondSight. *Second Sight Announces First Age Related Macular Degeneration Patient Receives the Argus II Retinal Prosthesis System as Part of Groundbreaking Study* 2015.

43. Jobling AI, Guymer RH, Vessey KA, Greferath U, Mills SA, Brassington KH *et al.* Nanosecond laser therapy reverses pathologic and molecular changes in age-related macular degeneration without retinal damage. *FASEB journal : official publication of the Federation of American Societies for Experimental Biology* 2015; **29**(2)**:** 696-710.

44. Flood MT, Gouras P, Kjeldbye H. Growth characteristics and ultrastructure of human retinal pigment epithelium in vitro. *Investigative ophthalmology & visual science* 1980; **19**(11)**:** 1309-1320.

45. Boulton ME, Marshall J, Mellerio J. Human retinal pigment epithelial cells in tissue culture: a means of studying inherited retinal diseases. *Birth defects original article series* 1982; **18**(6)**:** 101-118.

46. Hu DN, Del Monte MA, Liu S, Maumenee IH. Morphology, phagocytosis, and vitamin A metabolism of cultured human retinal pigment epithelium. *Birth defects original article series* 1982; **18**(6)**:** 67-79.

47. Mason C, Dunnill P. Quantities of cells used for regenerative medicine and some implications for clinicians and bioprocessors. *Regenerative medicine* 2009; **4**(2)**:** 153-157.

48. Li LX, Turner JE. Inherited retinal dystrophy in the RCS rat: prevention of photoreceptor degeneration by pigment epithelial cell transplantation. *Experimental eye research* 1988; **47**(6)**:** 911-917.

49. Dowling JE, Sidman RL. Inherited retinal dystrophy in the rat. *The Journal of cell biology* 1962; **14:** 73-109.

50. Gouras P, Kong J, Tsang SH. Retinal degeneration and RPE transplantation in Rpe65(-/-) mice. *Investigative ophthalmology & visual science* 2002; **43**(10)**:** 3307-3311.

51. Hawkins BS, Bressler NM, Miskala PH, Bressler SB, Holekamp NM, Marsh MJ *et al.* Surgery for subfoveal choroidal neovascularization in age-related macular degeneration: ophthalmic findings: SST report no. 11. *Ophthalmology* 2004; **111**(11)**:** 1967-1980.

52. Chen FK, Patel PJ, Uppal GS, Tufail A, Coffey PJ, Da Cruz L. Long-term outcomes following full macular translocation surgery in neovascular age-related macular degeneration. *The British journal of ophthalmology* 2010; **94**(10)**:** 1337-1343.

53. Cahill MT, Stinnett SS, Banks AD, Freedman SF, Toth CA. Quality of life after macular translocation with 360 degrees peripheral retinectomy for age-related macular degeneration. *Ophthalmology* 2005; **112**(1)**:** 144-151.

54. Eckardt C, Eckardt U. Macular translocation in nonexudative age-related macular degeneration. *Retina (Philadelphia, Pa)* 2002; **22**(6)**:** 786-794.

55. Peyman GA, Blinder KJ, Paris CL, Alturki W, Nelson NC, Jr., Desai U. A technique for retinal pigment epithelium transplantation for age-related macular degeneration secondary to extensive subfoveal scarring. *Ophthalmic surgery* 1991; **22**(2)**:** 102-108.

56. Stanga PE, Kychenthal A, Fitzke FW, Halfyard AS, Chan R, Bird AC *et al.* Retinal pigment epithelium translocation and central visual function in age related macular degeneration: preliminary results. *International ophthalmology* 2001; **23**(4-6)**:** 297-307.

57. van Meurs JC, Van Den Biesen PR. Autologous retinal pigment epithelium and choroid translocation in patients with exudative age-related macular degeneration: short-term follow-up. *American journal of ophthalmology* 2003; **136**(4)**:** 688-695.

58. van Zeeburg EJ, Maaijwee KJ, Missotten TO, Heimann H, van Meurs JC. A free retinal pigment epithelium-choroid graft in patients with exudative age-related macular degeneration: results up to 7 years. *American journal of ophthalmology* 2012; **153**(1)**:** 120-127 e122.

59. Binder S, Stolba U, Krebs I, Kellner L, Jahn C, Feichtinger H *et al.* Transplantation of autologous retinal pigment epithelium in eyes with foveal neovascularization resulting from age-related macular degeneration: a pilot study. *American journal of ophthalmology* 2002; **133**(2)**:** 215-225.

60. Carr AJ, Vugler AA, Hikita ST, Lawrence JM, Gias C, Chen LL *et al.* Protective effects of human iPS-derived retinal pigment epithelium cell transplantation in the retinal dystrophic rat. *PloS one* 2009; **4**(12)**:** e8152.

61. Girman SV, Wang S, Lund RD. Cortical visual functions can be preserved by subretinal RPE cell grafting in RCS rats. *Vision research* 2003; **43**(17)**:** 1817-1827.

62. Lee E, MacLaren RE. Sources of retinal pigment epithelium (RPE) for replacement therapy. *The British journal of ophthalmology* 2011; **95**(4)**:** 445-449.

63. Thumann G, Viethen A, Gaebler A, Walter P, Kaempf S, Johnen S *et al.* The in vitro and in vivo behaviour of retinal pigment epithelial cells cultured on ultrathin collagen membranes. *Biomaterials* 2009; **30**(3)**:** 287-294.

64. Lawrence JM, Sauve Y, Keegan DJ, Coffey PJ, Hetherington L, Girman S *et al.* Schwann cell grafting into the retina of the dystrophic RCS rat limits functional deterioration. Royal College of Surgeons. *Investigative ophthalmology & visual science* 2000; **41**(2)**:** 518-528.

65. McGill TJ, Cottam B, Lu B, Wang S, Girman S, Tian C *et al.* Transplantation of human central nervous system stem cells - neuroprotection in retinal degeneration. *The European journal of neuroscience* 2012; **35**(3)**:** 468-477.

66. Lund RD, Wang S, Lu B, Girman S, Holmes T, Sauve Y *et al.* Cells isolated from umbilical cord tissue rescue photoreceptors and visual functions in a rodent model of retinal disease. *Stem Cells* 2007; **25**(3)**:** 602-611.

67. Abe T, Yoshida M, Yoshioka Y, Wakusawa R, Tokita-Ishikawa Y, Seto H *et al.* Iris pigment epithelial cell transplantation for degenerative retinal diseases. *Progress in retinal and eye research* 2007; **26**(3)**:** 302-321.

68. Hu DN, McCormick SA, Ritch R. Isolation and culture of iris pigment epithelium from iridectomy specimens of eyes with and without exfoliation syndrome. *Archives of ophthalmology* 1997; **115**(1)**:** 89-94.

69. Crafoord S, Geng L, Seregard S, Algvere PV. Experimental transplantation of autologous iris pigment epithelial cells to the subretinal space. *Acta ophthalmologica Scandinavica* 2001; **79**(5)**:** 509-514.

70. Crafoord S, Geng L, Seregard S, Algvere PV. Photoreceptor survival in transplantation of autologous iris pigment epithelial cells to the subretinal space. *Acta ophthalmologica Scandinavica* 2002; **80**(4)**:** 387-394.

71. Rezai KA, Kohen L, Wiedemann P, Heimann K. Iris pigment epithelium transplantation. *Graefe's archive for clinical and experimental ophthalmology = Albrecht von Graefes Archiv fur klinische und experimentelle Ophthalmologie* 1997; **235**(9)**:** 558-562.

72. Thumann G, Kociok N, Bartz-Schmidt KU, Esser P, Schraermeyer U, Heimann K. Detection of mRNA for proteins involved in retinol metabolism in iris pigment epithelium. *Graefe's archive for clinical and experimental ophthalmology = Albrecht von Graefes Archiv fur klinische und experimentelle Ophthalmologie* 1999; **237**(12)**:** 1046-1051.

73. Dintelmann TS, Heimann K, Kayatz P, Schraermeyer U. Comparative study of ROS degradation by IPE and RPE cells in vitro. *Graefe's archive for clinical and experimental ophthalmology = Albrecht von Graefes Archiv fur klinische und experimentelle Ophthalmologie* 1999; **237**(10)**:** 830-839.

74. Kociok N, Heppekausen H, Schraermeyer U, Esser P, Thumann G, Grisanti S *et al.* The mRNA expression of cytokines and their receptors in cultured iris pigment epithelial cells: a comparison with retinal pigment epithelial cells. *Experimental eye research* 1998; **67**(2)**:** 237-250.

75. Gouras P, Algvere P. Retinal cell transplantation in the macula: new techniques. *Vision research* 1996; **36**(24)**:** 4121-4125.

76. Hayflick L, Moorhead PS. The serial cultivation of human diploid cell strains. *Experimental cell research* 1961; **25:** 585-621.

77. Dunn KC, Aotaki-Keen AE, Putkey FR, Hjelmeland LM. ARPE-19, a human retinal pigment epithelial cell line with differentiated properties. *Experimental eye research* 1996; **62**(2)**:** 155-169.

78. Davis AA, Bernstein PS, Bok D, Turner J, Nachtigal M, Hunt RC. A human retinal pigment epithelial cell line that retains epithelial characteristics after prolonged culture. *Investigative ophthalmology & visual science* 1995; **36**(5)**:** 955-964.

79. Lund RD, Adamson P, Sauve Y, Keegan DJ, Girman SV, Wang S *et al.* Subretinal transplantation of genetically modified human cell lines attenuates loss of visual function in dystrophic rats. *Proceedings of the National Academy of Sciences of the United States of America* 2001; **98**(17)**:** 9942-9947.

80. Alge CS, Suppmann S, Priglinger SG, Neubauer AS, May CA, Hauck S *et al.* Comparative proteome analysis of native differentiated and cultured dedifferentiated human RPE cells. *Investigative ophthalmology & visual science* 2003; **44**(8)**:** 3629-3641.

81. Vinores SA, Derevjanik NL, Mahlow J, Hackett SF, Haller JA, deJuan E *et al.* Class III beta-tubulin in human retinal pigment epithelial cells in culture and in epiretinal membranes. *Experimental eye research* 1995; **60**(4)**:** 385-400.

82. Thomson JA, Itskovitz-Eldor J, Shapiro SS, Waknitz MA, Swiergiel JJ, Marshall VS *et al.* Embryonic stem cell lines derived from human blastocysts. *Science* 1998; **282**(5391)**:** 1145-1147.

83. Ramsden CM, Powner MB, Carr AJ, Smart MJ, da Cruz L, Coffey PJ. Stem cells in retinal regeneration: past, present and future. *Development* 2013; **140**(12)**:** 2576-2585.

84. Schwartz SD, Hubschman JP, Heilwell G, Franco-Cardenas V, Pan CK, Ostrick RM *et al.* Embryonic stem cell trials for macular degeneration: a preliminary report. *Lancet* 2012; **379**(9817)**:** 713-720.

85. Schwartz SD, Regillo CD, Lam BL, Eliott D, Rosenfeld PJ, Gregori NZ *et al.* Human embryonic stem cell-derived retinal pigment epithelium in patients with age-related macular degeneration and Stargardt's macular dystrophy: follow-up of two open-label phase 1/2 studies. *The Lancet* 2014.

86. Carr AJ, Smart MJ, Ramsden CM, Powner MB, da Cruz L, Coffey PJ. Development of human embryonic stem cell therapies for age-related macular degeneration. *Trends in neurosciences* 2013.

87. Takahashi K, Yamanaka S. Induction of pluripotent stem cells from mouse embryonic and adult fibroblast cultures by defined factors. *Cell* 2006; **126**(4)**:** 663-676.

88. Zhao T, Zhang ZN, Rong Z, Xu Y. Immunogenicity of induced pluripotent stem cells. *Nature* 2011; **474**(7350)**:** 212-215.

89. Sancho-Martinez I, Li M, Izpisua Belmonte JC. Disease correction the iPSC way: advances in iPSC-based therapy. *Clinical pharmacology and therapeutics* 2011; **89**(5)**:** 746-749.

90. Yu J, Vodyanik MA, Smuga-Otto K, Antosiewicz-Bourget J, Frane JL, Tian S *et al.* Induced pluripotent stem cell lines derived from human somatic cells. *Science* 2007; **318**(5858)**:** 1917-1920.

91. Stadtfeld M, Nagaya M, Utikal J, Weir G, Hochedlinger K. Induced pluripotent stem cells generated without viral integration. *Science* 2008; **322**(5903)**:** 945-949.

92. Lu X, Zhao T. Clinical Therapy Using iPSCs: Hopes and Challenges. *Genomics, Proteomics & Bioinformatics* 2013; **11**(5)**:** 294-298.

93. Okita K, Yamakawa T, Matsumura Y, Sato Y, Amano N, Watanabe A *et al.* An efficient nonviral method to generate integration-free human-induced pluripotent stem cells from cord blood and peripheral blood cells. *Stem Cells* 2013; **31**(3)**:** 458-466.

94. Obokata H, Wakayama T, Sasai Y, Kojima K, Vacanti MP, Niwa H *et al.* Stimulus-triggered fate conversion of somatic cells into pluripotency. *Nature* 2014; **505**(7485)**:** 641-647.

95. Obokata H, Sasai Y, Niwa H, Kadota M, Andrabi M, Takata N *et al.* Bidirectional developmental potential in reprogrammed cells with acquired pluripotency. *Nature* 2014; **505**(7485)**:** 676-680.

96. Obokata H, Wakayama T, Sasai Y, Kojima K, Vacanti MP, Niwa H *et al.* Retraction: Stimulus-triggered fate conversion of somatic cells into pluripotency. *Nature* 2014; **511**(7507)**:** 112.

97. Peyman GA, Fishman GA, Sanders DR, Apple DJ, Vlchek JK. Biopsy of human scleral-chorioretinal tissue. *Investigative ophthalmology* 1975; **14**(9)**:** 707-710.

98. Lane C, Boulton M, Marshall J. Transplantation of retinal pigment epithelium using a pars plana approach. *Eye (London, England)* 1989; **3 (Pt 1):** 27-32.

99. Wongpichedchai S, Weiter JJ, Weber P, Dorey CK. Comparison of external and internal approaches for transplantation of autologous retinal pigment epithelium. *Investigative ophthalmology & visual science* 1992; **33**(12)**:** 3341-3352.

100. Gouras P, Flood MT, Kjedbye H, Bilek MK, Eggers H. Transplantation of cultured human retinal epithelium to Bruch's membrane of the owl monkey's eye. *Current eye research* 1985; **4**(3)**:** 253-265.

101. Lopez R, Gouras P, Brittis M, Kjeldbye H. Transplantation of cultured rabbit retinal epithelium to rabbit retina using a closed-eye method. *Investigative ophthalmology & visual science* 1987; **28**(7)**:** 1131-1137.

102. Weichel J, Valtink M, Engelmann K, Richard G. Use of an oil-hydraulic microinjection pump for subretinal infusions. *Ophthalmic surgery and lasers* 2002; **33**(4)**:** 340-342.

103. Tezel TH, Del Priore LV. Repopulation of different layers of host human Bruch's membrane by retinal pigment epithelial cell grafts. *Investigative ophthalmology & visual science* 1999; **40**(3)**:** 767-774.

104. Booij JC, Baas DC, Beisekeeva J, Gorgels TG, Bergen AA. The dynamic nature of Bruch's membrane. *Progress in retinal and eye research* 2010; **29**(1)**:** 1-18.

105. Moore DJ, Clover GM. The effect of age on the macromolecular permeability of human Bruch's membrane. *Investigative ophthalmology & visual science* 2001; **42**(12)**:** 2970-2975.

106. Huang JD, Presley JB, Chimento MF, Curcio CA, Johnson M. Age-related changes in human macular Bruch's membrane as seen by quick-freeze/deep-etch. *Experimental eye research* 2007; **85**(2)**:** 202-218.

107. Ohno-Matsui K, Ichinose S, Nakahama K, Yoshida T, Kojima A, Mochizuki M *et al.* The effects of amniotic membrane on retinal pigment epithelial cell differentiation. *Molecular vision* 2005; **11:** 1-10.

108. Kiilgaard JF, Scherfig E, Prause JU, la Cour M. Transplantation of amniotic membrane to the subretinal space in pigs. *Stem cells international* 2012; **2012:** 716968.

109. Thumann G, Schraermeyer U, Bartz-Schmidt KU, Heimann K. Descemet's membrane as membranous support in RPE/IPE transplantation. *Current eye research* 1997; **16**(12)**:** 1236-1238.

110. Turowski P, Adamson P, Sathia J, Zhang JJ, Moss SE, Aylward GW *et al.* Basement membrane-dependent modification of phenotype and gene expression in human retinal pigment epithelial ARPE-19 cells. *Investigative ophthalmology & visual science* 2004; **45**(8)**:** 2786-2794.

111. Lee CJ, Huie P, Leng T, Peterman MC, Marmor MF, Blumenkranz MS *et al.* Microcontact printing on human tissue for retinal cell transplantation. *Archives of ophthalmology* 2002; **120**(12)**:** 1714-1718.

112. Langer R, Vacanti JP. Tissue engineering. *Science* 1993; **260**(5110)**:** 920-926.

113. Temenoff JS, Mikos AG. Review: tissue engineering for regeneration of articular cartilage. *Biomaterials* 2000; **21**(5)**:** 431-440.

114. Atala A. Tissue engineering for bladder substitution. *World journal of urology* 2000; **18**(5)**:** 364-370.

115. Pomahac B, Svensjo T, Yao F, Brown H, Eriksson E. Tissue engineering of skin. *Critical reviews in oral biology and medicine : an official publication of the American Association of Oral Biologists* 1998; **9**(3)**:** 333-344.

116. Stanzel BV, Binder S, Blumenkranz MS, Marmor MF. Culture of Human RPE From Aged Donors on a Potential Bruch's Membrane Prosthesis. *Invest Ophthalmol Vis Sci* 2006; **47**(5)**:** 1407-.

117. Tomita M, Lavik E, Klassen H, Zahir T, Langer R, Young MJ. Biodegradable polymer composite grafts promote the survival and differentiation of retinal progenitor cells. *Stem Cells* 2005; **23**(10)**:** 1579-1588.

118. Tao S, Young C, Redenti S, Zhang Y, Klassen H, Desai T *et al.* Survival, migration and differentiation of retinal progenitor cells transplanted on micro-machined poly(methyl methacrylate) scaffolds to the subretinal space. *Lab on a chip* 2007; **7**(6)**:** 695-701.

119. Redenti S, Neeley WL, Rompani S, Saigal S, Yang J, Klassen H *et al.* Engineering retinal progenitor cell and scrollable poly(glycerol-sebacate) composites for expansion and subretinal transplantation. *Biomaterials* 2009; **30**(20)**:** 3405-3414.

120. Christiansen AT, Tao SL, Smith M, Wnek GE, Prause JU, Young MJ *et al.* Subretinal implantation of electrospun, short nanowire, and smooth poly(epsilon-caprolactone) scaffolds to the subretinal space of porcine eyes. *Stem cells international* 2012; **2012:** 454295.

121. Ho TC, Del Priore LV, Kaplan HJ. Tissue culture of retinal pigment epithelium following isolation with a gelatin matrix technique. *Experimental eye research* 1997; **64**(2)**:** 133-139.

122. Lu L, Yaszemski MJ, Mikos AG. Retinal pigment epithelium engineering using synthetic biodegradable polymers. *Biomaterials* 2001; **22**(24)**:** 3345-3355.

123. Williams RL, Krishna Y, Dixon S, Haridas A, Grierson I, Sheridan C. Polyurethanes as potential substrates for sub-retinal retinal pigment epithelial cell transplantation. *Journal of materials science Materials in medicine* 2005; **16**(12)**:** 1087-1092.

124. Shadforth AM, George KA, Kwan AS, Chirila TV, Harkin DG. The cultivation of human retinal pigment epithelial cells on Bombyx mori silk fibroin. *Biomaterials* 2012; **33**(16)**:** 4110-4117.

125. Xiang P, Wu KC, Zhu Y, Xiang L, Li C, Chen DL *et al.* A novel Bruch's membrane-mimetic electrospun substrate scaffold for human retinal pigment epithelium cells. *Biomaterials* 2014; **35**(37)**:** 9777-9788.

126. Lu B, Zhu D, Hinton D, Humayun MS, Tai YC. Mesh-supported submicron parylene-C membranes for culturing retinal pigment epithelial cells. *Biomedical microdevices* 2012; **14**(4)**:** 659-667.

127. Krishna Y, Sheridan C, Kent D, Kearns V, Grierson I, Williams R. Expanded polytetrafluoroethylene as a substrate for retinal pigment epithelial cell growth and transplantation in age-related macular degeneration. *The British journal of ophthalmology* 2011; **95**(4)**:** 569-573.

128. Stanzel BV, Liu Z, Somboonthanakij S, Wongsawad W, Brinken R, Eter N *et al.* Human RPE Stem Cells Grown into Polarized RPE Monolayers on a Polyester Matrix Are Maintained after Grafting into Rabbit Subretinal Space. *Stem cell reports* 2014; **2**(1)**:** 64-77.

129. Subrizi A, Hiidenmaa H, Ilmarinen T, Nymark S, Dubruel P, Uusitalo H *et al.* Generation of hESC-derived retinal pigment epithelium on biopolymer coated polyimide membranes. *Biomaterials* 2012; **33**(32)**:** 8047-8054.

130. Formhals A, inventor; Google Patents, assignee. Process and apparatus for preparing artificial threads, 1934.

131. Pitt DW, Treharne AJ, Thomson HA, Scott JA, Lotery AJ, Grossel MC. Improving cellular adhesion on scaffolds for transplantation: synthesising a poly(MMA-co-PEGM) network. *Journal of Materials Chemistry B* 2013; **1**(48)**:** 6627.

132. Klintworth GK. The cornea--structure and macromolecules in health and disease. A review. *The American journal of pathology* 1977; **89**(3)**:** 718-808.

133. Hollyfield JG. Hyaluronan and the functional organization of the interphotoreceptor matrix. *Investigative ophthalmology & visual science* 1999; **40**(12)**:** 2767-2769.

134. Hussain AA, Starita C, Hodgetts A, Marshall J. Macromolecular diffusion characteristics of ageing human Bruch's membrane: implications for age-related macular degeneration (AMD). *Experimental eye research* 2010; **90**(6)**:** 703-710.

135. Ramsey DJ, Arden GB. Hypoxia and Dark Adaptation in Diabetic Retinopathy: Interactions, Consequences, and Therapy. *Current diabetes reports* 2015; **15**(12)**:** 118.

136. Curcio CA, Johnson M. Structure, Function and Pathology of Bruch's Membrane. In: Ryan SJ, Schachat AP, Wilkinson CP, Hinton DR, Sadda SR, Wiedemann P (eds). Retina, 5th Ed. ed. Elsevier: London; 2013.

137. Thomson HA. Personal communication; 2013.

138. Stanzel BV, Thieltges F, Liu Z, Braun N, Wongsawad W, Somboonthanakij S *et al.* Localized RPE removal with a loop instrument in rabbits. *Invest Ophthalmol Vis Sci* 2014; **55**(5)**:** E-abstract 1179.

139. Bird AC, Marshall J. Retinal pigment epithelial detachments in the elderly. *Transactions of the ophthalmological societies of the United Kingdom* 1986; **105 (Pt 6):** 674-682.

140. Starita C, Hussain AA, Pagliarini S, Marshall J. Hydrodynamics of ageing Bruch's membrane: implications for macular disease. *Experimental eye research* 1996; **62**(5)**:** 565-572.

141. Liu Z, Yu N, Holz FG, Yang F, Stanzel BV. Enhancement of retinal pigment epithelial culture characteristics and subretinal space tolerance of scaffolds with 200 nm fiber topography. *Biomaterials* 2014; **35**(9)**:** 2837-2850.

142. Kay P, Yang YC, Paraoan L. Directional protein secretion by the retinal pigment epithelium: roles in retinal health and the development of age-related macular degeneration. *Journal of cellular and molecular medicine* 2013; **17**(7)**:** 833-843.

143. Boulton ME. Studying melanin and lipofuscin in RPE cell culture models. *Experimental eye research* 2014; **126:** 61-67.

144. Lehmann GL, Benedicto I, Philp NJ, Rodriguez-Boulan E. Plasma membrane protein polarity and trafficking in RPE cells: past, present and future. *Experimental eye research* 2014; **126:** 5-15.

145. de SSP, Calabro A, Nishiyama K, Hu JG, Bok D, Hollyfield JG. Glycosaminoglycan synthesis and secretion by the retinal pigment epithelium: polarized delivery of hyaluronan from the apical surface. *Journal of cell science* 2001; **114**(Pt 1)**:** 199-205.

146. Tombran-Tink J, Chader GG, Johnson LV. PEDF: a pigment epithelium-derived factor with potent neuronal differentiative activity. *Experimental eye research* 1991; **53**(3)**:** 411-414.

147. Tombran-Tink J, Mazuruk K, Rodriguez IR, Chung D, Linker T, Englander E *et al.* Organization, evolutionary conservation, expression and unusual Alu density of the human gene for pigment epithelium-derived factor, a unique neurotrophic serpin. *Molecular vision* 1996; **2:** 11.

148. Tombran-Tink J, Shivaram SM, Chader GJ, Johnson LV, Bok D. Expression, secretion, and age-related downregulation of pigment epithelium-derived factor, a serpin with neurotrophic activity. *The Journal of neuroscience : the official journal of the Society for Neuroscience* 1995; **15**(7 Pt 1)**:** 4992-5003.

149. Senger DR, Galli SJ, Dvorak AM, Perruzzi CA, Harvey VS, Dvorak HF. Tumor cells secrete a vascular permeability factor that promotes accumulation of ascites fluid. *Science* 1983; **219**(4587)**:** 983-985.

150. Ide A, Baker N, Warren S. Vascularization of the Brown Pearce rabbit epithelioma transplant as seen in the transparent ear chamber. *Am J Roentgenol* 1939; **42:** 891-899.

151. Ferrara N. Vascular endothelial growth factor. *Arteriosclerosis, thrombosis, and vascular biology* 2009; **29**(6)**:** 789-791.

152. Nowak DG, Woolard J, Amin EM, Konopatskaya O, Saleem MA, Churchill AJ *et al.* Expression of pro- and anti-angiogenic isoforms of VEGF is differentially regulated by splicing and growth factors. *Journal of cell science* 2008; **121**(Pt 20)**:** 3487-3495.

153. Blaauwgeers HG, Holtkamp GM, Rutten H, Witmer AN, Koolwijk P, Partanen TA *et al.* Polarized vascular endothelial growth factor secretion by human retinal pigment epithelium and localization of vascular endothelial growth factor receptors on the inner choriocapillaris. Evidence for a trophic paracrine relation. *The American journal of pathology* 1999; **155**(2)**:** 421-428.

154. Rofagha S, Bhisitkul RB, Boyer DS, Sadda SR, Zhang K, Group S-US. Seven-Year Outcomes in Ranibizumab-Treated Patients in ANCHOR, MARINA, and HORIZON: A Multicenter Cohort Study (SEVEN-UP). *Ophthalmology* 2013.

155. Nguyen QD, Shah SM, Khwaja AA, Channa R, Hatef E, Do DV *et al.* Two-year outcomes of the ranibizumab for edema of the mAcula in diabetes (READ-2) study. *Ophthalmology* 2010; **117**(11)**:** 2146-2151.

156. Campochiaro PA, Heier JS, Feiner L, Gray S, Saroj N, Rundle AC *et al.* Ranibizumab for macular edema following branch retinal vein occlusion: six-month primary end point results of a phase III study. *Ophthalmology* 2010; **117**(6)**:** 1102-1112 e1101.

157. Fromter E, Diamond J. Route of passive ion permeation in epithelia. *Nature: New biology* 1972; **235**(53)**:** 9-13.

158. Rizzolo LJ, Peng S, Luo Y, Xiao W. Integration of tight junctions and claudins with the barrier functions of the retinal pigment epithelium. *Progress in retinal and eye research* 2011; **30**(5)**:** 296-323.

159. Pfeffer BA, Philp NJ. Cell culture of retinal pigment epithelium: Special Issue. *Experimental eye research* 2014; **126:** 1-4.

160. Corning. Transwell® Permeable Supports Selection and Use Guide. Available at: http://csmedia2.corning.com/LifeSciences/media/pdf/transwell_guide.pdf.

161. Anderson JM, Van Itallie CM. Physiology and function of the tight junction. *Cold Spring Harbor perspectives in biology* 2009; **1**(2)**:** a002584.

162. Rizzolo LJ. Barrier properties of cultured retinal pigment epithelium. *Experimental eye research* 2014; **126:** 16-26.

163. Mazzoni F, Safa H, Finnemann SC. Understanding photoreceptor outer segment phagocytosis: use and utility of RPE cells in culture. *Experimental eye research* 2014; **126:** 51-60.

164. Gan SD, Patel KR. Enzyme immunoassay and enzyme-linked immunosorbent assay. *The Journal of investigative dermatology* 2013; **133**(9)**:** e12.

165. Sino-Biological. ELISA for Home Pregnancy Test. Available at: http://www.elisa-antibody.com/ELISA-applications/home-pregnancy-test. Accessed 3rd August, 2015.

166. Kanemura H, Go MJ, Nishishita N, Sakai N, Kamao H, Sato Y *et al.* Pigment epithelium-derived factor secreted from retinal pigment epithelium facilitates apoptotic cell death of iPSC. *Scientific reports* 2013; **3:** 2334.

167. Ts'o MO, Friedman E. The retinal pigment epithelium. I. Comparative histology. *Archives of ophthalmology* 1967; **78**(5)**:** 641-649.

168. Samuelson DA. Ophthalmic Anatomy. In: Gelatt KN, Gilger BC, Kern TJ (eds). Veterinary Ophthalmology. Vol. 1, 5th ed. Wiley-Blackwell: Hoboken, NJ, USA.; 2013. pp 135-136.

169. Luo Y, Zhuo Y, Fukuhara M, Rizzolo LJ. Effects of culture conditions on heterogeneity and the apical junctional complex of the ARPE-19 cell line. *Investigative ophthalmology & visual science* 2006; **47**(8)**:** 3644-3655.

170. Ablonczy Z, Dahrouj M, Tang PH, Liu Y, Sambamurti K, Marmorstein AD *et al.* Human retinal pigment epithelium cells as functional models for the RPE in vivo. *Investigative ophthalmology & visual science* 2011; **52**(12)**:** 8614-8620.

171. Gouras P, Lopez R. Transplantation of retinal epithelial cells. *Investigative ophthalmology & visual science* 1989; **30**(8)**:** 1681-1683.

172. Aylward GW. 25th RCOphth Congress, President's Session paper: 25 years of progress in vitreoretinal surgery. *Eye (London, England)* 2014; **28**(9)**:** 1053-1059.

173. Arshinoff SA. Understanding Ophthalmic Viscoelastic Devices. *XXXI Congress of the European Society of Cararact and Refractive Surgeons*; 5th-9th October; Amsterdam, 2013.

174. Van den Bruel A, Gailly J, Devriese S, Welton NJ, Shortt AJ, Vrijens F. The protective effect of ophthalmic viscoelastic devices on endothelial cell loss during cataract surgery: a meta-analysis using mixed treatment comparisons. *The British journal of ophthalmology* 2011; **95**(1)**:** 5-10.

175. Arshinoff SA, Jafari M. New classification of ophthalmic viscosurgical devices--2005. *Journal of cataract and refractive surgery* 2005; **31**(11)**:** 2167-2171.

176. El Rayes EN, Elborgy E. Suprachoroidal buckling: technique and indications. *Journal of ophthalmic & vision research* 2013; **8**(4)**:** 393-399.

177. Veritti D, Lanzetta P, Bandello F, Chiodini RG. Viscoelastic agent retention and failed macular hole surgery. *Retinal cases & brief reports* 2009; **3**(1)**:** 77-79.

178. Fernandez-Vigo J, Refojo MF, Verstraeten T. Evaluation of a viscoelastic solution of hydroxypropyl methylcellulose as a potential vitreous substitute. *Retina (Philadelphia, Pa)* 1990; **10**(2)**:** 148-152.

179. Maaijwee K, Koolen T, Rosenbrand D, Jacobs E, Kleinheerenbrink S, Knulst A *et al.* Threshold Amplitude and Frequency for Ocular Tissue Release from a Vibrating Instrument: An Experimental Study. *Investigative ophthalmology & visual science* 2008; **49**(4)**:** 1629-1632.

180. Knulst AJ, Maaijwee K, van Meurs JC, Wieringa PA, Breedveld P, Schutte S. Micro-scale thermal tissue gripper. *Minimally Invasive Therapy & Allied Technologies* 2009; **18**(1)**:** 8-14.

181. Stanzel BV, Liu Z, Brinken R, Braun N, Holz FG, Eter N. Subretinal delivery of ultrathin rigid-elastic cell carriers using a metallic shooter instrument and biodegradable hydrogel encapsulation. *Investigative ophthalmology & visual science* 2012; **53**(1)**:** 490-500.

182. Chan FK, Moriwaki K, De Rosa MJ. Detection of necrosis by release of lactate dehydrogenase activity. *Methods in molecular biology* 2013; **979:** 65-70.

183. Kirchhof B, Sorgente N. Pathogenesis of proliferative vitreoretinopathy. Modulation of retinal pigment epithelial cell functions by vitreous and macrophages. *Developments in ophthalmology* 1989; **16:** 1-53.

184. Coffey P, da Cruz L, Cheetham K, inventors; UCL Business PLC assignee. Patent 20130218167: device for deploying a flexible implant, 2013.

185. Remtulla S, Hallett PE. A schematic eye for the mouse, and comparisons with the rat. *Vision research* 1985; **25**(1)**:** 21-31.

186. Stein JD, Zacks DN, Grossman D, Grabe H, Johnson MW, Sloan FA. Adverse events after pars plana vitrectomy among medicare beneficiaries. *Archives of ophthalmology* 2009; **127**(12)**:** 1656-1663.

187. Admitted Patient Care - England. *Hospital Episode Statistics*. Available at: http://www.hscic.gov.uk/searchcatalogue?productid=9161&topics=1%2fHospital+care%2fInpatient+admissions&sort=Relevance&size=10&page=1 - top.

188. Warrier SK, Jain R, Gilhotra JS, Newland HS. Sutureless vitrectomy. *Indian journal of ophthalmology* 2008; **56**(6)**:** 453-458.

189. Machemer R, Buettner H, Norton EW, Parel JM. Vitrectomy: a pars plana approach. *Transactions - American Academy of Ophthalmology and Otolaryngology American Academy of Ophthalmology and Otolaryngology* 1971; **75**(4)**:** 813-820.

190. O'Malley C, Heintz RM, Sr. Vitrectomy with an alternative instrument system. *Annals of ophthalmology* 1975; **7**(4)**:** 585-588, 591-584.

191. Jackson TL, Donachie PH, Sparrow JM, Johnston RL. United Kingdom National Ophthalmology Database Study of Vitreoretinal Surgery: report 1; case mix, complications, and cataract. *Eye (London, England)* 2013; **27**(5)**:** 644-651.

192. Sawa M, Ohji M, Kusaka S, Sakaguchi H, Gomi F, Saito Y *et al.* Nonvitrectomizing vitreous surgery for epiretinal membrane long-term follow-up. *Ophthalmology* 2005; **112**(8)**:** 1402-1408.

193. Reibaldi M, Longo A, Avitabile T, Bonfiglio V, Toro MD, Russo A *et al.* TRANSCONJUNCTIVAL NONVITRECTOMIZING VITREOUS SURGERY VERSUS 25-GAUGE VITRECTOMY IN PATIENTS WITH EPIRETINAL MEMBRANE: A Prospective Randomized Study. *Retina (Philadelphia, Pa)* 2015; **35**(5)**:** 873-879.

194. Yang CM, Cousins SW. Quantitative assessment of growth stimulating activity of the vitreous during PVR. *Investigative ophthalmology & visual science* 1992; **33**(8)**:** 2436-2442.

195. Understanding animal research (Website - accessed September 2015). Available at: http://www.understandinganimalresearch.org.uk/resources/faqs/.

196. Research NCftRRRoAi. The 3Rs. Available at: https://http://www.nc3rs.org.uk/the-3rs (accessed October 2015).

197. Dubielzig D. Ocular Anatomy and Variations in Laboratory Animals. Available at: http://www.google.co.uk/url?sa=t&rct=j&q=&esrc=s&source=web&cd=1&ved=0CDAQFjAA&url=http%3A%2F%2Fwww.vetmed.wisc.edu%2Fpbs%2Fdubielzig%2Fpages%2Fcoplow%2FPowerPoints%2FAmColToxRed2008Anat.pdf&ei=rJiDUZSKHc-m0wWByIBQ&usg=AFQjCNG0zCy_jKdTZR5dSpo08e_CHCQ-bA&sig2=5YRoQHssiHhecc9wf0b3hA&bvm=bv.45960087,d.d2k&cad=rja. Accessed 02 May, 2013.

198. Deering MF. A Photon Accurate Model of the Human Eye. *SIGGRAPH* 2005.

199. Vakkur GJ, Bishop PO. THE SCHEMATIC EYE IN THE CAT. *Vision research* 1963; **61:** 357-381.

200. Sanchez I, Martin R, Ussa F, Fernandez-Bueno I. The parameters of the porcine eyeball. *Graefe's archive for clinical and experimental ophthalmology = Albrecht von Graefes Archiv fur klinische und experimentelle Ophthalmologie* 2011; **249**(4)**:** 475-482.

201. Mutti DO, Zadnik K, Murphy CJ. Naturally occurring vitreous chamber-based myopia in the Labrador retriever. *Investigative ophthalmology & visual science* 1999; **40**(7)**:** 1577-1584.

202. Hughes A. A schematic eye for the rabbit. *Vision research* 1972; **12**(1)**:** 123-138.

203. Lapuerta P, Schein SJ. A four-surface schematic eye of macaque monkey obtained by an optical method. *Vision research* 1995; **35**(16)**:** 2245-2254.

204. Massof RW, Chang FW. A revision of the rat schematic eye. *Vision research* 1972; **12**(5)**:** 793-796.

205. Jayaram H, Becker S, Eastlake K, Jones MF, Charteris DG, Limb GA. Optimized feline vitrectomy technique for therapeutic stem cell delivery to the inner retina. *Veterinary ophthalmology* 2014; **17**(4)**:** 300-304.

206. Anderson DH, Guerin CJ, Erickson PA, Stern WH, Fisher SK. Morphological recovery in the reattached retina. *Investigative ophthalmology & visual science* 1986; **27**(2)**:** 168-183.

207. Fraunfelder FT, Potts AM. An experimental study of retinal detachments. *American journal of ophthalmology* 1966; **62**(3)**:** 561-568.

208. Jackson TL, Hillenkamp J, Williamson TH, Clarke KW, Almubarak AI, Marshall J. An Experimental Model of Rhegmatogenous Retinal Detachment: Surgical Results and Glial Cell Response. *Investigative Opthalmology & Visual Science* 2003; **44**(9)**:** 4026.

209. Bhatt NS, Newsome DA, Fenech T, Hessburg TP, Diamond JG, Miceli MV *et al.* Experimental transplantation of human retinal pigment epithelial cells on collagen substrates. *American journal of ophthalmology* 1994; **117**(2)**:** 214-221.

210. Crafoord S, Algvere PV, Kopp ED, Seregard S. Cyclosporine treatment of RPE allografts in the rabbit subretinal space. *Acta ophthalmologica Scandinavica* 2000; **78**(2)**:** 122-129.

211. Crafoord S, Algvere PV, Seregard S, Kopp ED. Long-term outcome of RPE allografts to the subretinal space of rabbits. *Acta ophthalmologica Scandinavica* 1999; **77**(3)**:** 247-254.

212. Crafoord S, Dafgard Kopp E, Seregard S, Algvere PV. Cellular migration into neural retina following implantation of melanin granules in the subretinal space. *Graefe's archive for clinical and experimental ophthalmology = Albrecht von Graefes Archiv fur klinische und experimentelle Ophthalmologie* 2000; **238**(8)**:** 682-689.

213. Leng T, Fishman HA. Carbon nanotube bucky paper as an artificial support membrane for retinal cell transplantation. *Ophthalmic surgery, lasers & imaging retina* 2013; **44**(1)**:** 73-76.

214. Oganesian A, Gabrielian K, Ernest JT, Patel SC. A new model of retinal pigment epithelium transplantation with microspheres. *Archives of ophthalmology* 1999; **117**(9)**:** 1192-1200.

215. Wang F, Xu P, Wu JH, Xia X, Sun HL, Xu X *et al.* [Long-term outcome of gfp gene modified human RPE xenografts into the subretinal space of rabbits]. *Sheng wu hua xue yu sheng wu wu li xue bao Acta biochimica et biophysica Sinica* 2002; **34**(5)**:** 643-649.

216. Yaji N, Yamato M, Yang J, Okano T, Hori S. Transplantation of tissue-engineered retinal pigment epithelial cell sheets in a rabbit model. *Biomaterials* 2009; **30**(5)**:** 797-803.

217. Yamana T, Kita M, Ozaki S, Negi A, Honda Y. The process of closure of experimental retinal holes in rabbit eyes. *Graefe's archive for clinical and experimental ophthalmology = Albrecht von Graefes Archiv fur klinische und experimentelle Ophthalmologie* 2000; **238**(1)**:** 81-87.

218. Kroll AJ, Machemer R. Experimental retinal detachment and reattachment in the rhesus monkey. Electron microscopic comparison of rods and cones. *American journal of ophthalmology* 1969; **68**(1)**:** 58-77.

219. Lewis GP, Charteris DG, Sethi CS, Fisher SK. Animal models of retinal detachment and reattachment: identifying cellular events that may affect visual recovery. *Eye (London, England)* 2002; **16**(4)**:** 375-387.

220. Kim SH, Choi KS. Changes of intraocular pressure during experimental vitrectomy. *Current eye research* 2012; **37**(8)**:** 698-703.

221. Boscher C, Schmidt-Morand D, Holopherne D, Gauthier O. Experimental vitreoretinal surgery in porcine eyes. *Graefe's archive for clinical and experimental ophthalmology = Albrecht von Graefes Archiv fur klinische und experimentelle Ophthalmologie* 2013; **251**(1)**:** 405-406.

222. Thumann G, Aisenbrey S, Schaefer F, Bartz-Schmidt KU. Instrumentation and technique for delivery of tissue explants to the subretinal space. *Ophthalmologica Journal international d'ophtalmologie International journal of ophthalmology Zeitschrift fur Augenheilkunde* 2006; **220**(3)**:** 170-173.

223. Bertschinger DR, Beknazar E, Simonutti M, Safran AB, Sahel JA, Rosolen SG *et al.* A review of in vivo animal studies in retinal prosthesis research. *Graefe's archive for clinical and experimental ophthalmology = Albrecht von Graefes Archiv fur klinische und experimentelle Ophthalmologie* 2008; **246**(11)**:** 1505-1517.

224. Chow AY, Pardue MT, Chow VY, Peyman GA, Liang C, Perlman JI *et al.* Implantation of silicon chip microphotodiode arrays into the cat subretinal space. *IEEE transactions on neural systems and rehabilitation engineering : a publication of the IEEE Engineering in Medicine and Biology Society* 2001; **9**(1)**:** 86-95.

225. Pardue MT, Stubbs EB, Jr., Perlman JI, Narfstrom K, Chow AY, Peachey NS. Immunohistochemical studies of the retina following long-term implantation with subretinal microphotodiode arrays. *Experimental eye research* 2001; **73**(3)**:** 333-343.

226. Bragadottir R, Narfstrom K. Lens sparing pars plana vitrectomy and retinal transplantation in cats. *Veterinary ophthalmology* 2003; **6**(2)**:** 135-139.

227. Okuma M. [Transmission and scanning electron microscopic observations of the experimentally detached retina in the rabbit. I. Early changes of the detached retina]. *Nippon Ganka Gakkai zasshi* 1972; **76**(5)**:** 303-311.

228. Faude F, Francke M, Makarov F, Schuck J, Gartner U, Reichelt W *et al.* Experimental retinal detachment causes widespread and multilayered degeneration in rabbit retina. *J Neurocytol* 2001; **30**(5)**:** 379-390.

229. Gwon A. The rabbit in cataract/IOL surgery. In: Tsonis PA (ed). Animal Models in Eye Research. Academic Press: San Diego, CA, USA.; 2009.

230. Williams D. Rabbit and Rodent Ophthalmology. *EJCAP* 2007; **17**(3)**:** 242-252.

231. Henderson T *Principles of Ophthalmology*. William Heinemann: London; 1950.

232. Funk RH. The vessel architecture of the pars plana in the cynomolgus monkey, rat and rabbit eye. A scanning electron microscopic study of plastic corrosion casts. *Ophthalmic research* 1993; **25**(6)**:** 337-348.

233. Machemer R. Development of Vitreous Surgery. In: Blankenship GW, Binder S, Gonvers M, Stirpe M (eds). Basic and Advanced Vitreous Surgery. Liviana Press: Padova; 1986.

234. Christoforidis JB, Williams MM, Wang J, Jiang A, Pratt C, Abdel-Rasoul M *et al.* Anatomic and pharmacokinetic properties of intravitreal bevacizumab and ranibizumab after vitrectomy and lensectomy. *Retina (Philadelphia, Pa)* 2013; **33**(5)**:** 946-952.

235. Vurgese S, Panda-Jonas S, Jonas JB. Scleral thickness in human eyes. *PloS one* 2012; **7**(1)**:** e29692.

236. Famiglietti EV, Sharpe SJ. Regional topography of rod and immunocytochemically characterized "blue" and "green" cone photoreceptors in rabbit retina. *Visual neuroscience* 1995; **12**(6)**:** 1151-1175.

237. Leeson TS. Freeze-etch studies of rabbit eye. I. Choriocapillaris, lamina elastica (vitrea) and pigment epithelium. *Journal of anatomy* 1971; **108**(Pt 1)**:** 135-146.

238. Stalmans P, Benz MS, Gandorfer A, Kampik A, Girach A, Pakola S *et al.* Enzymatic vitreolysis with ocriplasmin for vitreomacular traction and macular holes. *The New England journal of medicine* 2012; **367**(7)**:** 606-615.

239. Render J. The Eye in Safety Studies: Preparation for Microscopic Assessment. *NE Division Symposium on Toxicologic Pathology of the Eye*, 2007.

240. McLeod D. Giant retinal tears after central vitrectomy. *The British journal of ophthalmology* 1985; **69**(2)**:** 96-98.

241. Stanzel BV. Personal Communication; 2014.

242. Keane PA, Balaskas K, Sim DA, Aman K, Denniston AK, Aslam T *et al.* Automated Analysis of Vitreous Inflammation Using Spectral-Domain Optical Coherence Tomography. *Transl Vis Sci Technol* 2015; **4**(5)**:** 4.

243. Nakano T, Ando S, Takata N, Kawada M, Muguruma K, Sekiguchi K *et al.* Self-formation of optic cups and storable stratified neural retina from human ESCs. *Cell stem cell* 2012; **10**(6)**:** 771-785.

244. Liew G, Michaelides M, Bunce C. A comparison of the causes of blindness certifications in England and Wales in working age adults (16-64 years), 1999-2000 with 2009-2010. *BMJ open* 2014; **4**(2)**:** e004015.